

DNA Hypomethylation, Radiosensitivity and Genomic Stability

Thesis submitted for the degree of

Doctor of Philosophy

at the University of Leicester

Christine Armstrong

University of Leicester Department of Genetics

September 2010

Abstract

Christine Armstrong

DNA Hypomethylation in Radiosensitivity and Genomic Stability

Exposure to ionising radiation can result in genome destabilisation. Genomic instability is observed in many cancers and is thought to lead to tumourigenesis. A correlation between genomic instability and global hypomethylation, another common feature of tumour cells, has been demonstrated and attributed to dysregulated gene expression, retroviral activation and increased homologous recombination. Furthermore, global hypomethylation has been correlated with increased radiosensitivity, and ionising radiation has been demonstrated to reduce methylation levels.

Using mouse embryonic stem cell lines containing wild type or catalytically inactive DNA methyltransferase enzymes (DNMT1, DNMT3A and DNMT3B), this thesis investigated the effect of radiation on global methylation, and the effect of global hypomethylation on radiosensitivity and genomic stability.

Global hypomethylation was not found to increase radiation sensitivity in these cells, and did not correlate with genomic instability on a genome wide scale, or at specific gene loci. However, the DNMT3A and DNMT3B enzymes specifically appeared to influence radiosensitivity, whilst absence of catalytically active DNMT1 resulted in a 10-fold increase of instability at the *Hprt* gene locus, indicating the importance of this enzyme for maintaining genomic stability.

Ionising radiation did not induce hypomethylation or delayed chromosomal instability in these cells. However, the wild type cell line displayed radiation induced delayed genomic instability at *Hprt*, indicated by a 5-fold increase of mutation rate. Furthermore, disruption of the normal methylation pattern, or absence of the DNMTs, resulted in failure to manifest radiation-induced delayed genomic instability. This is the first direct evidence that normal DNA methylation levels, or the presence of functional DNMTs, are required for the propagation of radiation induced delayed genomic instability in murine embryonic stem cells.

Acknowledgements

There are many people in the department I would like to thank for their help, advice and support during my PhD.

First and foremost I would like to thank my original supervisors Mark Plumb and Cristina Tufarelli, who together came up with the original idea behind this project. I would especially like to thank Mark for his ability to inspire and for giving me the confidence to see this project through. I hope he would have approved of how it has turned out. I am also extremely grateful to Cristina for sticking with me throughout the whole project, and for the tremendous support and guidance she has given at every step. A huge acknowledgement is also due to my adoptive supervisors, Chris Talbot and Don Jones (Snr), for actually taking me on in the first place, and for their immense support and patience throughout.

I would like to thank my collaborators, Raj and Jodie for their help with the HPLC, and Rhona Anderson, Munira Kadhim and Debbie Bowler for their help with the cytogenetic work. Also my two fabulous MSc students, Pooja and Deepan, for their valuable contributions to the work presented in this thesis. I am very grateful to Yuri Dubrova and Ruth Barber for their willing advice and support; to Jenny Foxon and Nicola Royle for their assistance in matters of cell culture and microscopes; to Don's lab group for teaching me the comet assay; and to all of my lab colleagues (Rohan, Rob M, George T, Raj) for the assistance they have given in this work and for making the lab an enjoyable place to work. An especially big 'thank you' goes to George G. for his help, advice and support at the most critical time. I may not have even made it through the first year without you. That brings me on to friends.

Thanks to my wonderful flatmates (Dee, Cynthia and Becky) and to all my friends in the department for making Leicester such a friendly and welcoming place to live. Thanks to Rob M. and Jon for numerous hearty Sunday dinners and fabulous profiteroles; to the Monkeys, and to Kat for being there to share the good times and sometimes to provide a much needed hug; Aline and George for their ability to get everyone to the pub; Allan for posting treats and not moaning that he's hardly seen me the last 2 months; and last but certainly not least, my parents and brother for their unconditional love and support in whatever I decide to do. Thank you.

Contents

1	Chapter 1. Introduction	12
1.1	DNA methylation and the DNMTs.....	12
1.2	DNA methylation in cancer	17
1.3	DNA methylation and genomic stability	21
1.4	Ionising radiation.....	29
1.4.1	Interaction with biological matter	31
1.5	The response of mammalian cells to DNA damage	32
1.5.1	Mammalian cell cycle regulation and checkpoints.....	32
1.5.2	Apoptosis/Necrosis in response to IR.....	36
1.5.3	Mammalian DNA repair processes	37
1.6	Radiosensitivity and DNA methylation	45
1.7	Radiation-induced delayed genomic instability.....	48
1.7.1	Mechanisms of radiation-induced DNA hypomethylation.....	53
1.7.2	Radiation-induced chromosomal instability.....	55
1.7.3	The role of telomeres in maintaining genomic stability.....	57
1.8	Project Rationale and aims	61
2	Chapter 2. Methods and Materials.....	63
2.1	Chemicals and Reagents	63
2.2	Routine cell culture	66
2.2.1	ES Cell Culture Media.....	66
	Complete ES Media.....	66
2.2.2	ES cell lines.....	67
2.2.3	Growth of ESCs from frozen aliquots	67
2.2.4	Routine passaging of ESCs	67
2.2.5	Freezing aliquots of ESCs	68
2.2.6	Screening cells for Mycoplasma infection	68
2.2.7	Pelleting cells for DNA extraction	69
2.3	DNA Extraction	70
2.3.1	Phenol-Chloroform Extraction.....	70
2.3.2	DNA extraction for HPLC.....	71
2.3.3	DNA extraction from single colonies	71
2.4	Irradiations	72
2.5	Polymerase Chain Reaction (PCR).....	72
2.6	Sequencing.....	74
2.6.1	Clean-up of PCR products	74
2.6.2	Sequencing reaction	74
2.6.3	Clean-up after sequencing.....	75
2.6.4	Sequence Analysis.....	75
2.7	Southern Blotting	75
2.7.1	Production of Probes	77
2.7.2	Radiolabelling of probes and membrane hybridisation	79
2.7.2.1	Oligonucleotide end-labelling	79
2.7.2.2	dsDNA labelled by random priming	80

2.7.3	Visualisation	81
2.7.4	Stripping a Southern blot.....	81
3	Chapter 3. Characterisation and Radiosensitivity of the Cell Lines	82
3.1	Introduction	82
3.2	Chapter-Specific Methods and Materials	86
3.2.1	HPLC.....	86
3.2.1.1	Stock solutions of authentic standards	86
3.2.1.2	Enzymatic hydrolysis of DNA.....	87
3.2.1.3	HPLC-UV detection	87
3.2.1.4	Calculation of the percentage 5-MedC in DNA	88
3.2.2	Clonogenic Assays: Radiosensitivity	88
3.2.2.1	Clonogenic assay using semi-solid agarose	88
3.2.2.2	Clonogenic assay using gelatinised dishes	89
3.2.3	Growth curves.....	90
3.2.4	FACS cell cycle analysis	91
3.2.4.1	Sample Preparation	91
3.2.4.2	Flow Cytometry: FACS (Fluorescence Activated Cell Sorting).....	92
3.3	Results	93
3.4	Discussion.....	110
3.4.1	The ESC lines display a range of states of hypomethylation in comparison to somatic cells	110
3.4.2	ESCs lack a G1 checkpoint and exit G2 arrest around 24 hours post irradiation	111
3.4.3	Radiosensitivity does not correlate with hypomethylation	113
3.4.4	Summary	114
4	Chapter 4. Genomic Stability: Mutation Rate at the <i>Hprt</i> Gene Locus and the Influence of Hypomethylation at Specific Repeats.....	116
4.1	Introduction	116
4.2	Chapter-Specific Methods and Materials	119
4.2.1	Genomic Stability Measured by Mutation Rate at the <i>Hprt</i> Gene	119
4.2.1.1	Establishment of clones.....	120
4.2.1.2	Selection of cells containing mutation(s) within the <i>Hprt</i> gene.....	121
4.3	Results	122
4.3.1	<i>Hprt</i> mutation rate.....	122
4.3.2	<i>Hprt</i> mutation spectrum	125
4.3.3	Methylation of structural repeats and endogenous retroviral elements 132	
4.4	Discussion.....	140
4.4.1	Lack of DNMT1, but not DNMT3A and/or DNMT3B, leads to an increased <i>de novo</i> mutation rate	140
4.4.2	Radiation-induced delayed genomic instability is observed in wild type ESCs, but not in <i>Dnmt</i> deficient ESCs.....	142
4.4.3	Mutation spectra analysis reveals a link between non-contiguous exonic deletions and hypomethylation or radiation exposure.....	144
4.4.4	Mutation spectra analysis reveals active retrotransposition in <i>Dnmt1</i> ^{-/-} ESCs	147

4.4.5	Summary	150
5	Chapter 5. Genomic Stability: Frequency of Aberrations on a Genome-wide Scale	152
5.1	Introduction	152
5.2	Chapter-specific Methods and Materials.....	155
5.2.1	Alkaline Single-Cell Gel Electrophoresis (Comet) Assay	155
5.2.1.1	Slide preparation and cell lysis	155
5.2.1.2	Treatment with FPG enzyme	156
5.2.1.3	Electrophoresis	157
5.2.1.4	Staining and visualisation	157
5.2.2	Genomic Stability Measured by Frequency of Cytogenetic Aberrations	158
5.2.2.1	Preparation and irradiation of cells.....	158
5.2.2.2	Accumulation of cells in metaphase.....	159
5.2.2.3	Harvesting.....	159
5.2.2.4	Fixation	160
5.2.2.5	Preparing slides	160
5.2.2.6	Staining slides	161
5.2.2.7	Mounting slides	161
5.2.2.8	Scoring aberrations.....	162
5.2.2.9	Statistical Analysis	162
5.3	Results	163
5.3.1	Comet assay for strand break damage detection.....	163
5.3.2	Comet Assay for oxidative stress damage detection.....	165
5.3.3	Frequency of structural cytogenetic aberrations	166
5.3.4	Frequency of numerical chromosome aberrations	176
5.4	Discussion.....	180
5.4.1	Global hypomethylation does not alter the level of endogenous or delayed DNA damage measured by the comet assay	180
5.4.2	Radiation-induced delayed genomic instability at <i>Hprt</i> in wild type ESCs is not a result of increased oxidative damage	184
5.4.3	Structural Cytogenetic Aberrations	186
5.4.4	Cytogenetic instability did not correlate with hypomethylation and was not observed at a delayed period after 3Gy X-irradiation	187
5.4.5	Aberrations of the satellite arms were more frequent in hypomethylated ESCs than wild type ESCs	190
5.4.6	Hypomethylation correlates with reduced frequency of aneuploidy	196
5.4.7	Chromosome gains/losses formed a cell line-specific trend.....	200
5.4.8	Summary	202
6	Chapter 6. Discussion.....	204
6.1	Radiosensitivity does not correlate with hypomethylation.....	205
6.2	Lack of DNMT1, but not DNMT3A or DNMT3B, leads to an increased <i>de novo</i> mutation rate	206
6.3	Radiation-induced delayed genomic instability is observed in wild type ESCs, but not in <i>Dnmt</i> deficient ESCs	208
6.4	Mutation spectra analysis reveals a link between non-contiguous exonic deletions and hypomethylation or radiation exposure.....	209

6.5	Global hypomethylation does not alter the level of endogenous or delayed DNA damage measured by the comet assay	211
6.6	Radiation-induced delayed genomic instability at <i>Hprt</i> in wild type ESCs is not a result of increased oxidative damage	212
6.7	Cytogenetic instability did not correlate with hypomethylation and was not observed at a delayed period after 3Gy X-irradiation	213
6.8	Aberrations of the satellite arms were more frequent in hypomethylated ESCs than wild type ESCs.....	214
6.9	Hypomethylation correlates with reduced frequency of aneuploidy	215
6.10	Chromosome gains/losses formed a cell line-specific trend	217
6.11	Final conclusions	217
7	Appendices.....	221
7.1	Appendix 1	221
7.2	Appendix 2	222
7.3	Appendix 3	223
7.4	Appendix 4	225
7.5	Appendix 5. License Agreement.	226

List of Figures

Figure 1-1. The mammalian somatic cell cycle and checkpoints.	34
Figure 1-2. Diagrams illustrating the mammalian DNA repair pathways.....	39
Figure 1-3. The correlation between DNA methylation level and tissue radiosensitivity	46
Figure 3-1. Proteins and catalytic region DNA sequences of the DNMTs.....	84
Figure 3-2. HPLC-UV spectra showing separation of 2' deoxynucleosides.....	93
Figure 3-3. HPLC spectrum spiked with standards for 5MedC and G.....	94
Figure 3-4. Methylation levels of the ESC lines and tissue controls.....	95
Figure 3-5. Methylation levels post 3Gy X-irradiation.....	97
Figure 3-6. Methylation levels post 3Gy X-irradiation: shorter time points.....	99
Figure 3-7. Growth Curves of the ESC lines.....	101
Figure 3-8. Cell cycle distribution of wild type ESCs before and after irradiation.....	103
Figure 3-9. Cell cycle progression of the ESC lines post irradiation.....	104
Figure 3-10. Clonogenic dose-response curve of ESC radiosensitivity.....	108
Figure 4-1. Schematic outline of the <i>Hprt</i> mutation rate procedure.....	119
Figure 4-2. <i>Hprt</i> gene mutation rates 23-25 population doublings post 3Gy X-irradiation or sham treatment.....	124
Figure 4-3. Spectrum of the <i>Hprt</i> gene mutations observed.....	126
Figure 4-4. Schematic of the murine <i>Hprt</i> gene.....	128
Figure 4-5. Sequence of <i>Hprt</i> gene intron/exon 3 and B2 SINE insertion.....	129
Figure 4-6. Sequence of <i>Hprt</i> gene intron/exon 6 and B1 SINE/Alu insertion.....	129
Figure 4-7. <i>Hprt</i> exon PCR products showing mutations.....	131
Figure 4-8. Southern blots: ESC methylation at minor satellites and IAPs.....	134
Figure 4-9. Southern blots: ESC methylation at LINE1 subfamilies.....	136
Figure 4-10. Southern blots: ESC methylation at L1 A compared to tissues.....	138
Figure 4-11. Southern blots: ESC methylation at SINE subfamilies.....	139
Figure 5-1. Comet images displaying increasing levels of DNA damage.....	163
Figure 5-2. DNA damage levels of the ESCs measured by comet assay.....	164
Figure 5-3. Levels of oxidative damage in the ESCs measured by comet assay.....	165
Figure 5-4. Frequencies of structural cytogenetic aberrations in the ESCs.....	171
Figure 5-5. Mitotic spreads showing a translocation and long satellite arms.....	172

Figure 5-6. Mitotic spreads showing multi-centric chromosome aberrations.....	173
Figure 5-7. Frequencies of chromosome aberrations involving the satellite arms.....	174
Figure 5-8. Mitotic spread showing a multi-radial chromosome.....	175
Figure 5-9. Frequency of aneuploidy and polyploidy.....	176
Figure 5-10. Characteristic distributions of chromosome counts in each ESC line.....	178

List of Tables

Table 2-1. Stock solutions.....	64
Table 2-2. Primers used to characterise mutations within the <i>Hprt</i> gene.....	73
Table 2-3. Primers used to generate longer sequence probes for Southern blotting...78	
Table 2-4. Satellite DNA sequences used as oligonucleotide probes for Southern blotting.....	79
Table 3-1. ESC line plating efficiencies and mean lethal doses (D_0) of X-irradiation...109	
Table 4-1 Fraction of the genome comprised by various transposable elements.....	118
Table 4-2. Details of the <i>Hprt</i> selections for each cell line and treatment condition..122	
Table 4-3. Illustration of the observed non-contiguous exonic deletions.....	127

Abbreviations

°C	degree centigrade
µg	microgram
µl	microlitre
*OH	hydroxyl radical
5MedC	5-methyl-2'-deoxycytidine
95% CI	95% confidence interval
AML	acute myeloid leukaemia
ASO	allele specific oligonucleotide
BER	base excision repair
BM	bone marrow
βME	beta mercaptoethanol
bp	base pair
BSA	bovine serum albumin
CHO	Chinese hamster ovary cell
CpG	Cytosine-phosphate-Guanine
D ₀	mean lethal dose
dA	2'-deoxyadenosine
dC	2'-deoxycytidine
dCTP	2'-deoxycytosine 5'-triphosphate
dG	2'-deoxyguanosine
dH ₂ O	distilled water
DMSO	dimethylsulphoxide
DNA	deoxyribonucleic acid
DNMT	DNA methyltransferase
dNTPs	2'-deoxyribose 5'-triphosphates
EAR	excess absolute risk
EDTA	ethylenediaminetetra acetic acid
ENV	Glutamate (E), Asparagine (N) and Valine (V)
ERR	excess relative risk
ESCs	embryonic stem cells
ESTR	expanded simple tandem repeat
EtBr	ethidium bromide
EtOH	ethanol
FACS	fluorescent activated cell sorting
FCS	foetal calf serum
FISH	fluorescence <i>in situ</i> hybridisation
Fpg	formamidopyrimidine DNA glycosylase
G	guanosine
Gy	gray
HDAC	histone deacetylase
hESCs	human embryonic stem cells
HPLC	high performance liquid chromatography

HPRT	hypoxanthine rybosyl transferase
HR	homologous recombination
HSC	haemopoietic stem cell
IAP	intracisternal A particle
ICF	immunodeficiency, centromeric instability, facial anomalies syndrome
IR	ionising radiation
Kb	kilobases
KO	knock out
LET	linear energy transfer
LIF	leukaemia inhibitory factor
LINE1	long interspersed nuclear element 1
LTR	long tandem repeat
Mol	Mole
mESCs	mouse embryonic stem cells
MMR	mismatch repair
mRNA	messenger RNA
NER	nucleotide excision repair
ng	nanogram
NHEJ	non homologous end joining
PBS	phosphate buffered saline
PC	prolylcysteinyI
PCNA	Proliferating Cell Nuclear Antigen
PCR	polymerase chain reaction
PI	propidium iodide
pMol	picomole
PWWP	Pro-Trp-Trp-Pro
RNA	ribose nucleic acid
ROS	reactive oxygen species
RPA	replication protein A
SEM	standard error of the mean
SINE	short interspersed nuclear element
Sv	Sievert
T	thymidine
T-DMR	tissue differentially methylated region
TE	tris-EDTA
UV	ultraviolet
V	volt
w/v	weight per volume
WT	wild type

1 Chapter 1. Introduction

It has long been recognized that there is a causative link between exposure to radiation and the development of cancer. Nevertheless, the molecular basis for the development of genomic instability and tumourigenesis are not thoroughly understood (Lengauer *et al*, 1998). Although several studies indicate that radiation-induced genomic instability may be mediated by an epigenetic mechanism, the processes involved remain unclear (Dubrova *et al*, 2003; Wright, 2010). Cancer cells often display low global levels of DNA methylation (Wahlfors *et al*, 1992; Lin *et al*, 2001; Kim *et al*, 1994), and aberrantly reduced methylation levels have been associated with instability through the activation of mobile DNA elements and increased frequencies of chromosomal rearrangements (Tuck-Muller *et al*, 2000; Symer *et al*, 2002). It has been proposed that demethylation is a direct effect of exposure to ionizing radiation and that this in turn may promote genomic instability (Koturbash *et al*, 2006). In addition, evidence indicates that cells and tissues with decreased levels of DNA methylation may be more radiosensitive (Dote *et al*, 2005). The work reported in this thesis aimed to investigate the relationship between DNA methylation, radiosensitivity and genomic stability using mouse embryonic stem cells as a model system.

1.1 DNA methylation and the DNMTs

Methylation of mammalian DNA involves the addition of a methyl group to carbon 5 of the Cytosine pyrimidine ring (5-MeC). In vertebrates this predominantly occurs at CpG

dinucleotides (Ramsahoye *et al*, 2000), 60-90% of which are methylated. The level of mammalian DNA cytosine methylation varies between different cell and tissue types (Gama-Sosa *et al*, 1983a). Generally, methylation levels increase with cellular differentiation, corresponding to differential regulation of genes and cell specialisation (Ehrlich *et al*, 1982; Shiota *et al*, 2002). In ESCs approximately 65% of the total CpG dinucleotides are methylated (Jackson *et al*, 2004) compared to roughly 80% in differentiated somatic cells (Razin and Szyf, 1984). Similarly, tissues which vary in the proportional content of immature and differentiated cells have been shown to demonstrate varying overall levels of methylation (Ehrlich *et al*, 1982; Gama-Sosa *et al*, 1983; Giotopoulos *et al* 2006). Bone marrow, which has a high stem cell content, is one of the most hypomethylated somatic tissues in the adult mouse (Giotopoulos *et al*, 2006).

The majority of the methylated CpG dinucleotides occur at low density throughout the genome due to spontaneous deamination of methylcytosine (see section 1.3). However, many of the unmethylated CpG dinucleotides occur in clusters, called CpG islands. These are often found in the 5' regulatory regions of genes (Ng and Bird, 1999; Lethe *et al*, 1998). Approximately 70% of human gene promoters have a high CpG content and 30% have a low CpG content (Saxonov *et al*, 2006). In promoters with a high CpG content, regulation of gene expression is thought to occur via histone modifications rather than DNA methylation (Meissner *et al*, 2008; Weber *et al*, 2007). The occurrence of DNA methylation at such CpG islands is rare, and causes repression of gene expression (Shen *et al*, 2007). On the other hand, gene promoters which

contain low numbers of CpG dinucleotides often exhibit DNA methylation. However, this is not thought to affect gene expression, as methylation of the few CpG dinucleotides within the promoter may be insufficient to cause repression (Weber *et al*, 2007). Although the majority of CpG islands in both mice and humans lack DNA methylation, roughly 5% of the CpG islands that contain a high density of CpGs are methylated in a tissue dependent manner. These are called tissue-differentially methylated regions (T-DMRs) and DNA methylation at these regions is strongly correlated with gene repression (Shen *et al*, 2007; Song *et al*, 2005).

Methylation of DNA cytosine bases at carbon 5 is an important cellular phenomenon. It is reversible and causes a heritable effect, without altering the base sequence of the DNA (Li and Bird, 2007). DNA methylation plays a key role in a wide variety of biological functions such as control of gene transcription (Song *et al*, 2005), imprinting (Davis *et al*, 2000), stabilisation of X-inactivation (Norris *et al*, 1994; Lee and Jaenisch, 1997), silencing of transposable elements (Takai *et al*, 2000) and maintenance of genome stability (Chen *et al*, 1998; Gisselsson *et al*, 2005). Generally, methylated DNA is associated with a compact, transcriptionally silent chromatin state in mammals (Choy *et al*, 2010; Lee and Jaenisch, 1997). The methyl group can directly block the binding of transcription factors (Watt and Molloy, 1988) and RNA polymerase II (Lorincz *et al*, 2004). In addition it promotes the recruitment of other proteins that mediate repressive local chromatin changes. For example, methylated CpGs provide a binding site for the methyl binding domain proteins (MBD1 to 4 and MeCP1 and 2) (Ohki *et al*, 2001), which in turn recruit co-repressor proteins such as histone

deacetylases (HDACs) (Nan *et al*, 1998). Furthermore, repressive factors such as HDACs, histone methyltransferases (HMTs) and ATP-dependent chromatin-remodelling proteins, can be recruited directly through interaction with the DNA methyltransferase enzymes themselves (Geiman *et al*, 2004).

Mammalian CpG DNA methylation is catalysed by three DNA methyltransferase enzymes (DNMT1, DNMT3A, and DNMT3B), using S-adenosyl methionine (SAM or AdoMet) as a methyl donor (Chen *et al*, 1991; Pradhan and Esteve, 2003). The roles of the enzymes overlap slightly, but DNMT1 is primarily a maintenance methyltransferase and copies the established methylation pattern onto the newly synthesised DNA strand at each round of DNA replication (Schermelleh *et al*, 2007). DNMT1 is ubiquitously expressed in the nucleus of all proliferating cells, and predominantly methylates hemi-methylated DNA, which it is targeted to by the Np95 protein (Sharif *et al*, 2007). The efficiency of the methylation activity of DNMT1 is enhanced via transient localisation to the replication fork during S phase, where it binds to Proliferating Cell Nuclear Antigen (PCNA) (Schermelleh *et al*, 2007). DNMT1 interacts with a range of chromatin modifying enzymes, such as HDACs, HMTs, polycomb group proteins and Hp1, to ensure the establishment of the full range of repressive marks and chromatin structure at heterochromatin and silenced euchromatic loci (Esteve *et al*, 2006, Fuks *et al*, 2000, Smallwood *et al*, 2007; Vire *et al*, 2006). DNMT1 is also recruited to repair foci at sites of DNA damage, presumably for the purpose of restoring epigenetic information (Mortusewicz *et al*, 2005).

The DNMT3 family of enzymes (DNMT3A and DNMT3B) are primarily *de novo* methyltransferases, responsible for establishing the DNA methylation pattern during early mammalian embryonic development and gametogenesis (Okano *et al*, 1999). They are strongly expressed in ESCs, early embryos and developing germ cells, but only occur in low levels in differentiated somatic cells (Okano *et al*, 1998). DNMT3A and DNMT3B have both overlapping and distinct roles in the establishment of DNA methylation (Watanabe *et al*, 2002) and exhibit preferential methylation activity for specific sites or sequences within the genome (Oka *et al*, 2006; Okano *et al*, 1999). They function together in a synergistic manner and have been shown to interact with each other (Li *et al*, 2007), and with a variety of other components of the transcriptional silencing pathways, in a similar manner to DNMT1 (Fuks *et al*, 2003, Geiman *et al*, 2004; Tachibana *et al*, 2008; Vire *et al*, 2006).

Establishment of *de novo* methylation patterns during gametogenesis is assisted by a further DNMT3 family protein called DNMT3L (Bourc'his *et al*, 2001). DNMT3L shares significant sequence homology with DNMT3A and DNMT3B but lacks a catalytic domain and, as such, has no methyltransferase activity or the ability to bind directly to DNA (Ooi *et al*, 2007). However, it interacts with DNMT3A, DNMT3B, the four core histone proteins (Ooi *et al*, 2007) and also binds directly to HDAC1 (Aapola *et al*, 2002). It is thought that DNMT3L assists *de novo* methylation by specifically recognizing and interacting with histone H3 tails that are unmethylated at lysine 4, and inducing recruitment or activation of DNMT3A (Ooi *et al*, 2007).

Each of the catalytically active mammalian DNA methyltransferase enzymes are essential for mammalian development (Li *et al*, 1992; Okano *et al*, 1999). Homozygous inactivation of the DNMT1 gene is embryonic lethal in mice (Li *et al*, 1992). *Dnmt3a3b*^{-/-} mouse embryos also exhibit an early lethal phenotype, whilst *Dnmt3b*^{-/-} embryos die later during development and *Dnmt3a*^{-/-} embryos show the least severe phenotype, surviving for roughly 4 weeks postnatally (Okano *et al*, 1999). Embryonic stem cells deficient for any of the DNMTs are viable and proliferate normally (Jackson *et al*, 2004; Li *et al*, 1992; Tsumura *et al*, 2006). However, *Dnmt1*^{-/-} ESCs die upon differentiation (Damelin and Bestor, 2007) and somatic cells and cancer cells containing conditional knock outs of *Dnmt1* apoptose within a few cell divisions after gene deletion (Chen *et al*, 2007; Jackson-Grusby *et al*, 2001). Differentiation ability of *Dnmt3a3b*^{-/-} ESCs depends on their residual level of DNA methylation, which decreases with increasing passage number (see section 3.3). Low passage number *Dnmt3a3b*^{-/-} ESCs with intermediate levels of DNA methylation are able to terminally differentiate along a limited range of cell lineages, and can form cardiomyocytes and haematopoietic cells. However, late passage *Dnmt3a3b*^{-/-} ESCs with very low levels of DNA methylation fail to initiate differentiation upon withdrawal of LIF and continue to express markers of undifferentiated ESCs (Jackson *et al*, 2004).

1.2 DNA methylation in cancer

Aberrant DNA methylation has frequently been observed in a wide variety of different cancers (Wahlfors *et al*, 1992; Lin *et al*, 2001; Kim *et al*, 1994; Costello *et al*, 2000; Esteller *et al*, 2001). Hyper- and hypo- methylation can occur in tumour cells

individually or together, and are thought to arise/contribute to carcinogenesis through independent processes (Ehrlich, 2002; Widschwendter *et al*, 2004). Abnormal hypermethylation is usually specific to CpG-rich sequences, such as the 5' regulatory regions of genes, and can result in transcriptional repression of tumour suppressor genes (Costello *et al*, 2000; Esteller *et al*, 2001; Pulukuri and Rao, 2006). Such an effect was illustrated recently in a study by Hannigan *et al* (2010).

Aberrant hypomethylation, however, usually has a global effect and occurs mainly at repeated sequences (Ehrlich, 2002; Gama-Sosa *et al*, 1983b). A wide range of cancers demonstrate global hypomethylation in comparison to corresponding normal tissue controls (Wahlfors *et al*, 1992; Lin *et al*, 2001; Kim *et al*, 1994). The link between hypomethylation and carcinogenesis is less obvious, but there is increasing evidence for an association between DNA hypomethylation and genomic instability (Chen *et al*, 1998; Gonzalo *et al*, 2006; Wang and Shen, 2004), which is thought to be an intrinsic part of the process leading to carcinogenesis (Nowell, 1976; Loeb, 1991; Lengauer *et al*, 1998). This will be discussed further in section 1.3.

Aberrantly high expression levels of the DNA methyltransferase enzymes 1, 3a and 3b have been observed in both leukaemic and solid tumour cells in comparison to corresponding controls from healthy donors (Mizuno *et al*, 2001; Robertson *et al*, 1999). In some samples, this increased expression of the DNMTs has been associated with hypermethylation of specific genes (Mizuno *et al*, 2001). Significantly reduced expression of DNMT1 in cancer cells and normal somatic cells is lethal. However, depletion of DNMT3B has been shown to cause a more severe phenotype in cancer

cells than in normal cells, characterised by reduced rates of proliferation and increased propensity for apoptosis (Beaulieu *et al*, 2002).

The differing severity of response between DNMT1 and DNMT3B depleted cells was suggested by Beaulieu *et al* (2002) to reflect the fact that DNMT1 determines the methylation status of a far greater number of CpG dinucleotides than DNMT3B in differentiated cells. However, the exaggerated response of cancer cells to DNMT3B depletion in comparison to that of normal cells was suggested to reflect a specific role for DNMT3B in the generation of the aberrant methylation patterns observed in cancer cells (Beaulieu *et al*, 2002). The phenotype of reduced proliferation and increased apoptosis caused by DNMT3B depletion in cancer cells could not be rescued by exogenous expression of DNMT1, and was not induced by down-regulation of DNMT3A. Splice variant isoforms of DNMT3B, however, were able to rescue this phenotype, indicating that at least some specific targets of DNMT3B in cancer cells are not shared by the other DNMT enzymes, and that these targets may be involved in controlling cancer cell proliferation and survival. One such identified target that was re-expressed in DNMT3B-depleted cancer cells was the RASSF1A tumour suppressor gene (Beaulieu *et al*, 2002).

Indeed, expression of a range of novel abnormally spliced transcripts of DNMT3B, in addition to expression of normal full-length DNMT3B transcripts, has been shown to be a common occurrence in cancer cell lines and primary leukaemia and lung cancer cells (Ostler *et al*, 2007; Wang *et al*, 2006a and 2006b). In a study by Ostler *et al* (2007), over 20 aberrant DNMT3B transcripts were detected in 53 out of 55 human primary

cancer cell samples or established cancer cell lines, 2-5% of which contained sequences that were normally intronic. Correspondingly, truncated DNMT3B proteins could be detected in nuclear protein extracts from the cancer cell lines. In contrast, no aberrant DNMT3B transcripts were detected in any of the 8 normal human tissue samples analysed (Ostler *et al*, 2007).

All of the aberrant DNMT3B transcripts identified in cancer cells by Ostler *et al* (2007) and Wang *et al* (2006a and 2006b) were predicted to encode truncated DNMT3B proteins, which contain novel amino acids and lack the catalytic domain. Expression of these aberrant DNMT3B transcripts was found to correlate with alterations in the expression level of several genes. Interestingly, 75% of the over-expressed genes were located on chromosomes 1, 16 and the X chromosome (Ostler *et al*, 2007). Furthermore, expression of aberrant DNMT3B transcripts also correlated with changes in methylation of several gene promoters including p16 and RASSF1A (Wang *et al*, 2006a).

It was proposed that such truncated proteins could potentially interfere with the normal DNA methylation machinery by binding directly to DNA or by binding to one or more of the proteins known to interact with DNMT3B in order to create a repressive chromatin state, such as HDAC1. Such interference could result in altered DNA methylation, and consequently gene expression. Thus, truncated DNMT3B proteins could potentially influence the DNA methylation state of cancer cells (Ostler *et al*, 2007).

1.3 DNA methylation and genomic stability

Genomic instability is frequently observed in tumour cells, and is thought to be an intrinsic part of the process leading to carcinogenesis (Nowell, 1976; Loeb, 1991; Lengauer *et al*, 1998). Several previous research groups have demonstrated a link between reduced levels of DNA methylation and genomic instability. Genome-wide DNA hypomethylation induced by treatment with a drug (Zebularine), which inhibits the activity of the DNA methyltransferase enzymes, has been associated with prolonged expression of elevated levels of γ H2AX foci in a range of human tumour cell lines compared to untreated tumour cells after 2Gy X-irradiation (Dote *et al*, 2005). γ H2AX foci are indicative of the presence of DNA DSBs. The persistence of this mark at elevated levels in hypomethylated cells suggests either a decrease in their capacity to repair radiation-induced DNA DSBs (Dote *et al*, 2005) or indicates *de novo* formation of new DSBs.

Furthermore, Chen *et al* (1998) analysed the mutation rate at two specific gene loci in hypomethylated and methylation proficient mESC lines: the X-linked hypoxanthine phosphoribosyltransferase (*Hprt*) gene locus and a viral thymidine kinase transgene (*tk*). They found that hypomethylated *Dnmt1*^{-/-} ESCs displayed a significantly elevated mutation rate at the *Hprt* locus in comparison to wild type ESCs, and at the *tk* locus in comparison to *Dnmt*^{+/-} ESC controls. Thus, it was suggested that DNA hypomethylation can lead to elevated levels of gene mutation and, based on the types of mutations detected, that DNA methylation may play an important role in

suppressing mitotic recombination and/or enabling faithful chromosome segregation (Chen *et al*, 1998).

In addition, several studies have shown that cell lines derived from patients with immunodeficiency, centromeric region instability and facial anomalies (ICF) syndrome are hypomethylated at genomic DNA satellite repeat sequences (Jeanpierre *et al*, 1993; Miniou *et al*, 1994) and display chromosomal instability (Sawyer *et al*, 1995; Tiepolo *et al*, 1979; Tuck-Muller *et al*, 2000). ICF syndrome is a rare disorder characterised by loss of DNMT3B activity due to mutations in the catalytic domain (Hansen *et al*, 1999; Xu *et al*, 1999) and/or increased expression of aberrantly spliced DNMT3B transcripts that are predicted to lack catalytic activity (Jiang *et al* 2005). Hypomethylation is seen in all patients at the classical satellite repeats 2 and 3, and on the inactive X chromosome in females (Miniou *et al*, 1994). However, hypomethylation can also involve other sequences including the centromeric alpha satellites (Miniou *et al*, 1997b), Alu sequences (Miniou *et al*, 1997a) and certain imprinted genes (Xu *et al*, 1999). As a result of the anomalous hypomethylation, large regions of pericentromeric heterochromatin on chromosomes 1, 9 and 16 are markedly decondensed and elongated (Jiang *et al*, 2005; Xu *et al*, 1999). This results in an increased frequency of chromosome and chromatid breaks, gaps, whole arm deletions, and the formation of rearrangements such as multiradial chromosomes, in comparison to cells from unaffected controls (Maraschio *et al*, 1988; Sawyer *et al*, 1995; Tiepolo *et al*, 1978; Tuck-Muller *et al*, 2000).

Finally, hypomethylation of subtelomeric DNA sequences has been associated with increased rates of telomeric recombination and sister chromatid exchange (Gonzalo *et al*, 2006). Sub-telomeric DNA repeats have a high density of CpG dinucleotides, which are methylated in mammalian somatic cells (Benetti *et al*, 2007; Brock *et al*, 1999). However, as telomeres become shorter during normal cell proliferation, repressive histone modifications and DNA methylation are lost from these regions (Benetti *et al*, 2007; Steinert *et al*, 2004). It is thought that when telomeres become very short, significantly less of the protective shelterin complex is able to bind, leaving the telomere end relatively unprotected (de Lange, 2005). Such unprotected ends cannot be distinguished from DNA DSBs and may undergo “repair” via degradation, recombination or chromosome fusion by the cellular DNA repair machinery (Artandi *et al*, 2000; Hande *et al*, 1999; Xin & Broccoli, 2004).

There are multiple ways in which aberrant or dysregulated DNA methylation could contribute to genomic instability. First of all, the presence of a methyl group at CpG dinucleotides is inherently mutagenic, as it facilitates the deamination of cytosine to thymine, resulting in a G-T base pair mismatch (Shen *et al*, 1994). Such mismatches are recognised by the DNA mismatch repair machinery (MMR), and thymines are preferentially replaced with cytosine (Brown and Jiricny, 1987). However, this repair is relatively inefficient compared to that of other mismatches such as U-G, and the rate of spontaneous deamination is higher for methylcytosine than cytosine, causing methylated CpGs to be hotspots for transition mutations (Lutsenko and Bhagwat *et al*, 1999). In addition, the G-T mismatch is occasionally incorrectly repaired as A-T,

resulting in a C to T transition mutation (Tornaletti and Pfeifer, 1995). As a result, CpG dinucleotides have become under-represented in the genome: they are present at roughly one fifth of the expected frequency based on calculations determining the frequency of cytosine and guanine occurring together by chance (Brena *et al*, 2006; Zilberman, 2007).

Aberrant DNA methylation could also contribute to genomic instability through inappropriate silencing of tumour suppressor genes (Goto *et al*, 2010) or genes involved in DNA repair or regulation of cell proliferation (Yamamoto *et al*, 2002). Dysregulation of DNA methylation, usually as a consequence of aberrant expression of the DNMTs, has been implicated in carcinogenesis (Costello *et al*, 2000; Esteller *et al*, 2001; Mizuno *et al*, 2001). Aberrant establishment of promoter-specific methylation at tumour suppressor genes such as P16 (Goto *et al*, 2010), DNA repair enzymes such as MLH1 and regulators of cellular proliferation such as CDKN2A (Yamamoto *et al* 2002) could potentially affect mutation rates and genomic stability.

At non-coding sequences, aberrant hypomethylation rather than hypermethylation has been implicated in genomic instability. As discussed above, increased incidences of recombination and rearrangements are observed at hypomethylated sub-telomeric repeats and pericentromeric classical satellite sequences (Gonzalo *et al*, 2006; Tuck-Muller *et al*, 2000). In addition, DNA hypomethylation has been associated with elevated levels of microsatellite instability (Guo *et al*, 2004; Kim *et al*, 2004; Wang and Shen, 2004), and also affects the stability of triplet repeat sequences (Dion *et al*, 2008; Wöhrle *et al*, 1998).

Microsatellite instability is frequently observed in a range of cancers (Burks *et al*, 1994; Merlo *et al*, 1994; Yee *et al*, 1994) and is commonly associated with mutations affecting the fidelity/processivity of DNA replication or mismatch repair (MMR) (Wang and Shen, 2004). Several research groups have demonstrated that DNMT1 deficient embryonic stem cell (ESC) lines have increased levels of microsatellite instability in comparison to wild type ESCs (Guo *et al*, 2004; Kim *et al*, 2004; Wang and Shen, 2004). It was suggested that *Dnmt1*^{-/-} induced genome wide hypomethylation may alter gene expression, and subsequently the cells physiological balance, resulting in increased DNA adduct formation and saturation of the DNA adduct recognition/signalling and MMR pathways (Wang and Shen, 2004). Alternatively, absence of DNMT1 could impair the integrity of the DNA replication machinery and consequently the replication-associated MMR processes, as PCNA is thought to provide the physical link between MMR and DNA replication complexes (Umar *et al*, 1996). Finally, it has also been suggested that DNMT1 may recognise the hemimethylated undamaged template strand during DNA replication, and through its interaction with PCNA, provide the signal for strand discrimination for the MMR complex (Wang and Shen, 2004).

Interestingly, however, the predominant form of alteration observed during hypomethylation-induced microsatellite instability involved contraction of the repeats (Kim *et al*, 2004). This is similar to the predominant alterations observed in CGG triplet repeat tracts residing within genes containing unmethylated promoters, in somatic cells (Wöhrle *et al*, 1998). The frequency of CAG repeat contractions was also significantly increased in hypomethylated mammalian somatic cells, caused by

treatment with the cytidine analogue 5-aza-CdR, or hydralazine (a drug which inhibits the expression of DNMT1), or siRNA against DNMT1 (Gorbunova *et al*, 2004; Dion *et al*, 2008). The occurrence of such contraction mutations has been suggested to be partly caused by transcription through the repeats inducing the formation of secondary structures, which are resolved by DNA repair processes such as nucleotide excision repair (NER) and MMR (Lin and Wilson, 2007; Lin and Wilson, 2009). Although CAG repeats contain no CpG sites, methylation of the surrounding DNA is thought to play a role in suppressing transcription, and thereby stabilising the length, of triplet repeats (Dion *et al*, 2008).

During germline transmissions to offspring, however, methylation proficient mice were found to display a bias towards contractions at the murine spinocerebellar ataxia type 1 (Sca1) locus CAG repeat tract, whilst methylation deficient (*Dnmt1*^{+/-}) mice demonstrated increased frequencies of CAG repeat expansions (Dion *et al*, 2008). The cause of such a disparate effect of hypomethylation on the form of length alteration induced at triplet repeats in somatic cells and the germline is currently unknown. The observed expansions were not found to be a result of altered transcription, and no evidence was found for the involvement of NHEJ (Dion *et al*, 2008). Such expansion of triplet repeat tracts during germline transmission to progeny is, however, responsible for causing several neurodegenerative diseases, such as Huntington Disease and Fragile X syndrome (Dion *et al*, 2008; Laccone and Christian, 2000; Wöhrle *et al*, 1998).

Finally, genomic instability has been associated with altered DNA methylation and activation of endogenous retroviral elements (Takai *et al*, 2000; Symer *et al*, 2002;

Howard *et al*, 2008). There are four main classes of retroviral elements in mammals: long interspersed nuclear elements (LINEs), short interspersed nuclear elements (SINEs), LTR transposons and DNA transposons (Lander *et al*, 2001). DNA transposons have become almost completely inactive in the human genome (Lander *et al*, 2001). However, LINEs, SINEs, and a form of LTR retrotransposons specific to mice called intracisternal A-particles (IAPs), all display high rates of retrotransposition (Carnell and Goodman, 2003; Mouse Genome Sequencing Consortium, 2002; Dewannieux *et al*, 2004; Druker *et al*, 2004; Goodier *et al*, 2001; Lander *et al*, 2001).

Transcription and transposition of endogenous retroviral elements is usually suppressed in mammalian somatic cells by DNA methylation (Gaudet *et al*, 2004; Hata and Sakaki, 1997; Kochanek *et al*, 1993 and 1995; Kuff and Leuders, 1988; Yoder *et al*, 1997). However, hypomethylation of these elements has been reported in a diverse range of cancers (Dante *et al*, 1992; Jürgens *et al*, 1996; Takai *et al*, 2000; Mendez *et al*, 2004; Chalitchagorn *et al*, 2004).

Elevated levels of IAP transcripts and *de novo* IAP insertions have been observed in a range of mouse tumour cells (Canaani *et al*, 1983; Tanaka *et al*, 1995; Lee *et al*, 1999). In addition, mice carrying a hypomorphic *Dnmt1* allele were found to exhibit a high incidence of hypomethylation-induced lymphomas associated with IAP insertions in the *Notch1* gene (Howard *et al*, 2008). Similarly, there have been reports of cancer-associated insertions involving LINE1 sequences (Iskow *et al*, 2010; Miki *et al*, 1992; Morse *et al*, 1988). In particular, one recent study has demonstrated that new somatic

LINE1 insertions occur in high frequencies in hypomethylated lung cancer tumours (Iskow *et al*, 2010).

Such aberrant demethylation and transcriptional activation of retrotransposable elements could contribute to genomic instability in several ways. For example, insertional mutagenesis can directly disrupt gene sequences (Holmes *et al*, 1994), or disturb the transcriptional regulation of nearby genes, as could simple reactivation of existing elements (Han *et al*, 2005; Roman-Gomez *et al*, 2005). Chimeric RNA transcripts of a range of genes have been identified, which are unique to breast cancer cell lines, primary tumours and colon cancer cells. These were found to occur as a direct result of hypomethylation, activation and transcription from the antisense promoter of existing human L1 insertions, as expression of the cancer-specific chimeric transcripts could be induced in non-malignant cells using the DNA demethylating agent 5-azacytidine (Cruickshanks and Tufarelli, 2009). Alternatively, if an active retrotransposon promoter is inserted in the opposite orientation to that of the host gene, and if transcription extends into the exon sequences downstream of the transposon, it could result in antisense RNA-mediated silencing of the gene (Yoder *et al*, 1997).

The presence of multiple copies of long repeats such as LINEs throughout the genome can also contribute to genomic instability by causing an enhancement in levels of homology-based ectopic recombination, resulting in the formation of deletions and duplications (Gilbert *et al*, 2002; Kazazian and Goodier, 2002). Furthermore, active L1 elements have been shown to possess the ability to co-transpose non-L1 DNA at their

3' ends to new genomic locations, resulting in genome duplications. This is thought to be the result of occasional bypassing of the L1 polyadenylation signal by the 3' end processing machinery, resulting in use of another downstream polyadenylation site (Goodier *et al*, 2000; Symer *et al*, 2002). Finally, L1 insertions have been associated with numerous other forms of DNA damage at the insertion sites, such as deletions, inversions and the insertion of between 1 and 100 “extra nucleotides”, which are all thought to be associated with the retrotransposition event itself (Symer *et al*, 2002).

1.4 Ionising radiation

Ionising radiation (IR) is energy that is emitted in a particulate or electromagnetic form, which is capable of producing an electrically charged ion, as a result of the energy deposited when it interacts with an atom or molecule, ejecting an electron. Non-ionising radiation does not have the energy required to displace the electrons surrounding an atom, and therefore does not cause ionisation (Wakeford, 2004).

Particulate forms of IR include β -particles (electrons and positrons), protons, neutrons and α -particles (Hall, 2000). Electrons are negatively charged and have a very small mass. Protons, on the other hand, are positively charged and have a much larger mass. The mass of neutrons is similar to that of protons, but they have no net charge. Alpha-particles consist of 2 protons and 2 neutrons and are essentially a helium nucleus (Dainiak, 2002). Electrons can travel very fast and are able to penetrate tissue for a limited distance, depositing their energy along the way. Protons have a lower speed, however, and are halted upon entry into tissue, resulting on the deposition of all of

their energy within one area (the Bragg peak) (Dainiak, 2002). The even larger α -particles are slower still, and are unable to pass through a sheet of paper. Neutrons, however, are highly penetrating due to their lack of charge (Hall, 2000). Electromagnetic forms of IR, such as X-rays and γ -rays, have no mass or charge (Dainiak, 2002), and are highly penetrating (Wakeford, 2004). X-rays and γ -rays are indistinguishable except for their source: γ -rays are emitted from within the nucleus of an atom whilst X-rays are emitted from the surrounding electrons (Hall, 2000).

The energy released from IR is not deposited uniformly when it enters tissues, but is located where the ionisation reactions occur (Hall, 2000). IR which creates dense ionisation along its track is referred to as having high linear energy transfer (LET), whilst IR which causes sparse ionisation along its track is referred to as having low linear energy transfer (LET). Thus, α -particles and neutrons are high-LET radiation, whilst X-rays and γ -rays are low-LET radiation (Dainiak, 2002). Given the differing density of the ionisation reactions, the damage produced by high-LET radiation is qualitatively different from that produced by low-LET radiation, and is much more difficult for the cell to repair (Hall, 2000).

The 'absorbed dose' of radiation is measured in gray (Gy). It is the energy deposited by the radiation in a unit mass of matter, where 1Gy is equal to 1 Joule of energy absorbed per Kilogram of matter (Wakeford, 2004). Alternatively the 'effective dose' can be used, usually when comparing the effect of different radiation types. This is measured in Sievert (Sv) and allows the difference in ionisation density between high-LET and low-LET radiation, and so the consequential biological effect, to be taken into

account. In the case of low-LET radiations, 1Gy is equal to 1Sv. However, this varies for high-LET radiations such as α -particles, 1Gy of which is equal to 20Sv (Wakeford, 2004).

Throughout the course of the current project, X-rays were the sole source of IR. Therefore, the effect of exposure to low-LET radiation, and X-rays in particular, will form the focus of this thesis.

1.4.1 Interaction with biological matter

IR can cause both direct and indirect damage to cellular DNA. Direct damage is caused by interaction between the radiation and the DNA. Indirect damage is caused via interaction of the DNA with reactive species created through collision of the radiation with another molecule, such as water. The majority of the damage caused to DNA by low-LET IR occurs indirectly, as a result of hydroxyl radicals (OH*) generated by the interaction of IR with water (Breen and Murphy, 1995). The accepted approximate quantity of DNA damage produced in a single cell by 1Gy of low-LET ionising radiation is 1,000 DNA single strand breaks (SSBs), 40 DNA double strand breaks (DSBs), 150 DNA-protein crosslinks, >1,000 single base damages (Frankenberg-Schwager, 1990; Ward, 1988; Wouters and Begg, 2009). It is widely accepted that this damage is untargeted (Lorimore *et al*, 2003) and occurs within seconds after exposure (Joiner *et al*, 2009). Complex lesions can also be formed, in which multiple damages occur within the locality of a single site (Hall, 2000). This is frequently observed at DSBs, which are often accompanied by extensive base damage (Ward, 1985).

1.5 The response of mammalian cells to DNA damage

In response to DNA damage, mammalian cells may either undergo cell cycle arrest, apoptosis, or attempt to repair the DNA damage (Wouters and Begg, 2009). These protective mechanisms are described in sections 1.5.1 to 1.5.3 below. The cells used throughout this project were murine embryonic stem cells (mESCs). It is essential for ESCs to maintain genomic integrity, as any mutations that develop could subsequently affect the entire organism. Several differences therefore exist between the DNA damage responses employed by ESCs and somatic cells (Tichy and Stambrook, 2008; Maynard *et al*, 2008). These will be highlighted in the relevant sections (1.5.1 to 1.5.3).

1.5.1 Mammalian cell cycle regulation and checkpoints

The eukaryotic cell cycle can be divided into several phases, depicted in Figure 1-1. The two main phases are mitosis (M), during which the chromosomes are assembled and cell division occurs; and interphase, which can be subdivided into the G₁, S and G₂ phases. S phase is the fraction of the cell cycle during which DNA synthesis occurs. G₁ and G₂ are gap phases, which provide the cell with time to ensure the correct segregation of chromosomes after mitosis and the accurate replication of DNA, respectively (Pardee, 2002). The majority of mammalian somatic cells are not actively dividing and therefore reside in the quiescent (G₀) phase *in vivo* (White and Dalton, 2005). Quiescent cells can enter the cell cycle at G₁ phase, and depending on endogenous and exogenous stimuli, cycling cells can also exit the cycle, from G₁ to G₀ (Pardee, 2002). The cell cycle of mESCs, however, differs in several aspects from the classic somatic cell cycle. ESCs grown *in vitro* are continually proliferating, and

therefore a comparatively large proportion of the population reside in S phase. In addition, the G₁ and G₂ phases are reduced, resulting in a relatively short cell cycle time (Aladjem *et al*, 1998; Savatier *et al*, 2002). Furthermore, it is not possible to induce quiescence in ESCs without also initiating differentiation (Burdon *et al*, 2002).

Cell cycle regulation is achieved by periodic activation of various cyclin dependent kinase (CDK)-cyclin complexes, as shown in Figure 1-1. These, in turn, activate a number of downstream substrates, which drive the different cell cycle events. After completion of each cell cycle transition, the appropriate CDK-cyclin complex is inactivated by ubiquitin-mediated degradation of the cyclin subunit (Hall, 2000).

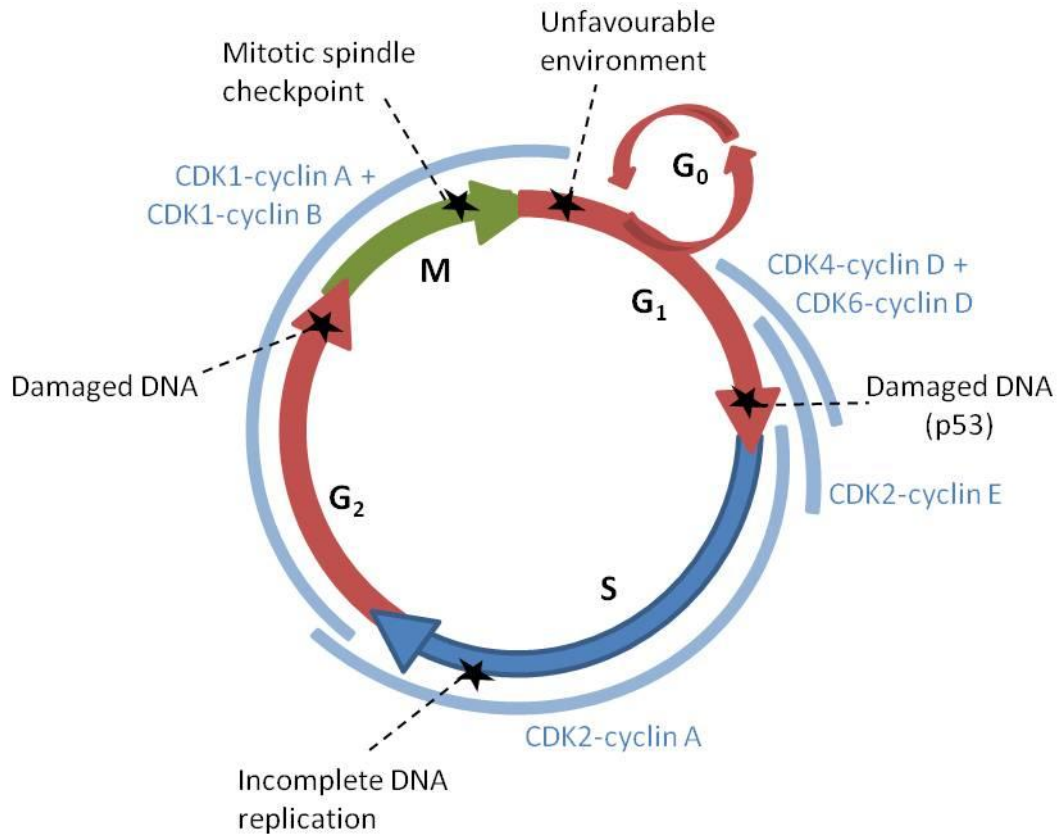


Figure 1-1. The mammalian somatic cell cycle and checkpoints. M, mitosis; G₁, gap phase 1; S, synthesis; G₂, gap phase 2; G₀, Gap phase 0 or quiescence. Checkpoints are indicated by black stars. The portions of the cell cycle mediated by the various CDK-cyclin complexes are indicated by the adjacent curved blue lines.

A number of cell cycle checkpoints exist in mammalian cells, which help to preserve genomic integrity. These are indicated in Figure 1-1. Two major checkpoints are activated in response to DNA damage (G₁/S and G₂/M) via a network of detection, signalling (ATM, ATR, CHK1+2), and effector (p53, p21, Cdc25, CDK) genes (Bartek and Lucas, 2001). In ESCs, however, the G₁ DNA damage checkpoint is not active (Aladjem *et al*, 1998; Hong and Stambrook, 2004). Activation of the G₁ checkpoint requires inhibition of CDK2 activity. This can occur via 2 pathways in somatic cells:

1. ATM/ATR activates Chk2/Chk1, which stimulates the degradation of Cdc25A (the protein that usually activates the CDK2-cyclin E complex). This is a rapid but transient response to DNA damage (Bartek and Lucas, 2001).
2. ATM or Chk2 activate and stabilise p53, thereby inducing expression of p21 (an inhibitor of CDKs). This response is slightly delayed due to the requirement for p21 threshold levels, but results in sustained G₁ arrest (Bartek and Lucas, 2001; Meek, 2004).

In mESCs, however, Chk2 is localised to the centrosomes instead of being diffuse within the nucleus as it is in somatic cells. Thus, it is unavailable to phosphorylate Cdc25A and stimulate its degradation (Hong and Stambrook, 2004). In addition, cytoplasmic p53 is inefficiently translocated to the nucleus in ESCs and as a result, levels of the CDK inhibitors p21 and p27 are undetectable (Aladjem *et al*, 1998). However, if ESCs are induced to differentiate, the G₁ phase becomes longer, and the G₁ DNA damage checkpoint is restored (Aladjem *et al*, 1998).

Activation of the G₂/M checkpoint requires inhibition of activation of CDK1-cyclin B. This is achieved in much the same pathway as activation of the G₁/S checkpoint (Vermeulen *et al*, 2003). However, whilst Chk2 appears to be of greater importance during the G₁/S checkpoint, Chk1 appears to be essential for activation of the G₂/M checkpoint in mammalian cells (Koniaras *et al*, 2001). As such, this checkpoint is functional in ESCs (Chuykin *et al*, 2008).

1.5.2 Apoptosis/Necrosis in response to IR

The main form of cell death after exposure to IR is mitotic catastrophe, as a result of cells attempting to divide with chromosome damage. However, programmed cell death/apoptosis can also remove damaged cells from the population (Hall, 2000). Activation and stabilisation of p53 in response to DNA damage involves inhibition of its main negative regulator (MDM2), allowing it to accumulate in the nucleus without being degraded. P53 is a transcription factor and, in addition to up-regulating genes involved in cell cycle checkpoint control, can induce the transcription of genes predisposing to cell cycle arrest (Cdc25, etc) or apoptosis (caspase 3, etc). However, no single gene product is solely responsible for the effects of p53. Rather, it is thought that the p53 pathway regulates the expression of genes leading to a certain outcome as a result of a complex feedback loop involving possibly hundreds of genes. Basically, if DNA repair has been successful the p53 response is reduced, allowing the cell to exit arrest. However, if the damage signals persist, the p53 response is maintained or promoted, sustaining the arrest and eventually leading to apoptosis (Meek, 2004 Fig.2).

Apoptosis is also thought to occur via p53 independent mechanisms, as seen in ESCs for example (Aladjem *et al*, 1998). In comparison to differentiated cells, ESCs have an increased propensity to undergo apoptosis in response to DNA damage (Roos *et al*, 2007). This is thought to be linked to the lack of a G1 checkpoint, as Hong and Stambrook (2004) have demonstrated that induction of the G1 checkpoint via ectopic expression of Chk2 protects ESCs from apoptosis. However, several studies also

indicate that the elevated apoptotic response of ESCs to DNA damage may partly be a result of elevated expression or activity of the MMR proteins (Claij and Riele, 2002; DeWeese *et al*, 1998; Roos *et al*, 2007).

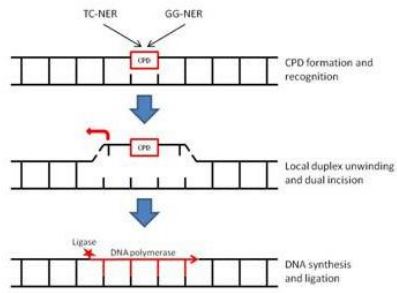
1.5.3 Mammalian DNA repair processes

Mammalian cells have evolved several different repair processes to cope with the multiple forms of DNA damage that can be induced by exposure to mutagens such as IR. Three of these repair pathways involve excision of the damaged/aberrant region from the DNA: Nucleotide Excision Repair (NER), Base Excision Repair (BER) and Mismatch Repair (MMR) (Maynard *et al*, 2008). These will be described first.

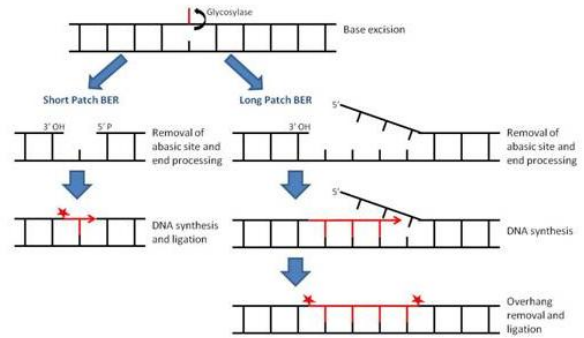
NER is used to remove a wide range of bulky, helix-distorting lesions such as UV-induced cyclobutane pyrimidine dimers (CPDs), which form between adjacent pyrimidine bases (Sinha and Häder, 2002) and can cause RNA polymerase II to stall (Protic-Sabljić and Kraemer, 1986). Roughly 30 proteins are involved in NER, including PARP1, ERCC1, and XPA, B, C, D, F and G. The proteins involved in the damage recognition step differ depending on whether the NER process is transcription-coupled (TC-NER) or part of the global genome repair process (GG-NER) that occurs in non-transcribed regions of the genome (Sinha and Häder, 2002). After recognition, the main steps of NER involve local duplex unwinding, dual incision of the DNA strand, DNA synthesis and ligation (Sinha and Häder, 2002) (see Figure 1-2). Defects in the NER genes cause several cancer-prone UV-sensitivity syndromes, such as Xeroderma Pigmentosum (Khan *et al*, 2009).

BER corrects non-bulky base modifications produced by oxidation (ie, 8-oxoguanine), alkylation and hydrolysis (ie, U resulting from deamination of C) (Krokan *et al*, 2002). Downstream elements of the BER machinery are also involved in the repair of DNA SSBs (Maynard *et al*, 2008; Sinha and Häder, 2002). The major enzymes in BER are the DNA glycosylases, which have the ability to cleave the bond between the altered base and the sugar residue and excise the damaged base, leaving an abasic site. There are several different DNA glycosylases that specifically recognise different kinds of base damage (Sinha and Häder, 2002). For example, Ogg1 recognises 8-oxoguanine (Radicella *et al*, 1997). After excision, the abasic site is cleaved and processed to create a 3' hydroxyl end from which DNA polymerase can extend. In short-patch BER, a single nucleotide is added and ligated. However, long-patch BER repair can also occur, wherein DNA polymerase synthesises multiple nucleotides, and the displaced overhang is removed by a flap endonuclease (Peterson and Côté, 2004). See Figure 1-2.

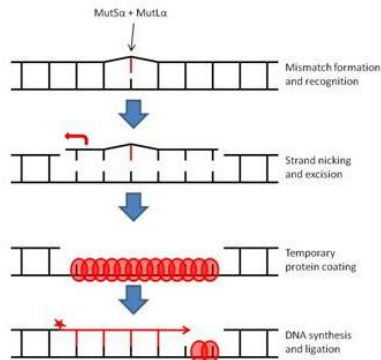
A. Nucleotide Excision Repair (NER)



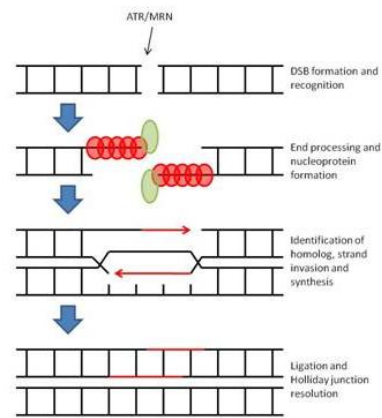
B. Base Excision Repair (BER)



C. Mismatch Repair (MMR)



D. Homologous Recombination (HR)



E. Non Homologous End Joining (NHEJ)

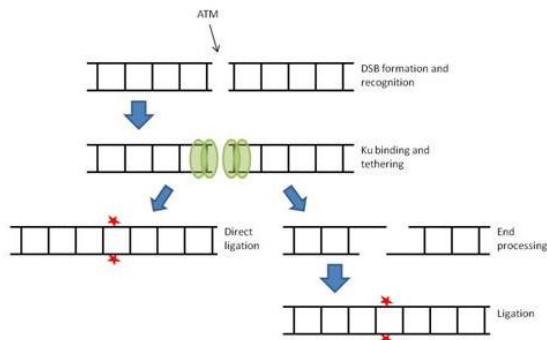


Figure 1-2. Diagrams illustrating the mammalian DNA repair pathways of Nucleotide Excision Repair (A); Base Excision Repair (B); Mismatch Repair (C); Homologous Recombination (D); and Non Homologous End Joining (E).

MMR is utilised by mammalian cells to correct errors that are incorporated into the newly synthesised strand during DNA replication. These include base-base mismatches formed as a result of the incomplete fidelity of DNA polymerases, and also

insertion/deletion loops created by misincorporation or strand slippage (Hsieh and Yamane, 2008). The precise mechanism of strand discrimination in mammals is not known, although DNMT1 has been implicated (see section 1.3). Recognition of mismatches is mediated by either of the MutS α or MutS β complexes, in combination with MutL α . Base-base mismatches and insertion/deletions of only 1 nucleotide are recognised primarily by MutS α , whilst larger insertion/deletions are recognised by MutS β . The mammalian MMR process remains largely undefined. Essentially, strand nicks are created on either side of the mismatch, and excision is carried out by EXO1 and other exonucleases which have not yet been identified. The resulting single-stranded gap is temporarily coated with a protein called replication protein A (RPA) before synthesis and ligation of the new strand occur (Hsieh and Yamane, 2008). See Figure 1-2. MMR deficiency frequently results in microsatellite instability, and has been shown to predispose to several forms of cancer (Buermeier *et al*, 1999; Jiricny and Nystrom-Lahti, 2000).

Single strand breaks (SSBs) are produced in high frequencies, as a result of actual damage to the DNA and also as intermediates during the repair of other forms of DNA damage. In proliferating cells, unrepaired SSBs can cause blockage or collapse of DNA replication forks, potentially leading to the formation of DSBs (Kuzminov, 2001) whilst in non-proliferating cells blockage of the transcription machinery could result in cell death (Kathe *et al*, 2004). SSBs are repaired readily using the opposite DNA strand as a template. The majority of radiation-induced SSBs are repaired within 20 minutes, and almost all within 2 hours, after exposure (van Loon *et al*, 1992) via a process that

involves the strand processing, DNA synthesis and ligation elements of the BER machinery (Caldecott, 2008). However, the formation of two SSBs either opposite each other, or separated by only a few base pairs, may lead to the formation of a DNA double strand break (Hall, 2000).

DNA double strand breaks (DSBs) are believed to be the most toxic lesions produced by IR (Valerie and Povirk, 2003). One of the main reasons for this is that DSBs can result in the formation of chromosome aberrations, potentially resulting in cell death or cancer (Bryant, 1984; Elliott and Jasin, 2002). In addition, the induction of cell killing correlates tightly with the induction of DSBs (Hall, 2000). Mutation or loss of the proteins involved in DNA DSB repair have been shown to lead to accelerated aging, genomic instability and carcinogenesis (Ham *et al*, 2006; Wong *et al*, 2003).

DNA DSBs are repaired using the non-homologous end joining (NHEJ) or homologous recombination (HR) pathways. In mammalian somatic cells, NHEJ is the major DSB repair mechanism. It is preferentially used during G1/G0 phases of the cell cycle, but is active in all phases, whilst HR occurs primarily in late S and G2 phases when sister chromatids are available (Rothkamm *et al*, 2003). In contrast, ESCs, which are continually proliferating and spend a greater proportion of the cell cycle time in S phase, primarily use HR for DNA repair (Adams *et al*, 2010; Tichy and Stambrook, 2008). The HR pathway enables high fidelity repair of DNA DSBs due to the use of a template sequence (Adams *et al*, 2010). NHEJ is considered to be more error-prone in comparison, due to small insertions and deletions introduced as a result of end

processing without the use of an undamaged template (Honma *et al*, 2007; van Attikum and Gasser, 2005).

DNA DSBs are detected by the ataxia telangiectasia mutated (ATM) and ataxia telangiectasia and RAD3-related (ATR) proteins (Cimprich and Cortez, 2008). One of the first events mediated by these proteins is the phosphorylation of the histone protein isoform H2AX to generate γ H2AX (Rogakou *et al*, 1998). This modification is thought to aid in the recruitment of other DSB repair proteins, including those that contribute to the formation of a more accessible chromatin structure (Paull *et al*, 2000; van Attikum and Gasser, 2005). It is also commonly used as a marker for the presence and repair of DSBs (Rogakou *et al*, 1999; Lassmann *et al*, 2010).

A comprehensive review of the processes and proteins involved in HR and NHEJ can be found in Hartlerode and Scully (2009). Essentially, HR involves processing of the free 5' ends of the DSB by the MRN complex (Mre11, Rad50, Nbs1) to produce long single-stranded 3' tails. These tails are temporarily coated with RPA and form nucleoprotein structures with Rad51, Rad52 and several other proteins, which function to locate a homologous sequence with which to align. When a homolog is found, strand invasion and DNA synthesis occur, followed by ligation. Finally, resolution of the Holliday junction restores the DNA template structure. BRCA1 and BRCA2 play various roles throughout the HR process, including anchoring, coordinating and loading the various proteins involved (Kinner *et al*, 2008; Peterson and Côté, 2004; Valerie and Povirk, 2003). See Figure 1-2.

Single-strand annealing (SSA) is an alternative form of HR, in which homologous sequences occurring on the resected 3' ends are aligned. After synthesis (gap filling) the 5' overhangs are removed by the FEN-1 endonuclease, and the strands are ligated. This mechanism frequently results in deletions (Kinner *et al*, 2008; Peterson and Côté, 2004).

NHEJ is mechanistically a much simpler process than HR in terms of the number of steps required. Essentially, it involves binding of the Ku heterodimer and recruitment of DNA-PKcs to the two broken ends, which tethers them together. If the ends are compatible, this is followed by direct ligation. Alternatively, end processing by artemis and/or the MRN complex occurs to remove any damaged bases, followed by ligation (Adams *et al*, 2010; Kinner *et al*, 2008; Peterson and Côté, 2004; Valerie and Povirk, 2003). See Figure 1-2.

Finally, inter-strand cross-links are also highly toxic lesions in which the two strands of DNA are covalently linked together by a chemical. Such damage results in blockage of DNA replication and transcription. The mechanism responsible for the repair of inter-strand cross-links in mammalian cells is poorly understood. However, it is accepted to occur via the generation of a DSB intermediate. Essentially, the damage is recognised and incision occurs near the cross-link, producing a DSB, which could then undergo several forms of processing. HR is thought to be a primary mechanism involved in cross-link repair, due to the involvement of the Fanconi Anaemia (FA) pathway, and the putative role of ERCC1 in processing (trimming) of overhanging DNA ends in order to promote strand invasion and non-allelic HR (McCabe *et al*, 2009). However, NER and

translesion DNA synthesis have also been implicated in cross-link repair (De Silva *et al*, 2000; Zheng *et al*, 2003). Models have been suggested for a single unified pathway (Niedernhofer *et al*, 2005). However, it is also possible that several independent pathways for cross-link repair exist in mammals (McCabe *et al*, 2009).

The mutation frequency at specific loci and the frequency of mitotic recombination are approximately 100-fold lower in mESCs than in adult somatic cells or mouse embryonic fibroblasts (MEFs) (Cervantes *et al*, 2002; Hong *et al*, 2007). This is partly due to the increased propensity for ESCs to undergo apoptosis (Tichy and Stambrook, 2008; de Waard *et al*, 2003). However, it is also partly due to differences in DNA repair. A study by Maynard *et al* (2008) found that several types of DNA damage, including oxidative damage, SSBs and DSBs, and inter-strand cross-links, were repaired more efficiently in hESCs than fibroblasts and HeLa cells. Correspondingly, endogenous levels of 8-oxoG were significantly lower in untreated hESCs than fibroblasts. Analysis of gene expression revealed that several of the genes involved in BER, NER, DSB repair and crosslink repair were up-regulated in hESCs in comparison to embryo bodies (hEBs), especially after exposure to DNA damage (Maynard *et al*, 2008).

Similar findings were observed in a study by Saretzki *et al* (2004) in which mESCs were shown to possess superior antioxidant capacity compared with various mEBs and embryonic fibroblasts. Differentiation of the cell lines, however, resulted in decreased antioxidant capacity, increases in cellular ROS levels and frequency of γ H2AX foci, and decreased expression of several DNA repair genes (Saretzki *et al*, 2008). Thus, it has been proposed that ESCs exhibit more rigorous responses to DNA damage than

differentiated cells (Hong *et al*, 2007; Maynard *et al*, 2008; Saretzki *et al*, 2008; Tichy and Stambrook, 2008).

1.6 Radiosensitivity and DNA methylation

In clinical studies, the relative radiosensitivity of different tissues is reflected by their radiation tolerance doses. This is the maximum cumulative dose of radiotherapy fractions associated with an “acceptable complication probability” of 1-5% (Joiner and van der Kogel, 2009). Clinical data demonstrates a wide range of sensitivities to ionising radiation in different tissue types (Dörr, 2009). Although there are exceptions to the trend, tissues with low methylation levels and high proliferative capacity, such as bone marrow, testis and ovary generally have low tolerance doses to radiation (1.5-4Gy). More heavily methylated tissues which have lower capacity for self-renewal, such as cerebrum and spinal cord, have much higher tolerance doses (55Gy and 35Gy respectively) (Dörr, 2009 table 13.2). Thus, there is an apparent inverse correlation between methylation levels and radiosensitivity in somatic tissues. There are, however, some exceptions to this trend, such as lung, which is more radiosensitive than predicted.

Interestingly, studies of Japanese Atomic bomb survivors reveal that people exposed to acute doses of whole body ionising radiation have a notable excess relative risk (ERR) of developing leukaemia compared to solid cancers (ERR at 1Sv for leukaemia incidence is 4.4 compared to <2 for solid cancers) (Wakeford, 2004). Furthermore, within the leukaemia subcategory, the highest Excess Absolute Risk (EAR) is observed

for acute myeloid leukaemia (AML) (Dainiak, 2002). AML is believed to be a malignancy of the bone marrow haemopoietic stem cells (HSCs) (Dainiak, 2002), whilst B- cell leukaemias and thymic lymphomas arise from committed lymphoid progenitor cells that are slightly more differentiated and less proliferative than HSCs (Metcalf, 1990). Furthermore, previous work within our laboratory has demonstrated that DNA methylation levels tend to increase with increasing haemopoietic differentiation (Giotopoulos *et al*, 2006). Thus, not only is bone marrow indicated as being one of the most hypomethylated and radiosensitive tissues in the adult human body (Ehrlich *et al*, 1982; Gama-Sosa *et al*, 1983; Van der Kogel, 1993), but within the bone marrow itself, the HSC compartment displays increased radiosensitivity in comparison to the committed progenitor cells (Lorimore *et al*, 1990), and increased susceptibility to malignant transformation (Dainiak, 2002).

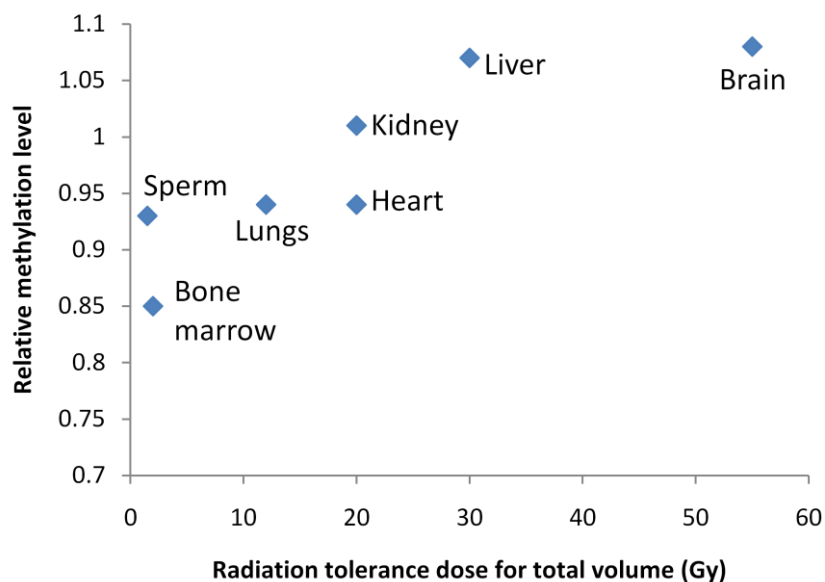


Figure 1-3. Scatter graph illustrating the correlation between DNA methylation level and tissue radiosensitivity as reflected by the radiation tolerance dose. Methylation

data is taken from Giotopoulos et al (2006) and is expressed relative to spleen, which was assigned a methylation value of 1. Radiosensitivity data is taken from Dörr (2009).

Several *in vitro* studies indicate a similar inverse correlation between aberrantly reduced methylation levels and increased sensitivity to ionising radiation in human cell lines. For example, lymphocyte cell lines from patients with ICF syndrome, which are hypomethylated at various genomic repeat sequences, display elevated radiosensitivity in comparison to lymphocytes from unaffected individuals (Narayan *et al*, 2000). In addition, Zebularine-induced genome-wide DNA hypomethylation has been shown to enhance tumour cell radiosensitivity in comparison to untreated tumour cells (Dote *et al*, 2005).

The sensitivity of cell lines to IR is most often assessed *in vitro* using the clonogenic assay. This provides a measure of the surviving fraction of cells in response to a specific dose of IR, and reflects the extent of reproductive cell death in addition to immediate cell killing (Hall, 2000). Survival curves for most mammalian cells exposed to low LET radiation such as X-rays show downward curvature, and can be described according to a linear-quadratic correlation: $SF = \exp(-\alpha D - \beta D^2)$ where SF is the surviving fraction of cells at a given dose D, and α and β are constants representing the degree of curvature. The initial slope in the low dose region, the shoulder of the curve (α), is thought to reflect decreases in SF resulting from single lethal events. The exponential section of the curve (β) in the higher dose region is thought to reflect decreases in SF resulting from the accumulation of multiple sub-lethal events (Hall, 2000). Linear survival curves without any shoulder are usually only obtained with high LET radiation. In such instances, the relationship between the surviving fraction and the dose can be

described by D_0 (the mean lethal dose). D_0 is the dose of radiation which produces on average one lethal event per cell and in so doing reduces the SF to 37% (Hall, 2000).

Numerous other factors are known to affect cellular radiosensitivity. For example, cells are generally most radiosensitive in the G_2/M phase of the cell cycle and least sensitive during the latter part of S phase (Pawlik and Keyomarsi, 2004). In addition, the level of available radical scavengers to mop up ROS, and the supply of oxygen itself can modulate cellular radiosensitivity. Such an effect is observed in tumours, whereby cells surrounding the blood vessels that have high oxygen levels are often killed in response to radiotherapy. Meanwhile, the cells more distant from the blood vessels, which are under conditions of hypoxia, are often found to be radio-resistant (Höckel and Vaupel, 2001; Rofstad *et al*, 2000). As such, the expression levels of hypoxia associated genes, such as HIF1 α , are useful markers for the progression of certain cancers and may be promising therapeutic targets to increase tumour radiosensitivity (Griffiths *et al*, 2007).

1.7 Radiation-induced delayed genomic instability

Genomic instability can manifest as many biological endpoints, such as gene mutations, lethal mutations, cytogenetic aberrations, micronucleus formation and minisatellite, microsatellite and ESTR mutations (Barber *et al*, 2006; Dubrova *et al*, 2002; Kadhim *et al*, 1995; Little *et al*, 1997; Maluf and Erdtmann, 2001; Mothersill *et al*, 1998; Uchida *et al*, 1994). Radiation-induced delayed genomic instability is characterised by the persistent expression of elevated levels of such (non-clonal) markers at a delayed period after irradiation, which are detected in the unirradiated

progeny of the irradiated cells (Morgan, 2003) or animals (Barber *et al*, 2006) several generations after irradiation (Huang *et al*, 2004).

The mechanism by which radiation-induced delayed genomic instability is propagated is currently poorly understood (Wright, 2010). However, it is a genome-wide process (Li *et al*, 1992; Grosovsky *et al*, 1996) and does not appear to arise from mutation of genes involved in genome maintenance (Lorimore *et al*, 2003; Kaup *et al*, 2006). Such mutations, caused by mis-repair of radiation-induced DNA damage, would be expected to manifest at the time of irradiation rather than at an arbitrary delayed period after (Kaup *et al*, 2006). Furthermore, gene mutations would be inherited and segregate in a mendelian fashion in the progeny of the irradiated animal, whilst in cells the effect would be clonal and all progeny would exhibit the same mutation as the original parental cell (Lorimore *et al*, 2003). In contrast, several research groups have shown that radiation-induced delayed genomic instability manifests in a non-clonal manner in clonal cell populations (Kadhim *et al*, 1994; Grosovsky *et al*, 1996). Furthermore, significantly elevated mutation rates were observed in the germline and somatic cells of the majority of the F1 and F2 offspring of every irradiated F0 male mouse (Barber *et al*, 2002; Barber *et al*, 2009). The lack of phenotypic segregation through the generations indicates non-mendelian inheritance of radiation-induced delayed genomic instability. Moreover, it is highly unlikely that the same genes would be affected, resulting in similar phenotypes, in the offspring produced from different paternally irradiated mice (Dubrova *et al*, 2003). Thus, it is thought that radiation-

induced delayed genomic instability is propagated through an epigenetic mechanism (Dubrova *et al*, 2003; Wright, 2010).

Several processes have been suggested as possible causes of radiation-induced delayed genomic instability, including inflammatory type responses resulting in oxidative stress (Clutton *et al*, 1996; Lorimore *et al*, 2003) and alterations in the balance of epigenetic factors such as DNA methylation (Dubrova *et al*, 2003; Kaup *et al*, 2006; Koturbash *et al*, 2005).

Cells are subjected to oxidative stress when the natural balance of antioxidant and pro-oxidant chemical species becomes imbalanced (Clutton *et al*, 1996). Normal cellular metabolism and extracellular processes, such as secretion of cytokines from nearby damaged cells (Lorimore *et al* 2003), both result in the production of highly reactive oxygen species (ROS), which have the potential ability to damage DNA (Cao and Wang, 2007). Saturation of the cellular defences to oxidative damage by exposure of cells to high extracellular levels of ROS has been shown to result in cytogenetic instability (Duell *et al*, 1995; Emerit and Cerutti, 1981). In addition, cultures of cells derived from gamma-irradiated bone marrow have been found to display increased activation of pathways that produce ROS (such as lipid peroxidation) and increased base oxidation, DNA fragmentation and cell death, in comparison to cultures derived from unirradiated bone marrow (Clutton *et al*, 1996). Furthermore, cells irradiated in the presence of free radical scavengers were found to display reduced frequencies of chromosome instability compared to cells irradiated in the absence of scavengers (Limoli *et al*, 2001). Thus, it has been proposed that the persistent elevation of ROS

found in the progeny of irradiated cells may be one mechanism leading to the molecular events responsible for radiation-induced delayed genomic instability (Clutton *et al*, 1996; Limoli *et al*, 2001; Limoli *et al*, 2003).

However, it has been argued that elevated levels of ROS are unlikely to lead to the transgenerational instability observed in animal studies (Dubrova, 2003), due to the minimal cytoplasmic content of mature sperm and its spatial separation from the nucleus (Cooper *et al*, 2004). Given that the trans-generational instability observed in the studies by Dubrova *et al* (1998; 2002) was inherited paternally, the factor(s) responsible for propagating radiation-induced delayed genomic instability must be transmissible from the sperm to the zygote. As a DNA-associated factor, DNA methylation is a suitable candidate for such transmission and potential propagation of the radiation memory (Dubrova *et al*, 2003).

Mammalian gametes, particularly sperm, contain significant levels of DNA methylation (Howlett and Reik, 1991; Oswald *et al*, 2000). However, global levels of DNA methylation decrease upon fertilization. The paternal genome is demethylated within a few hours via an active process, prior to the first round of DNA replication (Mayer *et al*, 2000; Oswald *et al*, 2000) whilst the maternal genome becomes demethylated in a passive manner during subsequent cleavage divisions (Howlett and Reik, 1991; Mayer *et al*, 2000). Nevertheless, some imprinted genes and repetitive elements, such as IAP retrotransposons and centric and pericentric heterochromatin, remain methylated in the paternal and maternal genomes throughout both of these de-methylation processes (Lane *et al*, 2003; Reik and Walter, 2001; Rougier *et al*, 1998; Santos *et al*,

2002). Thus, it is possible that aberrant methylation patterns established at such regions in the gametes of the irradiated paternal mouse could be transmitted and contribute, at least in part, to the observed transgenerational instability (Dubrova, 2003).

Indeed, reduced global methylation levels have been observed in thymus tissue in the offspring of irradiated mice, accompanied by decreased levels of the DNA methyltransferases and the methyl-CpG-binding protein MeCP2, and significant accumulation of DNA strand breaks (Koturbash *et al*, 2006). Furthermore, several research groups have shown that the offspring of irradiated male mice have persistently altered patterns of gene expression, including genes encoding cytokines involved in haematopoiesis, immunity and neoplasia (Daher *et al*, 1998), and genes encoding proteins involved in the regulation of cell proliferation, such as protein kinase C, MAP kinase, p53 and p21 (Baulch *et al*, 2001; Vance *et al*, 2002). In addition, significant increases in DNA damage detected by the comet assay have been observed in somatic tissues in the F1 and F3 offspring of paternally irradiated F0 mice (Barber *et al*, 2006; Vance *et al*, 2002). And Daher *et al* (1998) found that the offspring of paternally irradiated mice had an increased risk of developing leukemia/lymphoma compared to the offspring of unirradiated mice (Daher *et al*, 1998).

Several studies have generated data which indicates that ionising radiation can itself induce persistent reductions of DNA methylation in the radiation target tissue *in vivo* (Giotopoulos *et al*, 2006; Koturbash *et al*, 2005; Kovalchuk *et al*, 2004; Pogribny *et al*, 2004; Tawa *et al*, 1998). In some instances this has been coupled with a reduction in

expression levels of the DNA methyltransferases (Raiche *et al*, 2004) and the methyl-binding protein MeCP2 (Loree *et al*, 2006). It has also been correlated with increased levels of DNA strand breaks following the initial exposure (Koturbash *et al*, 2005; Pogribny *et al*, 2004). However, the occurrence of radiation-induced DNA hypomethylation is sex- and tissue- specific (Pogribny *et al*, 2004; Tawa *et al*, 1998), and also appears to be genotype-dependent (Giotopoulos *et al*, 2006). Possible mechanisms responsible for radiation-induced DNA hypomethylation are discussed in section 1.7.1. Previous work from our lab has shown that the CBA/H mouse strain exhibits radiation-induced hypomethylation of the bone marrow 10-14 days after 3Gy X-irradiation, whilst C57BL/6 mice do not (Giotopoulos *et al*, 2006). Interestingly, susceptibility to radiation-induced chromosomal instability is also strongly influenced by genetic factors (Watson *et al*, 1997) with CBA/H and BALB/c mice being susceptible whilst C57BL/6 mice are relatively resistant (Ponnaiya *et al*, 1997; Watson *et al*, 2001). Chromosomal instability is one of the most well documented forms of radiation-induced genomic instability. As such, it will be described further in section 1.7.2.

1.7.1 Mechanisms of radiation-induced DNA hypomethylation

Several potential mechanisms have been proposed as possible causes of radiation-induced DNA hypomethylation. Kalinich *et al* (1989) observed persistent DNA hypomethylation in a Chinese hamster lung fibroblast cell line 24 to 72 hours after exposure to gamma radiation, which correlated with decreased activity of the DNA methyltransferases in the nucleus and increased activity in the cytoplasm. The authors therefore suggested that radiation-induced hypomethylation may be caused by

redistribution of the DNMTs to the cytoplasm, resulting in passive demethylation during subsequent rounds of cell division (Kalinich *et al*, 1989). However, the reductions in methylation level observed by Pogribny *et al* (2004), Koturbash *et al* (2005) and Tawa *et al* (1998) occurred within 6-8 hours after exposure, and it is unlikely that significant cell division occurred during this time (Pogribny *et al*, 2004).

Another proposed mechanism for radiation-induced DNA hypomethylation is via the action of an active DNA demethylation enzyme(s) (Pogribny *et al*, 2004), similar to the putative demethylases involved in the reprogramming of the paternal genome shortly after fertilisation and of primordial germs cells during embryogenesis (Hajkova *et al*, 2010; Mayer *et al*, 2000; Oswald *et al*, 2000). Several different mechanisms have been proposed by which active DNA demethylation could occur, including direct removal of the methyl group to leave an unmethylated CpG (Bhattacharya *et al*, 1999); direct excision of methylcytosine via base excision repair (BER) (Zhu *et al*, 2000); deamination of methylcytosine to thymine followed by BER of the T-G mismatch (Hendrich *et al*, 1999; Morgan *et al*, 2004; Rai *et al*, 2008); nucleotide excision repair (NER) (Barreto *et al*, 2007; Schmitz *et al*, 2009); oxidative demethylation (Cannon *et al*, 1988; Ito *et al*, 2010); and radical S-adenosylmethionine (SAM)-based demethylation (Okada *et al*, 2010).

These mechanisms are reviewed fully in Wu and Zhang (2010). Essentially, no single process has yet been identified which is solely responsible for the DNA demethylation observed in the paternal genome post fertilization (Santos *et al*, 2002; Santos and Dean, 2004; Wu and Zhang, 2010). Rather, it appears a combination of several may

occur. Furthermore, demethylation mechanisms may vary between different cell/tissue types (Hajkova *et al*, 2010), and may depend on the stimulus for demethylation (Wu and Zhang, 2010). With regard to radiation-induced hypomethylation, active demethylation mechanisms involving the DNA repair machinery are favoured (Pogribny *et al*, 2004), as ionising radiation induces a wide variety of DNA lesions (Frankenberg-Schwager, 1990).

1.7.2 Radiation-induced chromosomal instability

Induced chromosome instability is defined as “the ongoing production of *de novo* aberrations in cell cycles subsequent to clastogenic treatment” (Kadhim *et al*, 1992). Ionising radiation can produce structural aberrations at all stages of the cell cycle, giving rise to both primary chromosome-type and chromatid-type aberrations (Savage, 1980). >90% of IR-induced DSBs are rejoined in their original configuration. The remainder either remain unrepaired, leading to the appearance of gaps, breaks and deletions, or undergo aberrant rejoining with free ends from other DSBs resulting in exchanges between different chromosomes (Hall, 2000; Savage, 1976; Savage 1999). Such interactions are thought to be influenced by the degree of intermingling that occurs between different chromosomes at the edges of their nuclear territories (Branco and Pombo, 2006) or in the inter-chromatin space (Cremer and Cremer, 2001).

In a proliferating cell culture, the population analysed at delayed periods after IR exposure reflects the progeny of the survivors. Chromatid-type aberrations are converted to chromosome-type aberrations during subsequent rounds of cell division. Therefore, the occurrence of ongoing chromosomal instability is indicated by the

presence of a persisting chromatid-type aberration frequency on a background of chromosome-type aberrations (Kadhim *et al*, 1995; Savage, 1999). The most reliable method for observing chromosome instability induced by IR involves the analysis of all visible metaphases comprising a colony derived from a single irradiated cell. This method permits identification of the directly induced aberrations and allows their discrimination from *de novo* non-clonal aberrations which have developed subsequently over the course of colony growth. It also allows determination of the mutation rate (Kadhim *et al*, 1995).

However, IR-induced delayed chromosomal instability can also be identified in non-clonal cell populations, indicated by an elevated frequency of asymmetrical or complex aberrations on a background of symmetrical, transmissible aberrations. Asymmetrical aberrations are those which result in the loss of genetic material (Savage, 1975). These often produce mechanical separation problems during mitosis and as a result, are usually lethal for the cell (Savage, 1980). For this reason, most complex exchanges (those involving three or more breaks in two or more chromosomes) (Savage, 2002) are also non-transmissible. Thus, the continued presence of elevated levels of asymmetrical and complex aberrations at a delayed period post irradiation is indicative of ongoing genomic instability (Kadhim *et al*, 1995). Most “symmetrical” aberrations, however, are transmissible through mitosis (Savage, 1999; Anderson *et al*, 2003). As such, their presence is only indicative of ongoing instability in clonally expanded cell populations, in which the accumulation of *de novo* aberrations can be observed (Kadhim *et al*, 1995).

High LET radiations, such as α -particles, are efficient inducers of both delayed chromosomal instability and gene mutations (Harper *et al*, 1997; Kadhim *et al*, 1992; Kadhim *et al*, 1995; Kadhim and Wright, 1998). However, low LET radiations such as X-rays appear to be comparatively inefficient inducers of chromosomal instability (Kadhim *et al*, 1992). Conflicting reports have been published, some of which indicate that whilst low LET radiations are able to cause delayed gene mutations, the induction of delayed higher-order cytogenetic effects requires a property specific to high LET radiations (Harper *et al*, 1997). Meanwhile, numerous other research groups have found that X-rays are in fact capable of inducing delayed cytogenetic instability (Holmberg *et al*, 1993; MacDonald *et al*, 2001; Marder and Morgan, 1993).

These contradictory findings could be a result of many factors, including differences in the methodology (clonal or non-clonal) (Kadhim *et al*, 1995), the detection methods (solid staining, banding or FISH), the end points scored (apoptosis, non-transmissible aberrations, translocations or total aberrations), and the growth conditions, culture periods and cell proliferation rates. Finally, the radiation response of delayed chromosomal instability is thought to be dependent upon the cell type and its genetic characteristics (Ponnaiya *et al*, 1997; Watson *et al*, 1997).

1.7.3 The role of telomeres in maintaining genomic stability

Mammalian telomeres consist of arrays of TTAGGG repeats that range in length from approximately 2 to 20kb in humans (Royle *et al*, 2009) and 25 to 40kb in mice (Blasco, 2005), depending on the cell type and extent of proliferation (Wright and Shay, 2005). Telomeres function to cap the terminal 3' single stranded ends of chromosomes by

folding the G-rich overhang back and inserting it into the duplex telomeric DNA, where it pairs with the C-rich strand, to form a protective D-loop. This structure is reinforced by the binding of a group of telomeric proteins, which form the shelterin complex (de Lange, 2005), and protects the telomeric chromosome ends against degradation by exonucleases, chromosomal fusion and recombination (Hockemeyer *et al*, 2005; Lei *et al*, 2005; Yang *et al*, 2005).

Each time a normal mammalian somatic cell divides telomeric repeats are lost partly due to the inability of DNA polymerase to replicate the end of the lagging strand (Shay and Wright, 2005; Watson, 1972). When the telomere length becomes critically short, the protection afforded by shelterin is lost (de Lange, 2005), leading to cellular senescence (Baird *et al*, 2003). Critically short or dysfunctional telomeres are recognised as DNA DSBs by the DNA damage response machinery, resulting in the formation of repair foci (d'Adda di Fagagna *et al*, 2003; van Steensel *et al*, 1998). Repair of such apparent DSBs by NHEJ results in chromosome fusion (Artandi *et al*, 2000; Espejel *et al*, 2002; de Lange, 2005; van Steensel *et al*, 1998), which causes breakage-fusion-bridge cycles and increasing cytogenetic instability (Lo *et al*, 2002; Royle *et al*, 2009).

Interestingly, many of the premature ageing and chromosomal instability syndromes, such as Ataxia telangiectasia (*ATM*), Werner (*WRN*) and Bloom syndrome (*BLM*) and Fanconi anaemia (*FANC* genes), are a result of mutations in DNA repair or cell-cycle checkpoint proteins which interact with the shelterin protein TRF2. As a result they are often characterised by an accelerated rate of telomere shortening (Blasco, 2005).

Some cells avoid telomere shortening by activating the enzyme telomerase. Telomerase is an enzyme complex consisting of a reverse transcriptase (TERT) and a template RNA (TERC) that includes the complementary sequence to the TTAGGG repeats. It is able to add new repeats to the chromosome ends to offset the degradation that occurs with each cell division (Blasco, 2005). Normal human somatic cells do not express telomerase (Harley, 1991; Hayflick, 1965 and 1997). However, ESCs display high levels of telomerase activity that is down-regulated during differentiation (Armstrong *et al*, 2005). Germ cell and adult stem cells in self-renewing tissues also express low levels of telomerase, which is upregulated during periods of rapid proliferation (Haik *et al*, 2000; Hiyama and Hiyama, 2007). Finally, virtually all human tumour cell lines and approximately 90% of human cancer biopsy specimens exhibit telomerase activity (Calcagnile and Gisselsson, 2007).

Some immortal and cancer cell lines do not express telomerase and instead maintain telomere length via an alternative mechanism (ALT) (Murnane *et al*, 1994; Royle *et al*, 2009). The telomeres in ALT cell lines display large variations in length, due to the occurrence of events that cause sudden elongation or shortening. They also display single stranded regions (Henson *et al*, 2002; Jeyapalan *et al*, 2008; Nabetani and Ishikawa, 2009). ALT is thought to be driven by recombination-like processes (Dunham *et al*, 2000) and is dependent on the expression of genes required for HR (Lundblad and Blackburn, 1993).

It has been demonstrated that the repressive heterochromatic marks which characterise the telomeric and sub-telomeric DNA regions, in addition to DNA

methylation of the sub-telomeric region, are lost as a consequence of telomere shortening (Benetti *et al*, 2007). Conversely, several studies have demonstrated that loss of repressive histone modifications at the sub-telomeric regions coincides with aberrant telomere elongation (Garcia-Cao *et al*, 2002; Garcia-Cao *et al*, 2004; Gonzalo *et al*, 2005). Thus, it has been proposed that the heterochromatic marks present in the telomeric and sub-telomeric regions may act as negative regulators of telomere elongation (Gonzalo *et al*, 2006).

A study by Gonzalo *et al* (2006), using the same mESCs studied in this project, demonstrated that absence of DNMT1 or DNMT3A and DNMT3B results in the generation of abnormally long telomeres, greater heterogeneity in telomere length than wild type cells, and an increased frequency of telomeric sister chromatid exchanges (T-SCEs). Furthermore, the number of long telomeres was found to increase with passage number in the *Dnmt3a3b*^{-/-} cell line (Gonzalo *et al*, 2006), which progressively loses methylation with increasing passage number (Jackson *et al*, 2004). These observations were not accompanied by alterations in the levels of histone modifications, protein binding or telomerase activity (Gonzalo *et al*, 2006). Thus, the effects observed were attributed directly to DNA hypomethylation. The possibility that gene expression was affected was not ruled out. However, it was proposed that DNA methylation, or heterochromatic modifications, are independent regulators forming part of a negative feedback loop to regulate telomere length, either via stimulation of an ALT-based mechanism, or by permitting increased access of telomerase or other proteins to the telomere (Blasco, 2005; Gonzalo *et al*, 2006).

1.8 Project Rationale and aims

Evidence indicates that radiation-induced genomic instability may be mediated by an epigenetic mechanism (Dubrova *et al*, 2003; Wright, 2010). Aberrantly reduced methylation levels have been associated with elevated genomic instability (Tuck-Muller *et al*, 2000; Symer *et al*, 2002) and increased radiosensitivity (Dote *et al*, 2005). Additionally, radiation has itself been shown to alter methylation levels, indicating a role for aberrant DNA methylation in promoting radiation induced genomic instability (Koturbash *et al*, 2006). Nevertheless, the molecular basis for the development and propagation of radiation induced delayed genomic instability is not thoroughly understood (Dubrova *et al*, 2003; Wright, 2010).

This project aimed to investigate the apparent correlations between DNA hypomethylation, radiosensitivity and genomic instability. A murine embryonic stem cell system was used, allowing analysis of the impact of complete inactivation of each of the three main active mammalian DNA methyltransferase enzymes (DNMT1, DNMT3A and DNMT3B), and providing a range of states of hypomethylation. The global methylation levels of the ESC lines were characterised in unirradiated cells, and at several time points post irradiation with 3Gy X-rays using HPLC. The proliferation rates and cell cycle characteristics of each cell line were also determined (chapter 3). The ESCs were then investigated for differences in radiosensitivity using the clonogenic assay (chapter 3) and, genomic stability was assessed both at the *Hprt* gene locus (chapter 4) and on a genome-wide scale using the comet assay and cytogenetic analysis (chapter 5). Finally, the spectrum of mutations observed was characterised in

an attempt to determine the mutational mechanisms that may be occurring (chapters 4 and 5).

2 Chapter 2. Methods and Materials

2.1 Chemicals and Reagents

All routinely used buffers and solutions were prepared as described in Table 2-1 and stored at room temperature unless stated otherwise. All chemicals and reagents were analytical grade or higher, supplied by Amersham Biosciences, Chemos, Fisher Scientific, Invitrogen, Lonza, Millipore, New England Biolabs, Perkin Elmer, Qiagen, Roche Diagnostics, Sera Laboratories International, Sigma Aldrich, Sigma Life Sciences, and VWR International.

The following Kits were used: ABI Prism BigDye Terminator v3.1 Cycle Sequencing Kit (Applied Biosystems); EZ-PCR Mycoplasma Test Kit (Geneflow Ltd); QIAprep Maxiprep Kit, QIAprep Miniprep Kit, QIAquick Gel Extraction Kit, QIAamp DNA Mini Kit, QIAamp DNA Micro Kit (Qiagen Ltd), Random Primer DNA Labelling System (Invitrogen), Rediprime II Random Primer Labelling System (Amersham); TOPO TA cloning kit with One Shot Competent *E.Coli* (Invitrogen); and XL10-Gold Ultracompetent Cells (Stratagene).

DNA ladders used were Hyperladders I-V (Bioline), lambda-hind III, Phi X HaeIII, 1kb and 50bp DNA ladders (NEB), and FullRanger 100bp ladder (Norgen Biotek Corp).

Table 2-1. Stock solutions used.

Solution	Preparation
10x Kinase Mix	700mM Tris-HCl (pH7.5), 100mM MgCl ₂ , 50mM spermidine trichloride, 20mM dithiothreitol. Store at -20°C.
10x TBE	44.5mM Tris-borate (pH8.3), 1mM EDTA.
10xTE	100mM Tris-HCl (pH8.0), 10mM EDTA.
11.1x PCR Buffer	167µl 2M Tris-HCl [pH 8.8], 83µl 1M NH ₄ 2SO, 33.5µl 1M MgCl ₂ , 3.6µl β-mercaptoethanol, 3.4µl 10mM EDTA [pH 8.8], 75µl of each 100mM dNTP, and 85µl 10mg/ml BSA. Aliquot and store at -20°C.
20x SSC	3M NaCl, 0.3M Tri-Sodium Citrate.
20% SDS	100g SDS dissolved in 500ml dH ₂ O. Heat to 37°C to dissolve.
Ampicillin	10mg/ml (dissolved in dH ₂ O). Store at -20°C.
Church Buffer	250ml 14% SDS, 250ml NaHPO ₄ , 1ml 0.5M EDTA (pH8.0). Filter (0.4µm, Acrodisc) and store as aliquots at -20°C.
Column Wash	1xTE, 0.1% SDS (pH7.5)
Comet Assay Alkali electrophoresis buffer	300mM NaOH, 1mM Na ₂ EDTA. Final volume 2L with cold dH ₂ O. pH13. Make on day of use.
Comet Assay Enzyme Reaction Buffer (ERB)	40mM HEPES, 0.1M KCl, 0.5mM Na ₂ EDTA, 0.2mg/ml BSA. Final volume 1L with dH ₂ O. Adjust to pH8.0 with 2M KOH. Make day prior to use.
Comet Assay Lysis Buffer	2.5M NaCl, 100mM Na ₂ EDTA, 10mM Tris-HCl. Final volume 1L with dH ₂ O. Set pH to 10.0 with 10M NaOH. Store at 4°C. Add 1% Triton X-100 prior to use.
Comet Assay Neutralisation Buffer	0.4M Tris-HCl in 1L dH ₂ O. Set pH to 7.5 with HCl.
DNA Loading Dye (6x)	4ml 10xTBE, 3.5g sucrose, 10mg bromophenol blue. Final volume 10ml with dH ₂ O.
Ethidium Bromide	10mg/ml (dissolved in dH ₂ O).
Fixative Solution	3:1 ratio of methanol: acetic acid. Make on day of use.
HPLC Digestion Buffer	100mM sodium succinate, 50mM calcium chloride (pH6.0)
Hypotonic Solution	75mM KCl. Make on day of use.
Kinase Stop Solution	25mM disodium EDTA, 0.1%SDS, 10mM ATP. Stored at -20°C.
Lairds Lysis Buffer	5ml 1M Tris-HCl (pH8), 10ml 0.5M EDTA (pH8), 1.25ml 4M NaCl, 25ml 10% SDS. Final volume 500ml in dH ₂ O.
Micrococcal nuclease	0.4U/µl (dissolved in dH ₂ O). Store at 4°C. Sigma
Nuclease P1	2U/µl (dissolved in 0.28M NaAc, 0.5mM ZnCl) pH 5.0. Store at 4°C. Sigma
Proteinase K	10mg/ml (dissolved in 1xTE). Store at -20°C. Roche
Puromycin	10mg/ml (dissolved in 1x PBS). Store at -20°C.

RNase A	10mg dissolved in 975µl dH ₂ O, 10µl 1M Tris-HCl (pH7.5), 15µl 1M NaCl. Store at -20°C.
RNase Buffer (10x)	50ml 1M Tris-HCl (pH7.5), 50ml 0.5M EDTA (pH8), 300ml 5M NaCl, 100ml dH ₂ O.
Sodium Phosphate Buffer NaHPO ₄ (1M)	48.55g Na ₂ HPO ₄ , 24.65g NaH ₂ PO ₄ dissolved in 500ml dH ₂ O (pH7.2).
Southern Blot Denaturing Solution	0.5M NaOH, 1M NaCl.
Southern Blot Depurinating Solution	0.25M HCl.
Southern Blot Neutralising Solution	0.5M Tris-HCl (pH7.5), 3M NaCl.
Southern Blot Hybridisation Solution	5M TMAC, 10% (w/v) SDS, 0.5M disodium EDTA, 0.1M sodium phosphate (pH6.8), 50x Dernhardt's solution, 10mg/ml yeast RNA. Store at 4°C.
Southern wash Solutions	2x-, 0.2x-, or 0.1x-SSC, 0.1% SDS.
Staining Solution	500µl 1mg/ml PI, 500µl 10mg/ml RNase A, 9ml 1xPBS. Pass solution through 0.2µm filter before use.
TMAC wash Solution	5M TMAC, 10% (w/v) SDS, 0.5M disodium EDTA, 0.1M sodium phosphate (pH6.8). Stored at 4°C.
Versene	0.1g EDTA 4Na in 500ml 1x PBS.

2.2 Routine cell culture

2.2.1 ES Cell Culture Media

Complete ES Media

394ml DMEM (High Glucose 4.5g) with Glutamax (Invitrogen 61965)

90ml Foetal Bovine Serum (FBS) (Sera Labs International, batches 104006, R409008 and R509008)

5ml Sodium Pyruvate (Invitrogen 11360)

5ml Non-essential Amino Acids (Invitrogen 11140)

5ml Penicillin/Streptomycin (P/S) (Invitrogen 11140)

500µl 100mM Beta-mercaptoethanol (Sigma Aldrich M6250) Filter sterilised (0.4µm filter)

50µl Leukaemia Inhibitory factor (LIF) (Millipore ESG1107)

Freezing Media

1ml Dimethylsulphoxide (DMSO) (Sigma Aldrich D2650)

9ml FBS

Filter sterilised (0.4µm filter)

6-Thioguanine (6TG) Media

500ml Complete ES Media (see recipe above)

400µl 6-thioguanine (Sigma Aldrich A4660) 2.5mg powder dissolved in 1ml Complete ES media. Final concentration 2µg/ml

2.2.2 ES cell lines

E14Tg2a and J1 wild type (WT) murine Embryonic Stem (ES) cells were used. Cell lines containing partial deletions of the DNA Methyltransferase genes *Dnmt1*, *Dnmt3a* and *Dnmt3b* were generated from J1 cells via homologous recombination, as described in Li *et al* (1992) and Okano *et al* (1999), prior to initiation of the current project. The deletions, illustrated in Figure 3-1, result in loss of catalytic activity of the enzymes. The J1 WT, and the DNMT functional KO ES cell lines derived from this parental cell line, were kindly gifted from En Li and Taiping Chen for the purpose of this project.

2.2.3 Growth of ESCs from frozen aliquots

1ml aliquots containing 2×10^6 or 3×10^6 ESCs were stored in liquid nitrogen. These were defrosted in a 37°C water bath, transferred to a tube containing 3ml complete ES media, and centrifuged at 1,000rpm for 5 minutes. The supernatant, containing the cryo-preserved DMSO, was removed. The pellet was resuspended in 3-5ml complete ES media, transferred to a gelatinised well of a 6-well tissue culture dish, and swirled gently to ensure even distribution of the cells. A wide-gauge needle and syringe were used to break up any large clusters and the plate was incubated at 37°C with 5% CO₂. Medium was changed at least every 2 days until the cells reached confluence.

2.2.4 Routine passaging of ESCs

After thawing the mESCs (see section 2.2.3) they were passaged every 2 days to maintain confluency below 70% and prevent differentiation. The medium was removed by aspiration, and cells washed with analytical grade PBS (phosphate

buffered saline). They were then treated with trypsin-EDTA (0.25% trypsin with EDTA 4Na, Invitrogen) for 3 minutes at 37°C to detach the cells from the gelatinised surface of the culture dish. The detached cells were washed off the surface of the flask with complete ES media and transferred to a tube for centrifugation at 1,000rpm for 5 minutes. The supernatant was removed by aspiration, and the pellet resuspended in 3-5ml complete ES media. The number of cells in 10µl cell suspension was counted using a haemocytometer. ESCs were pipetted into a gelatinised flask of suitable size, depending on the number of cells present.

2.2.5 Freezing aliquots of ESCs

Multiple aliquots of each cell line were retained in liquid nitrogen storage at all times. Cells were trypsinised and counted as in section 2.2.4 above, and re-pelleted. The supernatant was removed by aspiration and cells resuspended in sufficient freezing media to give a concentration of 2 or 3×10^6 cells per ml. 1ml aliquots were transferred to labelled 2ml cryo tubes, placed inside a polystyrene box and incubated at -20°C overnight, before being transferred to -80°C for 24 hours and then into liquid nitrogen for long term storage.

2.2.6 Screening cells for Mycoplasma infection

A region of the 16S rRNA gene which is specific to mycoplasma, and conserved across mycoplasma species, was amplified by PCR using the EZ-PCR Mycoplasma Test Kit (Geneflow). Briefly, 1ml cell culture medium was removed from a growing culture of ESCs and centrifuged at 1,800rpm for 30 seconds to pellet cell debris. The supernatant was transferred to a fresh eppendorf and centrifuged at 14,000rpm for 10 minutes to

pellet mycoplasma. The supernatant was carefully removed and discarded. The pellet was resuspended in 50µl Buffer Solution and incubated at 95°C for 3 minutes to lyse the cells. 5µl of the test sample was added to 10µl reaction mix and 35µl dH₂O, and subjected to the following PCR cycle conditions: 94°C initial incubation followed by 36 cycles of denaturation for 30 seconds at 94°C, annealing for 2 minutes at 60°C and extension for 60 seconds at 72°C. During the final cycle, the extension time was altered to 5 minutes at 72°C. The remainder of the test sample was stored at -20°C for later use if required.

20µl of the PCR product was electrophoresed on a 2% agarose gel (SeaKem LE Agarose, Lonza) containing ethidium bromide at 100 volts for 1 hour, and visualised by UV illumination using a GeneFlash imager (Syngene Bio Imaging). Positive (supplied by kit) and negative controls were assayed simultaneously with test samples. The presence of mycoplasma is indicated by an amplified product at 270bp.

2.2.7 Pelleting cells for DNA extraction

Cells were trypsinised and centrifuged. The supernatant was removed by aspiration and the cell pellet was immediately frozen at -20°C.

2.3 DNA Extraction

2.3.1 Phenol-Chloroform Extraction

Cell pellets in 12ml Falcon tubes were lysed over night at 37°C with 2ml Lairds Lysis Buffer and 10µl of 10mg/ml Proteinase K. The next morning, 50µl RNase A (10mg/ml solution) was added and the sample incubated at 37°C for 1 hour.

2x volume of phenol was added to the sample, which was shaken thoroughly, and centrifuged at 4,000rpm for 15 minutes. Phenol-Chloroform extraction purifies DNA by removing protein contaminants, which separate out at the interphase between the aqueous and organic phases. The DNA is contained within the aqueous phase. The aqueous phase was carefully removed and transferred to a new 12ml Falcon tube. 0.5x volume of phenol and 0.5x volume of chloroform were added to the sample. It was shaken thoroughly, and centrifuged at 4,000rpm for 15 minutes. The aqueous phase was transferred to a new tube, and 2x volume of chloroform added. It was shaken thoroughly and centrifuged at 4,000rpm for 15 minutes. The aqueous phase was transferred to a new tube, and 2x volume of 100% Ethanol and 0.1x volume of Sodium Acetate (3M, pH5) added. The tube was inverted 20x or until the DNA precipitated. If the DNA did not become visible, the samples were placed at -20°C over night before centrifugation at 13,000rpm for 30 minutes to pellet the DNA. This should be done at 4°C. The supernatant was discarded and the pellet washed in 200µl 70% Ethanol. The sample was centrifuged at 13,000rpm for 15 minutes, the supernatant was discarded, and the pellet was allowed to air dry at room temperature. The DNA was resuspended

in an appropriate volume of 1x buffer TE, depending on the pellet size, and allowed to resuspend fully over several days at 4°C.

2.3.2 DNA extraction for HPLC

Genomic DNA was extracted using a modified method of the QIAamp DNA Mini Kit protocol. Cell pellets were washed with 1ml PBS and centrifuged at 1,000rpm for 5 minutes. The supernatant was removed by aspiration, removing any residual culture media, and the sample was resuspended in 145µl fresh PBS. 20µl 10x RNase buffer, 25µl RNase A and 10µl RNase T1 (Roche Diagnostics, 100,000U/ml) were added to each sample to remove any potential interference from RNA. They were incubated at 37°C for 6 hours with frequent mixing. After the RNase incubation, 200µl buffer AL from the QIAGEN kit and 20µl 10mg/ml proteinase K, were added to each sample. The samples were mixed and incubated at 56°C over night. In the morning, 200µl 100% ethanol was added to each sample. They were pulse vortexed for 15 seconds and transferred to labelled spin columns provided in the kit.

If the cell pellet was quite large, multiple spin columns were used, and the quantity of each reagent was doubled or tripled accordingly. The rest of the protocol was as described from step 7 onwards on page 27 of the QIAamp DNA Mini Kit Handbook.

2.3.3 DNA extraction from single colonies

DNA was extracted from single colonies which had survived selection with 6TG media, using the protocol described in the QIAamp DNA Micro Kit handbook.

2.4 Irradiations

ESCs underwent acute irradiation with 1Gy, 3Gy, 5Gy, 7Gy or 10Gy of X-rays delivered at 0.5Gy min^{-1} (250 kV constant potential, HVL 1.5 mm Cu) using a Pantak industrial X-ray machine. The dose administered was dependent on subsequent experimental procedures. Unless stated otherwise, irradiations were carried out at room temperature.

2.5 Polymerase Chain Reaction (PCR)

Oligonucleotides were ordered from Sigma Aldrich. DNA was amplified by Polymerase Chain Reaction using a DNA Engine DYAD/ TETRAD Peltier Thermal Cycler (MJ Research) and 0.2ml sterile tubes/96-well plates.

For characterisation of mutations within the *Hprt* gene, PCR was carried out in $15\mu\text{l}$ reaction volumes using primer sequences taken from Meng *et al* (2004). See Table 2-2. Each reaction mixture contained 5-10ng genomic DNA, 0.5U Taq polymerase, $1.5\mu\text{l}$ 10x Taq Buffer (ABgene), $1.9\mu\text{l}$ dNTPs, $1.35\mu\text{l}$ MgCl_2 , $0.75\mu\text{l}$ DMSO, 0.3- $1.5\mu\text{l}$ F and R primer and dH_2O . Optimisations to this basic reaction mixture are detailed in Table 2-2. PCR cycle conditions comprised 5 minutes at 96°C , followed by 35-40 cycles of: 1 minute at 96°C , 1 minute at the appropriate annealing temperature (T_m), and 1 minute at 72°C . This was followed by a final incubation at 72°C for 5 minutes. For some PCRs, detailed in Table 2-2, the T_m was replaced with a touchdown step (65°C - 0.3°C per cycle).

Primer Name	Sequence (taken from Meng <i>et al</i> , 2004).	Product size	Primer conc.	Alterations to basic conditions
Exon 1 F Exon 1 R	ATCAGGCCACCTAGTCAGA CTCTGCTGGAGTCCCCTTG	320bp	1.5µl 50mM	67°C Tm No DMSO 11.1x buffer
Exon 2 F Exon 2 R	GCAGATTAGCGATGATGAACC CCTGTCCATAATCAGTCCATGA	112bp	1µl 10mM	Touchdown
Exon 3 F Exon 3 R	CCTCATGCCCCAAAATCTTA CACAGTAGCTCTTCAGTCTGATAAAA	379bp	1.5µl 10mM	Touchdown No MgCl ₂
Exon 4 F Exon 4 R	AGCATAATTTTGTGGCCATT AAAATGTTCTTTCTTTCTTCAA	225bp	1.5µl 10mM	Touchdown No DMSO
Exon 5 F Exon 5 R	TTTAAGGGCTCTGGTGGATG CAACTCAGGCTAACCCAGGA	552bp	0.75µl 10mM	Touchdown
Exon 6 F Exon 6 R	TTAAGGCCACCAACCTGAAC GGCATAACATACCTTGCAACC	485bp	1µl 10mM	Touchdown No MgCl ₂
Exon 7.8 F Exon 7.8 R	CTGGTGAAGGACCTCTCG CAAGGGCATATCCAACAACA	262bp	0.4µl 10mM	Touchdown 1µl MgCl ₂ No DMSO
Exon 9 F Exon 9 R	CCCAGACAACGTAGGAGGAC TTACTAGGCAGATGGCCACA	196bp	1.5µl 10mM	Touchdown
K-ras F K-ras R	TTCTCAGGACTCCTACAGGAAA CCCACCTATAATGGTGAATATC	191bp	1.5µl 10mM	55°C Tm No DMSO 11.1x buffer

Table 2-2. Primers used to characterise mutations within the *Hprt* gene.

For Southern blot probe synthesis, DNA (10-100ng) was amplified in a 10µl reaction containing: 0.9µl (~1x) 11.1x reaction buffer, 0.3µl (0.3mM) each primer, 0.15µl (0.5U) *Taq* polymerase (ABgene) and dH₂O. The PCR cycle conditions used were the same as those described above. Details of the primers and reaction conditions used are contained in Table 2-3 and Table 2-4.

Amplified DNA fragments were separated by agarose gel electrophoresis. Agarose gels (0.8-3% w/v) were prepared by boiling agarose in 1xTBE, adding Ethidium Bromide to a concentration of 0.25mg/ml, pouring the mixture into sealed gel trays containing combs selected to produce wells of desired volume, and allowing the gel to solidify

inside a fume hood. DNA samples were mixed with 6x DNA loading dye and loaded into wells adjacent to an appropriate DNA size marker. Electrophoresed DNA was visualised using a Geneflash UV imager (Syngene Bio Imaging).

2.6 Sequencing

2.6.1 Clean-up of PCR products

5µl PCR product was added to 0.5µl Exo1 enzyme (20U/µl, NEB) and 1.5µl Shrimp Alkaline Phosphatase (SAP, 1U/µl, Fermentas). The reaction was mixed and incubated at 37°C for 1 hour to inactivate excess PCR primers and dNTPs. It was then incubated at 80°C for 15 minutes to inactivate the Exo1/SAP enzymes, and held at 15°C until removal from the PCR block for sequencing.

2.6.2 Sequencing reaction

DNA fragments were sequenced using an ABI PRISM BigDye Terminator Cycle Sequencing Ready Reaction kit version 3.1. The sequencing reaction consisted of 6.5µl maximum volume (20-40ng/kb) cleaned-up PCR product or purified plasmid DNA, 1µl of 3.2pM forward or reverse primer (see Table 2-2), 1µl Big Dye Terminator Ready Reaction Mix, and 1.5µl Big Dye Terminator Buffer made up to a total reaction volume of 10µl with dH₂O. Sequencing cycle conditions involved 25 cycles of: 10 seconds at 96°C, 5 seconds at 50°C and 4 minutes at 60°C.

2.6.3 Clean-up after sequencing

10µl dH₂O and 2µl 2.2% SDS were added to each sequencing sample, mixed and incubated at 98°C for 5 minutes, followed by 25°C for 10 minutes, to disrupt aggregation of the BigDye v3.1 terminators and allow more effective spin column purification. Performa DTR Gel Filtration Cartridges were used to remove dye terminators. Essentially, the columns were centrifuged at 3,400rpm for 3 minutes and the buffer eluted from the gel was discarded. The sample was added to the column and centrifuged at 3,400rpm for 3 minutes. The eluate, containing the fluorescently labelled products of the sequencing reaction, was submitted to the University genomics core facility, PNAAC (Protein Nucleic Acid Chemistry Lab) for processing using an Applied Biosystems 3730 sequencing system.

2.6.4 Sequence Analysis

DNA sequence data was analysed using MacVector software version 8.1.2. Sequences were authenticated and confirmed by comparing against the appropriate wild type sequence found at <http://www.ncbi.nlm.nih.gov/>.

2.7 Southern Blotting

Methylation levels at specific repeat elements were characterised by Southern blotting. 20µg DNA was digested with *HpaII* and 20µg with *MspI*, using 30µl NEB Buffer 1 or 4 respectively, 6µl enzyme (60-120U), and sufficient dH₂O to make a total reaction volume of 300µl. Samples were incubated at 37°C for 3 hours. A further 6µl enzyme was added and they were left at 37°C over night.

After digestion, the samples were ethanol precipitated, air-dried, resuspended in 40µl 1x buffer TE, and allowed to dissolve at 4°C. The DNA concentration was estimated using a Nanodrop spectrophotometer and 5µg of each sample was loaded on a 1.7% LE agarose gel and electrophoresed at 30 volts for ~16 hours. When the samples had migrated 16-18cm from the wells, the gel was visualised under UV light and cut to 19.5cm x 19.5cm with a scalpel. The gel was washed twice for 10 minutes on the shaker with depurinating solution. This reduces the molecular weight of any very large fragments so that they can be transferred more easily from the gel onto the membrane. The gel was then washed twice for 20 minutes with denaturing solution, which denatures the DNA to single strand. Finally, the gel was washed twice for 20 minutes with neutralising solution to reduce the pH to 7.4.

Four 20cm x 20cm squares and one larger rectangle were cut from 3mm blotting paper (Whatman). Apparatus was arranged so that the rectangle of blotting paper, soaked in 10x SSC, lay flat on a Pyrex plate with its ends immersed in a tray of 10x SSC below. The gel was placed face down on top of the blotting paper, and a sheet of nylon membrane (Magnaprobe) cut to 20cm x 20cm and soaked quickly in 10x SSC was placed on top. The 4 squares of blotting paper were soaked in 10x SSC and placed on top of the membrane. Care was taken to remove any air bubbles as these can interfere with DNA transfer. To aid capillary action, two equal stacks of paper towels were placed on top of the blotting paper, followed by a second Pyrex plate and a weight. Any exposed areas of the rectangular section of blotting paper were covered with cellophane to

reduce evaporation of the buffer. The apparatus was left at room temperature over night to allow the DNA to transfer to the membrane.

The next morning, complete DNA transfer was checked by viewing the gel under UV illumination. The membrane was baked at 80°C for 1 hour, and the DNA covalently bound to the membrane by exposure to 7×10^4 J/cm² UV light using an RPN 2500 ultraviolet crosslinker (Amersham Biosciences). Membranes were stored at 4°C until use.

2.7.1 Production of Probes

DNA sequences for primer design were obtained from the NCBI database (<http://www.ncbi.nlm.nih.gov>). Primers were designed using MacVector or Primer 3 (http://biotools.umassmed.edu/bioapps/primer3_www.cgi).

Table 2-3 and Table 2-4 list the murine DNA sequences used as Southern blot probes. The major and minor satellite sequences were simply ordered as oligonucleotides (Sigma Aldrich). They were radiolabelled using the oligonucleotide end-labelling protocol, described in section 2.7.2.1. Multiple copies of all other probe sequences were generated using PCR as described in section 2.5, with the addition of a proof-reading enzyme pfu (Stratagene, use in ratio 1U pfu: 20U Taq). Product size was confirmed by agarose gel electrophoresis and the probes were stored at 4°C until use. They were radiolabelled using a random priming method described in section 2.7.2.2.

Primer name	Primer sequence	Tm	Product size	Target sequence (murine)
LINE1f F LINE1f R	AAGCCACAGCAGCAGCGGT CGGAAGGTGGCCGGCTGT	68°C	172bp	5' monomer sequence of L1 F subfamily
LINE1gf F LINE1gf R	TGAGAGCACGGGGTCTG AGGAAGGTGGCCGGCTGT	67°C	204bp	5' monomer sequence of L1 GF subfamily
LINE1tf F LINE1tf R	CAGAGGAGAGGTGTCTGCC CAGGGAAGGTGCCCCGGATGT	65°C	205bp	5' monomer sequence of L1 TF subfamily
LINE1a F LINE1a R	GCCTGCCCAATCCAATC TGTGATCCACTCACCAGAGG	63°C	206bp	5' monomer sequence of L1 A subfamily
SINE B2B4 F SINE B2B4 R	AGCTGTCCTCAGACACTCCAG GGCTCAGTGGGTAAGAGCAC	61°C	179bp	B2-B4 SINE. Insert detected in <i>Hprt</i> exon 3.
SINE AluB1 F SINE AluB1 R	GGTTTTTCGAGACAGGGTTTC ACGCCTTTAATCCCAGCACT	61°C	142bp	Alu/B1 SINE. Insert detected in <i>Hprt</i> exon 6.
IAP F IAP R	Tgccggttacaagatggcgc tctccccgctttacttctga	63°C	700bp	5' LTR of IAP promoter. Genbank: M17551 bp22-721.
Mito F Mito R	ACACACCGCCCGTCACCCTCC GGCTGCTTTTAGGCCTACAATGG	63°C	720bp	MtDNA GenBank: J01420 bp901-1620.

Table 2-3. Primers used to generate longer sequence probes for Southern blotting.

Probe	Sequence	Source
Major Satellite	GTGAAATATGGCGAGGAAAAC	Kipling <i>et al</i> (1995)
Minor Satellite	AACAGTGTATATCAATGAGTTACAATGAG	Bourc'his and Bestor (2004)

Table 2-4. Murine satellite DNA sequences used as oligonucleotide probes.

2.7.2 Radiolabelling of probes and membrane hybridisation

2.7.2.1 Oligonucleotide end-labelling

Probes were labelled using an oligonucleotide end-labelling reaction. Briefly, 3µl of 8µg/µl oligonucleotide stock was incubated for 1-5 hours at 37°C in a reaction containing 4.3µl dH₂O; 3µl 10x Kinase Mix; 0.36µl γ-32P-ATP (10mCi/ml, Amersham Biosciences); and 1.05µl T4 Polynucleotide Kinase (T4-PK, 10,000U/ml, NEB). T4-PK end-labels the oligonucleotides by forming a phosphodiester bond with the γ end of the dATP molecule. To stop the reaction, 60µl kinase stop solution was added.

The membrane was soaked in 2x SSC buffer, placed into a hybridisation bottle with 10ml hybridisation solution and incubated in the hybridisation oven at 53°C for 30 minutes. The bottle contents were discarded, replaced with 10ml fresh hybridisation solution and the membrane was incubated for a further 30 minutes at 53°C. The probe mixture was added to the hybridisation bottle, and incubated over night at 53°C in the hybridisation oven.

The next day, the hybridisation solution was discarded and the membrane washed 3x with 10ml TMAC wash solution for 20 minutes at 56°C to remove any excess, unbound

probe. The membrane was rinsed twice with 3x SSC buffer before being blotted to remove excess liquid and wrapped in cling film.

2.7.2.2 dsDNA labelled by random priming

Probes were labelled by random priming. Briefly, 4µl probe DNA (50-100ng) was heat denatured by boiling in 18µl water for 6 minutes. It was then transferred to ice and incubated for 1 hour at 37°C in a reaction containing 6µl dNTPs (excluding dCTP); 5µl α-32P-dCTP (3000Ci/mmol, Amersham Biosciences); 15µl random primers; and 1µl (5U) Klenow enzyme. The reaction was then filtered through a G50 NICK Column (GE Healthcare). Briefly, the column was equilibrated twice with column wash, the probe was added, unincorporated dNTPs were washed through with 400µl column wash, and the probe was eluted and collected by adding a further 400µl column wash.

The membrane was soaked in 2x SSC buffer, placed into a hybridisation bottle with 10ml Church Buffer, and incubated at 65°C for 3-5 hours. Immediately prior to adding the probe mixture, the old Church buffer was discarded and a fresh 10ml aliquot was added to the hybridisation bottle. The membrane was incubated at 65°C over night in the hybridisation oven.

The next day, the hybridisation solution was discarded and excess probe was removed from the membrane by washing twice for 20 minutes at 65°C with buffer 1 (2x SSC with 0.1% SDS) then buffer 2 (0.2x SSC with 0.1%SDS) and then buffer 3 (0.1x SSC with 0.1x SDS). The membrane was blotted to remove excess liquid and wrapped in cling film.

2.7.3 Visualisation

Membranes were placed in autoradiographic cassettes (Autorads) containing either Fuji RX 100 or Kodak BIOMAX XAR film and incubated at -80°C for >24hours. They were developed using a Compact X4 automatic X-ray film processor (Xograph Imaging Systems).

2.7.4 Stripping a Southern blot

Membranes were stripped to enable re-probing, by immersion for 10-15 minutes in 1L boiling dH²O containing 10ml 10% SDS and 10ml 10x SSC buffer. This was repeated if radioactivity exceeding 5 counts per second was still detectable with a Geiger counter. Stripped membranes were placed against film for 1 night to ensure no background signal was detectable. They were wrapped in cling film to prevent drying and stored at 4°C.

3 Chapter 3. Characterisation and Radiosensitivity of the Cell Lines

3.1 Introduction

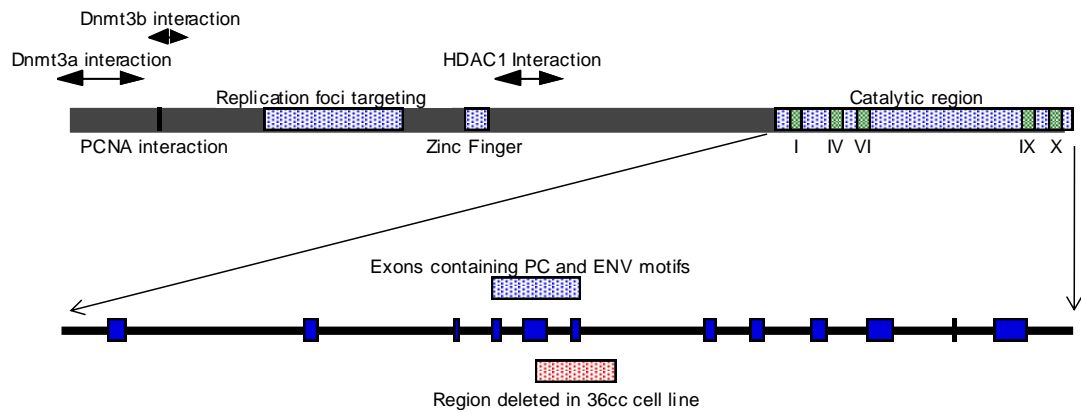
DNA cytosine methylation is an important cellular phenomenon in mammalian cells, due to its involvement in many essential biological functions (Chen *et al*, 1998; Davis *et al*, 2000; Gisselsson *et al*, 2005; Lee and Jaenisch, 1997; Norris *et al*, 1994; Song *et al*, 2005; Takai *et al*, 2000). The level of DNA methylation varies between different cell and tissue types. Generally, tissues containing higher proportions of fully differentiated cells, such as brain or spleen, possess higher methylation levels than those containing greater numbers of stem or progenitor cells, such as bone marrow (Ehrlich *et al*, 1982; Gama-Sosa *et al*, 1983; Giotopoulos *et al*, 2006). However, there are exceptions, such as heart, which contains comparatively little DNA cytosine methylation (Ehrlich *et al*, 1982).

Clinical data demonstrates that there is also a wide range of sensitivities to ionising radiation in different tissue types (Dörr, 2009). Although there are exceptions to the trend, tissues with low methylation levels generally have low radiation tolerance doses, whilst more heavily methylated tissues with lower capacity for self-renewal have much higher radiation tolerance doses. See section 1.6. Similarly, several *in vitro* studies using human cell lines imply a correlation between DNA hypomethylation and increased sensitivity to ionising radiation (Dote *et al*, 2005; Narayan *et al*, 2000). A

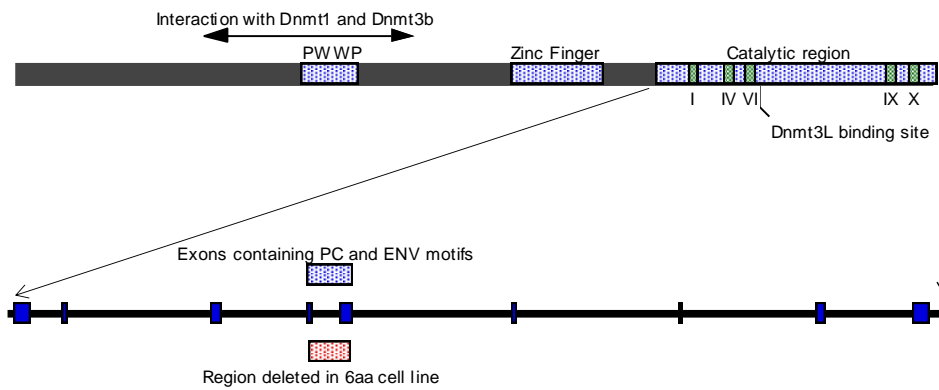
number of studies indicate that ionising radiation itself can induce sex- and tissue-specific reductions in levels of CpG methylation *in vivo* (Kovalchuk *et al*, 2004; Pogribny *et al*, 2004; Giotopoulos *et al*, 2006; Tawa *et al*, 1998). In some instances this has been coupled with a reduction in expression levels of the DNMTs (Raiche *et al*, 2004) and the methyl-binding protein MeCP2 (Loree *et al*, 2006).

The work presented in this chapter aims to investigate the apparent correlation between mammalian DNA cytosine methylation and radiosensitivity, and also to further investigate the effects of ionising radiation on genomic methylation levels. An established panel of mouse embryonic stem cell (ESC) lines were utilised, which have been derived from wild type J1 ESCs (129/SvJ). The derived ESC lines contain partial deletions of the three main active murine DNA Methyltransferase genes *Dnmt1*, *Dnmt3a* and *Dnmt3b*, generated via homologous recombination, as described in Lei *et al* (1996) and Okano *et al* (1999). The deletions span the exons encoding the PC (Proline and Cysteine) and ENV (Glutamate (E), Asparagine (N) and Valine (V)) motifs (see Figure 3-1), and result in loss of catalytic activity of the enzymes (Lei *et al*, 1996; Okano *et al*, 1999). The J1 wild type and the DNMT functional knock out (KO) ESC lines derived from this parental cell line were a kind gift from En Li and Taiping Chen for the purpose of this study.

A



B.



C.

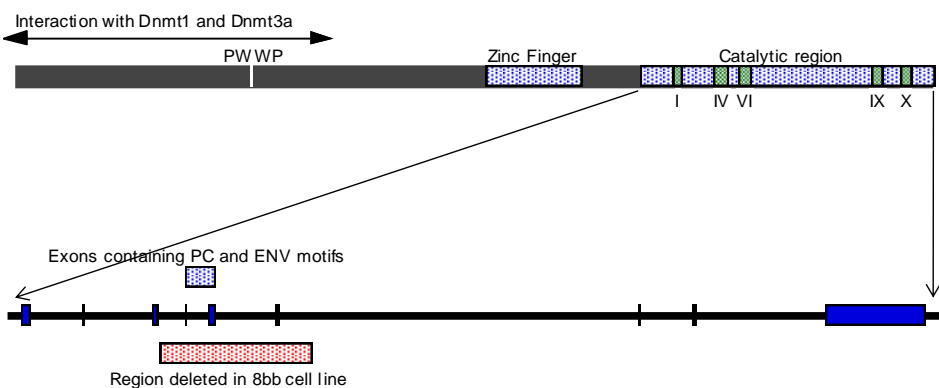


Figure 3-1. Schematics of the proteins and catalytic region genomic sequences for the 3 main murine DNA methyltransferase enzymes, DNMT1 (A), DNMT3A (B) and

DNMT3B (C). The deletions induced to generate the KO cell lines are indicated. The carboxyl-terminal region of each DNMT contains 10 conserved motifs. Motifs I and X create the AdoMet-binding site by folding together. Motif IV contains the prolylcysteiny (PC) dipeptide, which serves as the active site. Motif VI contains the ENV motif, which protonates the target cytosine. The target recognition domain is located between motifs VIII and IX (Lan *et al*, 2010). PCNA, Proliferating Cell Nuclear Antigen; HDAC, Histone Deacetylase; PWWP, conserved motif of Pro-Trp-Trp-Pro, involved in DNA binding.

Several techniques are available to determine global levels of genomic DNA methylation, including Klenow-based fill-in labelling reactions such as nearest neighbour analysis (Ramsahoye, 2002), CpG island microarrays, restriction landmark genomic scanning (RLGS), amplification of inter-methylated sites (AIMS), immunohistochemical staining, and high performance liquid chromatography (HPLC) (Esteller, 2005; Sulewska *et al*, 2007). Although, HPLC requires relatively large amounts of DNA, the results are unbiased by any kind of target sequence selectivity, and it can be coupled to an automated detection system, allowing accurate quantification of the level of DNA methylation.

Using HPLC-UV analysis, DNA methylation levels were characterised for each ESC line, and were re-assessed at several time points post irradiation with a clinically-relevant dose of X-rays (3Gy). In addition, growth curves were constructed to determine the rate of cell proliferation in irradiated/unirradiated cells, and cell cycle analysis was undertaken using flow cytometry. Finally, the radiosensitivity of the ESC lines was determined using the clonogenic assay.

3.2 Chapter-Specific Methods and Materials

3.2.1 HPLC

Global levels of DNA cytosine methylation were characterised using HPLC-ultraviolet (UV) detection. This method has been published and is described fully in Sandhu *et al* (2009). Briefly, genomic DNA was extracted from irradiated or unirradiated ESCs using an optimised procedure described in section 2.3.2, and enzymatically hydrolysed to 2'-deoxynucleosides. 10µg hydrolysed DNA was injected into a narrow-bore reverse phase HPLC column coupled with UV detection, for separation and quantification of the 2'-deoxynucleosides. Levels of 5-methyl-2'-deoxycytidine (5-MedC) were expressed as a percentage of the level of total cytosine (5-MedC and 2'-deoxycytidine (dC)).

3.2.1.1 Stock solutions of authentic standards

Stock solutions for the 2'-deoxynucleoside standards (dC, dG, dT and dA, Sigma) and the methyl standard (5-MedC, Chemos GmbH) were prepared and dissolved in HPLC grade water. The UV absorbance (λ_{\max}) for the peaks of interest: 5-MedC and dC, was 277 nm and 271 nm respectively. Typical retention times were: dC, 12.0 ± 1.0 min; 5-MedC, 19.7 ± 1.3 min; dG, 23.9 ± 1.5 min; dT, 25.1 ± 1.5 min; dA, 33.6 ± 1.0 min. A particularly stubborn RNA contaminant, Guanosine, was also sometimes detected at 21.4 ± 0.7 min. Sample peak identity was confirmed by co-elution with the corresponding authentic 2'-deoxynucleoside standard. See Figure 3-3.

3.2.1.2 Enzymatic hydrolysis of DNA

DNA samples (20–50µg) were dried using a Speed vac plus SC210A (Savant). They were resuspended in 10µl HPLC digestion buffer with 5µl micrococcal nuclease (0.4U/µl) which is an endo-exonuclease, and 35µl calf spleen phosphodiesterase (0.001U/µl, Calbiochem) which is a 5'-exonuclease. Samples were incubated at 37°C overnight. The following morning, 10µl nuclease P1 (2U/µl) was added and the samples were incubated for a further 4 hours at 37°C to catalyse cleavage of the phosphate groups. Samples were centrifuged at 14,000rpm for 20 minutes before transferring the supernatant to a new tube and drying in the Speed vac. The samples were resuspended with dH₂O to a final concentration of 1µg/µl and transferred to HPLC vials.

3.2.1.3 HPLC-UV detection

10µl each hydrolysed DNA sample was injected onto a Waters HPLC system consisting of an Alliance 2690 separations module and 2487 UV detector (Waters Ltd) connected to a Synergi Fusion-RP 80A C₁₈ (4µm, 250mm × 2mm) column attached to a Synergi Fusion-RP guard column of the same measurements and a KrudKatcher disposable pre-column filter (0.5µm, Phenomenex). DNA was eluted using a gradient with mobile phase solvent A (0.05M ammonium formate, pH 5.4, BDH) and solvent B (methanol, Fisher Scientific) at flow rate of 0.2ml/min. UV absorbance was monitored at 277 nm.

3.2.1.4 Calculation of the percentage 5-MedC in DNA

Genomic levels of DNA cytosine methylation were expressed as the percentage of total cytosines that were methylated. Calibration lines were constructed for each HPLC run using dilutions of stock standard solutions for 5MedC (0.0625–10nmol) and dC (0.125–25nmol). Based on these calibration lines, the level (nmol) of 5MedC and dC in the hydrolysed DNA samples could be determined from the area (UV*sec) of the dC and 5mdC peaks. Finally, the data was entered into the following formula:

$$\% \text{ 5MedC} = \left[\frac{\text{5MedC (nmol)}}{\text{dC (nmol) + 5MedC (nmol)}} \right] \times 100$$

3.2.2 Clonogenic Assays: Radiosensitivity

3.2.2.1 Clonogenic assay using semi-solid agarose

This method was adapted from Clutton *et al* (1996). Cells were trypsinised and counted. Aliquots of 3 million cells were transferred into 5 labelled eppendorf tubes (0Gy, 1Gy, 3Gy, 5Gy and 7Gy). The tubes were centrifuged at 1,000rpm for 5 minutes, and the supernatant removed by aspiration. The tubes were placed inside a polystyrene box for transport to/from the X-ray machine, where they were irradiated with the appropriate dose of X-rays. After irradiation the cells were resuspended in 3ml complete ES media to a concentration of 1 million cells per ml, before serially diluting to a concentration of 10,000 cells per ml.

9ml 3% LMP agarose, made with cell culture grade PBS, was heated in a microwave at full power for 30 seconds. It was allowed to cool slightly and diluted to 0.3% with 81ml warm complete ES media. Five 6-well plates were labelled, and 4ml warm agarose solution was transferred into 5 of the 6 wells. The remaining well was filled with dH₂O to keep the agarose moist.

The tubes containing the serially diluted ESCs were mixed thoroughly, and aliquots of the cell solutions were added to each agarose-containing well of the labelled 6-well plate as follows: 100µl for 0Gy and 1Gy, 200µl for 3Gy, 400µl for 5Gy and 500µl for 7Gy. PE was assessed by the proportion of cells seeded into the sham well which survived to produce colonies. The plates were swirled to ensure even dispersal of the cells, and left at room temperature for 10 minutes, to allow the agarose to become semi-solid, before transferring to the 37°C incubator. The agarose solution remains as a liquid if it is not permitted to set, causing larger numbers of cells to sink to the bottom of the well and form flat, sprawling colonies that are troublesome to count.

The colonies were grown in the incubator for 10 days, at which point all those visible by eye were counted, using a grid and low power (x2) dissection microscope.

3.2.2.2 Clonogenic assay using gelatinised dishes

This method was used in addition to the semi-solid agarose method described in section 1.1.7, and eventually replaced it. It was introduced to determine whether inability to change media in the semi-solid agarose method was slowing cell growth and biasing results, due to nutrient restriction and pH changes.

Five 6-well plates were gelatinised and labelled. Cells were trypsinised, counted, aliquotted, irradiated as pellets, and resuspended to a concentration of 10,000 cells per ml as described in section 3.2.2.1.

The tubes containing the serially diluted ESCs were mixed thoroughly, and aliquots of the cell solutions were added to each well of the correspondingly-labelled 6-well plate as follows: 100µl for 0Gy and 1Gy, 200µl for 3Gy, 400µl for 5Gy and 500µl for 7Gy. PE was assessed by the proportion of cells seeded into the sham well which survived to produce colonies. 3ml complete ES medium was added to each well and the plates were swirled to ensure even dispersal of the cells. The plates were placed in the 37°C incubator and colonies allowed to grow for 10 days, at which point all those visible by eye were counted. Medium was changed every second day during this 10-day incubation period.

3.2.3 Growth curves

Cells were trypsinised, counted and pelleted for irradiation as described in section 3.2.2.1. After 3Gy X-irradiation or sham treatment, 500,000 or 200,000 cells respectively were seeded into a single gelatinised well of a 6-well plate with 3ml complete ES media. After growth for 24 hours in the 37°C incubator, the cells were again trypsinised, centrifuged, resuspended and counted. A set number of cells were seeded (200,000 for sham cells, or 300,000 for cells irradiated <48 hours previously) into fresh gelatinised 6-well plates and incubated for a further 24 hours at 37°C. This process was repeated multiple times. The number of cells seeded and the number of cells harvested at each 24 hour time point was used to determine the cell population

doubling time. After several repeats, growth curves were generated to show the cumulative population doublings of each cell line over time, in X-irradiated or sham treated ESCs.

3.2.4 FACS cell cycle analysis

3.2.4.1 Sample Preparation

3 million cells were prepared for irradiation with 3Gy X-rays as described in section 3.2.2.1. After irradiation, the cells were seeded into 7 wells of 2 gelatinised 6-well plates at a concentration of 300,000 cells per well. 500,000 sham and 3Gy treated cells were sampled immediately, and at several time points thereafter (+5hours, +10hours, +24hours, +48hours, +72hours, +5days, +10days). Non-adherent cells were collected from the culture dish in a 50ml falcon tube. The adherent cells were incubated with trypsin at 37°C for 3 minutes, washed off the surface of the culture dish and added to the falcon tube. The cells were centrifuged at 1,000rpm for 5 minutes, the supernatant was removed by aspiration, and the cell pellet was resuspended in 200µl PBS. 2ml of 70% ethanol was added to fix the cells, and aggregates were broken up by pipetting x3. Samples were stored at -20°C until use (<11 days).

Immediately prior to analysis, the cells were pelleted by centrifugation at 2,000rpm for 10 minutes and the supernatant removed by aspiration. The pellet was resuspended in 1ml Staining Solution (see Table 2-1) and incubated at 37°C for 30 minutes before being run on the flow cytometer.

3.2.4.2 Flow Cytometry: FACS (Fluorescence Activated Cell Sorting)

Cell cycle distribution analysis was carried out using a Becton Dickinson FACScan flow cytometer coupled to a computer running CellQUEST software (Becton Dickinson). Complete reviews on the technique of flow cytometry can be found elsewhere (Givan, 2001). Briefly, the cells are intersected by a beam of light, and the resulting emitted light is detected and analysed. Cell diameter is determined from the forward-angle light scatter (FSC) and the surface texture and conformation of inner cellular structures are given by side-angle light scatter (SSC). In addition, the intensity of PI fluorescence is proportional to the DNA content of the cells (Givan, 2001). This varies throughout the cell cycle ($2n$ during G_1/G_0 ; $4n$ during G_2 /mitosis; $2n-4n$ during S phase), hence measurement should allow determination of the cell-cycle stage for each cell analysed.

This information (FSC, SSC and PI fluorescence) was acquired for a total of 10,000 cells per sample at a speed of 200 cells/events per second. Gating processes were applied to the data using CellQuest software, to exclude cell debris based on cell size and shape, and then to exclude aggregates or clumps from the analysis based on the area and width of the fluorescence peak. See appendix 7.1. The gated cells were plotted as a DNA histogram displaying the number of cells (Y) per PI fluorescence intensity (X). Finally, ModFit LT software (Becton Dickinson) was used to estimate the proportion of cells from each sample in the different phases of the cell cycle. Examples of the ModFit histograms are displayed in Figure 3-8.

3.3 Results

We first analysed the global levels of DNA cytosine methylation in wild type (J1) cells and in *Dnmt1*^{-/-}, *Dnmt3a*^{-/-}, *Dnmt3b*^{-/-} and *Dnmt3a3b*^{-/-} cells, using high performance liquid chromatography coupled with UV detection (HPLC-UV), as described in Sandhu *et al* (2009). Typical spectra are shown in Figure 3-2.

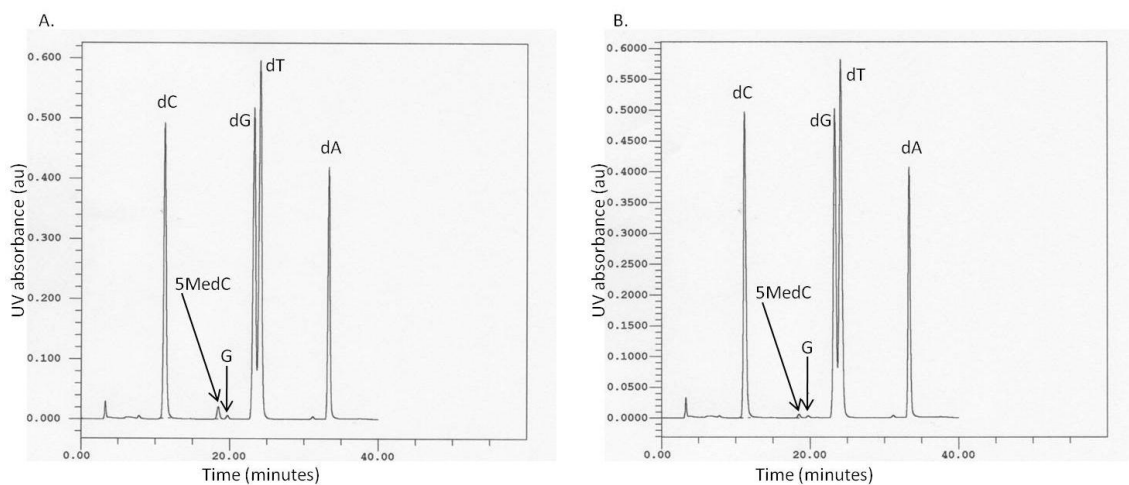


Figure 3-2. Example HPLC-UV spectra showing separation of 2'-deoxynucleosides in two samples with a range of levels of genomic DNA cytosine methylation. A) J1 wild type ESCs. B) *Dnmt1*^{-/-} ESCs. UV absorbance is measured in absorbance units (au). 2'-deoxycytidine, dC; 5-methyl-2'-deoxycytidine, 5MedC; 2'-deoxyguanosine, dG; thymidine, T; 2'-deoxyadenosine, dA; guanosine, G.

The presence of a small Guanosine peak (G) in the above spectra highlights the importance of the ribonuclease incubation to prevent co-elution of RNA contaminants with the 2'-deoxynucleosides and subsequent interference with HPLC-UV analysis. The identity of each peak was confirmed by spiking a sample with authentic standard solutions (Chemos GmbH; Sigma). A sample spiked with standards for 5MedC and G is shown in Figure 3-3.

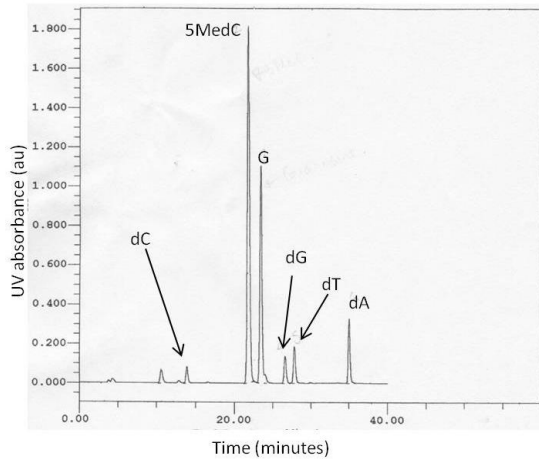


Figure 3-3. HPLC spectrum spiked with authentic standards for 5MedC and G.

DNA cytosine methylation levels of the ESC lines, as measured by HPLC-UV detection, are in agreement with previously published data (Jackson *et al*, 2004). The results are presented in Figure 3-4. All of the samples analysed were within the limits of detection and quantitation for cytosine and methylcytosine described in Sandhu *et al* (2009). Functional absence of the maintenance methyltransferase, DNMT1, causes a substantial decrease in genomic methylation in comparison to wild type cells, whilst knock out of a single *de novo* methyltransferase has only a very modest effect on genomic methylation. This implies a greater single requirement for DNMT1 than either of the *de novo* methyltransferase enzymes to maintain genomic DNA methylation levels in these ESCs. However, functional absence of both DNMT3A and DNMT3B results in a considerable decrease of cytosine methylation, emphasising their importance as co-factors for DNMT1.

As covered in section 1.1, all three DNA methyltransferase enzymes cooperate in the maintenance of DNA methylation (Kim *et al*, 2002), and DNMT1 also plays a role in *de*

novo methylation of cytosines (Jair *et al*, 2006). DNMT1 has maintenance fidelity of roughly 98% in ESCs. Due to its imperfect ability to maintain methylation levels alone, a fraction of genomic cytosine methylation is lost at every cell division in the *Dnmt3a3b*^{-/-} cell line (Jackson *et al*, 2004). We observed such a decline in the present study, with approximately 1.3% of total cytosines being methylated at px16, and only roughly 0.4% of total cytosines being methylated at px60 (see Figure 3-4). The methylation level of all other ESC lines studied remained constant throughout passaging.

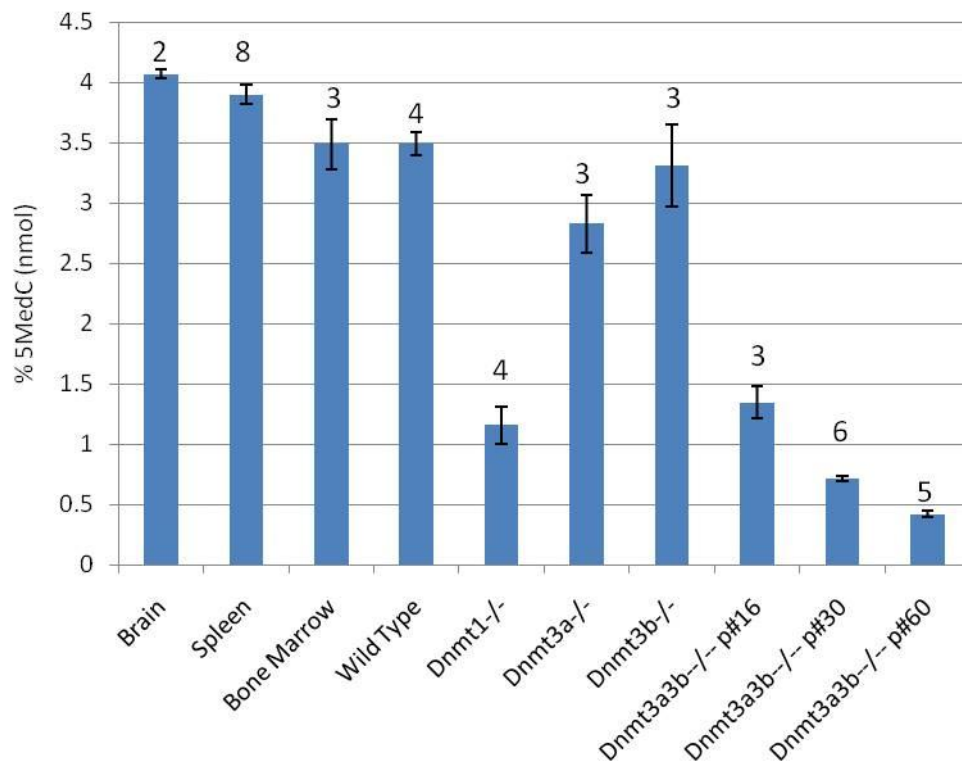


Figure 3-4. Genomic DNA cytosine methylation of unirradiated ESC samples and murine tissue controls, measured by HPLC-UV. Columns represent the average percentage of cytosine bases that were methylated, and the error bars represent the standard error of the mean (SEM). Results were combined from multiple independent experiments. The number of replicate measurements for each data point is displayed above the error bar. DNA extracted from one spleen sample was included as a control in each HPLC run to ensure consistency between experiments. Passage number (p#).

Population doublings were assessed using a method in which a set number of cells were seeded into a culture dish and 24 hours later the number of cells harvested were counted. See section 3.2.3 for a full description of the method. Based on these cell counts, during exponential growth the ESC lines underwent an average of 1.1 population doublings within 24 hours, except *Dnmt3a*^{-/-}, which underwent an average of 1.5 population doublings in 24 hours. The cell lines were maintained in exponential growth during routine culturing, by passaging approximately every 48 hours. The *Dnmt3a*^{-/-} cell line was split 1 in 6 whilst the others were split 1 in 4. Therefore, each passage represents 2.2 to 3 population doublings. The passage numbers of px16, px30 and px60 for the *Dnmt3a3b*^{-/-} ESC line therefore approximately represent 35, 66 and 132 population doublings, respectively.

Three mouse tissue controls (brain, spleen and bone marrow) were included in the HPLC-UV analysis for comparison with the ESCs. These had been harvested for similar previous work by a colleague, and DNA was extracted using the QIAamp DNA Mini Kit. Wild type ESCs have a similar methylation level to bone marrow, which as discussed in section 1.6, is one of the least methylated mammalian somatic tissues. This is thought to be due to the large proportion of stem and progenitor cells contained within bone marrow (Giotopoulos *et al*, 2006). In keeping with this theory, the tissues which contain fewer such cells, namely spleen and brain, have produced higher measurements of cytosine methylation using the current HPLC-UV method.

To determine whether ionising radiation would affect global methylation levels in ESCs as observed by previous groups *in vivo* (Kovalchuk et al, 2004; Pogribny et al, 2004; Giotopoulos et al, 2006; Tawa et al, 1998), the level of cytosine methylation in the cell lines was characterised post irradiation with 3Gy X-rays. The results are displayed in Figure 3-5. Cells were sampled for HPLC-UV analysis immediately prior to irradiation, 24 hours post irradiation and 10 days post irradiation. The analysis was repeated in triplicate for all cell lines and the values obtained were plotted as a ratio of the unirradiated average for each cell line.

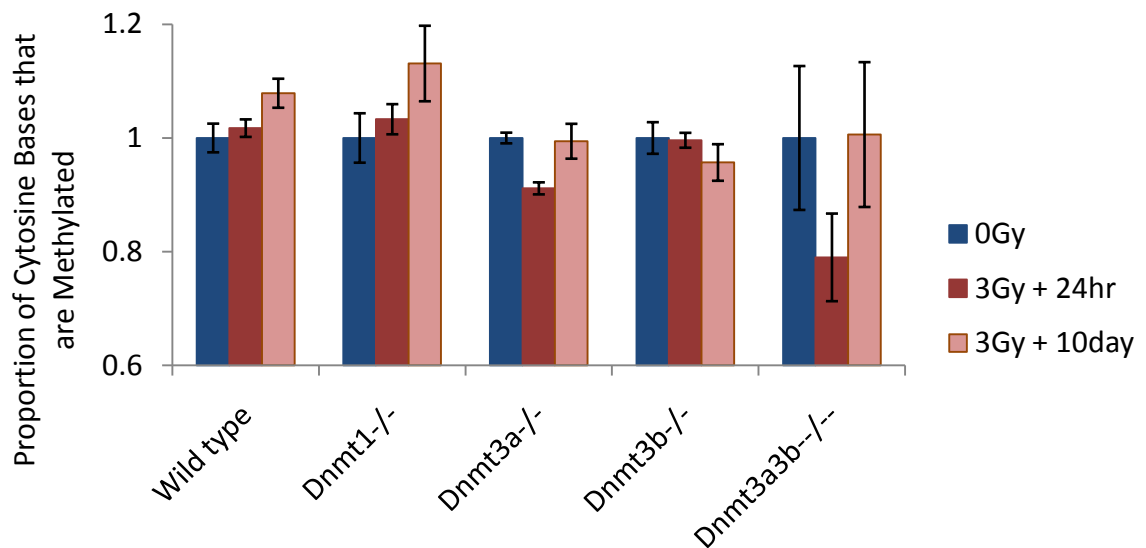


Figure 3-5. Genomic DNA cytosine methylation of the ESC lines before and after exposure to 3Gy X-rays, measured by HPLC-UV. The unirradiated sample (0Gy) for each ESC line was used as a reference and assigned a value of 1. Any detected alterations in DNA methylation were expressed as a ratio of the 0Gy value. Therefore, columns represent the average proportion of cytosine bases that were methylated, and the error bars represent the SEM, of 3 independent experiments with 2 replicates each.

Global cytosine methylation levels of the wild type and *Dnmt1*^{-/-} ESC lines appear to increase over time after irradiation. However, the difference is not statistically

significant ($p > 0.05$). In addition, the methylation level of the *Dnmt3b*^{-/-} cell line was not significantly altered 24 hours or 10 days post irradiation. However, the *Dnmt3a*^{-/-} cell line showed a significant decrease in cytosine methylation 24 hours post irradiation ($p = 0.0004$) with values returning to normal by 10 days. Although not significant ($p = 0.15$), the only other cell line without functional DNMT3A, the *Dnmt3a3b* double knock out, displayed a similar trend with methylation levels reduced 24 hours post irradiation and returning to normal by 10 days.

It was attempted to determine whether the apparent radiation-induced demethylation observed in the ESC lines lacking catalytic DNMT3A (Figure 3-5) was due to an active or a passive process (see section 1.7.1). The experiment was repeated for those cell lines which showed a reduction in methylation at 24 hours (*Dnmt3a*^{-/-} and *Dnmt3a3b*^{-/-/-}) and also for the wild type cell line. Several extra time points were introduced post irradiation (1 hour, 3 hours, 8 hours, 72 hours and 5 days) to enable a more accurate estimate of the timescale of any methylation changes. The analysis was repeated in triplicate for all cell lines and the values obtained were plotted as a ratio of the unirradiated average for each cell line. The results are displayed in Figure 3-6.

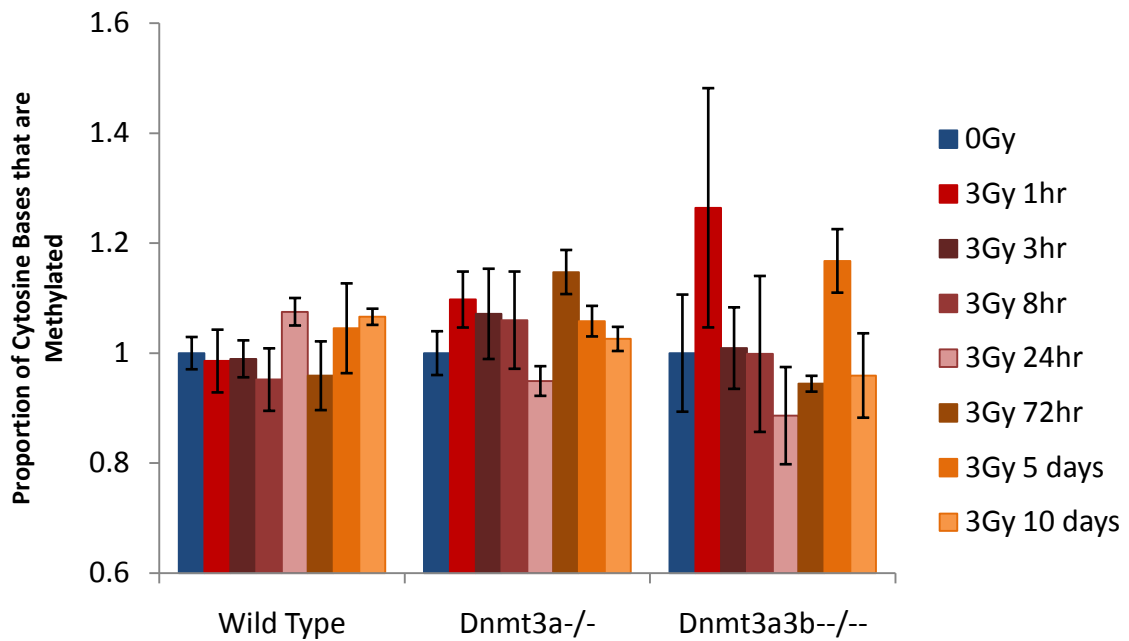


Figure 3-6. Genomic DNA cytosine methylation level of the wild type, *Dnmt3a*^{-/-} and *Dnmt3a3b*^{-/-} ESC lines post 3Gy X-irradiation. The unirradiated sample (0Gy) for each ESC line was used as a reference and assigned a value of 1. Any detected alterations in DNA methylation were expressed as a ratio of the 0Gy value. Columns represent the average proportion of cytosine bases that are methylated, and the error bars represent the SEM, of 3 independent experiments with 2 replicates each.

Repetition of the experiment revealed no statistically significant fluctuations in methylation level from that of the unirradiated control cells ($p > 0.06$) (Figure 3-6).

Therefore, it is likely that the original reduction in methylation observed in the *Dnmt3a*^{-/-} cell line 24 hours after irradiation (see Figure 3-5) was an anomaly.

Nevertheless, the shape of the graphs were consistent for each ESC line, with the lowest methylation levels in the *Dnmt3a*^{-/-} and *Dnmt3a3b*^{-/-} cell lines occurring at 24 hours post irradiation, whilst the wild type cell line displayed a slight increase in methylation levels 24 hours and 10 days post irradiation.

So far, it has been established that the wild type ESC line has a similar methylation level to bone marrow, and that the different *Dnmt* KO ESC lines have varying levels of hypomethylation, which remain largely unchanged after X-irradiation. Any differences in the proliferative ability of the ESC lines were also examined. Growth curves were constructed, as described in section 3.2.3, to characterise cell proliferation in sham treated and 3Gy X-irradiated cells (Figure 3-7, A and B respectively). Results were based on the cumulative population doublings observed over a period of one week.

In agreement with work undertaken by previous research groups, the *Dnmt* KO ESC lines showed no obvious abnormalities with respect to growth rate or morphology (See appendix 7.2) in comparison to the wild type cell line (Jackson *et al*, 2004 and Chen *et al*, 2003). Growth rates were similar between all five ESC lines, both in untreated and 3Gy X-irradiated cells, although the *Dnmt3a*^{-/-} ESC line proliferated slightly faster than the other ESC lines. Cell proliferation was, however, slightly reduced during the first 3 days post treatment in X-irradiated cells compared to sham treated controls, possibly as a result of radiation-induced cell death or cell cycle arrest. The plateau in population doublings post irradiation was most apparent in the wild type and *Dnmt3a3b*^{-/-} cell lines (Figure 3-7), indicating that it occurs irrespective of global methylation levels.

The growth curves appear to become slightly steeper at later time points (>72 hours) in the 3Gy X-irradiated cells, indicating a higher rate of cell proliferation compared to their unirradiated counterparts. This may be due to release from cell-cycle arrest and/or accelerated proliferation of surviving stem cells to recover the population. By

the 7th day, both irradiated and unirradiated cell populations had undergone near identical numbers of population doublings.

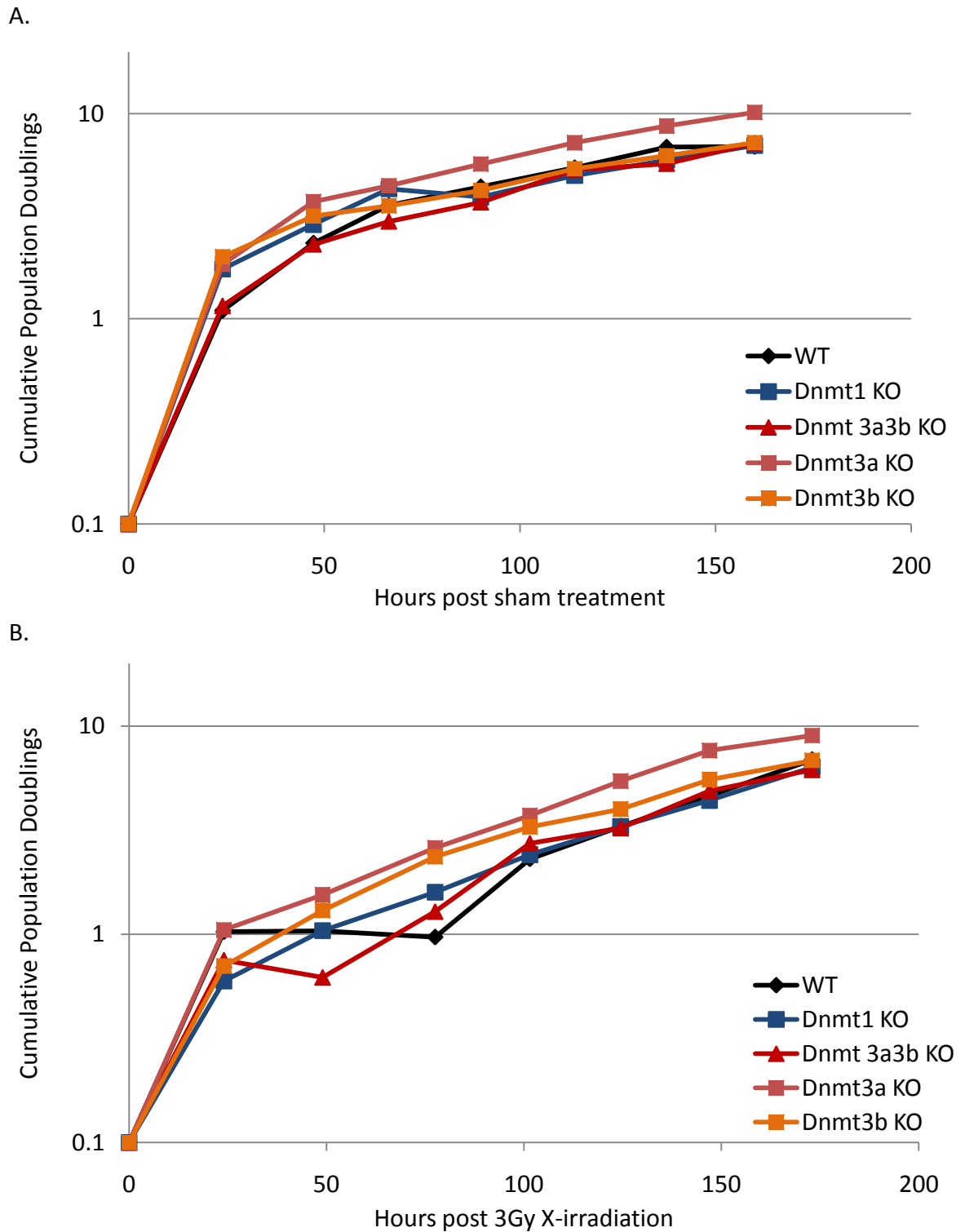


Figure 3-7. Growth Curves. Cumulative population doublings in unirradiated cells (A) and cells irradiated with 3Gy X-rays (B). Each point represents a single measurement.

Cell cycle analysis was carried out, using flow cytometry, to determine the cell-cycle response of the five ESC lines after irradiation with 3Gy X-rays. Asynchronous populations of cells, such as those being studied in the current investigation, contain cells in each phase of the cell cycle. The DNA content of a cell changes as it progresses through these phases, allowing the approximate cell cycle phase to be identified by measuring the nuclear DNA content. Cells in G_0 and G_1 have the normal diploid DNA content for that species ($2n$), whilst cells in G_2 and M phases contain double the amount of DNA ($4n$). Cells in S phase can have varying amounts of DNA anywhere between $2n$ and $4n$. In the current study, flow cytometry with a DNA-binding fluorochrome (PI) was used to determine the cell cycle distribution of cells within asynchronous cultures of each ESC line, as described in section 3.2.4.

Examples of the DNA histograms obtained by flow cytometry, gating and ModFit software analysis are shown for the wild type ESC line at each time point post irradiation (Figure 3-8). A clear change in cell cycle distribution can be seen with time post irradiation. Each of the *Dnmt* KO ESC lines displayed a very similar cell cycle distribution both before irradiation and at each time point thereafter (histograms not shown).

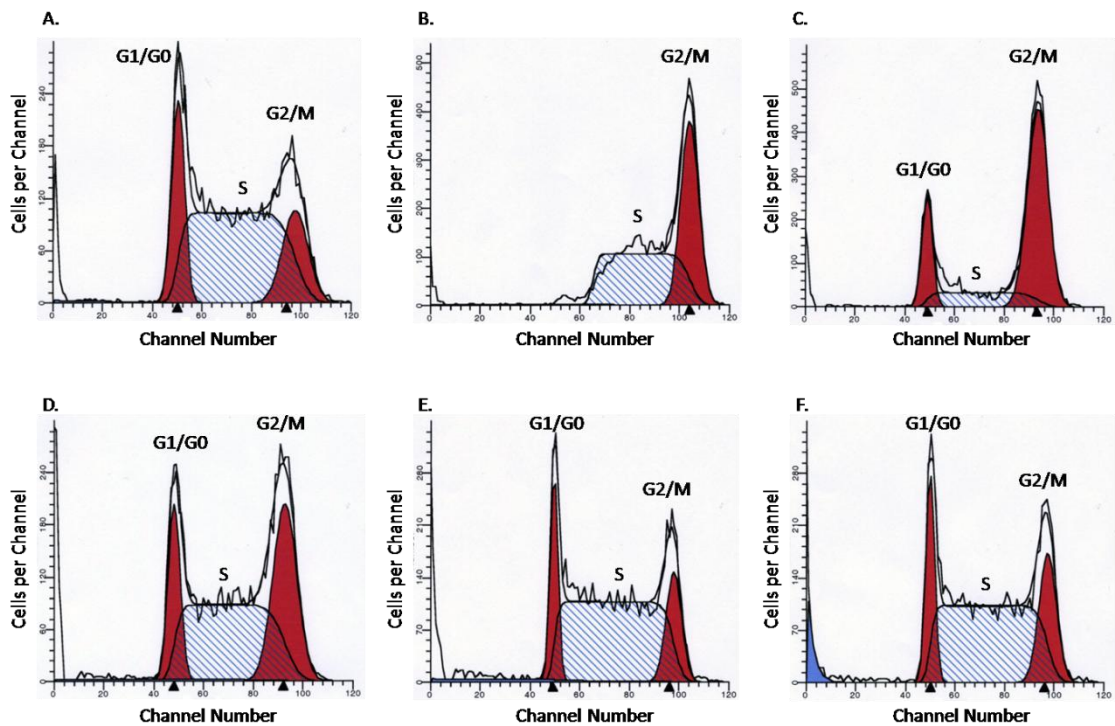


Figure 3-8. Histograms representing cell cycle distribution of the wild type cell line 4 hours post sham treatment (A) and at the following time points post irradiation with 3Gy X-rays: 4 hours (B), 8 hours (C), 24 hours (D), 120 hours/5 days (E), 240 hours/10 days (F).

As covered in section 1.5.1, ESCs differ from somatic cells in that they have a reduced G_1 phase and effectively absent G_1 cell cycle checkpoint in response to ionising radiation (Hong and Stambrook, 2004). This is evidenced in Figure 3-8, at the 4 hour time point post irradiation, by the progression of cells straight through G_0/G_1 and S phases to accumulate at the G_2/M checkpoint. The absence of G_1 arrest in ESCs is thought to be due to compromise of specific signalling pathways which respond to DNA damage. See section 1.5.1.

The cell cycle data generated using CellQuest was analysed using ModFit software to estimate the percentage of cells in each phase of the cell cycle. The combined results from three independent experiments are displayed in Figure 3-9 below.

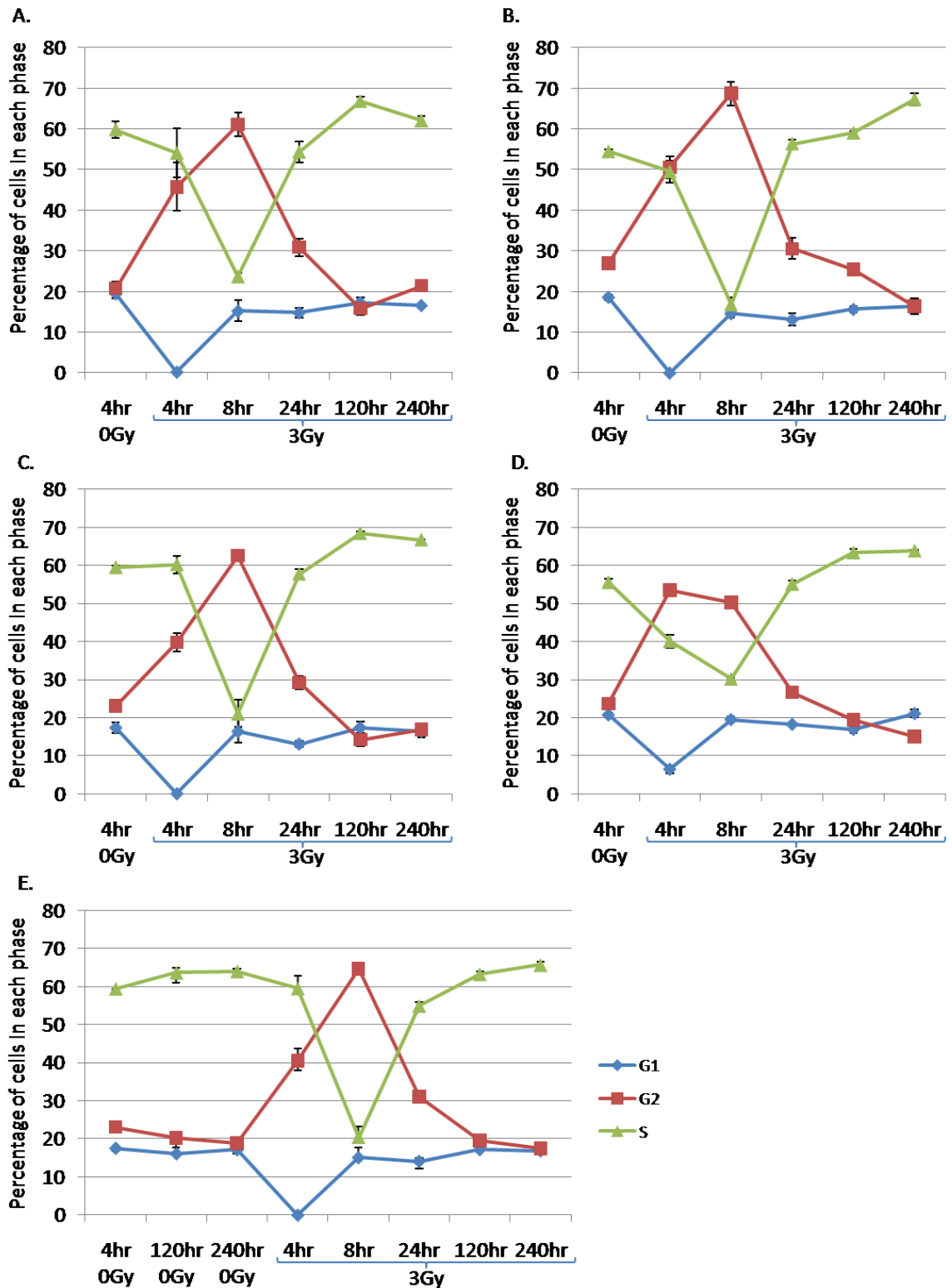


Figure 3-9. Relative percentages of cells in each phase of the cell-cycle at various time points post irradiation with 3Gy X-rays or sham treatment in the following cell lines: wild type (A), *Dnmt1*^{-/-} (B), *Dnmt3a*^{-/-} (C), *Dnmt3b*^{-/-} (D), and *Dnmt3a3b*^{-/-} (E). Each data point represents the mean and error bars represent the SEM.

Under normal growth conditions, all five ESC lines had approximately 20% of cells in the G₀/G₁ phases, 55-65% in the S-phase and less than 20-30% in the G₂ and/or M phases (Figure 3-9). There were small differences between the cell lines in cell-cycle distribution of sham treated cells, for example, *Dnmt1*^{-/-} had a slightly higher proportion of cells in G₂ (p=0.04). However, these differences were small and only marginally significant. In addition, the proportion of cells in each stage of the cell cycle did not alter significantly over the course of the experiment in unirradiated *Dnmt3a3b*^{-/-} cells (p>0.2). Therefore, cell-cycle distribution does not appear to be affected by the varying levels of hypomethylation in these ESC lines.

In response to 3Gy X-irradiation, all cell lines displayed a sharp reduction of cells in the G₀/G₁-phase of the cell-cycle to almost zero, by the 4 hour time point (p<0.0002). This was accompanied by a concomitant increase in the proportion of cells accumulating in the G₂/M phases (p<0.018), indicating arrest at the G₂/M cell-cycle checkpoint. By 8 hours post irradiation the number of cells accumulating in G₂/M phase was at its highest for most cell lines, and far fewer cells were in S phase. The proportion of cells in G₀/G₁ returned to near normal levels 8 hours post irradiation, and remained largely unchanging throughout the remaining time points (p>0.2). The *Dnmt1*^{-/-} cell line again showed a slightly different cell-cycle response to the other ESC lines, with the proportion of cells in G₀/G₁ remaining up to 5% lower than sham levels until between 5 and 10 days post irradiation (p=0.03). However, again this was only a minor deviation from the trend seen in the other ESC lines.

The largest difference in overall cell-cycle response to 3Gy X-irradiation was seen in the *Dnmt3b*^{-/-} cell line. G₂/M phase arrest peaks by 8 hours post irradiation in all cell lines except *Dnmt3b*^{-/-}. This peak in G₂/M is accompanied by a significant decrease in the proportion of cells in S-phase ($p < 0.0004$). In the *Dnmt3b*^{-/-} ESC line, G₂/M arrest, with a corresponding decrease in the proportion of cells in S phase, occurs earlier, peaking 4 hours post irradiation. In addition, there was a significant decrease in the proportion of cells in S phase for the *Dnmt3b*^{-/-} cell line at the 4 hour time point ($p = 0.001$). At the 8 hour time point the overall decrease in the number of cells in S-phase is not as pronounced as the other cell lines, resulting in an earlier decline of G₂/M arrested cells, and an overall smaller proportion of cells arresting in G₂/M at any one time, in *Dnmt3b*^{-/-} than the other cell lines ($p < 0.003$).

Nevertheless, in all cell lines the majority of cells (50-70%) were present in the G₂/M phases 8 hours post irradiation, indicating arrest at the G₂/M cell-cycle checkpoint in response to radiation. 24 hours post irradiation, the proportion of cells in G₂/M began to decrease whilst the proportion of cells in S-phase began to increase to normal levels in all cell lines. By 5-10 days the cell cycle distribution of X-irradiated cells resembled that of the unirradiated controls, with an even distribution of cells in the G₂/M and G₀/G₁ phases, and the majority of cells residing in S phase (Figure 3-9).

A trend was noted in 3Gy treated cells for all cell lines except *Dnmt3a3b*^{-/-}, whereby the proportion of cells in S phase overshot slightly at the 5 and/or 10 day time points compared to day one sham levels ($p < 0.04$). Although only marginally significant, this

small change in cell-cycle distribution may reflect the increased population doubling time observed in the ESC lines after 3Gy X-irradiation (Figure 3-7).

Finally, the radiosensitivity of the ESC lines was characterised to determine whether this correlates with their methylation levels. Bone marrow is one of the most radiosensitive mammalian somatic tissues (Dörr, 2009). Due to the apparent inverse correlation between methylation levels and radiosensitivity in somatic tissues (see Figure 1-3), it was hypothesised that the ESC lines containing the lowest levels of cytosine methylation would show the greatest sensitivity to ionising radiation.

Radiosensitivity was assayed using the clonogenic assay after acute irradiation as an asynchronous cell population with 0-7Gy X-rays. Two similar methods were used, which are described in section 3.2.2. The results were found to be similar for both methods ($p > 0.05$ for all cell lines) and were subsequently combined. Ten days after irradiation and seeding at low density, ESC colonies 0.5-3mm in diameter were clearly visible and were scored without staining. Plating efficiencies for the five ESC lines ranged between 11-21% (see Table 3-1). The surviving fraction (SF) of cells at each dose was calculated after correction for plating efficiency and is presented as a graph in Figure 3-10.

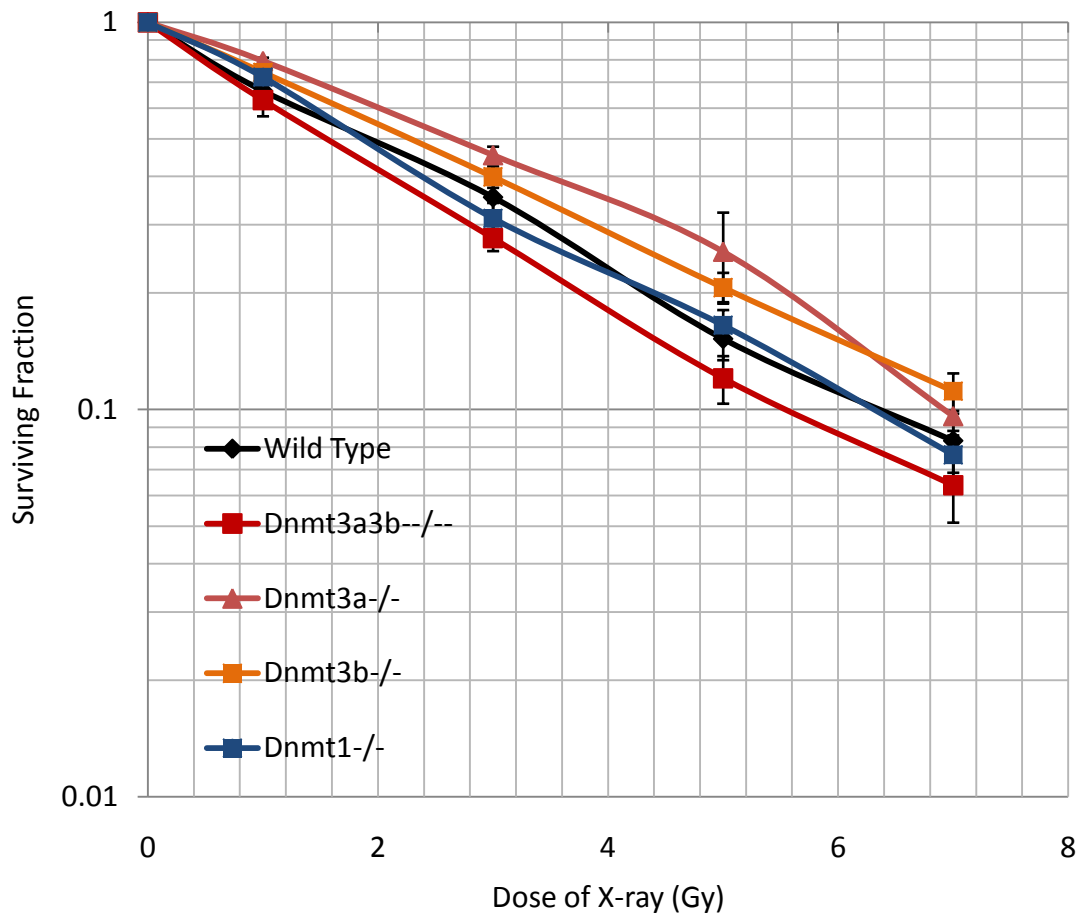


Figure 3-10. Dose-response curve of the ESC lines after irradiation with 0-7Gy X-rays. Each data point represents the mean and SEM of at least 3 independent experiments.

Irradiation resulted in a dose-dependent decrease of the surviving fraction (SF) in all five ESC lines. Survival curves for most mammalian cells exposed to low LET radiation such as X-rays show some downward curvature (Hall, 2000). However, none of the murine ESC lines in the present study showed any evidence of a shoulder or continuous curvature. Irradiation with X-rays resulted in a near exponential survival curve, similar to that described by Clutton *et al* (1996) in their study of three other wild type ESC lines. The mean lethal dose (D_0) for each cell line was therefore calculated using the least squares fitting procedure (see Table 3-1).

ESC Line	Mean Plating Efficiency	Mean Lethal Dose (D ₀ SF 37%)
Wild Type (J1)	21%	2.81Gy
<i>Dnmt1</i> ^{-/-}	15%	2.71Gy
<i>Dnmt3a3b</i> ^{-/-}	11%	2.29Gy
<i>Dnmt3a</i> ^{-/-}	19%	3.35Gy
<i>Dnmt3b</i> ^{-/-}	13%	3.19Gy

Table 3-1. ESC line plating efficiencies and mean lethal dose of X-irradiation.

Analysis of the survival curves (SF3Gy and D₀) using a 2-tailed T-test showed no significant difference between the wild type cell line and any of the hypomethylated *Dnmt* KO cell lines after correction for multiple testing. However, the *Dnmt3a3b*^{-/-} cell line was significantly more radiosensitive than *Dnmt3a*^{-/-} and *Dnmt3b*^{-/-} (SF3Gy, p=0.005 and p=0.015 respectively). Although not statistically significant, *Dnmt3a*^{-/-} and *Dnmt3b*^{-/-} were consistently more radio-resistant than the wild type and *Dnmt1*^{-/-} ESC lines, whilst *Dnmt3a3b*^{-/-} remained consistently more radiosensitive. This implies that the DNMT3 family of enzymes may contribute to a small extent in determination of cellular radiosensitivity, and that absence of a single *de novo* methyltransferase, particularly DNMT3A, may in fact be beneficial for these ESCs.

3.4 Discussion

3.4.1 The ESC lines display a range of states of hypomethylation in comparison to somatic cells

Using a panel of five ESC lines, derived from and including the J1 wild type, the roles played by each of the three main murine DNA methyltransferase enzymes in maintenance of DNA methylation, and cellular sensitivity to ionising radiation were investigated. Genetically, the cell lines differed only by the methyltransferase that was catalytically inactivated. This resulted in relatively large decreases in global cytosine methylation levels, measured by HPLC-UV (Figure 3-4). The wild type ESC line had a similar methylation level to that of murine bone marrow, and the *Dnmt* KO cell lines provided a range of states of hypomethylation with which to assess response to ionising radiation.

In contrast to results obtained by previous researchers working *in vivo*, cytosine methylation levels of the ESC lines were not significantly altered in response to ionising radiation exposure (Figure 3-5; Figure 3-6). However, this is not entirely surprising, as the phenomenon of radiation-induced alterations in DNA methylation level appears to be specific to certain cell/tissue types (Koturbash *et al*, 2005; Pogribny *et al*, 2004; Raiche *et al*, 2004; Tawa *et al*, 1998). For example, Tawa *et al* (1998) were able to show a ~40% reduction in murine liver methylcytosine levels within 8 hours after 4Gy X-irradiation, which persisted for >72 hours. However, brain and spleen samples harvested from the same mice showed no such alteration in methylation levels (Tawa *et al*, 1998). Thus, it is possible that ESCs simply do not display altered methylation

levels in response to 3Gy X-irradiation. Alternatively, radiation-induced DNA hypomethylation may be less likely to manifest under cell culture conditions than *in vivo*, possibly due to factors such as the supply of fresh folate in the media. Such a possible effect of cell culture variables on radiation-induced DNA hypomethylation is indicated by the fact that results produced using CHO cells by one research group (Kalinich *et al*, 1989) were not reproducible by another group using the same cell line (Tawa *et al*, 1998).

3.4.2 ESCs lack a G1 checkpoint and exit G2 arrest around 24 hours post irradiation

As discussed in section 1.5, cells undergo three possible reactions in response to radiation-induced DNA damage: cell cycle arrest; repair of the damage; or apoptosis or necrosis. The proliferative ability and cell-cycle response of the ESC lines were therefore investigated, both prior to and post irradiation with 3Gy X-rays.

The *Dnmt* KO ESC lines showed no obvious abnormalities in growth rate compared to the wild type cell line, both in untreated and X-irradiated cells. In response to irradiation, cell proliferation ability was reduced for ~3 days in all cell lines, irrespective of DNA cytosine methylation levels. The rate of cell proliferation then increased in the 3Gy irradiated cells compared to their unirradiated counterparts. It is not clear why such stimulation in cell proliferation might occur, but shortening of the cell cycle and rapid recovery to normal cell population levels after radiation-induced cell death and release of mitotic delay is a common phenomenon observed *in vivo* (Giotopoulos *et al*, 2006; Tsubouchi and Matsuzawa, 1974). Tumour repopulation by surviving tumour

stem cells is also commonly observed between radiotherapy fractions and after cessation of treatment (Kim and Tannock, 2005). Moreover, it is possible that the reduction in population size caused by radiation-induced cell death in the current study encouraged selection for ESCs with certain survival characteristics, such as increased ability to proliferate. The accumulation of such traits in ESCs throughout continued culturing is termed 'culture adaptation' (Harrison *et al*, 2007). Extension of the growth curve time points would allow determination of whether the increased growth rate in the X-irradiated cell lines slowed to that of the unirradiated controls (repopulation), or continued to exceed them (culture adaptation).

There were no marked differences between the ESC lines in their normal (unirradiated) cell cycle distributions. In addition, the cell cycle distribution of the *Dnmt3a3b*^{-/-} cell line remained consistent in sham treated cells throughout the duration of the experiment, indicating that global levels of DNA cytosine methylation do not affect the cell cycle distribution in these ESCs. In response to ionising radiation, the ESCs displayed a characteristic lack of the G₁ phase cell cycle checkpoint, and accumulation at the G₂/M checkpoint instead. The only notable difference in cell cycle response to irradiation was observed in the *Dnmt3b*^{-/-} cell line, which entered G₂ arrest and showed a decline of cell numbers in S phase slightly earlier than the other cell lines. However, the *Dnmt3b*^{-/-} cell line maintained G₂ arrest for longer than the other cell lines, with the effect of exiting at roughly the same time post irradiation. It is not clear why absence of DNMT3B in particular resulted in a slightly earlier and prolonged G₂ checkpoint activation, but it may reflect a role of this enzyme in the ESC cell cycle

response, or increased difficulty in repairing damage at sites which are usually the target for methylation by DNMT3B.

3.4.3 Radiosensitivity does not correlate with hypomethylation

Finally, there was no significant difference in sensitivity to ionising radiation between the wild type cell line and any of the *Dnmt* KO cell lines. This indicates that substantial reductions in global DNA methylation do not correlate with alterations in sensitivity to X-irradiation in ESCs. However, other groups have previously shown that reducing methylation levels in somatic and tumour cells results in increased sensitivity to ionising radiation (Dote *et al*, 2005; Narayan *et al*, 2000). Possible reasons for these conflicting results include cell type specific differences in the endogenous DNA methylation levels and expression levels of the DNA methyltransferase enzymes. It is possible that the methylation level of the wild type ESCs is already too low to allow any further effect on radiosensitivity to be seen in the hypomethylated *Dnmt* KO ESC lines. Furthermore, the observation by Narayan *et al* (2000) that hypomethylated lymphocytes derived from ICF syndrome patients are significantly more radiosensitive than lymphocytes from unaffected individuals is evidence of a correlation rather than cause and effect. It is therefore possible that the heightened radiosensitivity of cells from ICF syndrome patients is a result of another facet of the syndrome.

The lack of any shoulder on a survival curve is generally accepted as indicating sensitivity to ionising radiation or inability to repair sub-lethal damage (Hall, 2000). Exponential survival curves such as those displayed in Figure 3-10 have been observed previously for wild type ESCs, and the lack of a shoulder has been suggested to reflect

the propensity for ESCs to undergo apoptosis (Clutton *et al*, 1996; de Waard *et al*, 2003). It is tempting to speculate that this high propensity for apoptosis in ESCs (Roos *et al*, 2007) has masked the effect of reduced methylation levels on radiosensitivity in the *Dnmt* KO ESC lines. As the propensity of ESCs to undergo apoptosis in response to DNA damage decreases upon differentiation (Roos *et al*, 2007), future work could involve inducing differentiation in the mESC lines and then determining the effect of *Dnmt* KO on radiosensitivity.

Nevertheless, the results of the current study indicate that the *de novo* methyltransferase enzymes, DNMT3A and DNMT3B, may play a minor role in modulating sensitivity to X-rays in ESCs. Surprisingly, functional absence of one *de novo* methyltransferase enzyme was found to have a slight radioprotective effect, whilst KO of both resulted in comparative radiosensitisation ($p < 0.002$ and $p < 0.009$ at 3Gy and 5Gy respectively). This implies that absence of a single *de novo* methyltransferase, particularly DNMT3A, may in fact be beneficial for ESCs. However, the differences observed were still modest.

3.4.4 Summary

In a panel of five mouse ESC lines exhibiting varying degrees of hypomethylation, no large differences in radiosensitivity, growth characteristics or cell-cycle distribution were observed. All five ESC lines displayed an exponential survival curve, which may reflect the propensity for ESCs to undergo apoptosis in response to DNA damage (Clutton *et al*, 1996; de Waard *et al*, 2003). However, lack of a single *de novo* methyltransferase enzyme, particularly DNMT3A, was found to have a slight radio-

protective effect, whilst absence of both DNMT3A and DNMT3B was found to result in comparative radiosensitivity. In response to 3Gy X-irradiation the ESCs bypass the G₁ checkpoint and arrest in G₂/M phase. However, the cells start to come out of G₂/M checkpoint arrest by 24 hours post 3Gy X-irradiation. By 5-10 days after irradiation the ESCs display a normal cell cycle distribution and slightly increased doubling times.

Although these results differ from some previously published research correlating hypomethylation with radiosensitisation, possible reasons exist for the discrepancies, including cell type specific differences in endogenous DNA methylation levels and expression levels of the DNMT enzymes. In addition, it is tempting to speculate that the propensity of ESCs to undergo apoptosis may have masked the effect of hypomethylation on radiosensitivity. There appears to be a far more direct link between methylation levels and genomic stability. This was assessed in the panel of ESCs lines, and is discussed in chapter 4.

4 Chapter 4. Genomic Stability: Mutation Rate at the *Hprt* Gene Locus and the Influence of Hypomethylation at Specific Repeats.

4.1 Introduction

Radiation-induced delayed genomic instability is characterised by the persistent expression of elevated levels of cell death, mutations or cytogenetic aberrations at a delayed period after irradiation, which can be detected in the unirradiated progeny of irradiated cells (Morgan, 2003) or animals (Barber *et al*, 2006) several generations after irradiation. The mechanism by which radiation-induced delayed genomic instability is propagated is currently poorly understood (Wright, 2010). Radiation induced delayed genomic instability is a genome-wide process that does not appear to arise from mutation of genes involved in genome maintenance (see section 1.7).

Several processes have been suggested as a possible cause of radiation-induced delayed genomic instability, including oxidative stress (Clutton *et al*, 1996), the secretion of clastogenic factors by cells subjected to stresses (Emerit *et al*, 1994) and epigenetic factors such as microRNAs (Koturbash *et al*, 2007; Ilnytskyy *et al*, 2008; Valeri *et al* 2010) and DNA methylation (Kaup *et al*, 2006). Given that the trans-generational instability observed in the studies by Dubrova *et al* (1998; 2002) was inherited paternally, the factor(s) responsible for propagating radiation-induced delayed genomic instability must be transmissible through the male germ line. As a

DNA-associated factor, DNA methylation is a suitable candidate for such transmission and potential propagation of the radiation memory (Dubrova *et al*, 2003).

Previous research groups have demonstrated a link between DNA methylation levels and genomic instability (Chen *et al*, 1998; Dion *et al*, 2008; Gonzalo *et al*, 2006; Tuck-Muller *et al*, 2000; Wang and Shen, 2004; Yamamoto *et al*, 2002). There are multiple ways in which dysregulation of DNA methylation could contribute to genomic instability, including inappropriate silencing of tumour suppressor genes (Goto *et al*, 2010) or genes involved in DNA repair or regulation of cell proliferation (Yamamoto *et al*, 2002), hypomethylation of pericentromeric and sub-telomeric satellite repeats (Gonzalo *et al*, 2006; Tuck-Muller *et al*, 2000), and altered DNA methylation and activation of endogenous retroviral elements (Takai *et al*, 2000; Symer *et al*, 2002; Howard *et al*, 2008). See section 1.3.

To provide a measure of genomic stability in the five mouse ESC lines used in the current study, mutation rates were analysed at the X-linked *Hprt* gene. As the ESC lines were derived from a male mouse, this gene locus was hemizygous, allowing direct detection of mutants using selective media, as described in 4.2.1. Selection for mutants was conducted 23-25 population doublings post sham treatment or 3Gy X-irradiation to allow determination and comparison of the *de novo* mutation rate as well as the radiation-induced delayed mutation rate in the progeny of the irradiated cells. Any mutant colonies that were produced were picked and analysed for mutation type using a series of PCRs encompassing each exon of the *Hprt* gene. PCR products were sequenced if further characterisation was required.

The methylation levels of several endogenous retroviral elements were characterised using Southern blotting. Roughly 45% of the human genome is derived from transposable elements (see Table 4-1), which are methylated and silenced in normal mammalian somatic cells. Probes were designed to specifically bind to regions of the active transposable elements that may be differentially methylated according to their expression status. This included the 5' LTR of IAP elements, the 5' monomer sequences of the mouse L1 elements and entire B1 and B2 SINE sequences. However, it must be noted that hypomethylation of these repeats does not necessarily indicate active retrotransposition. Methylation levels of the structural minor satellite repeats were also analysed by Southern blotting. These sequences form the murine pericentromeric repeats corresponding to the human classical satellite sequences, which are hypomethylated and the main site for genomic rearrangements in lymphocytes from patients with ICF syndrome (Choo, 1997; Garagna *et al*, 2002; Sawyer *et al*, 1995; Tiepolo *et al*, 1979; Tuck-Muller *et al*, 2000).

Type of transposable element (subclass)	Fraction of human genome*	N ^o of copies in human genome (in thousands)*	Fraction of mouse genome*	N ^o of copies in mouse genome (in thousands)*
LINE	21%	870	19.2%	660
(LINE1)	17.4%	520	18.8%	600
SINE	13.6%	1,560	8.2%	1,500
(Alu human)	10.6%	1,090	-	-
(B1/B2/B4 mouse)	-	-	2.7%	560/350/390
LTR elements	8.5%	440	9.9%	630
DNA transposons	3%	290	0.9%	110

Table 4-1 The fraction of the draft human genome sequence (%) comprised by currently recognised members of each major class of transposable element, and the number of copies detected, taken from Lander *et al* (2001). Data for the mouse is

taken from the Mouse Genome Sequencing Consortium (2002). *All values given are approximate.

4.2 Chapter-Specific Methods and Materials

4.2.1 Genomic Stability Measured by Mutation Rate at the *Hprt* Gene

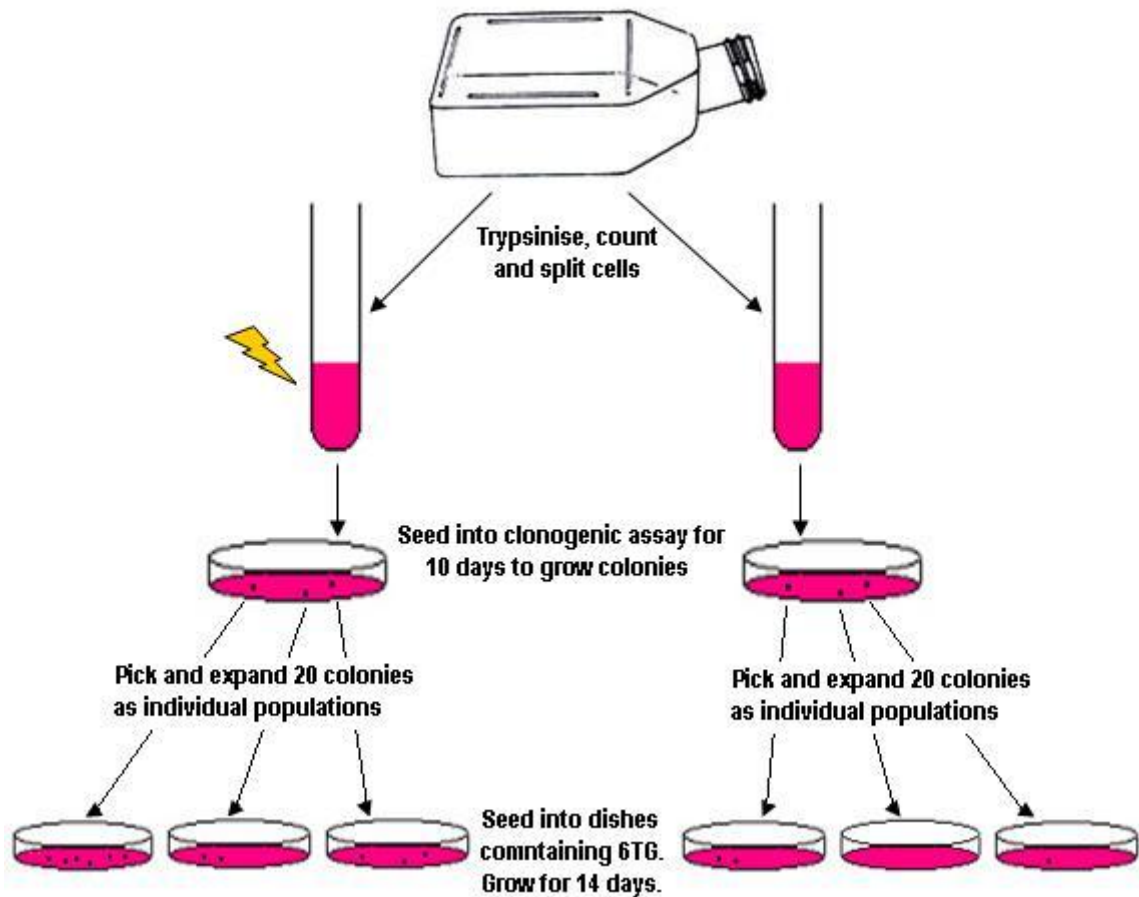


Figure 4-1. Schematic to outline the procedure for detecting mutations in the *Hprt* gene. The colonies that grew in media containing 6TG were picked and analysed.

4.2.1.1 Establishment of clones

Cells were trypsinised and counted. Three million cells were transferred into 2 labelled eppendorf tubes, which were centrifuged at 1,000rpm for 5 minutes, and the supernatant removed by aspiration. The tubes were placed inside a polystyrene box for transport to/from the X-ray machine. After irradiation with 3Gy X-rays or sham treatment, as described in section 2.4, the cells were resuspended in complete ES media to a concentration of 1 million cells per ml, mixed and serially diluted to a concentration of 10,000 cells per ml. 30 μ l of cell solution was added to a gelatinised well of a 6-well plate containing 3ml complete ES media, and the contents swirled to mix. The plate was placed in the 37°C incubator and colonies allowed to grow for 8-10 days. Medium was changed every second day.

For each cell line, 20-25 individual sham and 3Gy x-ray treated colonies were picked for expansion as individual clonal populations. Medium was removed from the well by aspiration, and the colonies covered with PBS. Individual colonies of a variety of sizes were randomly selected and removed from the gelatinised surface using a 20 μ l pipette. They were placed into separate round-bottom wells of 96 well plates containing 10 μ l trypsin-EDTA and incubated at 37°C for 2 minutes. 130 μ l complete ES medium was added to neutralise the trypsin, and the contents of the well were transferred to a gelatinised, flat-bottom well of a 96 well plate to grow. Medium was changed every 2 days until the cells had reached confluence, at which point they were passaged into a 24 well culture dish. When each clone reached confluence in a 6-well

plate, half of the cells were frozen as an aliquot for future use, using the method described in section 2.2.5. The remaining cells were maintained in culture.

4.2.1.2 Selection of cells containing mutation(s) within the *Hprt* gene

When each clone was confluent in a 75cm flask (T75), the cells were trypsinised and counted. When each clone had proliferated to $20\text{-}30 \times 10^6$ cells, 4×10^6 of the cells were seeded into a gelatinised 9cm petri dish containing $2\mu\text{g/ml}$ 6-thioguanine (6TG) in 10ml media and allowed to grow for 10 days in the 37°C incubator. To calculate the plating efficiency, 3 clonal populations were selected at random for each cell line and treatment condition and 1,000 of the cells were seeded into a petri dish containing complete ESC media without 6TG. These were allowed to grow alongside the cells in selective media, and the number of colonies produced after 10 days were counted. Medium was changed every second day.

The metabolites of 6TG are toxic to mammalian cells. However, cells which have a mutation in the *Hprt* gene do not metabolise this compound and proliferate to produce visible colonies during the 10-day incubation period. Colonies that were visible to the naked eye were counted, picked as described in section 4.2.1.1, transferred to a labelled eppendorf and stored at -20°C until DNA extraction and characterisation of the mutation by PCR and/or sequencing. See sections 2.3.3, 2.5 and 2.6 for methods. The mutation rate was calculated using Luria-Delbrück fluctuation analysis implemented by Salvador, which runs in Mathematica.

4.3 Results

4.3.1 *Hprt* mutation rate

Selection for ESCs carrying functional mutations in the *Hprt* gene was carried out using approximately 20 individual clonal populations, each expanded from a single irradiated or sham treated ESC, per cell line and treatment condition. See Figure 4-1. The exact number of selections carried out for each ESC line, the numbers of cells screened, the colony counts and the calculated mutation rates, are detailed in Table 4-2.

Cell line and condition	Number of independent selections	Number of cells screened per selection	Average plating efficiency	Number of mutations per selection†	Mutation rate‡
Wild Type sham	25	4×10^6	55%	0(22), 1(2), 3(1)	5.7×10^{-8}
<i>Dnmt1</i> ^{-/-} sham	19	4×10^6	52%	0(6), 1(7), 2(2), 3(1), 4(1), 12(1), 97(1)	4.4×10^{-7}
<i>Dnmt3a3b</i> ^{-/-} sham	25	4×10^6	51%	0(22), 1(2), 2(1)	6.0×10^{-8}
<i>Dnmt3a</i> ^{-/-} sham	19	4×10^6	38%	0(16), 1(2), 2(1)	1.1×10^{-7}
<i>Dnmt3b</i> ^{-/-} sham	22	4×10^6	51%	0(16), 1(1), 1(4), 16(1)	8.7×10^{-8}
Wild Type 3Gy	20	4×10^6	49%	0(11), 1(5), 2(1), 3(1), 9(1), 13(1)	2.8×10^{-7}
<i>Dnmt1</i> ^{-/-} 3Gy	19	4×10^6	49%	0(7), 1(5), 2(2), 3(2), 6(2), 29(1)	4.5×10^{-7}
<i>Dnmt3a3b</i> ^{-/-} 3Gy	20	4×10^6	45%	0(16), 1(3), 6(1)	1.2×10^{-7}
<i>Dnmt3a</i> ^{-/-} 3Gy	20	4×10^6	41%	0 (17), 1(2), 2(1)	9.5×10^{-8}
<i>Dnmt3b</i> ^{-/-} 3Gy	21	4×10^6	48%	0(18), 2(1), 7(1), 8(1)	8.5×10^{-8}

Table 4-2. Details of the *Hprt* mutation rate selections carried out for each cell line and treatment condition. † The number in brackets indicates the number of selections in which the adjacent number of drug-resistant colonies was observed. ‡ Calculated using

Luria Delbrück fluctuation analysis and corrected for plating efficiency. Average plating efficiency was calculated as described in section 4.2.1.2.

It could be confirmed from the colony counts that no founder mutations were present in any of the clonal populations, as no more than 97 colonies were observed in any selection dish, each of which was seeded with 4×10^6 ESCs. The plating efficiencies were very similar for each of the cell lines. After correction for plating efficiency, a total of approximately 28.9×10^6 - 55×10^6 cells were screened per ESC line and treatment condition. The majority of the clonal populations produced no colonies. However, greater numbers of petri dishes containing colonies were observed in selections of *Dnmt1*^{-/-} ESCs from both treatment groups, and wild type ESCs which had been subjected to 3Gy X-irradiation. In addition, greater variation in the number of colonies produced in each dish was observed in these ESC clones. Correspondingly, an elevated mutation rate was calculated in the *Dnmt1*^{-/-} sham and 3Gy-treated ESCs and the wild type 3Gy treated ESCs, compared to all other ESC lines and treatment conditions, using Luria-Delbrück fluctuation analysis. The calculated mutation rates at the *Hprt* locus are displayed graphically in Figure 4-2.

As discussed in section 3.3 all of the ESC lines had similar doubling times, and underwent 23-25 population doublings between sham treatment or 3Gy X-irradiation and being seeded into selective media containing 6TG. The *Dnmt3a3b*^{-/-} ESCs were p#14-17 at the time of treatment, and p#20-26 at the point of seeding into selective media. Thus, according to the results presented in Figure 3-4 they would have had very similar or lower methylation levels than the *Dnmt1*^{-/-} ESCs at the time of seeding into selective media.

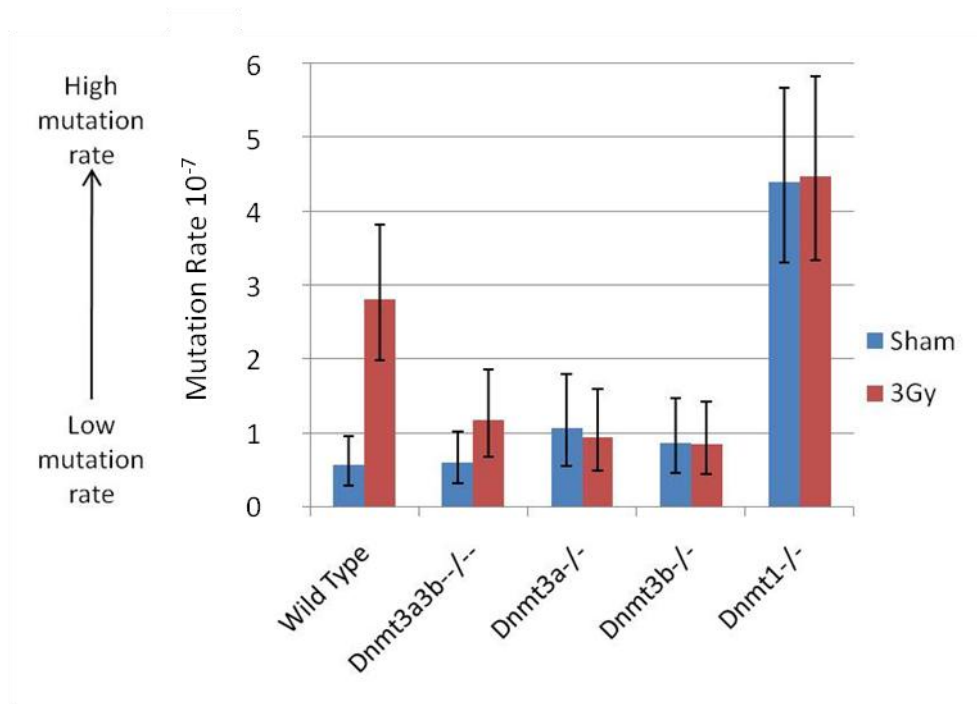


Figure 4-2. *Hprt* gene mutation rates 23-25 population doublings after 3Gy X-irradiation or sham treatment. Columns represent the mutation rate, calculated using Luria-Delbrück fluctuation analysis, \pm the 95% confidence intervals. *Dnmt3a3b*^{-/-} ESCs were p#20-26 at the time of selection for mutants.

However, the *Dnmt1*^{-/-} ESCs have a significantly elevated *de novo* mutation rate in comparison to all of the other ESC lines ($p < 5.6 \times 10^{-5}$), including *Dnmt3a3b*^{-/-} ($p = 3.2 \times 10^{-6}$). Although the *Dnmt3a3b*^{-/-} ESC line had a similar methylation level to the *Dnmt1*^{-/-} ESC line, the mutation rate determined from the sham treated clones was not significantly different from that of the wild type ESC line ($p = 0.9$). Thus, it appears that the elevated mutation rate detected in the *Dnmt1*^{-/-} ESC line is not simply a result of global hypomethylation, but a result of the absence of a property or function specific to DNMT1. The *Dnmt3a*^{-/-} and *Dnmt3b*^{-/-} ESCs were also found to have very similar low *de novo* mutation rates to the wild type ESC line ($p > 0.2$).

The *Dnmt1*^{-/-} ESCs also showed a significantly elevated mutation rate in the 3Gy X-irradiated clones. However, this was not significantly different to the *de novo* mutation rate for this cell line ($p=0.9$). Similarly, none of the other *Dnmt* knock out ESC lines showed a significantly elevated mutation rate in the 3Gy X-irradiated clones in comparison to the sham treated controls ($p>0.4$). Thus, the *Dnmt* knock out ESC lines showed no evidence of the classic occurrence of radiation-induced delayed genomic instability. The wild type ESC line, however, did display a significantly elevated mutation rate in the 3Gy X-irradiated clones in comparison to the sham treated control clones ($p=1.6\times 10^{-4}$), indicating the occurrence of radiation-induced delayed genomic instability. The fact that this was observed in the wild type cell line alone indicates that absence of the DNA methyltransferase enzymes, or disruption of the normal methylation pattern, may potentially inhibit the mechanism behind radiation-induced delayed genomic instability.

4.3.2 *Hprt* mutation spectrum

The types of mutations present at the *Hprt* gene in the picked colonies were characterised using PCR, in order to determine the mechanisms that might be responsible for the differing mutation rates between the ESC lines. Primers were taken from a previous paper by Meng *et al* (2004) and are listed in Table 2-2. These primers were designed to amplify each of the 9 exons within the X-linked *Hprt* gene, in addition to a control primer pair which amplified exon 2 of the unlinked K-ras gene on chromosome 6. This method allowed the detection of large deletions encompassing the whole gene, smaller deletions encompassing one or a few exons, and insertions or

deletions within the exons. Any mutations thought to be a result of insertions were confirmed and characterised by sequencing, as described in section 2.6. In the instances where no mutations could be detected by PCR, it was assumed that the colony had survived selection as a result of either an epigenetic alteration, point mutation of one or a few bases, or a frameshift mutation. These were grouped into a classification of 'other' mutations. Figure 4-3 displays the spectra of mutations obtained from the 6TG-surviving colonies that were successfully picked, extracted and characterised for each ESC line and treatment condition.

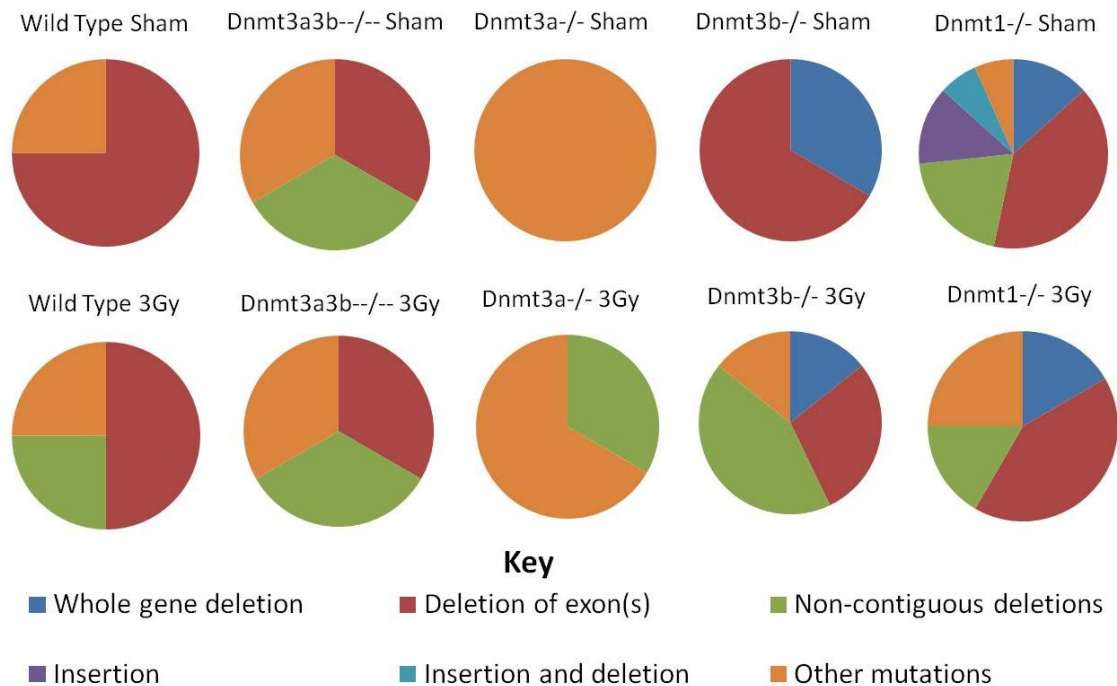


Figure 4-3. Spectrum of *Hprt* gene mutations observed in the ESC lines 23-25 population doublings after 3Gy X-irradiation or sham treatment.

The minimum range of mutations detected in each cell line and treatment condition are displayed in Figure 4-3. When multiple colonies from a single clonal population produced the same result during mutation analysis, they were assumed to share the

same clonal mutation, and have been represented as a single mutation. Interestingly, multiple deletions of non-contiguous exons were observed in sham-treated clones from the two most hypomethylated ESC lines (*Dnmt1*^{-/-} and *Dnmt3a3b*^{-/-}). For example, exon 1 and exons 5-9 were found to be deleted in a *Dnmt3a3b*^{-/-} sham colony, and exons 1-4, 6 and 9 were deleted in a single *Dnmt1*^{-/-} sham colony. See Table 4-3 below. Notably, all of the ESC lines displayed these non-contiguous exonic deletions in clones which were derived from 3Gy X-irradiated cells. The deletions do not appear to follow any particular pattern. They will be discussed in section 4.4.3.

Sample	<i>Hprt</i> Exons								Control
	1	2	3	4	5	6	7.8	9	K-ras
<i>Dnmt1</i> ^{-/-} sham	N	N	N	N	P	N	P	N	P
	N	N	P	P	P	N	P	P	P
	N	N	N	N	P	N	P	N	P
<i>Dnmt3a3b</i> ^{-/-} sham	N	P	P	P	N	N	N	N	P
Wild Type 3Gy	P	N	P	P	P	P	N	P	P
	P	P	P	N	P	P	N	P	P
<i>Dnmt1</i> ^{-/-} 3Gy	P	N	P	P	P	P	N	P	P
	P	N	P	P	P	P	N	P	P
<i>Dnmt3a3b</i> ^{-/-} 3Gy	N	N	P	P	N	P	N	N	P
	N	P	P	N	N	P	N	N	P
<i>Dnmt3a</i> ^{-/-} 3Gy	N	N	N	N	P	P	P	N	P
<i>Dnmt3b</i> ^{-/-} 3Gy	N	P	N	P	P	P	P	P	P
	N	N	P	P	N	P	P	P	P
	P	P	N	N	N	N	P	N	P

Table 4-3. The non-contiguous exonic deletions observed in the ESC lines are displayed. Exons for which a PCR product was present are identified by 'P' in a blue box. Exons for which no PCR product was detected are denoted 'N' in a red box.

Relative distances between the various deleted exons, and the sizes of the exons in the murine *Hprt* gene, are represented in Figure 4-4.

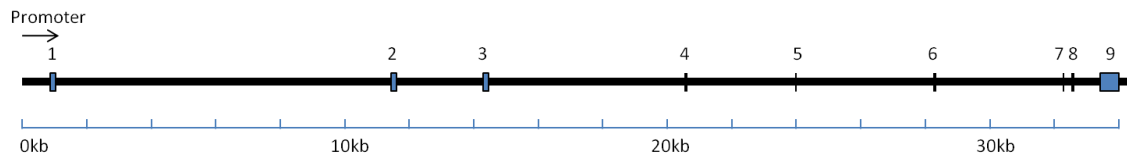


Figure 4-4. Schematic of the murine *Hprt* gene showing the promoter region and all 9 exons. The scale below indicates the size of the gene and relative distances between exons in kilobases.

The *Dnmt1*^{-/-} ESC line, which has the highest spontaneous mutation rate as calculated by Luria-Delbrück fluctuation analysis, was also found to display the widest variety of mutation types in comparison to the sham-treated clones from the other ESC lines. This indicates that a wider variety of different mutational processes may be contributing to the elevated mutation rate observed in the *Dnmt1*^{-/-} ESC line. In particular, *Dnmt1*^{-/-} cells were the only ESCs to demonstrate the occurrence of active retrotransposition, as indicated by the presence of insertions involving two different subfamilies of non-autonomous SINE retrotransposons. A B2 SINE was detected just 5' of exon 3 in the *Hprt* gene in a single colony produced by a *Dnmt1*^{-/-} sham-treated clonal expansion, and a B1 SINE/Alu insertion was detected just 5' of exon 6 in the *Hprt* gene in all ten colonies analysed from the *Dnmt1*^{-/-} sham-treated clonal expansion which produced 97 colonies in total. The sequences of these insertions and the surrounding *Hprt* genomic DNA are shown in Figure 4-5 and Figure 4-6.

5'-cctcatgccccaaatcttacctttggtatatgaaaaatagctccacttctgcaaaatattgctttatgaagtaagaatt
 cccttcatagagacaaggaatgtgtcctgtaaaagtttaatgtgtaagaagatttgttttttttttttttttttttttttttttttt
tttttttttttttttaaatatttatttattatataatgtaagtacactgtagctgtcctcagacactccagaagagggagtc
gatcttggtatggatggcgtgagccaccatgtggttgcctgggattgaaactcctgaccttcggaagagcagtcgggtgctctt
accactgagccatctcaccagccccagaagatttgtttataaaagataaatattcagaatcttcttttaattctgattttat
 ttctatagGACTGAAAGACTTGCTCGAGATGTCATGAAGGAGATGGGAGGCCATCACATTGTGG
 CCCTCTGTGTGCTCAAGGGGGGCTATAAGTTCTTTGCTGACCTGCTGGATTACATTAAGCACT
 GAATAGAAATAGTGATAGATCCATTCTATGACTGTAGATTTTATCAGACTGAAGAGCTACTG
Tgtaagataattaacttataattaaataatagggcc-3'

Figure 4-5. DNA sequence of *Hprt* gene exon 3 and surrounding introns, and the B2 SINE insert. Red underlined = primers; lower case = intron; upper case = exon; B2 SINE insert = black underlined; dark grey shading = duplicated DNA sequence adjacent to the insert; light grey shading = duplicated sequence adjacent to B2 SINE insert characterised in E14.1 wild type ESCs by Tsuda *et al* (1997).

5'-ttaaggccaccaacctgaactacatagcaagaccctgtgtgaaatacaacagaaagatttgtgtatgtgtgcagtgcct
 acatgtagacgttccatttactgttttgaccttgccacatctatgcaatctagttctggggactgacattacctctgcttactta
 gagccagataggttacaagttccagactatctctgtgtgaattgtggtgagattttgtataactaaaaatgaatggcattgt
 gtcgtggaatactagaatattgcatttgaattgtatgttgaataaggatgatttttttaattgtggtggtttatttacca
 ttaaagtctcttttctttttttttttttttttttttttttttttttggtttttcgagacagggtttctctgtatagccctggctgtcc
tggaacctcattttagaccaggctggcctcgaactcagaaatccacctgcctctgcctcccagtgctgggattaaaggcgt
gcgccaccacgccggctgtctcttttctttttaaaagGATATAATTGACTGGTAAAACAATGCAAACCTTT
 GCTTCCCTGGTTAAGCAGTACAGCCCCAAAATGGTTAAGGTTGCAAGgtatgtatgccactttaag
 tagaatgctttccttat -3'

Figure 4-6. DNA sequence of *Hprt* gene exon 6 and surrounding introns, and the B1 SINE/Alu insert. Red underlined = primers; lower case = intron; upper case = exon; B1 SINE/Alu insert = black underlined; dark grey shading = duplicated DNA sequence adjacent to the insert.

It is possible that increased expression of SINE elements and activation of endogenous retroviruses, which have the capacity to reverse transcribe and transpose SINEs, such as LINE1 elements, may contribute at least in part to the increased mutation rate observed in the *Dnmt1*^{-/-} ESC line. However, it is also possible that active retrotransposition has not been observed in the other ESC lines simply by chance, due to their lower spontaneous mutation rates.

The high *de novo* mutation rate of the *Dnmt1*^{-/-} ESC line was further demonstrated by the occurrence of second mutation events during the expansion of the sham-treated clones. For example, one of the ten colonies analysed in the clonal population carrying the B1 SINE insertion in exon 6, was also found to have a deletion of exon 4. This has been represented in Figure 4-3 as an 'insertion and deletion'. Given that the SINE insertion was present in several colonies and the deletion mutation was only detected in a single colony, it was assumed that the deletion of *Hprt* exon 4 had arisen at a delayed period after the SINE insertion had occurred. Figure 4-7 illustrates the PCR product banding patterns obtained by a range of the *Dnmt1*^{-/-} ESC colonies. Clone 3 colony 5 exhibited no detectable mutations in the *Hprt* exons and was therefore classed as an 'other' mutation type. Clone 11 colony 15 displayed a B1 SINE insertion in exon 6 (expected product size: 485bp) and clone 11 colony 16 showed the presence of a second mutation (deletion of exon 4) in addition to the B1 SINE insertion in exon 6. PCRs that failed to give a product were confirmed as deletions after repetition of the PCR alongside a positive and negative control sample.

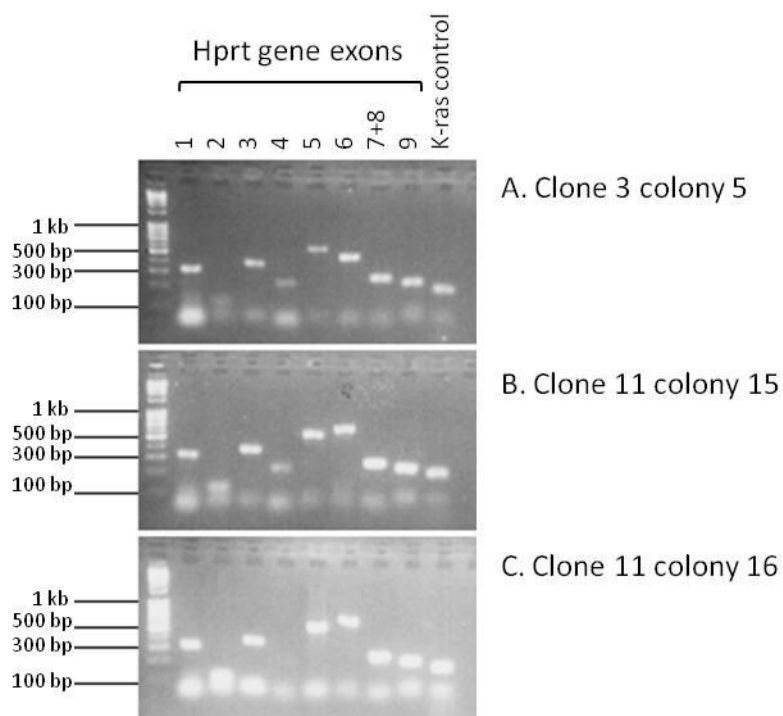


Figure 4-7. Images of the banding pattern produced in a range of *Dnmt1*^{-/-} ESC colonies from two sham-treated clones, after PCR amplification of the *Hprt* gene exons and K-ras control, and staining of the gel with ethidium bromide. A. Colony number 5 from clone 3 has no detectable mutation in the *Hprt* exons, but may carry another form of mutation. B. Colony 15 from clone 11 carries the B1 SINE insertion, as can be seen by the increased PCR product size for exon 6. C. Colony 16 from clone 11 carries the B1 SINE insertion in addition to deletion of exon 4.

Finally, the mutation spectrum data revealed a trend in which the ESC lines with lower *de novo* mutation rates either displayed no change or an increase in the number of different mutation types observed in the 3Gy-irradiated clones. Conversely, the *Dnmt1*^{-/-} cell line, which demonstrated a wider range of *de novo* mutations and an elevated *de novo* mutation rate, appeared to display a reduced range of mutation types in the 3Gy X-irradiated clones. In addition, no SINE insertions were observed in the irradiated clones, but it is hard to establish the significance of this observation.

4.3.3 Methylation of structural repeats and endogenous retroviral elements

The cytosine methylation levels of specific structural genomic repeat sequences and endogenous retroviral elements were analysed using Southern blotting, as described in section 2.7. Control for complete digestion (C.D.) was achieved using a probe specific to a mitochondrial DNA sequence which falls between two *Msp1/HpaII* restriction sites separated by 1.7kb. As mitochondrial DNA contains no CpG methylation, a single band of 1.7kb in size should be visible on the blot if restriction enzyme digestion with *Msp1* or *HpaII* has been complete. As can be seen from Figure 4-8 to Figure 4-11, all samples on the Southern blots were fully digested. An image of the ethidium bromide stained gel, pictured 10 minutes after loading the samples, was used as a control for loading (C.L.). This allowed direct comparison of the methylation levels between different samples.

DNA samples from each ESC line were digested with *HpaII*. An additional aliquot of DNA from the wild type ESC line was digested with *Msp1* and loaded into the first lane of every Southern blot. *HpaII* and *Msp1* are isoschizomers (restriction site: C'CG,G), but *HpaII* is methylation-sensitive and only cuts when the recognition sequence is not methylated. *Msp1* cuts regardless of the presence of methylation at the recognition sequence, and therefore provides an indication of the banding pattern that would be produced in *HpaII*-digested DNA that was entirely devoid of CpG methylation. Furthermore, the fragment sizes produced are proportional to the level of

methylation, with highly methylated samples producing more high molecular weight fragments than less methylated samples.

At the minor satellite region, the *Dnmt1*^{-/-} ESC line appeared to have the least methylation, followed by the *Dnmt3a3b*^{-/-} ESCs (px22). The single *de novo* *Dnmt3a*^{-/-} and *Dnmt3b*^{-/-} ESCs displayed levels of minor satellite methylation much closer to that of the wild type. Interestingly, however, slightly lower methylation levels were found in the ESCs nullizygous for *Dnmt3b*, the methyltransferase which carries mutations in ICF syndrome.

To allow semi-quantitative comparison of minor satellite methylation levels between the samples, the band at ~300bp and the load control band were quantified using Image J, and subjected to chi-square analysis. Reassuringly, a significantly different value was obtained when comparing wild type ESCs digested with *HpaII* and *MspI* ($p=0.002$). The *Dnmt1*^{-/-} ESCs were found to contain significantly less methylation at the minor satellite repeat sequences than the wild type cells ($p=0.001$). However, the differences in methylation level between the wild type ESC line and the *de novo* methyltransferase knock outs (*Dnmt3a*^{-/-}, *Dnmt3b*^{-/-} or *Dnmt3a3b*^{-/-}) were not statistically significant ($p>0.25$).

A. Minor Satellite Repeats

B. IAP LTR Retrotransposons

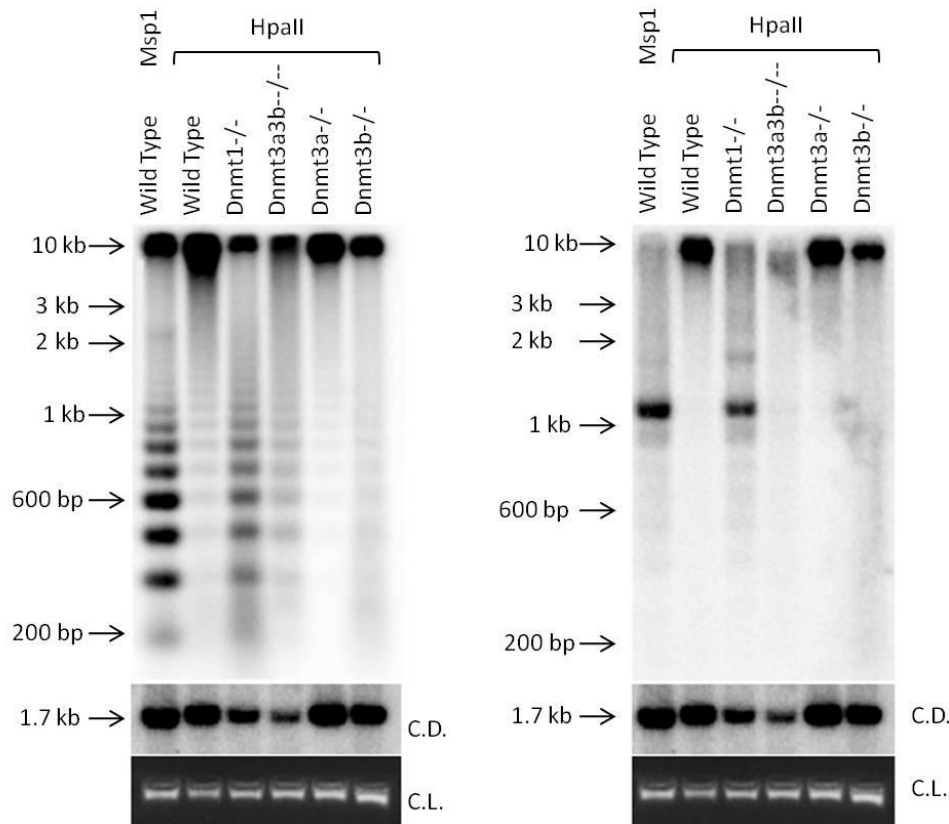


Figure 4-8. Southern blots of ESC DNA digested with *Msp1* or *HpaII*, as indicated above the blots, and visualised with probes specific for the structural minor satellite repeats (A) or intracisternal-A particle (IAP) LTR retrotransposons (B). Hyperladder 1 was used as a size marker. A mitochondrial DNA probe was used as a control for complete digestion (C.D.) and the ethidium bromide stained gel was used as a control for even loading (C.L.). The *Dnmt3a3b*^{-/-} ESCs were p#22.

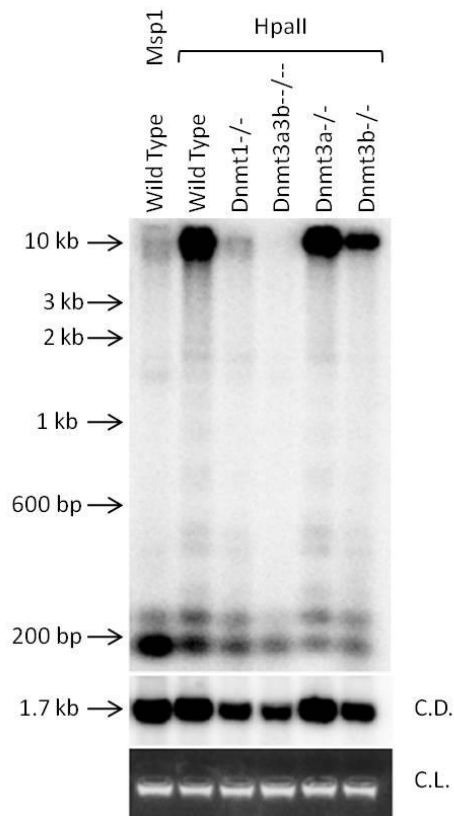
Labelling of the Southern blot membrane with a probe specific to IAP LTR retrotransposons revealed a strong band slightly greater than 1kb in size, which was indicative of complete digestion. This band was used for quantification, in addition to the loading control as a correction factor. Again, a significant difference was observed between the values for *HpaII* and *Msp1* digested DNA from the wild type ESCs ($p=0.002$). The *Dnmt1*^{-/-} ESCs were found to contain significantly less methylation at

IAP retrotransposon sequences in comparison to wild type ESCs ($p=0.002$). A faint band was also visible in the lane containing *HpaII* digested DNA from the *Dnmt3a3b*^{-/-} ESCs. However, the methylation level was not found to be significantly lower than that of the wild type ESC line ($p=0.4$).

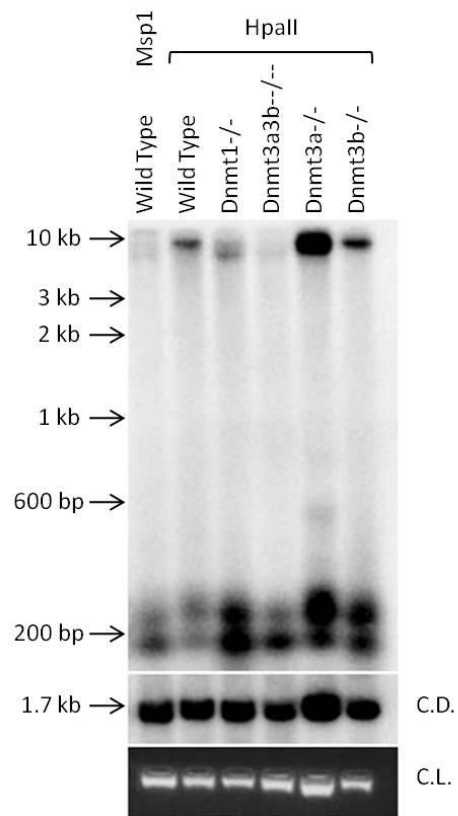
The results of the Southern blots using probes for LINE1 elements were much more difficult to interpret. The Southern blot image obtained using a probe specific to the TF subfamily of murine LINE1 elements was very un-informative. However, comparison of the other LINE1 blots by eye alone indicates that the *Dnmt3a3b*^{-/-} ESC line is the most hypomethylated at LINE1 A, F and GF sub-families, based on the smallest band (<200bp) being more intense than the band just above 200bp.

Quantification and comparison of the two bands around 200bp in size, and control for sample loading, revealed almost no significant difference in methylation level between any of the ESC lines at LINE1 elements. Significant differences were observed only when a probe specific to the LINE1 F-type subfamily was used (Figure 4-9 B), indicating hypomethylation of the *Dnmt1*^{-/-} and *Dnmt3a*^{-/-} ESC lines in comparison to the wild type ESCs ($p<0.0008$). However, these results were thought to be anomalous, as quantification implies that they are more hypomethylated than the wild type ESCs digested with *Msp1*. This is unlikely to be true, as it would require the *Dnmt* knock out ESCs to have acquired additional *HpaII*/*Msp1* restriction sites. Thus, it was concluded that this membrane may have developed areas prone to non-specific probe binding as a result of continual stripping and re-probing.

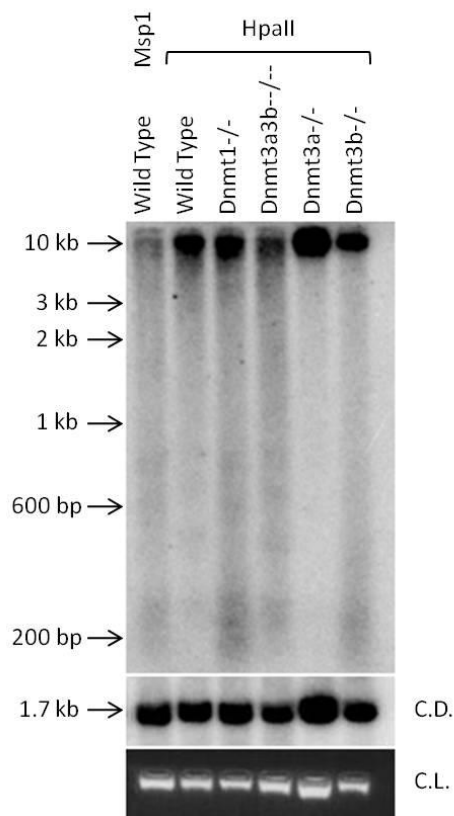
A. LINE1 A-type



B. LINE1 F-type



C. LINE1 TF-type



D. LINE1 GF-type

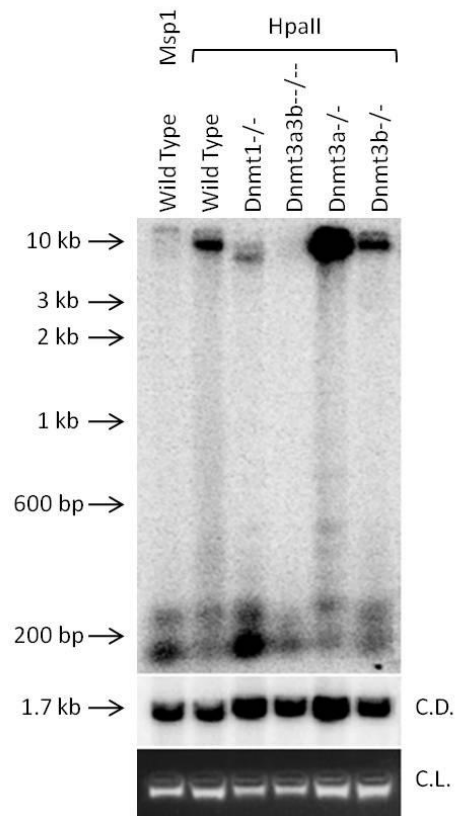


Figure 4-9. Southern blots of ESC DNA digested with *Msp1* or *HpaII*, as indicated above the blots, and visualised with probes specific for the long interspersed nuclear element 1 (LINE1) subfamilies defined by the 5' monomer types A, F, TF and GF. Hyperladder 1 was used as a size marker. A mitochondrial DNA probe was used as a control for complete digestion (C.D.) and the ethidium bromide stained gel was used as a control for even loading (C.L.).

Previous groups have reported that LINE1 elements are expressed during murine embryogenesis, particularly in the blastocyst cells (Packer *et al*, 1993) from which ESCs are derived (Evans and Kaufman, 1981). Thus, another membrane blotted with *Msp1/HpaII* digested DNA from the same ESC lines and some tissue controls from the CBA/H mouse strain was hybridised with the LINE1 A probe. See Figure 4-10. An ethidium bromide picture of the gel taken 10 minutes after loading was not available, but one taken immediately before blotting onto the membrane was. This was used to control for loading instead, using Image J to quantify the pixels within a slice/section down the centre of each lane (Figure 4-10 B).

A. LINE1 A with tissue controls.

B. Ethidium bromide stained gel.

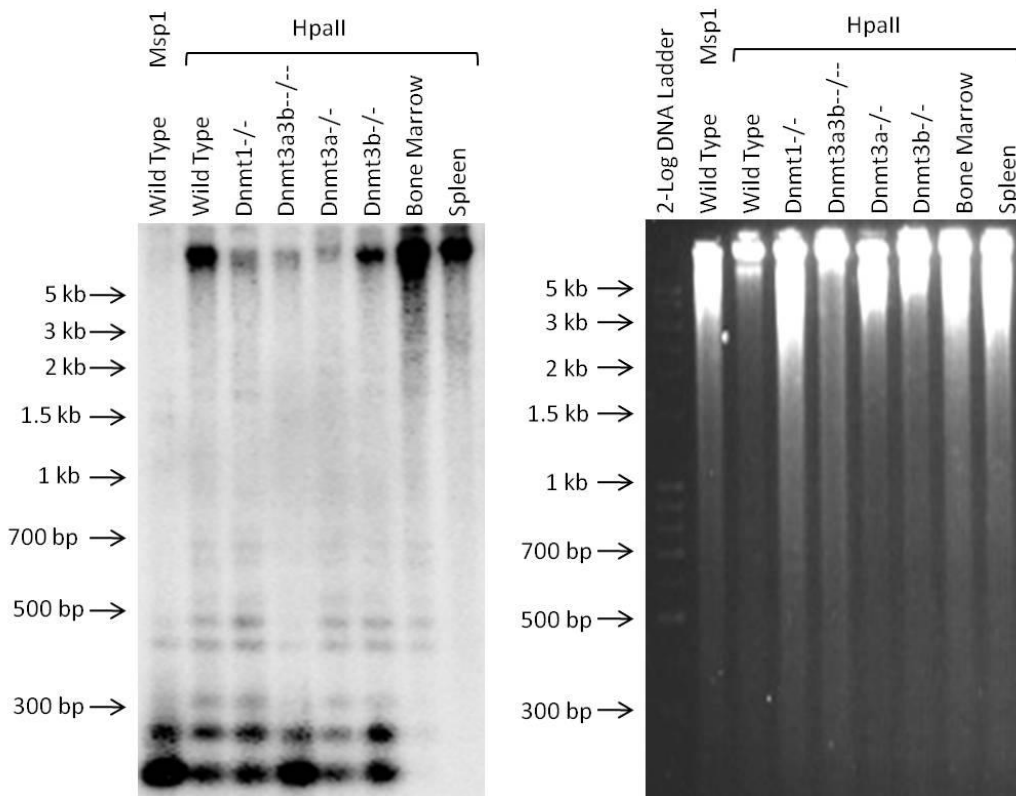


Figure 4-10. Southern blot of ESC DNA and DNA extracted from CBA/H mouse spleen and bone marrow, which has been digested with *Msp1* or *HpaII* and visualised with probes specific for the LINE1 subfamily A (A). Fullranger DNA ladder (NORGEN) was used as a size marker. The ethidium bromide stained gel was used to control for loading between samples (B). The *Dnmt3a3b*^{-/-} ESCs were p#16.

The banding patterns produced for the ESC lines were similar to those in the Southern blots shown in Figure 4-9. However, in Figure 4-10 the difference between the *Msp1* and *HpaII* digested wild type DNA is more prominent, and it can be seen that increased intensity of the smallest band (<200bp) is proportional to the extent of hypomethylation in the ESCs. Quantification of the smallest band using Image J and comparison between the ESC lines after controlling for loading revealed that a significant difference could be detected between the *Msp1* and *HpaII* digested wild type ESC DNA ($p=0.00001$). Furthermore, the *Dnmt1*^{-/-} and *Dnmt3a3b*^{-/-} ESCs were found to be significantly less methylated than the wild type ESCs at LINE1 elements of

the A-type subfamily ($p=0.04$ and $p=0.0005$ respectively). In comparison to the tissue controls, all of the ESC lines were found to be very hypomethylated at LINE1 elements. Moreover, in agreement with previous data from this lab, the DNA from CBA/H bone marrow contained lower levels of methylation at LINE1 elements than DNA from CBA/H spleen (Giotopoulos *et al*, 2006).

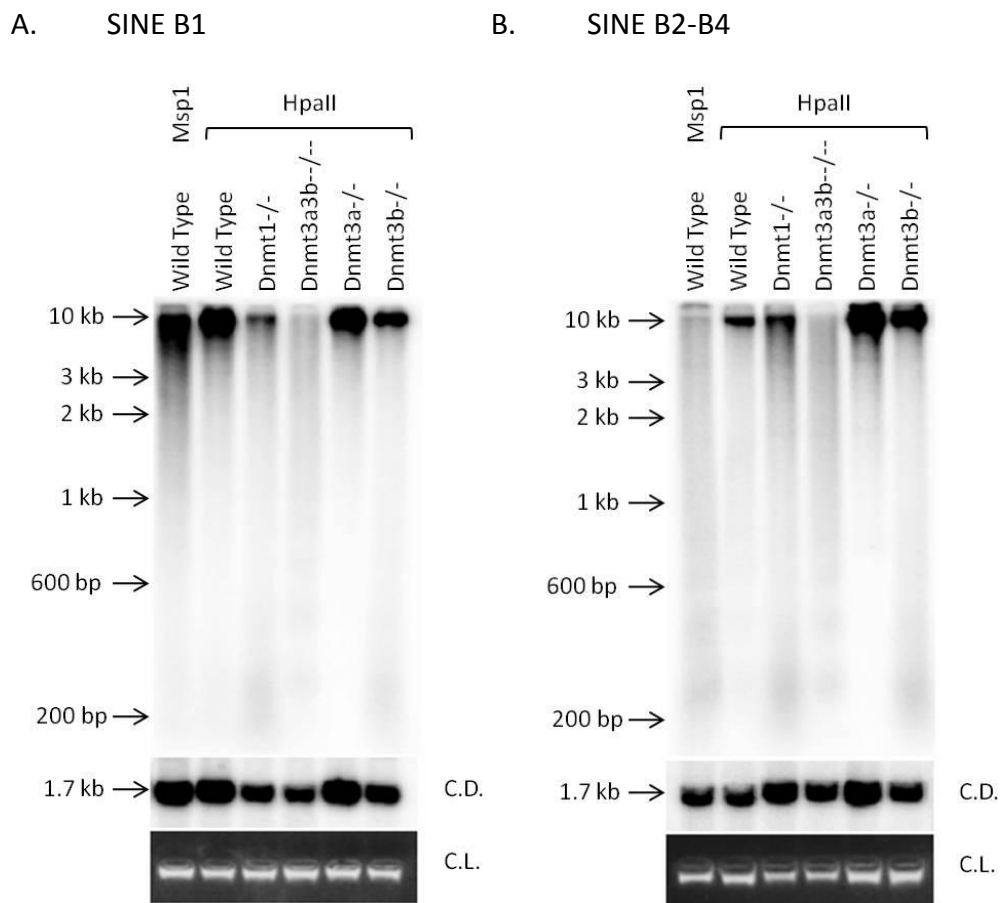


Figure 4-11. Southern blots of ESC DNA digested with *Msp1* or *HpaII*, as indicated above the blots, and visualised with probes specific for the short interspersed nuclear element (SINE) subfamilies (G-H). Hyperladder 1 was used as a size marker. A mitochondrial DNA probe was used as a control for complete digestion (C.D.) and the ethidium bromide stained gel was used as a control for even loading (C.L.).

Finally, the methylation level at SINE elements was compared between the ESC lines. The B1 and B2-B4 SINE sequences which formed the insertional mutations at exons 3 and 6 of the *Hprt* gene were used to generate the probes. As Figure 4-11 shows, the

signals detected from the SINE probes were weak and no discrete bands could be identified. However, visual comparison between the lanes indicated that *Dnmt1*^{-/-}, *Dnmt3a3b*^{-/-} and *Dnmt3b*^{-/-} ESCs are hypomethylated in comparison to the wild type ESCs. Semi-quantitative analysis using the bottom third of each lane and controlling for loading, however, revealed that these differences were not statistically significant ($P > 0.5$).

4.4 Discussion

4.4.1 Lack of DNMT1, but not DNMT3A and/or DNMT3B, leads to an increased *de novo* mutation rate

The first major observation from the mutation rate data was that the *Dnmt1*^{-/-} ESCs displayed a significantly elevated *de novo* mutation rate in comparison to the wild type ESC line. The mutation rate of the sham-treated *Dnmt1*^{-/-} ESCs was 10-fold higher than that of the sham-treated wild type ESCs (4.4×10^{-7} versus 5.7×10^{-8} respectively). The same trend was observed previously in a study by Chen *et al* (1998), and it was concluded by the authors that DNA hypomethylation leads to elevated *Hprt* mutation rates. However, Chen *et al* (1998) did not analyse the effect on mutation rate of functional absence of the *de novo* methyltransferase enzymes (DNMT3A and DNMT3B). In addition, they did not investigate mutation rate in the ESC lines after irradiation.

Thus, to build on the results of the study by Chen *et al* (1998), the current project also analysed the mutation rates of *Dnmt3a*^{-/-}, *Dnmt3b*^{-/-} and *Dnmt3a3b*^{-/-} ESCs. The

results demonstrate that the mutation rate of the *Dnmt1*^{-/-} ESC line is significantly elevated in comparison to the *Dnmt3a*^{-/-}, *Dnmt3b*^{-/-} and *Dnmt3a3b*^{-/-} ESC lines. Furthermore, each of the *de novo* methyltransferase KO ESC lines displayed a mutation rate that was not significantly different to that of the wild type ESC line. As discussed in section 3.3, each of the ESC lines used in this project have similar doubling times, and underwent 23-25 population doublings between sham treatment or 3Gy X-irradiation and being seeded into selective media containing 6TG. The *Dnmt3a3b*^{-/-} ESCs were p#14-17 at the time of treatment, and p#20-26 at the point of seeding into selective media. Thus, according to the results presented in Figure 3-4 they would have had very similar or lower methylation levels than the *Dnmt1*^{-/-} ESCs at the time of seeding into selective media. However, in contrast to expectations, the mutation rate of the sham treated *Dnmt3a3b*^{-/-} ESC clones was significantly lower than that of the *Dnmt1*^{-/-} ESC line ($p=3.2 \times 10^{-6}$).

Based on these observations, it can be inferred that the 10-fold elevated mutation rate detected in the *Dnmt1*^{-/-} ESC line is not simply a result of global hypomethylation as previously reported (Chen *et al*, 1998). Rather, it appears to be a result of the absence of a property or function specific to DNMT1. For example, it is possible that the specific genomic targets for DNA methylation by DNMT1, rather than DNMT3A or DNMT3B, may be important in maintaining genomic stability. Alternatively, the role of DNMT1 in DNA replication and repair may affect mutation rates at gene loci (see section 1.3).

4.4.2 Radiation-induced delayed genomic instability is observed in wild type ESCs, but not in *Dnmt* deficient ESCs

The second major observation from the *Hprt* mutation rate data was that the wild type ESCs demonstrated an elevated mutation rate 23-35 PDs after exposure to 3Gy X-rays, but the *Dnmt*^{-/-} ESCs did not. The wild type ESC line exhibited a 5-fold increase in mutation rate 23-25 PDs after exposure to 3Gy X-rays in comparison to sham treated wild type ESC controls. This is characteristic of the occurrence of radiation-induced delayed genomic instability, as seen previously at the *Hprt* locus in a study by Little *et al* (1997).

However, radiation-induced delayed genomic instability was not observed in any of the *Dnmt*^{-/-} ESC lines: the mutation rates of the 3Gy X-irradiated clones were not significantly different to the respective *de novo* mutation rates. This indicates that absence of the DNA methyltransferase enzymes, or disruption of the normal methylation pattern, may potentially inhibit the mechanism behind radiation-induced delayed genomic instability. However, it is not clear whether the failure to manifest radiation induced delayed genomic instability is a result of lack of the DNMT enzymes themselves, or simply a disruption of the normal methylation pattern.

It is possible that cell lines which are intrinsically unstable do not exhibit radiation induced delayed genomic instability because irradiation has the effect of eliminating those unstable cells from the population. This could explain the failure of the *Dnmt1*^{-/-} ESCs to show any increase in instability in the 3Gy treatment group. However, none of the *de novo* *Dnmt*^{-/-} ESC lines have a significantly higher *de novo* mutation rate than

the wild type ESCs. Thus, it is not thought that elimination of unstable cells from the population has resulted in the observed failure to manifest radiation-induced delayed genomic instability.

To our knowledge this is the first direct demonstration of a requirement for specific DNA methylation patterns and/or the DNA methyltransferase enzymes in the propagation of radiation induced delayed genomic instability. Further work is required to elucidate the possible roles of the DNMTs in this mechanism. Speculative effects of disruption to the normal methylation pattern are easier to envisage. Although the correlation of reduced levels of DNA methylation with apparently increased genomic stability after a radiation insult could be conceived as contrary to expectations, numerous possible explanations exist. For example, methylcytosine is thought to be a preferential target for DNA adduct-forming mutagens in comparison to unmethylated cytosine, and oxidative crosslink lesions have been found to be induced >10 times more efficiently in methylated DNA than unmethylated DNA (Cao and Wang, 2007).

Alternatively, the lower levels of DNA methylation and associated binding proteins in the *Dnmt*^{-/-} ESCs may permit increased access to the DNA for proteins involved in DNA damage signalling and repair (Amouroux *et al*, 2010). Finally, it is also possible that, if radiation induced delayed genomic instability is partly mediated by epigenetic dysregulation of the genes involved in the DNA damage response (ie, via aberrant promoter methylation), the lack of methyltransferase enzymes in the *Dnmt*^{-/-} ESCs may reduce this effect. Characterisation of the mutation types observed at the *Hprt*

locus in each of the ESC lines was carried out in an attempt to better understand the mechanisms that may be responsible for their differing mutation rates.

4.4.3 Mutation spectra analysis reveals a link between non-contiguous exonic deletions and hypomethylation or radiation exposure

An attempt was made to characterise the spectrum of mutation types contributing to the mutation rates of each ESC line, both in irradiated and sham-treated clones. It could be argued that due to the low numbers of colonies produced, the mutation spectra of the clones with a low mutation rate may not be entirely accurate. Nevertheless, for each cell line the mutation spectrum at a delayed period after 3Gy X-irradiation was found to roughly resemble the *de novo* mutation spectrum. Interestingly, multiple deletions of non-contiguous exons were observed in the sham-treated clones from the two most hypomethylated ESC lines (*Dnmt1*^{-/-} and *Dnmt3a3b*^{-/-}). In addition, all of the ESC lines displayed these non-contiguous exonic deletions in clones derived from 3Gy X-irradiated cells. See Table 4-3.

It is not clear from the available data whether the non-contiguous deletions are the result of a single mutation event or multiple mutational events which have occurred during expansion of the colonies. However, previous research groups have reported similar mutations in the *Hprt* gene using lymphocytes and Chinese hamster ovary (CHO) cells, and have associated them with the occurrence of radiation-induced delayed genomic instability (Caron et al, 1997; Mognato *et al*, 2001; Romney *et al*, 2001). Non contiguous exonic deletions are thought to be one phenotype of radiation-induced global instability, and are not specifically associated with the occurrence of

other markers of instability, including minisatellite mutations, changes in telomere length, and induction of chromosomal aberrations (Romney *et al*, 2001).

In this project, non-contiguous deletions were observed in as many as 40% of 3Gy X-irradiated clones, and also in 20-35% of clones derived from the hypomethylated *Dnmt1*^{-/-} and *Dnmt3a3b*^{-/-} ESCs, which had not been irradiated. Thus, these hypomethylated cell lines appear to display a type of instability that is characterised by similar mutational events to those observed at a delayed period after irradiation. Interestingly, it has been suggested that non-contiguous exonic deletions may arise via recombinational repair of DNA DSBs (Balestrieri *et al*, 2001). Previous studies have also attributed the occurrence of large deletions in the *Hprt* gene to illegitimate recombination (Morris and Thacker, 1993). In this project, large deletions involving several exons were observed in all ESC lines, and may simply reflect the fact that homologous recombination is the main mechanism by which DNA DSBs are repaired in ESCs (Adams *et al*, 2010; Tichy and Stambrook, 2008). However, it is also possible that the non-contiguous exonic deletions observed in the most hypomethylated sham treated ESC lines, and in all of the ESC lines exposed to 3Gy X-rays, indicate the occurrence of increased levels of illegitimate recombination.

The suggestion that DNA methylation can protect the genome from illegitimate recombination is not new (Bender, 1998; Chen *et al*, 1998), and several studies lend support to this hypothesis. Indeed, crossover at recombination hotspots in fungus has been shown to be reduced >100-fold when the hotspot is methylated on both homologs, and 50-fold when only one homolog is methylated (Maloisel and Rossignol,

1998). Furthermore, in murine ESCs Gonzalo *et al* (2006) demonstrated that deficiency of *Dnmt1*^{-/-} or *Dnmt3a3b*^{-/-} results in increased frequencies of recombination events at telomeres.

Thus, it is possible that homologous recombination could be responsible for some of the mutations observed in the ESC lines used in the present study. It should be noted that the *Hprt* gene is X-linked and as the parental J1 clone was derived from a male embryo, all the *Dnmt*^{-/-} derivatives are by default male. However, a complete homolog of this gene is available for homologous recombination after DNA replication, in late S-phase and G2 of the cell cycle. Alternatively, homologous recombination could potentially occur between relatively small sequences of homology on non-homologous chromosomes.

Repetitive sequences such as retroviral elements and satellite sequences, contain the majority of the methylated cytosines found in mammalian cells (Yoder *et al*, 1997) and have been found in at least some instances to be hotspots for recombination (Edelmann *et al*, 1989; Jeffreys *et al*, 1999). Southern blot analysis of the minor satellite region in the mESCs in this project revealed that the *Dnmt1*^{-/-} ESC line contained the lowest level of methylation at these sequences and was significantly hypomethylated in comparison to the wild type ESCs (=0.001). Given the apparent correlation between methylation levels and homologous recombination, it is possible that hypomethylation of the minor satellite sequences in the *Dnmt1*^{-/-} ESCs could cause increased recombination between centromeric regions. Such a phenomenon is observed in cell lines from patients with ICF syndrome (see section 1.3). However,

homologous recombination between pericentric satellite sequences is unlikely to be responsible for the elevated mutation rate observed in the *Dnmt1*^{-/-} ESCs at the *Hprt* gene.

4.4.4 Mutation spectra analysis reveals active retrotransposition in

***Dnmt1*^{-/-} ESCs**

The *Dnmt1*^{-/-} ESC line was found to display the widest variety of mutation types in comparison to the other ESC lines, indicating that a wide variety of different mutational processes were occurring. For example, it was the only cell line to demonstrate the occurrence of active retrotransposition. As described in section 4.3.2, a B2 SINE insertion was detected just 5' of *Hprt* exon 3 and a B1 SINE/Alu insertion was detected just 5' of *Hprt* exon 6, in clones derived from *Dnmt1*^{-/-} sham-treated cells. It was therefore considered that this cell line may have more active retrotransposition as a result of hypomethylation of endogenous retroviral repeats. However, SINE elements are thought to utilise the host cell or L1 machinery for transposition, and Southern blotting revealed that the L1 promoter was most hypomethylated in *Dnmt3a3b*^{-/-} ESCs, although in comparison to the tissue controls all of the ESC lines were significantly hypomethylated at LINE1 elements. Furthermore, the SINE elements themselves were hypomethylated to a very similar degree in the *Dnmt1*^{-/-}, *Dnmt3a3b*^{-/-} and *Dnmt3b*^{-/-} ESC lines. Thus, we cannot assume that endogenous retroviruses are active only in the *Dnmt1*^{-/-} cell line, as insertions may not have been detected in the other ESC lines simply by chance. Further support for this possibility comes from the fact that a very similar SINE insertion has previously been described in wild type

murine ESCs of the E14.1 strain. Tsuda *et al* (1997) reported the occurrence of a B2 SINE insertion in exon 3 of the *Hprt* gene, which arose spontaneously during selection in media containing 6-TG. This insertion was at the 3' end of *Hprt* exon 3, whilst the B2 SINE insertion detected in this project was in the intron 5' of exon 3. However, the occurrence of both of these insertions within/near the same exon indicates that this region of the *Hprt* gene may be a hotspot for SINE insertions. Whether it is simply coincidental that both insertions at exon 3 were of the B2 subfamily is unknown.

Interestingly, some of the genomic rearrangements described by Chen *et al* (1998) during their analysis of 6-TG resistant *Dnmt1*^{-/-} clones also appear to be insertions of a few hundred base pairs. It is not known whether they investigated the possibility, but it is tempting to speculate that rather than observing a high frequency of genomic rearrangements in the *Dnmt1*^{-/-} ESCs as reported, Chen *et al* (1998) actually detected some insertions of retroviral elements.

In the present study, IAP elements were also found to be significantly more hypomethylated in the *Dnmt1*^{-/-} ESCs than any of the other ESC lines. However, due to the PCR-based methodology used to characterise the mutation types and the large size of IAP elements, it was not possible to determine whether insertions of these elements had occurred. Similarly, the occurrence of LINE1 retrotransposition events could not be detected. If either of these elements actively retrotransposed to generate an insertion in the *Hprt* gene, it would most likely manifest as an exonic deletion if it occurred between the forward and reverse primers of a primer pair, or as an 'other' mutation type if it occurred within the *Hprt* promoter region or an intron sequence that was not

covered by a primer pair. Colonies exhibiting such mutation types were not sequenced in the current study. Thus, it is possible that increased expression of IAP and SINE elements and activation of endogenous retroviruses that have the capacity to mobilise SINEs, such as LINE1 elements, may have contributed at least in part to the increased mutation rate observed in the *Dnmt1*^{-/-} ESC line, in addition to a possible increased frequency of homologous recombination. However, the possibility that such insertions also occurred in the other ESC lines and were simply not detected cannot be excluded.

The high *de novo* mutation rate in the *Dnmt1*^{-/-} ESC line was further demonstrated by the occurrence of second mutation events during the expansion of the sham-treated clones. For example, one of the ten colonies analysed in the clonal population carrying the B1 SINE insertion in exon 6, was also found to possess a deletion of exon 4. See Figure 4-7. Given that the SINE insertion was present in several colonies and the deletion mutation was only detected in a single colony, it was assumed that deletion of *Hprt* exon 4 had arisen at a delayed period after the SINE insertion had occurred.

Other possible reasons for the elevated mutation rate observed in the *Dnmt1*^{-/-} ESC line may stem from the roles that DNMT1 plays in DNA repair. For example, DNMT1 has been shown to be recruited to sites of DNA damage repair by PCNA, whilst DNMT3A and DNMT3B are not (Mortusewicz *et al*, 2005). It was proposed that DNMT1 is recruited in order to restore the methylation pattern on the repaired strand, and also to help re-establish chromatin structure and histone modifications (Mortusewicz *et al*, 2005). However, it is possible that DNMT1 may play another more central role at DNA repair sites. For example, it is thought to be involved in mismatch repair (MMR)

and in maintaining the stability of triplet repeat tracts (Wang and Shen, 2004; Dion *et al*, 2008). The exact role of DNMT1 in MMR is not clear. However, *Dnmt1*^{-/-} ESCs have been shown to exhibit relatively high levels of microsatellite instability in comparison to wild type ESCs (Wang and Shen, 2004).

The final major observation made from analysis of the mutation spectrum in the current study was that the ESC lines with low *de novo* mutation rates tended to display either a plateau or an increase in the number of different mutation types observed in the 3Gy-irradiated clones. Conversely, the *Dnmt1*^{-/-} cell line, which demonstrated a wider range of *de novo* mutations and an elevated *de novo* mutation rate, appeared to display a reduced range of mutation types in the 3Gy X-irradiated clones. In addition, no SINE insertions were observed in the irradiated clones. This is consistent with the hypothesis that cells and tissues which are intrinsically unstable are often eliminated from the population after irradiation. This may well be the case for the *Dnmt1*^{-/-} ESCs, and may explain why no mutations involving insertion of endogenous retroviral elements were observed in the 3Gy X-irradiated clones, especially if there is only a subset of particularly unstable clones containing active retroviruses.

4.4.5 Summary

The results of the mutation rate analysis at the *Hprt* gene indicate that a low global level of CpG methylation does not necessarily lead to high levels of genomic instability as previously thought by Chen *et al* (1998). Instead, it appears that *Dnmt1*^{-/-} ESCs are unstable due to loss of a property specific to DNMT1 that is not shared by the *de novo* methyltransferase enzymes. Possible causes of the detected increased mutation rate

in *Dnmt1*^{-/-} ESCs include increased illegitimate homologous recombination, retroviral activation, and loss of the properties of DNMT1 that are required for efficient DNA replication and repair. The wild type ESC line displayed the classic occurrence of radiation-induced delayed genomic instability. However, knock out of any of the DNA methyltransferase enzymes appeared to inhibit transmission of the cellular memory of the radiation insult through the clonal progeny. This indicates that DNA methylation is indeed involved in the propagation of radiation induced delayed genomic instability in the mESC lines used in the present study. However, it is not clear whether the failure to manifest radiation induced delayed genomic instability is a result of loss of the DNMT enzymes themselves, or simply a disruption of the normal methylation pattern. The possible effects of varying DNA methylation levels on cellular capacity for DNA damage repair will be discussed further in section 5.4.

5 Chapter 5. Genomic Stability: Frequency of Aberrations on a Genome-wide Scale

5.1 Introduction

The mutation rate results discussed in chapter 4 are data obtained from analysis of a single locus: the *Hprt* house-keeping gene. The data reflects the rate and type of mutational processes occurring in coding regions of the DNA, which are functionally very important. However, hypomethylation in the *Dnmt* KO ESC lines occurs on a genome-wide scale and is expected to affect the stability of endogenous retroviral elements and structural satellite repeat sequences as well as coding regions.

Drug-induced genome-wide DNA hypomethylation has been shown to result in prolonged detection of increased levels of γ H2AX foci after irradiation, indicating the continuous presence of DSBs (Dote *et al*, 2005). Analysis of the levels of DNA strand breaks in the ESC lines would therefore provide a useful measure of instability on a genome-wide scale. A variety of techniques are available to detect and quantify DNA strand breaks, including γ H2AX and 53BP1 foci counting methods, alkaline and neutral filter elution sucrose gradient sedimentation, pulsed field gel electrophoresis (PFGE) and single-cell electrophoresis (the comet assay) (Hall, 2000; Iwabuchi *et al*, 2003; Rogakou *et al*, 1998). The comet assay has the advantage of being able to detect both SSBs and DSBs (in addition to alkali-labile sites), and has high sensitivity in comparison to PFGE or filter elution sucrose gradient sedimentation. It also requires fewer cells per

sample and has the ability to measure DNA damage at the single-cell level (Olive and Banáth, 2006; Tice *et al*, 2000).

For the results presented in this chapter, the comet assay was performed in three of the mESC lines which had produced distinctive signatures of mutation rate at the *Hprt* locus. Analysis was performed 23-25 population doublings after 3Gy X-irradiation or sham treatment. As such, the level of DNA damage, mostly strand breaks, present in each of the cell lines at the time of selection for *Hprt* mutants was determined (see section 5.3.1). It was hypothesised that global levels of DNA strand breaks would correlate with mutation rates at the *Hprt* locus, so that the hypomethylated *Dnmt1*^{-/-} cell line would display relatively high levels of endogenous strand breaks, whilst the wild type ESCs would display increased strand breaks 23-25 PDs after exposure to 3Gy X-rays.

The comet assay can also be used to measure levels of DNA damage caused as a result of oxidative stress. This is achieved through conversion of oxidised base lesions (such as 8-oxoG) into strand breaks by treatment with enzymes that cut at the site of oxidised base lesions, such as the glycosylase/endonuclease Fpg (Johansson *et al*, 2010; Olive and Banáth, 2006). Oxidative stress is one of the proposed mechanisms by which radiation-induced delayed genomic instability is propagated (Wright, 2010), and oxidative crosslink lesions have been shown to form >10 times more efficiently in methylated DNA than unmethylated DNA (Cao and Wang, 2007). Therefore, the levels of oxidative damage were determined in the three ESC lines giving distinctive *Hprt* mutation rate signatures 23-25 PDs post sham treatment or exposure to 3Gy X-rays.

The results are presented in section 5.3.2. It was hypothesised that only the wild type ESC line would display an elevated level of oxidative DNA damage 23-25 PDs post irradiation, whilst the *Dnmt1*^{-/-} ESC line may exhibit higher endogenous levels of oxidative damage.

Finally, DNA hypomethylation has been associated with an increased frequency of recombination and cytogenetically detectable chromosome rearrangements in mammals (Gonzalo *et al*, 2006; Tuck-Muller *et al*, 2000). A pilot study was therefore carried out to provide an indication of whether chromosomal instability may be occurring in the hypomethylated ESC lines. The results are presented in sections 5.3.3 and 5.3.4. Methylation proficient ESCs (wild type) and the two most hypomethylated ESC lines (*Dnmt1*^{-/-} and *Dnmt3a3b*^{-/-}) were harvested for cytogenetic analysis at two delayed time points post 3Gy X-irradiation or sham treatment: 10-14 and 23-25 population doublings (PDs). The latter time point corresponds to the delayed period at which cells were seeded into selective media for detection of mutations in the *Hprt* gene.

The frequency of cytogenetically detectable aberrations was assessed in 200-300 metaphases per treatment condition per cell line in order to achieve sufficient statistical power. Thus, cells were harvested from non-clonal cell populations and multiple slides were made. Metaphases were visualised using solid staining with Giemsa, as this staining method permits the preferential detection of aberrations which are indicative of ongoing genomic instability within a non-clonal cell population. Asymmetrical aberrations, and non-transmissible complex exchanges involving several

chromosomes, are easily visible using solid staining (Savage, 1999), whilst the majority of the symmetrical, transmissible exchanges are not (Savage, 1980).

5.2 Chapter-specific Methods and Materials

5.2.1 Alkaline Single-Cell Gel Electrophoresis (Comet) Assay

5.2.1.1 Slide preparation and cell lysis

Single frosted glass microscope slides were labelled according to the cell samples to be analysed. They were coated on one side with 1% LE agarose, made with dH₂O, and laid flat to dry over night at 37°C.

The next day the cells to be analysed, which had been exposed to sham treatment or 3Gy X-irradiation 23-25 PDs previously, were trypsinised and counted. 60,000 to 240,000 cells per sample were aliquotted into labelled eppendorfs. This provided sufficient cells to make 6 slides for each sample: 2 x no treatment; 2 x buffer; 2 x buffer and FPG. The eppendorfs were centrifuged at 1,000rpm for 5 minutes at 4°C, the supernatant was removed by aspiration and the cells were resuspended in 120µl PBS. 20µl aliquots were transferred into 6 labelled eppendorfs, 1 for each slide, and placed on ice. In each subsequent step the samples remained on ice to prevent repair of any single strand breaks, and in dim lighting to prevent light-induced DNA damage. All of the samples were transported to the x-ray machine in a polystyrene box filled with ice. Eppendorfs containing control cells prepared in the same manner were irradiated with 0Gy, 5Gy and 10Gy x-rays, whilst remaining on ice. The test samples, which had been

exposed to sham treatment or 3Gy X-irradiation 23-25 PDs previously, were not irradiated.

0.6% low melting point agarose (Invitrogen) was made with 1x PBS and allowed to cool to 37°C in a water bath. Once at 37°C, 170µl was added to the 20µl aliquot of cells, briefly mixed by pipetting, and dispensed onto the correspondingly labelled slide in 2 aliquots of 80µl. A 22x22mm coverslip was swiftly placed on top of each aliquot to form 2 evenly spread squares of gel. The slides were placed on an ice cold metal tray for 10-15 minutes to set the agarose. The coverslips were gently removed, and the slides placed in Coplin jars filled with ice-cold lysis buffer containing 1% triton X-100. They were stored in the dark over night in a polystyrene box filled with ice.

5.2.1.2 Treatment with FPG enzyme

Slides were removed from the lysis buffer, placed on a tray and submersed in ice-cold dH₂O for 5 minutes. The water was removed by aspiration. Trays containing slides to be treated with buffer or FPG were submersed three times in ice cold Enzyme Reaction Buffer (ERB) for 5 minutes each time. Slides which were to undergo no treatment were immersed in fresh ice cold dH₂O. Care was taken not to disturb the gels, and the trays were covered with a black sheet of plastic during incubations to prevent any light-induced DNA damage.

Slides to be treated with enzyme or buffer were laid in moistened black boxes. Those to undergo no treatment remained in dH₂O covered with black sheeting. 50µl ERB was pipetted onto each gel square on the buffer treatment slides. 50µl of a 1/500 dilution

of FPG enzyme in ERB was pipetted onto each gel square on the FPG treatment slides. Fresh coverslips were placed on top of each gel and the slides were incubated for 30 minutes at 37°C in the dark.

5.2.1.3 Electrophoresis

The coverslips were removed and all of the slides were laid lengthwise in an electrophoresis tank, with the frosted end of each slide towards the anode. The slides were covered with ice-cold alkali electrophoresis buffer and incubated for 20 minutes in the dark. Electrophoresis was then carried out at 30V (300mA) for 20 minutes, in the dark.

After electrophoresis, the slides were removed from the tank and laid on a tray. Each slide was flooded with 1ml neutralisation buffer and incubated for 20 minutes at room temperature. The slides were then rinsed by submersion with ice cold dH₂O. This was immediately removed by aspiration, and the slides were submersed in fresh dH₂O for a further 10 minutes. The water was removed and the slides were allowed to dry at 37°C over night.

5.2.1.4 Staining and visualisation

The next morning, the slides were rehydrated with dH₂O for 30 minutes. The water was drained and each slide was flooded twice with 1ml freshly made 2.5µg/ml propidium iodide (PI) solution (Sigma Aldrich, 1mg/ml stock diluted in dH₂O). After incubation at room temperature in the dark for 15-20 minutes, excess PI solution was drained from the trays and the slides were submersed in dH₂O. After incubation for

20-30 minutes at room temperature in the dark, the water was drained. The slides were dried in the 37°C oven, and stored in a slide box until image analysis. The slides can be re-stained if image analysis is not carried out within a few weeks.

Comets were visualised with an Olympus fluorescent microscope at magnification of x200. Images were captured using an online charge coupled device (CCD) camera and analysed using Komet 5.0 analysis software (Andor Bioimaging). A total of 200 cells were analysed per sample per experiment: 50 cells per gel; 2 gels per slide; 2 slides per sample. The percentage of the cellular DNA contained within the tail of each comet was calculated by the Komet 5.0 analysis software (% tail DNA). Results are expressed as the mean \pm the standard error of the mean (SEM) of three independent experiments.

5.2.2 Genomic Stability Measured by Frequency of Cytogenetic

Aberrations

5.2.2.1 Preparation and irradiation of cells

For each cell line under analysis, 3x 75cm² flasks of ESCs were grown to 70% confluence and labelled “Sham” or “3Gy+0hr” and “3Gy+1hr”. They were transported to the X-ray machine in a polystyrene box and either irradiated with 3Gy x-rays or sham treated.

As soon as possible after irradiation, the cells in flasks labelled “sham” or “3Gy+0hr” were trypsinised and counted. 10⁶ cells were seeded into a fresh gelatinised 75cm²

flask with 15ml complete ES media and incubated at 37°C with 5% CO₂ until harvesting 9 hours later (see section 5.2.2.3). 500,000 cells were seeded into a gelatinised well of a 6-well plate with 3ml complete ES media and cultured for several more days to allow harvesting at delayed time points. The cells in flasks labelled “3Gy+1hr” were placed back into the 37°C incubator for 1 hour before being trypsinised, counted and re-seeded as described above. This 1 hour incubation allows cells to repair radiation-induced DNA damage such as single strand breaks before entering a new round of cell division (see section 5.3.3).

5.2.2.2 Accumulation of cells in metaphase

One hour prior to harvesting, 45µl KaryoMAX colcemid solution (10µg/ml, GIBCO) was added to the media in the flask of ESCs (final concentration 0.03µg/ml). The flask was swirled to mix, and placed back into the incubator. Colcemid is a spindle inhibitor which arrests cells in metaphase. 1 hour incubation with colcemid, 8 hours after seeding the cells into a fresh flask, produced the greatest yield of metaphases with good quality chromosomes in these ESCs.

5.2.2.3 Harvesting

Medium was decanted into a labelled 50ml falcon tube. The cells were washed with 5ml Versene (also decanted into the 50ml falcon tube) and incubated with 2ml trypsin-EDTA for 5 minutes at 37°C. The trypsinised cells were washed off the surface of the flask with 5ml media/PBS from the falcon tube, and pipetted into the same 50ml falcon tube for centrifugation at 5,000rpm for 5 minutes. The supernatant was removed by aspiration, leaving ~0.5ml. The tube was flicked to resuspend the pellet,

and 3ml pre-warmed hypotonic solution was added slowly. The solution was transferred to a labelled 15ml falcon tube and incubated at 37°C for 15 minutes. 2-3 drops of ice cold fresh fixative solution were added to help keep the cells swollen before centrifuging for 5 minutes at 5,000rpm.

5.2.2.4 Fixation

All but 1ml of the supernatant was discarded using a Pasteur pipette, and the tube flicked to resuspend the cells. Single drops of fresh ice cold fixative were slowly added to the tube whilst flicking continually to avoid clumping of the cells. Once 5ml fixative had been added the samples were placed at -20°C for >30 minutes. Samples were centrifuged for 5 minutes at 5,000rpm and all but 1ml of the supernatant was removed with a Pasteur pipette. The samples were flicked to resuspend the pellet, 4ml fresh ice cold fixative was added, and the sample was centrifuged again at 5,000rpm for 5 minutes. The process of adding fresh fixative and centrifuging was repeated twice more. Samples were stored at -20°C in a re-sealable plastic bag containing a sachet of dessicant.

5.2.2.5 Preparing slides

Immediately before use, the fixed cells were centrifuged at 5,000rpm for 10 minutes, the supernatant was removed, and the cells were resuspended in 1-5ml freshly made fixative, depending on the size of the pellet. They were kept on ice, and replaced in the -20°C freezer in a sealed bag with dessicant immediately after use.

Single frosted glass microscope slides, which had been washed and stored at 4°C in 70% ethanol, were dried with lint-free tissue and labelled. The slides were held over steam from a clean waterbath (70°C) for 5 seconds, to create a humid surface, before swiftly pipetting 3x 12µl aliquots of cell suspension along the length of the slide. As the fixative began to dry, Newton's rings became visible. At this point the slide was held over steam for a further 3 seconds before being laid flat to dry at room temperature. The steam aids chromosome spreading. Once dry, slide quality was checked using a phase contrast microscope to ensure sufficient good quality metaphases were present. Slides were allowed to age for a few days before staining and mounting.

5.2.2.6 Staining slides

Slide buffer was made by dissolving 1 Gurr phosphate buffer tablet (pH6.8, Invitrogen) in 1L dH₂O. It was stored at 4°C. 55ml slide buffer was added to a Coplin jar containing 4ml Giemsa stain (BDH Labb Supplies, Gurr), and two more empty Coplin jars. Slides were immersed in Giemsa/buffer solution for 5 minutes before being transferred into the buffer-only Coplin jars for a few seconds each. The quality of stain on the first slide was checked under the microscope and the incubation times adjusted accordingly before proceeding with the remaining slides. Once stained, the slides were left to air dry at room temperature in a vertical position with the frosted, labelled end of the slide at the base. Slides were dried for a minimum of 12-24 hours before mounting.

5.2.2.7 Mounting slides

Mounting was carried out in a fume hood. Stained slides were immersed in Xylene (Fisher Scientific) for 15 minutes-1 hour. Using a glass pipette, 2 drops of DPX

Mountant for Histology (Fluka BioChemika) were placed onto the slide and a cover slip carefully dropped on top. Pressure was applied to the coverslip to remove air bubbles, and excess mountant was removed with blotting paper. Slides were laid flat to dry inside the fume hood. Once dry, they were stored in a slide box with dessicant.

5.2.2.8 Scoring aberrations

Scoring was carried out using the bright field function and a green filter on a Carl Zeiss Microscope (Axioskop 2) with 63x and 100x oil immersion lenses (1,25 and 1,30 objectives respectively). The label on each slide was obscured with a coded sticker so that scoring was blind. Slides were scored in a raster fashion from top left to bottom right, recording details of the first 120 good quality metaphases for each cell line and treatment condition. The chromosomes were counted and any visible aberrations noted and described. The Vernier position was noted for each aberrant metaphase and a picture was taken using Ikaros (MetaSystems) or Smart Capture X (Digital Scientific UK) imaging software.

5.2.2.9 Statistical Analysis

P values were calculated using the chi-square test, as this method allows the comparison of different proportions.

5.3 Results

5.3.1 Comet assay for strand break damage detection

Essentially, the comet assay involves lysis of single cells embedded in agarose, and removal of all membranes and the majority of cellular proteins to leave a nucleoid body composed of supercoiled DNA. The nucleoid bodies are exposed to an unwinding buffer and subjected to a short period of electrophoresis. This has the effect of causing the DNA to migrate out of the nucleoid body, to form a 'comet' with a head and a tail. Examples are shown in Figure 5-1. The extent of migration of DNA from the head to the tail of the comet is dependent upon the degree of coiling of the DNA and also the integrity of the DNA strands. As such, the proportion of the DNA contained within the tail of the comet (the percentage tail DNA) is proportional to the combined level of SSBs, DSBs and alkali-labile sites present within the nucleoid body (Olive and Banáth, 2006).

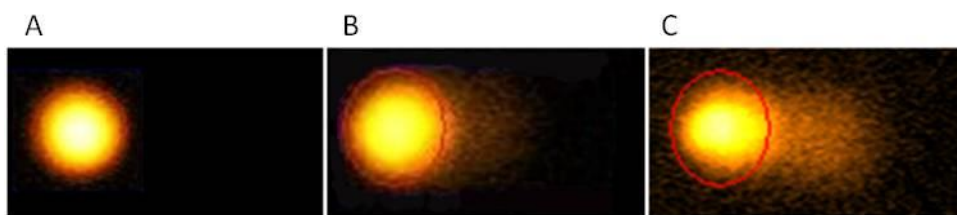


Figure 5-1. Comet images obtained using Komet 5.0 analysis software and displaying increasing levels of DNA damage (% tail DNA) from no damage (A) to high levels of damage (C).

Using this procedure, the average level of single and double DNA strand breaks in the wild type, *Dnmt1*^{-/-} and *Dnmt3a3b*^{-/-} ESCs was determined 23-25 PDs after sham treatment or 3Gy X-irradiation. The results are displayed in Figure 5-2 below,

expressed as the percentage tail DNA, averaged from 600 cells (200 cells per experiment, carried out in triplicate).

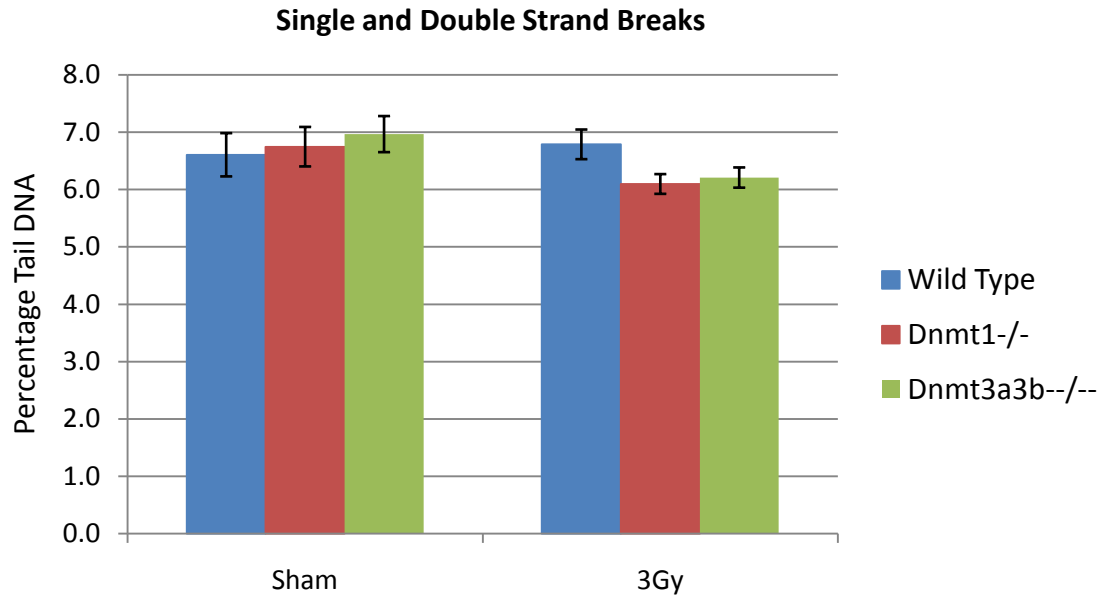


Figure 5-2. Percentage tail DNA of three mESC lines, 23-25PDs post 3Gy X-irradiation or sham treatment. Results are expressed as an average of 3 independent experiments, each comprising 200 separate cell measurements. Error bars represent the SEM of the averages of the 3 independent experiments.

The average level of strand breaks was very similar between all of the cell lines and treatment conditions analysed. After Bonferroni correction for multiple testing, there was no significant difference in the average level of strand breaks between any of the cell lines ($p > 0.1$), or between the 3Gy and sham treatment conditions ($p > 0.07$).

5.3.2 Comet Assay for oxidative stress damage detection

Fpg is a DNA glycosylase that generates SSBs at sites containing oxidized purines such as 8oxoG lesions (Maynard *et al*, 2008). By subtracting the results of cells treated with buffer alone from those treated with Fpg and buffer, the relative level of Fpg-sensitive oxidized bases could be specifically assessed. The results are presented in Figure 5-3 below, expressed as the percentage tail DNA averaged from 600 cells (200 cells per experiment, carried out in triplicate).

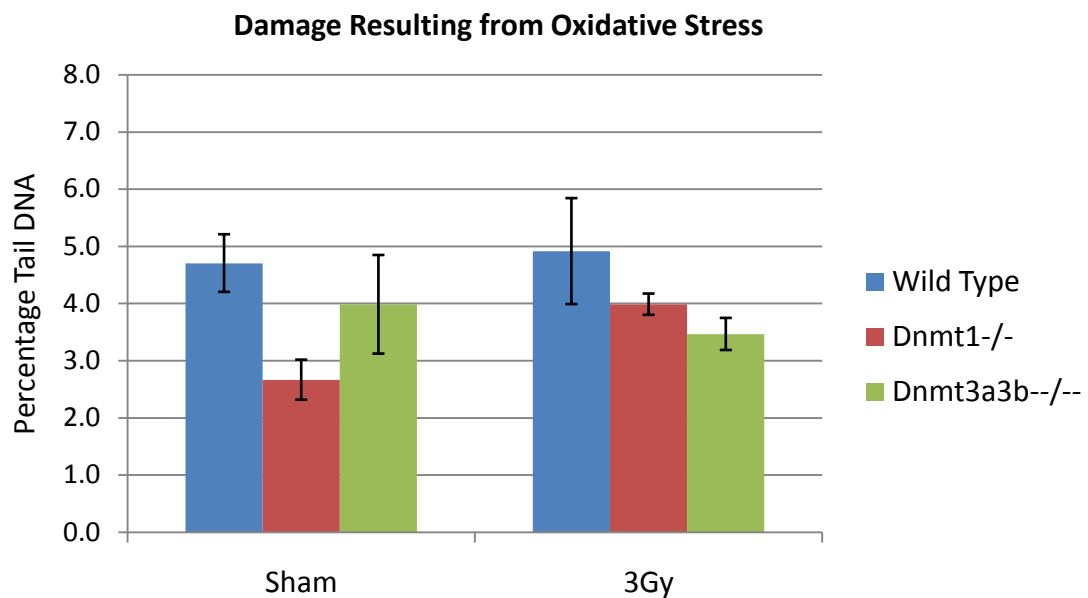


Figure 5-3. Percentage tail DNA of three mESC lines, 23-25PDs post 3Gy X-irradiation or sham treatment. Results are expressed as an average of 3 independent experiments, each comprising 200 separate cell measurements. Error bars represent the SEM of the averages of the 3 independent experiments.

As Figure 5-3 shows, there was more variation in the average level of lesions indicative of oxidative stress between the cell lines and treatment conditions than the average level of strand breaks. However, there was also greater variation between and within

experiments, as reflected by the larger error bars. As a result, after correction for multiple testing, there was no significant difference in the average level of lesions indicating oxidative stress induced DNA damage between any of the cell lines ($p>0.07$), or between the 3Gy and sham treatment conditions ($p>0.06$).

5.3.3 Frequency of structural cytogenetic aberrations

Many cell types are contact inhibitive and will accumulate in G1 phase of the cell cycle when grown to high density in the culture flask. This allows the majority of the cells to be irradiated at the same phase of the cell cycle. Re-seeding the cells in a lower concentration post irradiation then stimulates them to undergo a new round of cell division (Nilausen and Green, 1965). Thus, the cells are synchronised and a high mitotic index should be obtained at the next mitosis. Some research groups allow an incubation period of ≥ 1 hour post irradiation before re-seeding the cells. This enables the cells to repair any potentially lethal radiation-induced DNA damage before they enter a new round of cell division, and as such significantly increases their survival in comparison to cells allowed no recovery period (Kano and Little, 1984).

However, the ESCs used in the present study are not contact-inhibitive, and do not accumulate in G1 phase when grown to confluence (Burdon *et al*, 2002). Therefore, it is questionable whether the presence of the 1 hour recovery period would make any difference to the results. To investigate this possibility, at the 10-14 PD time point post treatment, the 3Gy X-irradiated cells grown from cultures plated immediately after irradiation and 1hr post irradiation were analysed separately. The results between the cells with/without a recovery period were not statistically different ($p>0.05$). Thus,

they were added together and used as a single “3Gy” treatment condition. At the 23-25 PD post treatment time point only the cells permitted the 1 hour recovery period were used.

Approximately 120 cells or metaphases (40 per slide) were scored at each time point for each treatment condition for each of the wild type, *Dnmt1*^{-/-} and *Dnmt3a3b*^{-/-} ESC lines. Thus, >200 metaphases were scored per cell line at the 23-25 PD time point, and >300 metaphases were scored per cell line at the 10-14 PD time point due to the inclusion of an extra treatment condition (1 hour recovery post 3Gy) at this time point. Table 5.1 and Table 5.2 list the precise number of metaphases scored for each cell line and treatment group. The number of chromosomes in each metaphase were counted and recorded, and have been analysed in section 5.3.4. The presence and number of any visible structural aberrations were also recorded. Tables of the raw data, detailing the numbers of each aberration observed can be found in appendix 7.3. Illustrations of the appearance of each aberration type are displayed in appendix 7.4.

Table 5-1 and Table 5-2 list the frequency of metaphases containing any detectable structural aberrations for each time point. At the 10-14 PD time point there was no significant difference in the frequency of total structural aberrations between any of the cell lines, or between the sham and 3Gy treatment groups ($p > 0.22$) as calculated using the chi-square test. The same was true for the later time point of 23-25 PDs ($p > 0.39$). In addition, there was no significant difference in the frequency of structural aberrations between the two time points ($p > 0.14$). The average number of aberrations per metaphase was also not significantly different between any of the cell lines or

between the sham and 3Gy treatment conditions at the 10-14 PD time point ($p>0.12$) or the 23-25 PD time point ($p>0.27$).

10-14 PD	Total number of metaphases scored	Metaphases with structural aberrations %	Average number of aberrations per metaphase ($\pm 95\%$ CI)	Ratio of chromatid to chromosome type aberrations
Cell line/condition				
Wild Type Sham	119	12	0.15 \pm 0.07	0.8
Wild Type 3Gy	238	9	0.10 \pm 0.04	1.1
<i>Dnmt1</i> ^{-/-} Sham	118	14	0.19 \pm 0.08	0.4*
<i>Dnmt1</i> ^{-/-} 3Gy	248	12	0.15 \pm 0.05	0.9
<i>Dnmt3a3b</i> ^{-/-} Sham	120	11	0.13 \pm 0.07	1.5
<i>Dnmt3a3b</i> ^{-/-} 3Gy	232	16	0.20 \pm 0.06	1.6

Table 5-1. Frequencies and ratios of structural cytogenetic aberrations observed 10-14 population doublings (PD) post irradiation with 3Gy X-rays or sham treatment. *The ratio of chromatid to chromosome aberrations is significantly different between the sham and 3Gy treatment groups for *Dnmt1*^{-/-} ($p=0.024$ after Bonferroni correction).

23-25 PD	Total number of metaphases scored	Metaphases with structural aberrations %	Average number of aberrations per metaphase ($\pm 95\%$ CI)	Ratio of chromatid to chromosome type aberrations
Cell line/condition				
Wild Type Sham	119	15	0.17 \pm 0.08	0.8
Wild Type 3Gy	139	13	0.14 \pm 0.07	1
<i>Dnmt1</i> ^{-/-} Sham	119	15	0.20 \pm 0.08	0.9
<i>Dnmt1</i> ^{-/-} 3Gy	120	11	0.14 \pm 0.07	1.1
<i>Dnmt3a3b</i> ^{-/-} Sham	119	13	0.18 \pm 0.08	0.8
<i>Dnmt3a3b</i> ^{-/-} 3Gy	120	10	0.13 \pm 0.07	1

Table 5-2. Frequencies and ratios of structural cytogenetic aberrations observed 23-25 population doublings (PD) post irradiation with 3Gy X-rays or sham treatment.

The proportion of chromatid-type to chromosome-type aberrations observed in the wild type cell line was comparable at both time points, and did not differ significantly between the 3Gy and sham treatment groups. The ratio of chromatid to chromosome type aberrations observed in the *Dnmt3a3b*^{-/-} ESCs also did not differ significantly between the treatment groups. However, a significantly elevated ratio of chromatid-type aberrations were observed in the *Dnmt3a3b*^{-/-} ESC line in comparison to the wild type ESCs at the 10-14 PD time point ($p=0.003$). This difference is not thought to reflect an effect of global hypomethylation, as the difference was found to be even greater between the *Dnmt3a3b*^{-/-} and *Dnmt1*^{-/-} ESC lines ($p=4 \times 10^{-7}$). In addition, the ratio of chromatid-type aberrations displayed by the *Dnmt3a3b*^{-/-} cell line was significantly lower at the 23-25 PD time point ($p=0.02$). Thus, it is possible that the elevated ratio of chromatid-type aberrations observed at the 10-14 PD time point was an anomaly.

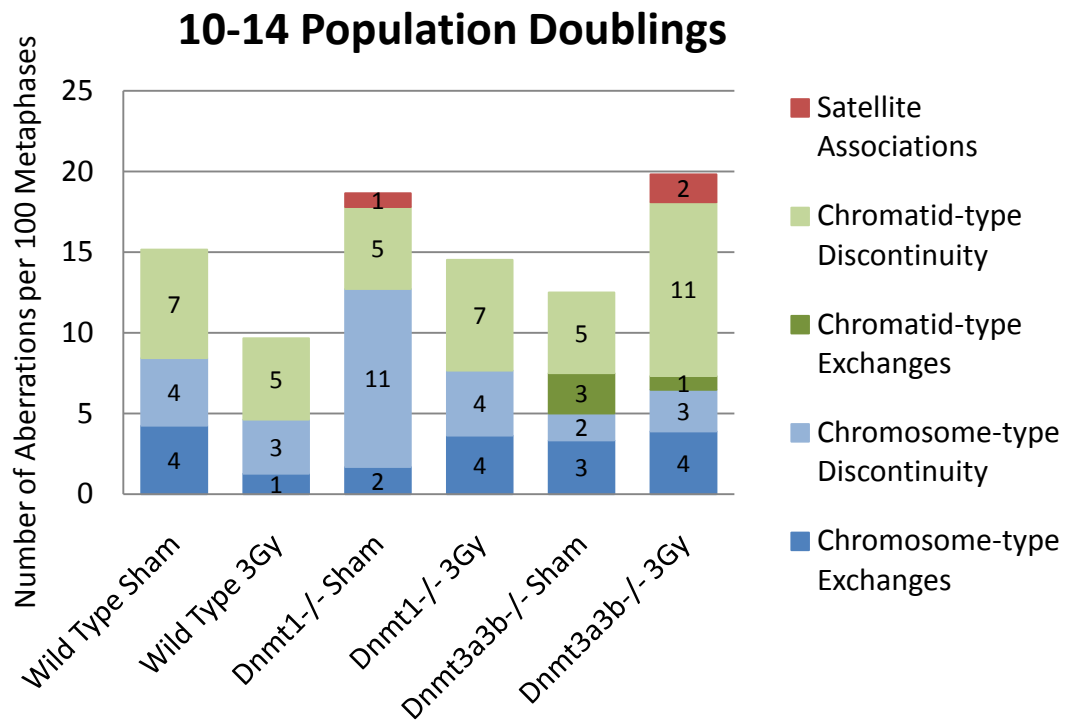
A trend was apparent at both time points, in which 3Gy X-irradiated ESCs appear to display a higher proportion of chromatid-type aberrations than unirradiated ESCs. This shift in the ratio was small in the wild type and *Dnmt3a3b*^{-/-} cell lines. However, the *Dnmt1*^{-/-} cell line displayed a significantly higher proportion of chromatid-type aberrations in the 3Gy treated cells compared to the sham treated cells, at the 10-14 PD time point ($p=0.008$). This will be discussed further in section 5.4.3.

To enable more detailed analysis of the structural cytogenetic aberrations observed, they were grouped according to classifications defined by John Savage (Savage, 1999). The results are displayed in Figure 5-4. No significant difference was observed in the

frequency of any class of structural aberration between any of the cell lines or treatment groups, after correction for multiple testing ($p>0.11$). The same was true when the aberrations were grouped simply into either exchanges or discontinuities, regardless of chromosome- or chromatid-type ($p>0.14$). In addition, there was no significant difference in the frequency of aberrations in each class between the two time points for each cell line (3Gy or sham) ($p>0.11$).

The structural aberrations observed in the present study were re-grouped into those cited in the literature as being transmissible forms and those cited as being non-transmissible forms (Savage, 1999). Only four transmissible aberrations were detected in total: one chromatid-type reciprocal translocation in the 3Gy-treated *Dnmt3a3b*^{-/-} cell line at the 10-14 PD time point (see Figure 5-5 A); and an aberration involving the appearance of abnormally long satellite arms, which was observed once in the 3Gy-treated wild type cells, 8 times in the 3Gy-treated *Dnmt1*^{-/-} cells, and 5 times in the sham-treated *Dnmt1*^{-/-} cells (see example in Figure 5-5 B). Thus, the long satellite arm aberration was observed almost exclusively in the *Dnmt1*^{-/-} cell line ($p=0.001$). It was seen multiple times at the 23-25 PD time point, but was not noted at the 10-14 PD time point ($p=0.0003$). Accordingly, it was counted only once towards the total aberration frequency for each cell line/treatment condition in which it was observed.

A.



B.

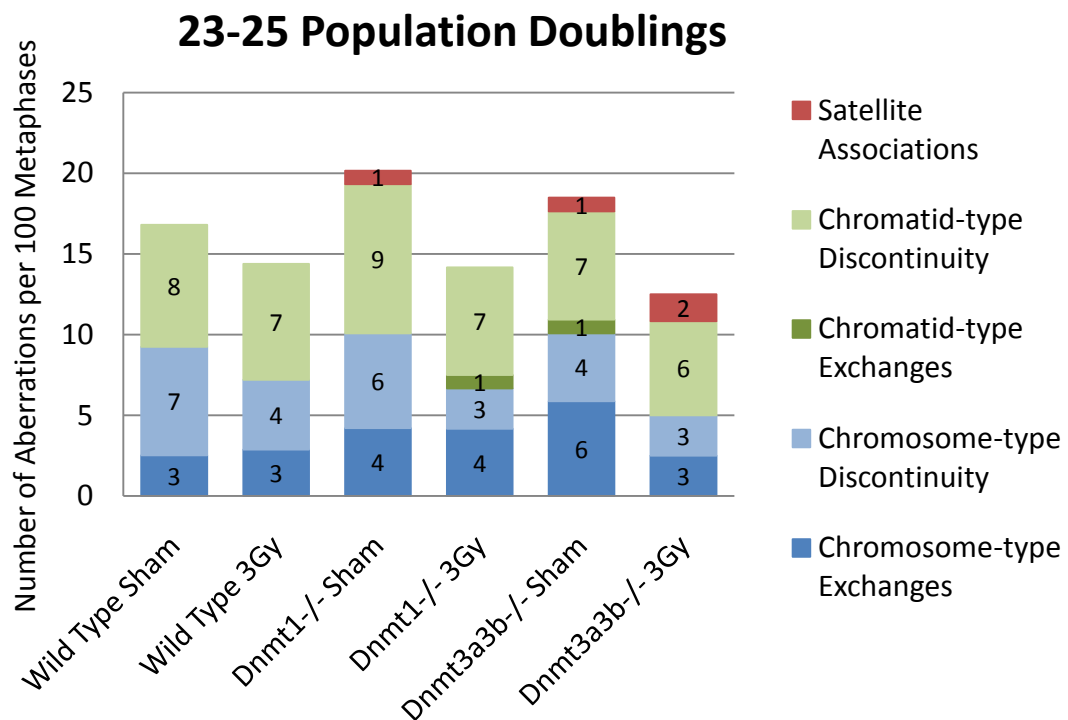


Figure 5-4. Classifications of structural cytogenetic aberrations as defined by Savage (1999). The results are displayed as the number of each class of aberration observed per 100 metaphases. Graph A displays the results 10-14 PDs post treatment; Graph B displays the results 23-25 PDs post treatment.

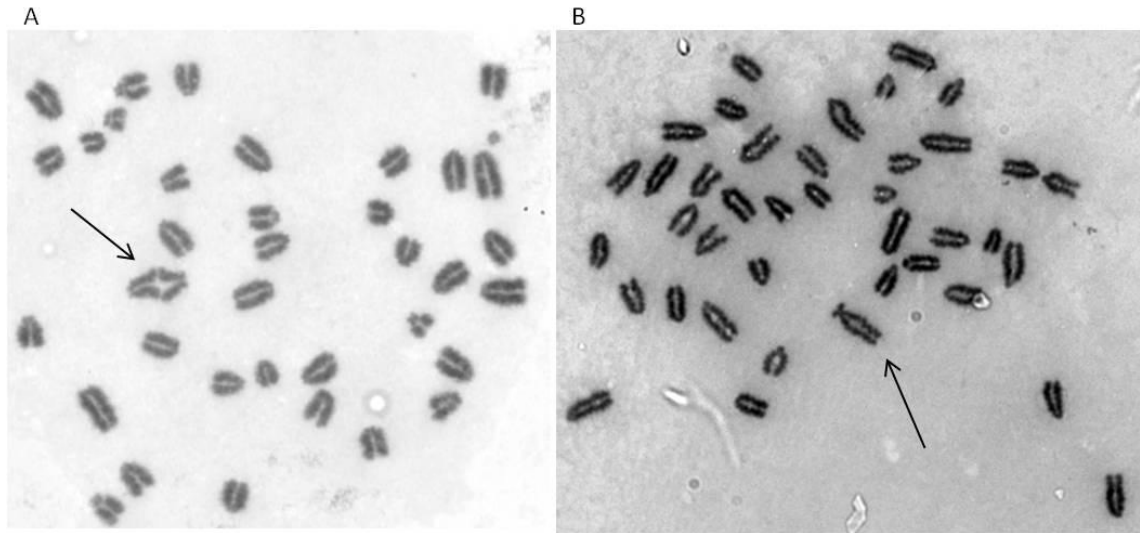


Figure 5-5. Mitotic spreads of Giemsa-stained chromosomes from the *Dnmt3a3b*^{-/-} ESC line 10-14 PDs post 3Gy X-irradiation, showing a chromatin-type reciprocal translocation (A) and the *Dnmt1*^{-/-} ESC line 23-25 PDs after sham treatment, showing a chromosome with very long satellite arms.

Several complex exchanges involving the satellite arms of three or more chromosomes were observed in the hypomethylated *Dnmt* knock out ESC lines, at both time points, irrespective of the treatment condition. No such aberrations were observed in the wild type cell line. These complex exchanges between three or more different chromosomes are unlikely to be transmitted to daughter cells in an intact state due to mechanical separation problems encountered during mitosis (Savage, 1980). Examples are shown in Figure 5-2 below.

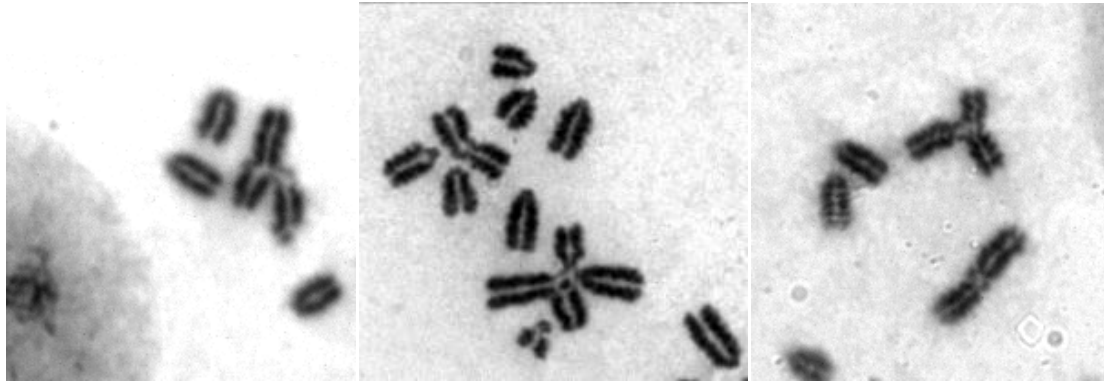
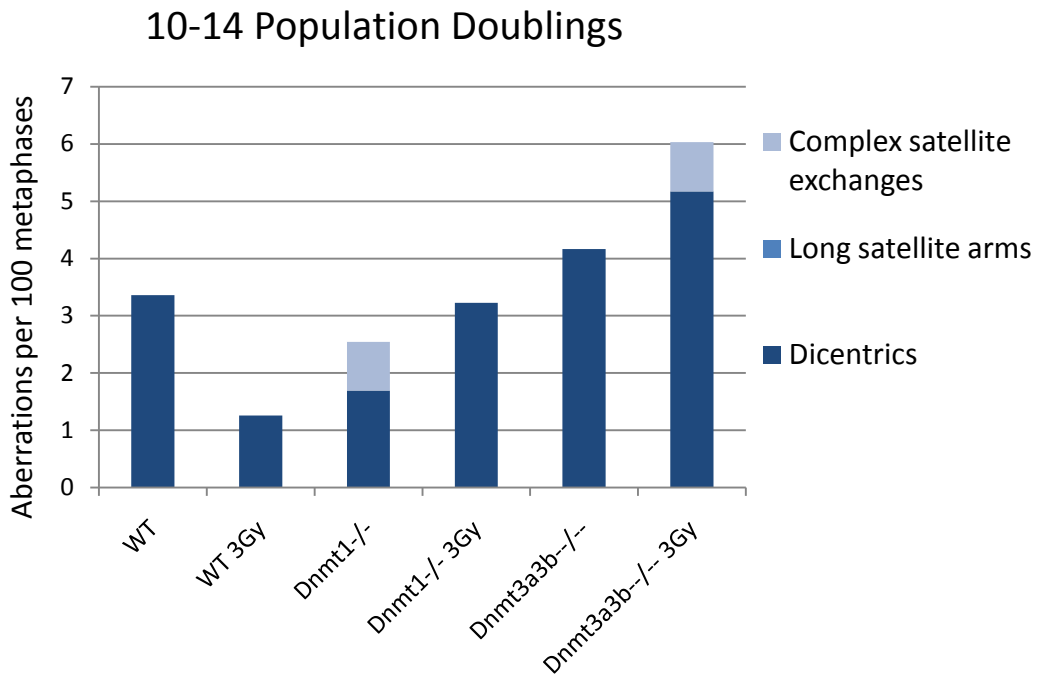


Figure 5-6. Dicentric, tri-centric and tetra-centric chromosome-type aberrations observed in Giemsa-stained metaphase spreads of *Dnmt1*^{-/-} and *Dnmt3a3b*^{-/-} mESCs.

The frequencies of the three aberration types observed that appear to involve associations or exchanges of the satellite arms (long satellite arms, dicentrics and complex satellite exchanges) were combined. The results are displayed for each cell line/treatment condition and time point in Figure 5-7.

The difference in the frequency of each of these aberrations between the wild type and the *Dnmt*^{-/-} cell lines, or between the sham and 3Gy treatment groups, was not statistically significant when analysed individually ($p > 0.13$). The aberrations were subsequently grouped together as associations or exchanges of the satellite arms, and the time points and treatment conditions were combined. This revealed that the elevated frequency of aberrations observed in the *Dnmt3a3b*^{-/-} ESC line in comparison to the wild type cell line, was bordering on significant ($p = 0.051$). However, the frequency of associations or exchanges involving the satellite arms that were observed in the *Dnmt1*^{-/-} ESC line was not significantly different to that of the wild type cell line ($p = 0.3$).

A.



B.

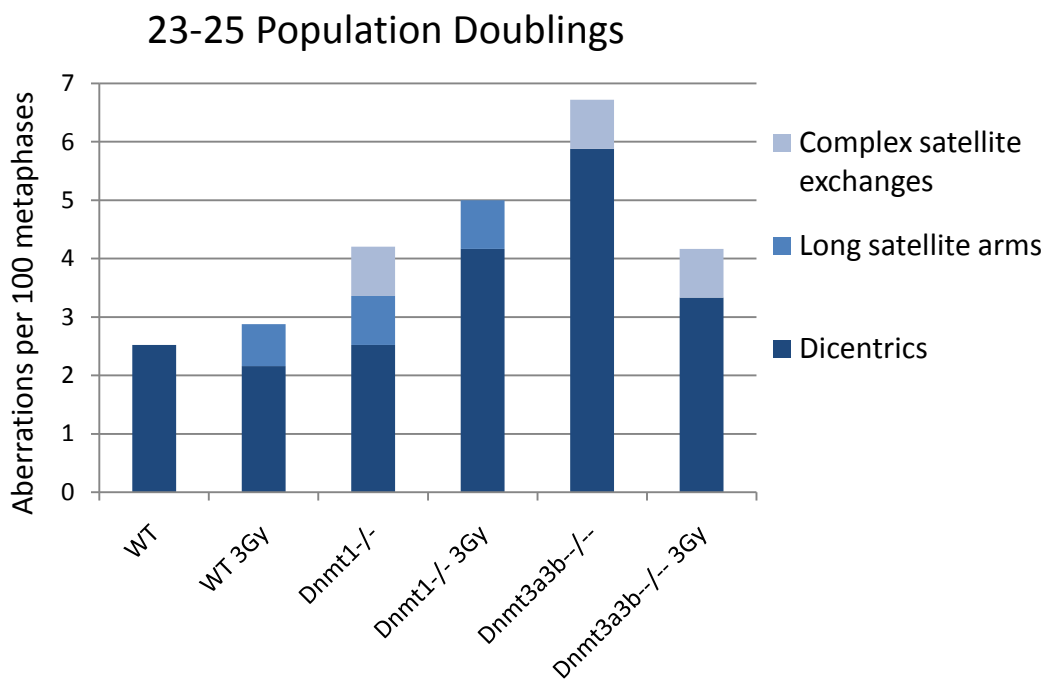


Figure 5-7. Graphs showing the frequency of chromosome aberrations involving associations or exchanges of the satellite arms at the 10-14 PD and 23-25 PD time points (graphs A and B respectively). Frequencies are expressed as the number of aberrations per 100 metaphases scored.

Finally, a multi-radial chromosome was observed in a single metaphase which showed a high level of background damage, indicated by the presence of multiple breaks and fragments. This metaphase, shown in Figure 5-8, was observed at the 23-25 PD time point, in the wild type cell line which had been exposed to 3Gy X-irradiation.

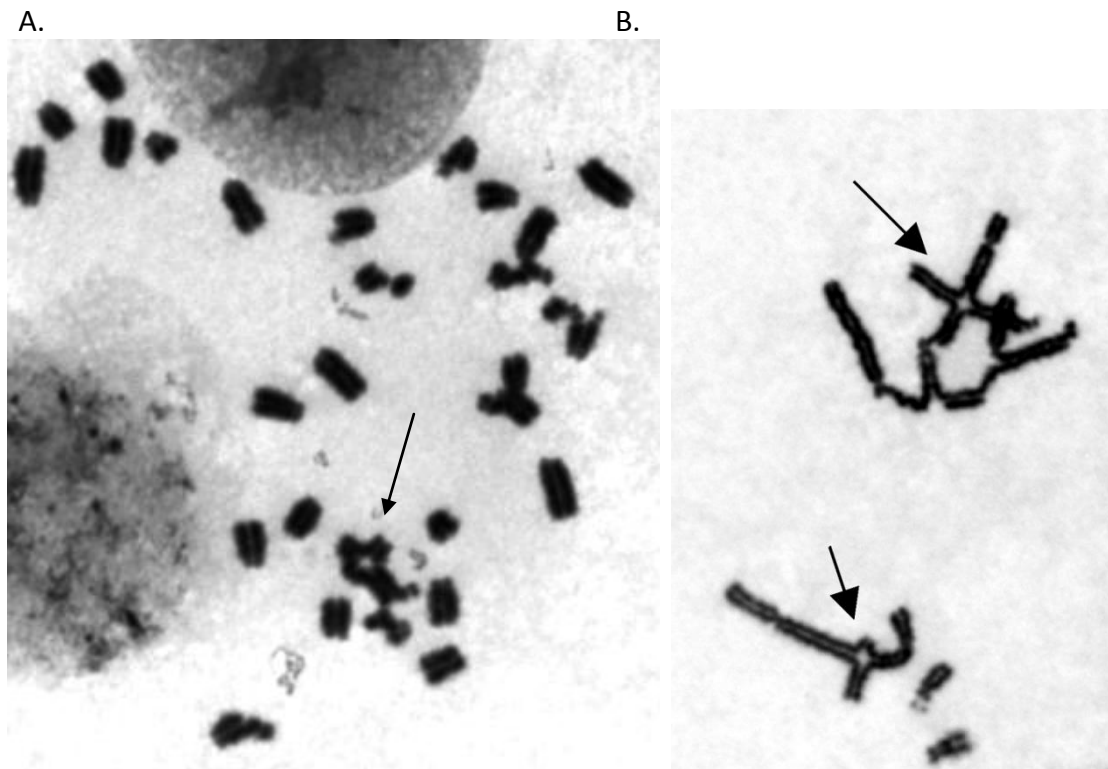


Figure 5-8. A: Giemsa stained metaphase harvested 23-25 population doublings post exposure to 3Gy X-irradiation in the wild type ESC line. The multi-radial chromosome is indicated by an arrow. B: Giemsa-stained chromosomes from a patient with Fanconi anaemia following treatment with the crosslinking agent mitomycin C. The characteristic quadri- and tri-radial chromosome aberrations are indicated by arrows. Image from Howlett *et al* (2005). See License Agreement in appendix 7.5.

5.3.4 Frequency of numerical chromosome aberrations

In addition to structural aberrations, the frequency of numerical chromosome aberrations was also noted during the analysis. Haploid metaphases could not reliably be distinguished from overspread metaphases, so any metaphases with a chromosome count of ≤ 35 were excluded from the analysis. The results are shown in Figure 5-9.

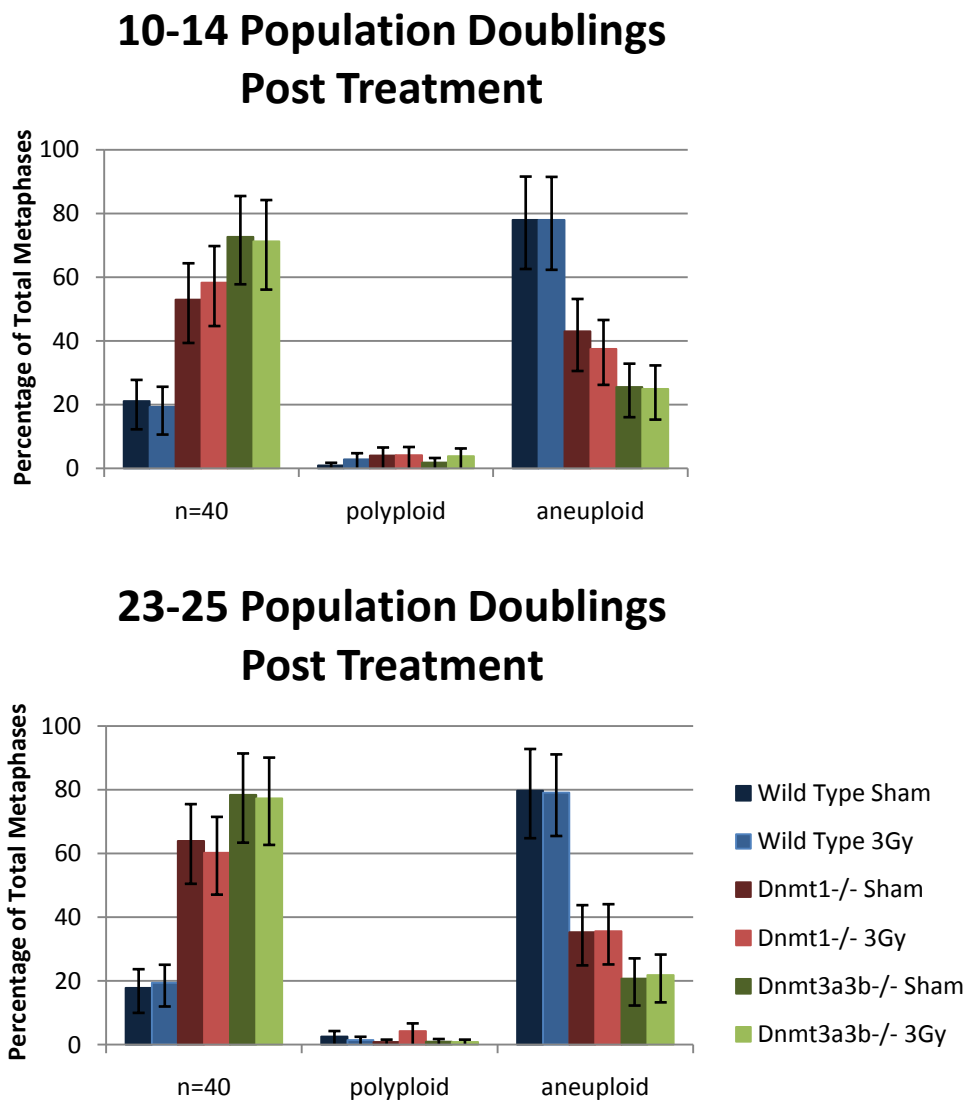


Figure 5-9. Graphs illustrating the percentage of metaphases scored for each cell line and treatment condition which were diploid (n=40), polyploid or aneuploid. A separate graph has been constructed for each time point.

At both the 10-14 PD and 23-25 PD time points, the treatment condition (sham or 3Gy) had no discernable effect on the frequency of numerical chromosome aberrations ($p > 0.11$). There were, however, significant differences in the frequency of numerical aberrations between the cell lines. The wild type cell line showed a significantly higher frequency of aneuploid metaphases than either of the *Dnmt* knock out (KO) cell lines ($p < 0.02$ and $p < 0.0005$ for the 10-14 PD and 23-25 PD time points respectively). The frequency of aneuploidy was not significantly different between the *Dnmt1*^{-/-} and *Dnmt3a3b*^{-/-} cell lines ($p = 0.08$ and $p = 0.07$ for the early and late time points respectively). In addition, the frequency of polyploid cells did not differ significantly between any of the cell lines or treatment conditions ($p \geq 0.09$). Finally, there were no significant differences in the frequency of numerical chromosome aberrations between the two time points for each cell line and/ or treatment condition ($p > 0.15$).

The level of aneuploidy in the *Dnmt3a3b*^{-/-} cell line is slightly higher at the 10-14 PD time point than at the 23-25 PD time point. The methylation level of this cell line decreases with increasing passage number (see Figure 3-4). At the 10-14 PD time point the *Dnmt3a3b*^{-/-} ESC line is p#31, and p#41 by the 23-25 PD time point. Thus, the methylation level of this ESC line would have decreased slightly between the two time points. Furthermore, the methylation level of the *Dnmt3a3b*^{-/-} cell line was lower than that of the *Dnmt1*^{-/-} cell line at both time points and it displays a lower frequency of aneuploidy. Possible mechanisms responsible for the comparatively low frequency of aneuploidy observed in the *Dnmt1*^{-/-} and *Dnmt3a3b*^{-/-} ESC lines compared to the wild type are discussed in section 5.4.6.

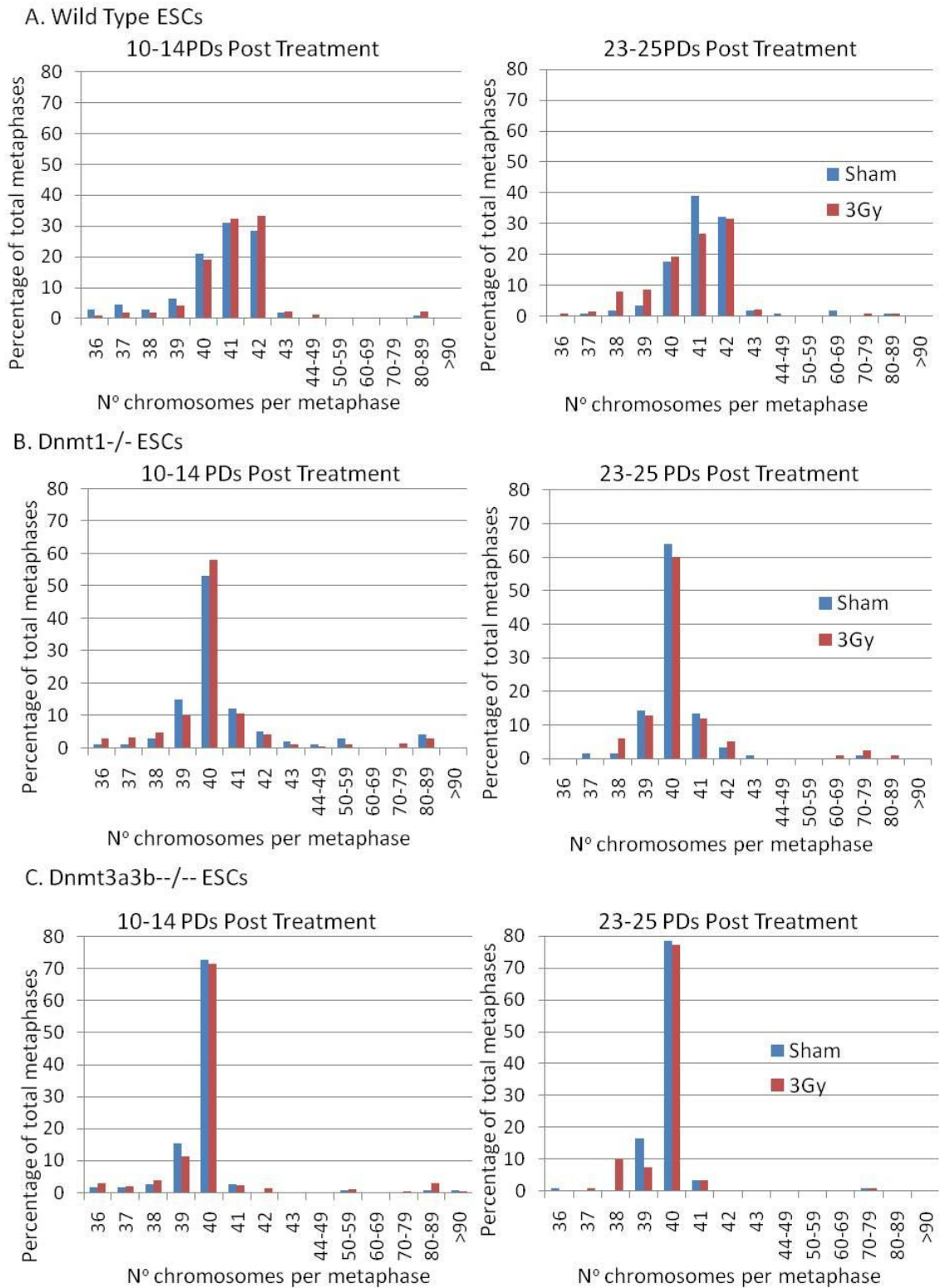


Figure 5-10. Graphs showing the spread of chromosome counts in each of the cell lines at the 10-14 PD and 23-25 PD time points. A. Wild type ESCs; B. *Dnmt1*^{-/-} ESCs; and C. *Dnmt3a3b*^{-/-} ESCs.

In addition to the differing overall frequency of aneuploidy between the ESC lines, the mean chromosome number was also slightly different. This is illustrated by the spread of the chromosome counts for each cell line, displayed in Figure 5-10. The spread of chromosome numbers in the metaphases was consistent at both time points for each cell line. As Figure 5-10 shows, the majority of the aneuploid metaphases detected in the wild type ESCs, have extra copies of one or two chromosomes, forming a skewed distribution. In the *Dnmt1*^{-/-} ESCs, the spread of aneuploidy appeared to follow a much more normal/Gaussian distribution. There was a roughly equal distribution of gain and loss of chromosomes in the aneuploid metaphases, with gain or loss of just one chromosome being most common. The spread of aneuploidy was tightest in the *Dnmt3a3b*^{-/-} ESCs, with the majority of metaphases displaying aneuploidy in this cell line arising as a result of loss of a single chromosome.

5.4 Discussion

5.4.1 Global hypomethylation does not alter the level of endogenous or delayed DNA damage measured by the comet assay

Global levels of DNA damage (mainly strand breaks) were measured using the alkaline comet assay with the aim of characterising the effect of DNA hypomethylation on a genome-wide scale. The alkaline comet assay was used, rather than the neutral comet assay, due to its increased sensitivity for detecting low levels of DNA damage (Speit *et al*, 2004). Three of the mESC lines (wild type, *Dnmt1*^{-/-} and *Dnmt3a3b*^{-/-}) were analysed 23-25 PDs post 3Gy X-irradiation or sham treatment. This delayed time point is equivalent to that at which cells were seeded into selective media for detection of mutations in the *Hprt* gene. As such, a direct comparison could be made between the genome-wide levels of strand breaks and the types and rates of mutations detected at the *Hprt* locus.

Previous studies demonstrate that treatment of tumour and lymphocyte cell lines with drugs that induce genome-wide DNA hypomethylation or inhibit histone deacetylation, results in a persistence of elevated levels of γ H2AX foci after irradiation compared to untreated control cells (Camphausen *et al*, 2004; Camphausen *et al*, 2005; Dote *et al*, 2005; Stoilov *et al*, 2000). This indicates either inhibition of DSB repair (Dote *et al*, 2005) or *de novo* formation of new DSBs. Based on these observations it was expected that the hypomethylated *Dnmt1*^{-/-} and *Dnmt3a3b*^{-/-} ESC lines used in the present study would show increased endogenous levels of strand breaks in comparison to the wild type ESCs. The *Dnmt1*^{-/-} ESC line, in particular, was postulated to exhibit a

significantly higher frequency of strand breaks due to its roles in DNA damage repair (see section 1.3), and the elevated spontaneous mutation rate observed in this cell line at the *Hprt* locus.

As shown in Figure 5-2, each of the ESC lines analysed displayed a percentage tail DNA value of 6-7%. This is similar to the endogenous levels of strand breaks detected in murine bone marrow (6.3% tail DNA) and slightly higher than the levels in kidney (5.2% tail DNA) (Oshida *et al*, 2008). However, the level of endogenous strand breaks detected in the sperm of unirradiated mice is higher still (~10% tail DNA) (Haines *et al*, 2002). Thus, there appears to be a trend of increasing levels of strand breaks in tissues with lower methylation levels. However, care should be taken when comparing results between different studies. Nevertheless, the results of this project are within the expected range.

No significant difference was observed in the level of endogenous strand breaks between the wild type and *Dnmt* KO cell lines. Therefore, if the level of DNA methylation does affect the level of strand breakage in the ESC model system, this occurs at a level that is below the resolution of the comet assay. Nevertheless, this finding does not contradict those of the studies by Dote *et al* (2005) and Stoilov *et al* (2000), as treatment with Zebularine or iHDACs did not induce significantly increased levels of γ H2AX foci in comparison to untreated control cells in the absence of irradiation. Nor did it elevate the level of γ H2AX foci induced initially by irradiation. Rather, hypomethylation or hyperacetylation appeared to inhibit the ability of the cells to repair the radiation-induced DNA damage (Camphausen *et al*, 2004; Camphausen *et*

al, 2005; Dote *et al*, 2005; Stoilov *et al*, 2000). It was suggested that this could be a result of altered activity or expression of the proteins required for efficient DNA damage response (Stoilov *et al*, 2000). Indeed, administration of Zebularine or iHDACs has been shown to alter the expression of key DNA repair genes (Ku70, Ku86, DNA-PKcs) and cell cycle and apoptosis regulatory proteins (p16, p21) in unirradiated cell lines (Cheng *et al*, 2004; Munshi *et al*, 2005).

In this project, no significant difference was detected in the level of DNA damage (SSBs, DSBs and ALSs) between the sham and 3Gy-treated cells. This indicates that the elevated mutation rates observed at the *Hprt* locus in the wild type ESCs 23-25 PDs post 3Gy X-irradiation, and in the *Dnmt1*^{-/-} ESCs in both sham and 3Gy treatment conditions, are not a result of increased levels of strand breaks. It also indicates that, in contrast to the study by Dote *et al* (2005), DNA hypomethylation does not suppress the cellular DNA repair capacity. However, the extent of alterations in gene expression observed by Cheng *et al* (2004) and Munshi *et al* (2005) as a result of Zebularine or iHDAC treatment were cell-type specific. Interestingly, the induced alterations in gene expression and increases in radiosensitivity were greater in tumour cell lines than normal controls, possibly reflecting cell/tumour-specific differences in the transcriptional control of DNA repair (Cheng *et al*, 2004; Munshi *et al*, 2005).

In addition, it should be noted that the delayed time point used in this project was much longer than the 24 hour time point used by Dote *et al* (2005). Thus, a comparison is being made between the levels of strand breaks persisting in the original irradiated cells (Dote *et al*, 2005) and the levels of strand breaks persisting in the progeny of the

irradiated cells after 23-25 population doublings. DNA DSB repair exhibits a rapid component with a half-life of 5-30 minutes and a slow component with a half-life of 1-20 hours (Wang *et al*, 2001). The fast component is thought to correspond to the NHEJ repair process, and deficiency in proteins involved in NHEJ causes an increased number of DSBs to be repaired with slow kinetics (DiBiase *et al*, 2000; Wang *et al*, 2001). It is therefore possible that Zebularine-induced hypomethylation caused changes in gene expression that resulted not in an inability to repair DSBs, but a shift in the repair mechanism to one with much slower kinetics. As such, an elevated level of DSBs would be present in the cell lines 24 hours post irradiation, as reported by Dote *et al* (2005). The possibility that an inhibition of DNA repair would have been seen within the first 24 hours after X-irradiation in the hypomethylated ESC lines in this project cannot be ruled out, and is something that could be investigated in the future.

Alternatively, the apparent deficit in cellular repair capacity observed by Dote *et al* (2005) may reflect an effect specific to Zebularine-induced hypomethylation. Treatment resulted in a significant level of G2 cell cycle arrest (Dote *et al*, 2005), suggesting that the covalent attachment of Zebularine to the DNA methyltransferase enzymes (Champion *et al*, 2010) may generate obstacles for the cellular replication machinery, resulting in damage formation during S phase. Such an effect would not be seen in the hypomethylated cell lines used in this project.

5.4.2 Radiation-induced delayed genomic instability at *Hprt* in wild type

ESCs is not a result of increased oxidative damage

Oxidative stress is one of the proposed mechanisms by which radiation-induced delayed genomic instability is propagated (Wright, 2010). Several studies indicate that methylated DNA is a preferential target for adduct-forming physical and chemical mutagens, such as BPDE and solar UV light, in comparison to unmethylated DNA (Denissenko *et al*, 1997; Tomassi *et al*, 1997; Yoon *et al*, 2001; You *et al*, 1999). In addition, oxidative intrastrand cross link lesions have been shown to form >10 times more efficiently in methylated than unmethylated DNA, suggesting that the presence of methylation at CpG dinucleotides can lead to increased levels of certain types of oxidative damage in response to oxidative stress (Cao and Wang, 2007). Furthermore, Amouroux *et al* (2010) found that oxidation of guanine to form 8-oxoG results in preferential recruitment of the BER machinery to euchromatin regions and almost complete exclusion from heterochromatin in HeLa cells. Moreover, the induction of a compact chromatin state using hypertonic shock triggered by sucrose resulted in inhibition of the repair of 8-oxoG (Amouroux *et al*, 2010).

Based on these observations, it was expected that the wild type ESC line, which was the only cell line to demonstrate the occurrence of radiation-induced delayed genomic instability at the *Hprt* locus, would exhibit elevated levels of oxidative stress 23-25 population doublings (PD) post irradiation with 3Gy X-rays. This hypothesis was investigated using a modified form of the alkaline comet assay described in section

5.2.1 which incorporates a glycosylase enzyme (Fpg) that converts oxidized purines such as 8-oxoG into strand breaks (Tchou et al, 1991).

In contrast to expectations, the results revealed no significant difference in the average level of lesions indicating oxidative-stress between the wild type and hypomethylated ESC lines, or between the sham and 3Gy treatment groups. Thus, it appears that the radiation-induced delayed genomic instability observed at the *Hprt* locus in the wild type cell line is not a result of persistently increased levels of oxidative stress. However, the oxidative lesions detected in the present study were those oxidised purines such as 8-oxoG, which could be converted to strand breaks by the glycosylase enzyme, Fpg. Thus, it is possible that the crosslink lesions observed at elevated levels in methylated DNA by Cao and Wang (2007) were simply not detected in this project.

Alternatively, the difference between the results of this project and those of Cao and Wang (2007) could reflect the fact that whilst genomic DNA has been the substrate in this project, Cao and Wang (2007) used synthetic DNA fragments to demonstrate the link between methylation levels and oxidative damage. Thus, the possible influences of higher order chromatin structure and the radical-scavenging abilities of histone proteins (Milligan *et al*, 2004) have not been taken into account.

Finally, ESCs are reported to differ from somatic cells in their response to DNA damage (see section 1.5), including damage caused by oxidative stress (Maynard *et al*, 2008). Endogenous levels of the oxidative lesion 8-oxoG have been shown to be significantly

lower in hESCs than fibroblasts. In addition, hESCs were found to repair Fpg-sensitive oxidative DNA lesions more rapidly (Maynard *et al*, 2008). Another group has shown that mESCs have superior antioxidant capacity in comparison to various differentiated murine cells (Saretzki *et al*, 2004). Furthermore, as hESCs differentiate, major antioxidant genes become down-regulated and ROS levels increase (Saretzki *et al*, 2008). Thus, it is possible that whilst somatic cells manifest radiation-induced delayed genomic instability at least in part through oxidative stress, the occurrence of such lesions are not detected in elevated levels in ESCs due to their increased capacity for repair of such damage.

5.4.3 Structural Cytogenetic Aberrations

A pilot study was performed using a non-clonal bulk culture method. The analysis was designed to complement the mutation rate results generated at the *Hprt* locus, within the time frame of this PhD. As such, the wild type, *Dnmt1*^{-/-} and *Dnmt3a3b*^{-/-} ESC lines, which gave distinctive *Hprt* mutation rate results, were analysed 23-25 PDs after exposure to 3Gy X-rays or sham treatment. A natural extension of this work would involve a more detailed analysis of cultures derived clonally from single irradiated cells.

The presence of transmissible chromosome aberrations in a non-clonal bulk culture does not necessarily indicate the occurrence of ongoing genomic instability, as it is not possible to determine whether they have arisen *de novo* or simply been transmitted clonally through the progeny. The staining method used in this project, however, preferentially allowed detection of unstable or non-transmissible aberrations characterised either by gross structural abnormalities or the presence of gaps, breaks

and fragments. See appendix 7.4. In addition, the cell cycle and growth curve data presented in sections 3.2.3 and 3.2.4 demonstrate that the ESC lines exit cell cycle arrest around 24 hours, and cycle normally within 5-10 days (<10 PDs) post 3Gy X-irradiation. Furthermore, quiescence cannot be induced in undifferentiated ESCs (Burdon *et al*, 2002). Therefore, it can be assumed with reasonable confidence that any unstable or lethal aberrations observed in this project are indicative of ongoing instability, rather than indicative of the presence of radiation-induced aberrations in cells which have simply arrested or delayed. A total of 4 transmissible aberrations were detected in this project. When similar aberrations appeared multiple times in a single culture, they were counted as a single, possibly transmissible aberration (ie, the long satellite arms).

5.4.4 Cytogenetic instability did not correlate with hypomethylation and was not observed at a delayed period after 3Gy X-irradiation

There was no significant difference in the frequency of total structural aberrations between any of the cell lines, between the sham and 3Gy treatment groups, or between the two time points. In addition, the proportion of aberrations that were chromosome-type was very similar to the proportion of chromatid-type aberrations (~50:50 ratio) for most of the cell lines. The occurrence of ongoing chromosomal instability in cultures of cells is indicated by the presence of a persisting chromatid-type aberration frequency on a background of chromosome-type aberrations (Kadhim *et al*, 1995; Savage, 1999). Thus, these results indicate that cytogenetic instability was not observed in any of the ESC lines analysed, in either treatment group.

It has been shown that X-rays are a relatively inefficient inducer of chromosomal instability in comparison to high LET radiation such as α -particles (Kadhim *et al*, 1992). However, several previous studies have demonstrated that delayed cytogenetic instability can be induced after exposure to X-irradiation (Holmberg *et al*, 2001; MacDonald *et al*, 2001; Marder and Morgan, 2003). Possible reasons for the difference between these studies and the results of the current project include the fact that the predominant types of mutation observed in these studies using either FISH (MacDonald *et al*, 2001; Marder and Morgan, 1993) or G-banding (Holmberg *et al*, 1993) were symmetrical aberrations such as transmissible translocations, deletions or insertions, which solid staining cannot reliably detect (Savage, 1980). In addition, susceptibility to radiation-induced chromosomal instability is strongly influenced by genetic factors (Watson *et al*, 1997) with some mouse strains being susceptible whilst others are relatively resistant (Ponnaiya *et al*, 1997; Watson *et al*, 2001). Thus, it is possible that ESCs derived from the 129SvJ strain of mouse simply do not display chromosomal instability in response to X-irradiation.

Nevertheless, for each of the ESC lines analysed in this project, a trend was apparent at both time points, in which 3Gy X-irradiated cells appeared to display a higher proportion of chromatid-type aberrations than unirradiated cells. The possibility that this may indicate a slight elevation of instability-induced cytogenetic aberrations in the 3Gy X-irradiated samples was considered. However, the only cell line in which this shift in contribution to total mutations was statistically significant was the *Dnmt1*^{-/-} cell line, at the 10-14 PD time point: a significantly higher proportion of chromosome-type

aberrations were observed in the sham treatment group compared to the 3Gy treatment group. This may indicate that a higher proportion of the DSBs introduced in the sham-treated *Dnmt1*^{-/-} cell line may occur prior to DNA synthesis, rather than during or after DNA synthesis (Hall, 2000; Savage, 1999). However, at the 23-25 PD time point, the ratio of chromatid-type to chromosome-type aberrations in the *Dnmt1*^{-/-} sham cells was very similar, with both types contributing roughly 50% of the total aberrations. Thus, the increased proportion of chromosome-type aberrations observed at the 10-14 PD time point may simply be an anomaly.

It is also interesting that the two hypomethylated ESC lines demonstrated highly contrasting ratios of chromatid to chromosome type aberrations in comparison to the wild type ESC line at the 10-14 PD time point (see table Table 5-1). These contrasts were not sustained at the later time point. However, it may indicate that the hypomethylated ESCs exhibit greater fluctuations in the ratio of chromatid and chromosome type aberrations than do wild type ESCs.

Previous groups have observed almost exclusively chromatid-type aberrations in unirradiated somatic cells (Kadhim *et al*, 1995). However, the unirradiated ESCs in this project displayed a near 50:50 ratio of chromatid-type to chromosome-type aberrations. This disparity may reflect intrinsic differences between the cell lines. For example, in somatic cells, the vast majority of *de novo* aberrations are thought to arise as a result of interference with, or abnormality in, the process of DNA replication, leading to the formation of chromatid-type aberrations at the next mitosis (Savage, 1999). However, ESCs lack an efficient G1 checkpoint, which usually delays progression

into S phase in response to DNA damage such as strand breaks (Nelson and Kastan, 1994). Thus, it is possible that increased replication of chromatid-type strand breaks could occur, resulting in an increased frequency of chromosome-type aberrations in ESCs.

Moreover, it is possible that the checkpoint deficiencies characteristic of ESCs could cause a higher overall frequency of *de novo* cytogenetic aberrations in these cell lines. Indeed, in the study by Kadhim *et al* (1995) the unirradiated control somatic cell lines demonstrated a lower frequency of total cytogenetic aberrations (<4 aberrations per 100 metaphases) than the control ESCs in this project. Alternatively, the elevated frequency of cytogenetic aberrations observed in this project may simply reflect previous observations that rodent cells have a higher level of *de novo* chromosome instability than human cells (Tanaka *et al*, 2008).

The aberrations observed were grouped in Figure 5-4 according to the classifications of chromosome-type and chromatid-type exchanges and discontinuity defined by John Savage (1999). See appendix 7.4. There was no significant difference in the frequency of any class of structural aberration between any of the cell lines or treatment groups, or between the two time points.

5.4.5 Aberrations of the satellite arms were more frequent in hypomethylated ESCs than wild type ESCs

Although the aberration frequencies indicate that cytogenetic instability was not observed in any of the ESC lines analysed, some interesting observations were made.

For example, a presumably transmissible aberration was observed that was characterised by the appearance of abnormally long satellite arms. All of the chromosomes in mice are acrocentric (Mouse Genome Sequencing Consortium, 2002). The p arms are composed entirely of large blocks of repeated DNA (Garagna *et al*, 2002), consisting of the major satellites, the minor satellites, one or both of two sequences called tL1 and TLC, and the telomeric repeats (Kalitsis *et al*, 2006). Unfortunately, the use of solid staining does not permit the identification of the extra DNA sequences that appear to be present in the p arms of the long satellite arm aberration. However, the aberration arose independently in three separate cultures (*Dnmt1*^{-/-} sham, *Dnmt1*^{-/-} 3Gy and wild type 3Gy), and was only detectable at the 23-25 PD time point, indicating that it developed in each culture as a result of selective advantage. Thus, it is tempting to speculate that it may represent a small translocation containing a chromosomal region encoding genes which confer a proliferative advantage.

Selection pressure for aberrations which confer proliferative advantage is one mechanism proposed to lead to selection for tumorigenic cells in constantly renewing tissues (Savage, 1980). For example, allelic loss on chromosome 2 is observed in >95% of radiation-induced murine acute myeloid leukaemias (Hayata *et al*, 1983; MacDonald *et al*, 2001). The long satellite arm aberration was observed almost exclusively in the *Dnmt1*^{-/-} ESC line, in both treatment groups (5 times and 8 times respectively), and only once in the wild type cells that had been exposed to 3Gy X-rays. The significantly higher frequency of the aberration in *Dnmt1*^{-/-} ESCs (p=0.001)

indicates that selection for this aberration occurred earlier in *Dnmt1*^{-/-}. In addition, it was observed in both sham and 3Gy X-irradiated cells, possibly suggesting an elevated *de novo* mutation rate. As such, this observation reflects the results of the previous chapter, in which the *Dnmt1*^{-/-} ESC line was shown to have an increased *de novo* mutation rate in comparison with the other ESC lines. Furthermore, the occurrence of the long satellite arm aberration in the wild type cells exposed to 3Gy X-rays also correlates with the occurrence of genomic instability at the *Hprt* locus.

Alternatively, it is tempting to speculate that the long satellite arm aberration may have arisen as a result of abnormal elongation of the telomeres, by permitting increased access of telomerase to the telomere or stimulation of an alternative telomere lengthening mechanism (ALT) (Blasco, 2005). It has been proposed that the heterochromatic marks present in telomeric and sub-telomeric chromosome regions act as negative regulators of telomere elongation (Blasco, 2005), and several studies demonstrate that loss of repressive histone modifications in mice coincides with aberrant telomere elongation (Garcia-Cao *et al*, 2002; Garcia-Cao *et al*, 2004; Gonzalo *et al*, 2006). Furthermore, a study by Gonzalo *et al* (2006), demonstrated that the same *Dnmt1*^{-/-} and *Dnmt3a3b*^{-/-} mESCs analysed in this thesis show significant loss of DNA methylation at the sub-telomeric and pericentric satellite sequences, and display abnormally long telomere sequences in comparison to the wild type ESCs (Gonzalo *et al*, 2006). Moreover, the number of long telomeres was found to increase with passage number in the *Dnmt3a3b*^{-/-} cell line (Gonzalo *et al*, 2006), which progressively loses methylation with increasing passage number (see Figure 3-4). In

order to test the hypothesis that the long satellite arm aberration is a result of sub-telomeric DNA hypomethylation and abnormal telomere elongation, FISH could be conducted using probes specific to the telomeric repeats. However, it is unlikely that abnormal telomere elongation would be visible cytogenetically as such a large increase in satellite arm length.

Another interesting observation in the present study was that both hypomethylated *Dnmt1*^{-/-} and *Dnmt3a3b*^{-/-} ESC lines displayed complex exchanges or associations involving the satellite arms of three or more chromosomes, whilst the wild type ESC line did not. See Figure 5-6 and Figure 5-7. It is unlikely that such aberrations would be transmissible through mitosis in an intact state. Therefore they were assumed to have arisen *de novo*. Tri- or tetra-centric chromosome-type aberrations are usually only occasionally seen at high levels of overall damage (Savage, 2002). However, the complex satellite exchanges or associations were observed at similar frequencies in both unirradiated and irradiated *Dnmt* KO ESCs. Additionally, the frequency of these aberrations did not decrease significantly between the two time points analysed. Thus, the instability mechanism causing these aberrations appears to be specific to the *Dnmt* KO ESC lines rather than specific to the delayed effects of X-irradiation.

Use of the solid staining method in this project means that it has not been possible to determine exactly where, within the satellite arms, the fusions have occurred which caused the multicentric chromosome aberrations. It is tempting to speculate that these aberrations, and possibly also the long satellite arm aberrations, have arisen as a result of increased homologous recombination. DNA methylation has been proposed

to protect the genome from illegitimate recombination (Bender, 1998; Chen *et al*, 1998; Maloisel and Rossignol, 1998), and increased frequencies of telomeric sister chromatid exchanges (T-SCEs) were observed in *Dnmt1*^{-/-} and *Dnmt3a3b*^{-/-} ESCs by Gonzalo *et al* (2006). T-SCEs arise as a result of homologous recombination (HR) between telomeres on sister chromatids and can result in the lengthening of one telomere at the expense of another (De Lange, 2005). HR can also cause uncapping of the telomere via removal of the protective t-loop structure (Wang *et al*, 2004). Critically short or uncapped telomeres are recognised as DNA DSBs, and if repaired by the NHEJ machinery, can result in chromosome fusions (Van Steensel *et al*, 1998), complex aberrations (Gagos and Irminger-Finger, 2005) and the formation of multicentric chromosomes (Artandi *et al*, 2000; Hande *et al*, 1999).

Repetitive sequences contain the majority of the methylated cytosines found in mammalian cells (Yoder *et al*, 1997) and have been found in at least some instances to be hotspots for recombination (Edelmann *et al*, 1989; Jeffreys *et al*, 1999). Southern blot analysis of the minor satellite region in the mESCs in this project revealed that the *Dnmt1*^{-/-} and *Dnmt3a3b*^{-/-} ESC lines are hypomethylated in comparison to the wild type ESCs (see Figure 4-8). Given the apparent correlation between methylation levels and homologous recombination, it is possible that hypomethylation of the minor satellite sequences in the *Dnmt1*^{-/-} ESCs could cause increased recombination between centromeric regions. Such a phenomenon is observed in cell lines from patients with ICF syndrome, resulting in the generation of multiradial chromosomes (Ehrlich *et al*, 2006; Tuck-Muller *et al*, 2000). However, this hypothesis is purely

speculative and further work is required to determine the actual mechanism behind the long satellite arm and multicentric chromosome aberrations.

Finally, it should be noted that a total of 500-600 metaphases were analysed for each ESC line, and a total of 6 complex satellite associations/exchanges and 14 long satellite arm aberrations were observed. Thus, although these aberrations occurred almost exclusively in the hypomethylated *Dnmt1*^{-/-} and *Dnmt3a3b*^{-/-} cell lines (see appendix 7.3), their frequency was not significantly higher than in the wild type ESC line.

Contrary to expectations, no multi-radial star-shaped chromosomes resembling those characteristic of lymphocyte cell lines from patients with ICF syndrome were observed in the hypomethylated ESC lines. This is not entirely surprising, however, as there is thought to be a cell-type specificity to this chromosomal instability (Ehrlich *et al*, 2006). The pronounced cytogenetic aberrations observed in mitogen-stimulated lymphocytes derived from patients with ICF syndrome are observed at negligible frequencies in other tissues (Ehrlich *et al*, 2001; Maraschio *et al*, 1989), and possibly also in mESCs.

Nevertheless, a different kind of multi-radial chromosome was observed, which occurred in a single metaphase containing a high level of background damage. See Figure 5-8. This metaphase was observed at the 23-25 PD time point, in the wild type cell line which had been exposed to 3Gy X-irradiation, and is very similar to the typical radial chromatid-type aberrations found in cells from patients with Fanconi Anaemia (FA), a disorder characterised by genomic instability and hypersensitivity to cross-linking agents (Knipscheer *et al*, 2009). Such multi-radial chromosomes are also

frequently observed to occur in chromosomes from patients with other chromosome breakage syndromes, particularly Bloom syndrome (Hickson *et al*, 2001). The FA and BLM proteins are involved in the repair of DNA interstrand crosslinks (ICLs) via replication-coupled repair during S phase (Knipscheer *et al*, 2009). Thus, it is possible that this single cell carried a mutation in one of the genes involved in the repair of DNA inter-strand cross links.

5.4.6 Hypomethylation correlates with reduced frequency of aneuploidy

In addition to structural aberrations, the frequency of numerical chromosome aberrations was analysed. The treatment condition (sham or 3Gy) was not found to have any effect on the frequency of numerical chromosome aberrations. However, the wild type cell line did display a significantly higher frequency of aneuploid metaphases than either of the *Dnmt* KO cell lines, at both time points.

It has been well documented that human and murine ESCs grown in culture for long periods of time tend to develop very high levels of aneuploidy (Liu *et al*, 1997; Longo *et al*, 1997; Mitalipova *et al*, 2005). Longo *et al* (1997) demonstrated that the proportion of euploid metaphases dropped significantly with time in culture from roughly 100% at passage 5 to only 20-30% by passage 25 in three different ESC lines derived from a 129sv male embryo. This figure correlates very neatly with the approximately 80% level of aneuploidy observed in the WT cell line in the present study. However, both *Dnmt1*^{-/-} and *Dnmt3a3b*^{-/-} ESC lines displayed significantly lower frequencies of aneuploidy (see Figure 5-9).

The high level of aneuploidy in ESCs is thought to be due to decreased functioning of the decatenation and mitotic spindle assembly checkpoints in comparison to somatic cells (Damelin *et al*, 2005; Mantel *et al*, 2007). The spindle assembly checkpoint (SAC) blocks anaphase and is required for correct chromosome segregation in somatic cells. However, in mESCs the SAC is only transiently functional and after a prolonged period of SAC activation, rather than undergoing p53 mediated apoptosis as somatic cells do, mESCs re-enter mitosis irrespective of their chromosome number. This results in polyploid/aneuploid daughter cells (Mantel *et al*, 2007).

Although this explains the high level of tolerance for aneuploidy in ESCs, as observed in the wild type cell line, it does not explain the cause of the aneuploidy, or why significantly lower levels were detected in the *Dnmt1*^{-/-} and *Dnmt3a3b*^{-/-} cell lines. One of the main mechanisms through which aneuploidy is thought to arise in ESCs is the deficiency of another cell cycle checkpoint called the decatenation checkpoint (Damelin *et al*, 2005).

The decatenation checkpoint occurs in the G2 phase of the cell cycle but is independent from the G2/M DNA damage checkpoint. Its function is to delay entry into mitosis if the chromosomes have not been sufficiently decatenated or disentangled by topoisomerase II (topo II). Decreased efficiency of the decatenation checkpoint means that cells are able to complete mitosis in the presence of entangled chromosomes, resulting in aneuploidy in the daughter cells. As with SAC, efficiency of the decatenation checkpoint increases upon ESC differentiation (Damelin *et al*, 2005).

Previous research groups have shown that the activity of topo II can be inhibited by the presence of DNA cytosine methylation (Leteurtre *et al*, 1994; Boos and Stopper). The studies by Leteurtre *et al* (1994) and Boos and Stopper (2001) were conducted using bacterial plasmid DNA, or synthesized PCR fragments. Therefore, the results are independent of mammalian higher order chromatin structure and indicate that simply the presence of a methyl group on the cytosine base is enough to reduce topo II efficiency. It was proposed that the altered topological conformation of methylated DNA may disturb the interaction of enzymes like topo II with DNA (Boos and Stopper, 2001).

If the results of the studies by Leteurtre *et al* (1994) and Boos and Stopper (2001) can be extrapolated to mammalian genomic DNA, the inhibition of topo II by the presence of DNA methylation could potentially explain the low levels of aneuploidy observed in the hypomethylated *Dnmt1*^{-/-} and *Dnmt3a3b*^{-/-} ESC lines. It is tempting to speculate that wild type ESCs enter mitosis in the presence of entangled chromosomes, as the deficient decatenation checkpoint does not delay the cell sufficiently to allow completion of decatenation before mitosis. In the hypomethylated *Dnmt* KO ESCs, however, the reduced methylation level may allow more efficient processing of the DNA by topo II, resulting in more efficient decatenation and disentanglement of the chromosomes prior to mitosis, and a correspondingly reduced incidence of aneuploidy in the daughter cells.

At the 10-14PD time point in this experiment, the wild type ESCs were p#46 and the *Dnmt1*^{-/-} and *Dnmt3a3b*^{-/-} ESC lines were p#22 and p#23 respectively. Therefore, it

could be argued that the higher proportion of aneuploidy observed in the wild type cell line was due to its higher passage number. However, during the course of the experiment, all three cell lines underwent 10 passages between the 10-14 and 23-25PD time points. Therefore, based on the data in previous literature (Longo *et al*, 1997; Liu *et al*, 1997), a decline in the proportion of euploid metaphases should have been observed in all cell lines throughout the course of the experiment. However, no significant difference was observed in the level of aneuploidy between the two time points for any of the cell lines, indicating that the level of aneuploidy observed for each cell line is stable. Thus, it is unlikely that the differing levels of aneuploidy between the wild type and *Dnmt* KO ESC lines is a result of their differing passage numbers at the commencement of the experiment.

In addition, the passage numbers of the *Dnmt* KO ESC lines may be under-estimated. It is thought that the passage numbers supplied when the cell lines were received represent the number of passages the cells had undergone since the lines were established. If this is the case, their true passage number will be higher, as it is the sum of the passage number of the wild type cell line before targeting, plus the number of passages it underwent during targeting and establishment, plus the number of passages since the cell line was established.

A trend was noted whereby the level of aneuploidy in the *Dnmt3a3b*^{-/-} cell line was slightly higher at the 10-14 PD time point than at the 23-25 PD time point. The methylation level of this cell line decreases with increasing passage number (see Figure 3-4), and there are 10 passages between the two time points. The reduction in

aneuploidy between the two time points was not statistically significant. However, this may simply be because the difference in methylation between the two time points was not large enough to observe an effect.

Cells were also frozen at the first metaphase after treatment, when the experiment was carried out. These cells have not been used for analysis of structural cytogenetic aberrations, as it was deemed unnecessary based on the results of the later time points. However, as these *Dnmt3a3b*^{-/-} cells are p#23, they have a higher methylation level than the cells analysed at the 10-14 PD time point. Thus, a natural extension of this work would be to make slides of the *Dnmt3a3b*^{-/-} cells that were harvested at the first metaphase after treatment (p#23) and analyse the level of aneuploidy.

5.4.7 Chromosome gains/losses formed a cell line-specific trend

In addition to the differing overall frequency of aneuploidy observed between the ESC lines, the mean chromosome number also varied slightly (see Figure 5-10). The majority of the aneuploid metaphases detected in the wild type ESCs have extra copies of one or two chromosomes, forming a skewed distribution. In the *Dnmt1*^{-/-} ESCs, however, the spread of aneuploidy followed a normal/Gaussian distribution, with roughly equal preference for gain and loss of chromosomes. Additionally, gain or loss of more than one chromosome was very rare. The tightest spread of aneuploidy was observed in the *Dnmt3a3b*^{-/-} ESC line, in which the majority of aneuploid metaphases arose due to loss of a single chromosome.

The same trend in the spread of characteristic aneuploid chromosome numbers was observed in these ESC lines by Gonzalo *et al* (2006). Furthermore, consistent gain or loss of the same chromosomes has been observed recurrently in human and mouse ESCs maintained for long periods in culture (Mitalipova *et al*, 2005; Liu *et al*, 1997). Trisomy 8 is a particularly common recurrent aneuploidy that has been observed in cultures of mESCs (Liu *et al*, 1997). Interestingly, it was found to confer a selective growth advantage on the cells, resulting in depletion of euploid cells during further culture (Liu *et al*, 1997).

Thus, although the staining method used in the present study does not permit identification of the chromosomes present in each metaphase, it is possible that the selection pressures exerted by the different ESC lines resulted in preference for different chromosomes. It is tempting to speculate that certain genes required to maintain pluripotency and restrict differentiation may be expressed at elevated levels in the hypomethylated *Dnmt* KO ESC lines, whilst in the wild type cells, selective pressure for increased expression of these genes could result in selection for gain-of-chromosome type aneuploidy. In order to test this hypothesis, a technique with higher resolution, such as G-banding or FISH, would be required to identify the chromosomes present in the metaphases, and identify any recurring karyotypical abnormalities which may be characteristic of the cell lines.

5.4.8 Summary

DNA hypomethylation does not appear to affect the level of DNA damage in ESCs, either before or at a delayed period after irradiation, as measured by the alkaline comet assay. Thus, the increased *de novo* mutation rate observed in the *Dnmt1*^{-/-} ESC line at the *Hprt* gene and the radiation-induced delayed genomic instability observed in the wild type ESC line are unlikely to be a result of increased levels of DNA strand breaks and alkali labile sites (ALS).

In addition, no significant difference was found in the average level of Fpg-sensitive lesions between the wild type and hypomethylated ESC lines, or between the sham and 3Gy treatment groups. Thus, it appears that the radiation-induced delayed genomic instability observed at the *Hprt* locus in the wild type cell line is not a result of persistently increased levels of oxidative stress. However, it is possible that this reflects the fact that ESCs appear to have a particularly stringent damage response to oxidative DNA damage (Maynard *et al*, 2008; Saretzki *et al*, 2004; Saretzki *et al*, 2008).

The pilot study undertaking cytogenetic analysis of the wild type and *Dnmt* KO ESC lines indicates that no statistically significant alterations in chromosomal instability were observed either between hypomethylated and wild type ESC lines or between cells exposed 23-25 PDs previously to 3Gy X-rays or sham treatment. However, the resolution of the staining method used was reasonably low, restricting the range of aberrations that could be identified in comparison to techniques such as chromosome banding or FISH. Furthermore, two aberration types were identified which occurred almost exclusively in the hypomethylated *Dnmt1*^{-/-} and *Dnmt3a3b*^{-/-} ESCs. These

aberrations both involved the satellite arms, and it is speculated that they may have arisen as a result of homologous recombination between satellite sequences or translocation of a sequence which confers a proliferative or survival advantage. Further work is required to investigate these hypotheses.

High passage ESCs normally display a high frequency of aneuploidy due to deficiencies in the SAC and decatenation checkpoints. This was seen in WT ESCs but was found to be reduced in the hypomethylated *Dnmt1*^{-/-} and *Dnmt3a3b*^{-/-} cell lines. It is speculated that the elevated frequency of aneuploid metaphases observed in the wild type ESCs compared to the hypomethylated ESC lines may reflect the inhibitory effect of DNA methylation on the activity of topo II, as observed by previous groups *in vitro*. Finally, a characteristic preference for gain or loss of specific numbers of chromosomes was observed in each cell line, which may reflect differing selection pressures for proliferation and maintenance of pluripotency.

6 Chapter 6. Discussion

Exposure to ionising radiation can damage DNA and results in genome destabilisation (Barber *et al*, 2006; MacDonald *et al*, 2001). Genomic instability is a hallmark of many cancers and is thought to be one of the mechanisms leading to tumourigenesis (Nowell, 1976; Loeb, 1991; Lengauer *et al*, 1998). Multiple cancers demonstrate global DNA hypomethylation in comparison to normal tissue controls (Wahlfors *et al*, 1992; Lin *et al*, 2001; Kim *et al*, 1994) and several studies have established a correlation between DNA hypomethylation and increased genomic instability (Chen *et al*, 1998; Tuck-muller *et al*, 2000). Furthermore, global hypomethylation has been correlated with increased radiosensitivity (Dote *et al*, 2005; Narayan *et al*, 2000), and ionising radiation has itself been demonstrated to reduce methylation levels (Giotopoulos *et al*, 2006; Pogribny *et al*, 2004; Raiche *et al*, 2004; Tawa *et al*, 1998).

The aim of this project was to investigate the apparent correlations between DNA hypomethylation, radiosensitivity and genomic instability. A murine embryonic stem cell system was used, allowing analysis of the impact of complete inactivation of each of the three main active mammalian DNA methyltransferase enzymes. The global methylation level of the ESC lines was characterised before and after irradiation, as were the proliferation rates and cell cycle characteristics. The ESCs were then investigated for differences in radiosensitivity and genomic stability, both at a specific gene locus and on a genome-wide scale.

6.1 Radiosensitivity does not correlate with hypomethylation

Chapter 3 investigated the roles played by each of the three main murine DNA methyltransferase enzymes in cellular radio-response. The DNA methylation level of the wild type ESCs is similar to that of bone marrow, one of the least methylated of all adult somatic tissues, and the *Dnmt* KO ESC lines displayed varying degrees of hypomethylation. None of the cell lines exhibited radiation-induced DNA hypomethylation. However, this phenomenon appears to be cell- and tissue-type specific, and has previously only been demonstrated in somatic cells (Pogribny *et al*, 2004; Raiche *et al*, 2004; Tawa *et al*, 1998).

No significant differences in radiosensitivity were observed between the wild type and *Dnmt* KO cell lines, indicating that global DNA hypomethylation does not increase radiosensitivity in mESCs. This is in contrast to the results of previous groups, using somatic and tumour cell lines (Dote *et al*, 2005; Narayan *et al*, 2000). However, differentiated cell lines are less likely to undergo apoptosis in response to DNA damage in comparison to ESCs (Roos *et al*, 2007). All five ESC lines displayed an exponential survival curve, which is thought to reflect their high propensity for apoptosis (Clutton *et al*, 1996; de Waard *et al*, 2003). Therefore, it is tempting to speculate that the high level of apoptosis has masked the effect of reduced methylation levels on radiosensitivity in the *Dnmt* KO ESC lines. It would be interesting, therefore, to induce differentiation in the mESC lines and then determine the effect of *Dnmt* KO on radiosensitivity. Nevertheless, the *de novo* methyltransferase enzymes, DNMT3A and DNMT3B, may play a minor role in modulating sensitivity to X-rays in mESCs, as

absence of one was found to have a modest radioprotective effect, whilst KO of both resulted in comparative radiosensitisation.

The *Dnmt* KO ESC lines showed no significant differences in growth rate or cell cycle characteristics in comparison to the wild type, both in unirradiated and X-irradiated cells. In response to 3Gy X-irradiation the ESCs bypassed the G1 checkpoint and arrested in G2/M. The cells began to exit G2/M checkpoint arrest by 24 hours post 3Gy X-irradiation, and displayed a normal cell-cycle distribution by 5-10 days after irradiation. After release from radiation-induced cell cycle arrest, the slope of the growth curve increased in all cell lines, possibly reflecting the processes of repopulation or culture adaptation.

6.2 Lack of DNMT1, but not DNMT3A or DNMT3B, leads to an increased *de novo* mutation rate

Chapter 4 analysed the mutation rate and spectrum of the five mESC lines at the X-linked *Hprt* gene locus. This revealed an approximately 10-fold elevation of *de novo* mutation rate in the *Dnmt1*^{-/-} ESCs in comparison to the wild type ESCs. This is in agreement with previous work undertaken by Chen *et al* (1998). However, the *de novo* mutation rates of the *Dnmt3a*^{-/-}, *Dnmt3b*^{-/-} and *Dnmt3a3b*^{-/-} ESC lines were not significantly different from that of the wild type cell line. Based on the data provided in Figure 3-4, the *Dnmt3a3b*^{-/-} ESC line had a very similar level of DNA methylation to the *Dnmt1*^{-/-} ESC line at the time of selection for *Hprt* mutations. Therefore, it is unlikely that the elevated mutation rate detected in the *Dnmt1*^{-/-} ESC line is a result of

global hypomethylation as previously reported (Chen et al, 1998). Rather, it appears to be a result of the absence of a property or function specific to DNMT1. One potential mechanism that could be investigated is the possibility that absence of functional DNMT1 results in increased frequencies of replication fork stalling. This could be analysed using 2D gel electrophoresis to visualise replication intermediates, as described in Friedman and Brewer (1995).

Finally, the *Dnmt* KO ESCs used in this project contain large deletions in the catalytic region. Such deletions may potentially alter the structural conformation of the DNMT protein and prevent it from carrying out other possible roles required for normal cell function. This effect could be assessed by rescuing the *Dnmt1*^{-/-} ESC line with wild type and mutant *Dnmt1* minigenes, as described in Damelin and Bestor (2007). The mutant *Dnmt1* minigene contains only a 2bp mutation in the catalytic domain, which is not thought to affect protein conformation (Damelin and Bestor, 2007). Analysis of the *Hprt* mutation rate in *Dnmt1*^{-/-} ESCs rescued with these minigenes would permit determination of whether the elevated mutation rate originally observed was as a result of loss of DNA methylation specific to the function of DNMT1, or loss of another non-catalytic function. This work has been started, but unfortunately electroporation was unsuccessful.

6.3 Radiation-induced delayed genomic instability is observed in wild type ESCs, but not in *Dnmt* deficient ESCs

The wild type ESC line demonstrated a 5-fold increased mutation rate 23-25 PDs after exposure to 3Gy X-rays in comparison to sham treated wild type control cells. This is characteristic of the occurrence of radiation-induced delayed genomic instability. However, this phenomenon was not observed in any of the *Dnmt* KO lines: the mutation rates of the 3Gy X-irradiated clones were not significantly different to the *de novo* mutation rates. This indicates that absence of the DNA methyltransferase enzymes, or disruption of the normal methylation pattern, may potentially inhibit the mechanism behind radiation-induced delayed genomic instability.

To our knowledge this is the first direct demonstration of a requirement for specific DNA methylation patterns and/or the DNA methyltransferase enzymes in the propagation of radiation induced delayed genomic instability. The correlation of reduced levels of DNA methylation with apparently increased genomic stability after a radiation insult could be viewed as contrary to expectations. However, methylcytosine is known to be a preferential target for oxidative crosslink and adduct-forming mutagens in comparison to unmethylated cytosine (Cao and Wang, 2007; Denissenko *et al*, 1997; Yoon *et al*, 2001; You *et al*, 1999). In addition, there are several more speculative explanations. For example, radiation exposure has been shown to result in site-specific increases in DNA methylation as well as global hypomethylation (Kaup *et al*, 2006; Koturbash *et al*, 2005). Thus, if radiation induced delayed genomic instability is mediated by epigenetic dysregulation of genes involved in the DNA damage

response, the reduction of methyltransferase enzymes in the *Dnmt*^{-/-} ESCs may reduce this effect. Finally, it is possible that the lower levels of DNA methylation and associated binding proteins in the *Dnmt*^{-/-} ESCs may permit increased access to the DNA for proteins involved in the DNA damage response (Amouroux *et al*, 2010). This latter hypothesis may well be true for topo II, as indicated by the reduced frequency of aneuploidy in the *Dnmt*^{-/-} ESCs. Future studies could be designed to test these hypotheses in the ESC lines.

Finally, the results of this project indicate that radiosensitivity and genomic instability are mediated by independent mechanisms in ESCs, as the cell line which displayed the greatest level of instability at the *Hprt* locus (*Dnmt1*^{-/-}) was no more radiosensitive than the wild type cell line, which displayed a significantly lower *Hprt* mutation rate.

6.4 Mutation spectra analysis reveals a link between non-contiguous exonic deletions and hypomethylation or radiation exposure

Characterisation of the mutation types observed at the *Hprt* locus in each of the ESC lines was carried out in an attempt to better understand the mechanisms that may be responsible for their differing mutation rates. The ESC lines with low *de novo* mutation rates displayed either no change or an increase in the number of different mutation types observed in the 3Gy-irradiated clones. However, the *Dnmt1*^{-/-} cell line, which demonstrated a wider range of *de novo* mutations and an elevated *de novo* mutation rate, appeared to display a reduced range of mutation types in the 3Gy X-irradiated

clones. This is potentially consistent with the hypothesis that cells and tissues which are intrinsically unstable can be eliminated from the population after irradiation. However, this is unlikely to be true for the ESC lines containing KO of the *de novo* methyltransferase enzymes, DNMT3A and/or DNMT3B, as they exhibited a similar *de novo* mutation rate to the wild type cells.

The mutation spectra of each ESC line 23-25 PDs after 3Gy X-irradiation roughly resembled the *de novo* mutation spectrum. Interestingly, however, multiple deletions of non-contiguous exons were observed in the sham-treated clones from the two most hypomethylated ESC lines (*Dnmt1*^{-/-} and *Dnmt3a3b*^{-/-}), and in all of the ESC lines in clones derived from 3Gy X-irradiated cells. Previous research groups have associated such mutations with the occurrence of radiation-induced delayed genomic instability (Caron et al, 1997; Mognato et al, 2001; Romney et al, 2001), and suggested they may have arisen as a result of recombinational repair of DSBs (Balestrieri et al, 2001). Thus, it is possible that the most hypomethylated ESC lines (*Dnmt1*^{-/-} and *Dnmt3a3b*^{-/-}) may display increased levels of DNA DSBs and/or illegitimate recombination. This remains to be investigated. However, previous studies indicate that DNA methylation may play a role in suppressing recombination (Chen et al, 1998; Maloisel and Rossignol, 1998).

Repetitive sequences such as retroviral elements and satellite repeats contain the majority of the methylcytosine in mammalian cells (Yoder et al, 1997) and can be hotspots for recombination (Edelmann et al, 1989; Jeffreys et al, 1999). Southern blot analysis revealed that the *Dnmt1*^{-/-} ESC line was significantly hypomethylated in

comparison to the wild type ESCs at minor satellite sequences and Alu elements. In addition, L1 elements were hypomethylated in all ESC lines. Recombination between the pericentric minor satellites is unlikely to be responsible for the elevated mutation rate observed in the *Dnmt1*^{-/-} ESC line at the *Hprt* gene. However, detection of the presence of large retroviral elements, such as IAP and L1, in the *Hprt* gene was not achieved with the PCR-based approach used in this project. Nevertheless, several SINE insertions were detected in the *Dnmt1*^{-/-} ESCs indicating the occurrence of active retrotransposition in this hypomethylated cell line.

The high *de novo* mutation rate in *Dnmt1*^{-/-} ESCs was further demonstrated by the occurrence of secondary mutation events during expansion of the sham-treated clones containing SINE insertions. It is possible that loss of the properties of DNMT1 that are required for DNA replication and repair may contribute to the increased mutation rate of the *Dnmt1*^{-/-} ESC line (Dion *et al*, 2008; Mortusewicz *et al*, 2005; Wang and Shen, 2004).

6.5 Global hypomethylation does not alter the level of endogenous or delayed DNA damage measured by the comet assay

Chapter 5 investigated genomic instability on a genome-wide scale in the wild type, *Dnmt1*^{-/-} and *Dnmt3a3b*^{-/-} ESC lines 23-25 PDs post 3Gy X-irradiation or sham treatment. In this way, a direct comparison could be made between the markers of genomic instability and the types and rates of mutations detected at the *Hprt* locus.

The *Dnmt1*^{-/-} and *Dnmt3a3b*^{-/-} cell lines displayed no significant difference in the level of endogenous DNA damage compared to the wild type cells, as measured by the alkaline comet assay. In addition, the level of damage was not significantly different between cells that had undergone sham treatment and cells that were exposed to 3Gy X-irradiation. Thus, DNA hypomethylation does not affect the combined level of SSBs, DSBs and alkali-labile sites (ALS) in ESCs, either before or at a delayed period after irradiation. Furthermore, the increased *de novo* mutation rate observed in the *Dnmt1*^{-/-} ESC line at the *Hprt* gene and the radiation-induced delayed genomic instability observed in the wild type ESC line are unlikely to be a result of increased levels of such DNA damage.

6.6 Radiation-induced delayed genomic instability at *Hprt* in wild type ESCs is not a result of increased oxidative damage

Oxidative stress is one of the proposed mechanisms by which radiation-induced delayed genomic instability is propagated (Wright, 2010), and several studies indicate that methylated DNA is a preferential target for oxidative crosslink and adduct-forming physical and chemical mutagens in comparison to unmethylated DNA (Cao and Wang, 2007; Denissenko *et al*, 1997; Tomassi *et al*, 1997; Yoon *et al*, 2001; You *et al*, 1999). However, no significant difference was found in the average level of Fpg-sensitive lesions between the wild type and hypomethylated ESC lines, or between the sham and 3Gy treatment groups. Thus, it appears that the radiation-induced delayed genomic instability observed at the *Hprt* locus in the wild type cell line is not a result of persistently increased levels of oxidative stress. The discrepancy between these results

and those of the previous studies, which used DNA substrates lacking mammalian higher order chromatin structure, may reflect the impact of factors such as the radical-scavenging abilities of histone proteins (Milligan *et al*, 2004). Alternatively, it may reflect the fact that ESCs appear to have a particularly stringent damage response to oxidative DNA damage (Maynard *et al*, 2008; Saretzki *et al*, 2004; Saretzki *et al*, 2008).

6.7 Cytogenetic instability did not correlate with hypomethylation and was not observed at a delayed period after 3Gy X-irradiation

A pilot study was carried out using a non-clonal bulk culture method to assess the frequency of cytogenetic aberrations indicative of genomic instability in the wild type, *Dnmt1*^{-/-} and *Dnmt3a3b*^{-/-} ESC lines 23-25 PDs post X-irradiation or sham treatment. No significant difference was found in the frequency of total structural aberrations between any of the cell lines, between the sham and 3Gy treatment groups, or between the two time points. In addition, the proportion of aberrations that were chromosome-type was very similar to the proportion of those that were chromatid-type (~50:50 ratio). This indicates that cytogenetic instability was not observed in any of the ESC lines, in either treatment group. However, susceptibility to radiation-induced chromosomal instability is strongly influenced by genetic factors (Ponnaiya *et al*, 1997; Watson *et al*, 2001), and previous research groups have also found a disparity between the ability of X-rays to induce instability at the *Hprt* locus and on a cytogenetic scale (Harper *et al*, 1997). Furthermore, whilst indicators of genomic

instability such as elevated levels of recombination, SCEs, gene mutations and ESTR mutations are all thought to be related, genomic instability characterised by chromosomal instability (CIN) is thought to occur independently (Lengauer *et al*, 1998; Limoli *et al*, 1997).

6.8 Aberrations of the satellite arms were more frequent in hypomethylated ESCs than wild type ESCs

Some interesting observations were made from the cytogenetic pilot study, which indicate that certain mutational mechanisms may be operating to a greater extent in the hypomethylated cell lines than in the wild type ESC line. Specifically, a small increase in the frequency of aberrations involving the satellite arms of the chromosomes was observed in the hypomethylated ESC lines (*Dnmt1*^{-/-} and *Dnmt3a3b*^{-/-}) compared to the wild type. These aberrations included the occurrence of abnormally long satellite arms and complex exchanges/associations occurring between the satellite arms of 3 or more chromosomes. Such tri- or tetra-centric chromosome-type aberrations are normally only seen at high levels of overall damage (Savage, 2002). However, they were observed in both X-irradiated and unirradiated ESCs, indicating that the causal mechanism is specific to hypomethylation rather than irradiation.

Unfortunately, the use of solid staining did not permit the determination of the cause of these aberrations. However, several possibilities exist including translocation of a chromosomal region encoding genes which confer a selective advantage, or increased

frequencies of rearrangements or homologous recombination at the major and minor satellite repeats due to hypomethylation, as occurs in cell lines from patients with ICF syndrome (see section 1.3).

Several research groups have demonstrated a possible link between DNA methylation levels and recombination (Dominguez-Bendala and McWhir, 2004; Maloisel and Rossignol, 1998), indicating that DNA hypomethylation, such as that induced in the *Dnmt1*^{-/-} and *Dnmt3a3b*^{-/-} ESCs, may potentially result in increased frequencies of recombination at repeated regions throughout the genome (Gonzalo *et al*, 2006). This possibility could be investigated in the ESC lines using FISH to detect non-clonal aberrations, such as translocations and exchanges, arising in clonal cultures. Furthermore, the use of FISH could help to determine the cause of the long satellite arm aberration observed in the hypomethylated cell lines.

6.9 Hypomethylation correlates with reduced frequency of aneuploidy

In addition to structural aberrations, the frequency of numerical chromosome aberrations was analysed. Treatment condition (sham or 3Gy) was not found to have any effect on the frequency of numerical chromosome aberrations. However, the wild type cell line displayed a significantly higher frequency of aneuploid metaphases than either of the *Dnmt* KO cell lines, at both time points. The development of aneuploidy is a common occurrence in ESCs maintained for long periods in culture (Liu *et al*, 1997; Longo *et al*, 1997; Mitalipova *et al*, 2005), due to very transient functioning of the

mitotic spindle assembly checkpoint in comparison to somatic cells (Damelin *et al*, 2005; Mantel *et al*, 2007).

One of the main mechanisms through which aneuploidy is thought to arise in ESCs is via deficiency of the decatenation checkpoint (Damelin *et al*, 2005), allowing cells to complete mitosis in the presence of entangled chromosomes (Damelin *et al*, 2005). DNA topoisomerase II (topo II) is responsible for the decatenation or disentanglement of chromosomes prior to mitosis (Wang, 2002), and previous research groups have shown that the interaction of topo II with DNA is reduced by the presence of DNA cytosine methylation (Leteurtre *et al*, 1994; Boos and Stopper, 2001). It is therefore tempting to speculate that the hypomethylated ESC lines are able to undergo more efficient decatenation prior to mitosis than the wild type ESCs can, resulting in lower levels of aneuploidy.

If it is true that simply the presence of a methyl group can inhibit the efficiency of topo II, then it is also possible that similar effects may be seen with other DNA repair proteins. Assuming this hypothesis was true, the reduced levels of DNA methylation in the *Dnmt* KO ESC lines may permit greater access and more efficient interaction of the DDR proteins with the DNA, resulting in more effective repair. This could appear in Figure 4-2 as a reduction in the occurrence of radiation-induced delayed genomic instability, whilst in actual fact it may simply reflect an increased capacity to repair the damage. This hypothesis could be tested in the future by analysing the rate of formation and repair of DNA damage in each of the ESC lines, using the comet assay, γ H2AX or 53BP1.

Speculating further, if reduced methylation levels permit more efficient repair of DNA damage in the *Dnmt* KO ESC lines, then this may also partly explain the lack of variation in radiosensitivity. It may also explain why loss of a single *de novo* methyltransferase enzyme, particularly DNMT3A, results in apparently increased radioresistance.

6.10 Chromosome gains/losses formed a cell line-specific trend

In addition to the differing overall frequency of aneuploidy, the mean chromosome number also varied between the ESC lines. The reason for the differing spread of characteristic aneuploid chromosome numbers is unclear. However, the same trends were observed in these ESC lines by Gonzalo *et al* (2006), and recurrent trisomies have been proposed to be a result of selection for specific abnormalities which confer a proliferative advantage (Liu *et al*, 1997; Mitalipova *et al*, 2005). Further investigation using FISH could establish the identities of the characteristic gained and lost chromosomes observed in each of the ESC lines, and their possible roles in conferring selective advantage could be assessed via a candidate gene approach.

6.11 Final conclusions

Global genomic DNA hypomethylation *per se* does not cause increased radiosensitivity or genomic instability in mESCs. However, the *de novo* DNA methyltransferase enzymes may be involved in determining radiosensitivity, and absence of functional DNMT1 results in a ten-fold increase in mutation rate at the *Hprt* locus. This instability may be a result of increased illegitimate homologous recombination, retroviral

activation, or loss of the properties of DNMT1 that are required for efficient DNA replication and repair.

No instability was observed on a genome-wide scale as indicated by the frequency of strand breaks and cytogenetic aberrations. However, observations made during cytogenetic analysis indicate that elevated levels of recombination may occur in the hypomethylated *Dnmt1*^{-/-} and *Dnmt3a3b*^{-/-} ESC lines. Further investigation is required on this point. Radiation-induced delayed genomic instability was observed in the wild type ESC line at the *Hprt* locus. However, none of the *Dnmt* KO ESC lines exhibited this phenomenon, indicating that disruption of the normal methylation pattern, or functional absence of any of the DNA methyltransferase enzymes, may disrupt the mechanism responsible for propagating radiation-induced delayed genomic instability. Alternatively, it could be speculated that the lack of observed radiation-induced delayed genomic instability in the *Dnmt* KO ESC lines could be a result of reduced levels of DNA methylation permitting more efficient repair of DNA damage. Notably, the hypomethylated *Dnmt1*^{-/-} and *Dnmt3a3b*^{-/-} cell lines were found to display lower levels of aneuploidy than the wild type cell line, possibly as a result of more efficient decatenation by topo II prior to mitosis. However, this theory is speculative and requires further investigation.

Finally, the lack of radiosensitivity in the ESC line which demonstrated significantly increased genomic instability at the *Hprt* locus (*Dnmt1*^{-/-}) indicates that genomic instability and sensitivity to ionising radiation are mediated by independent mechanisms.

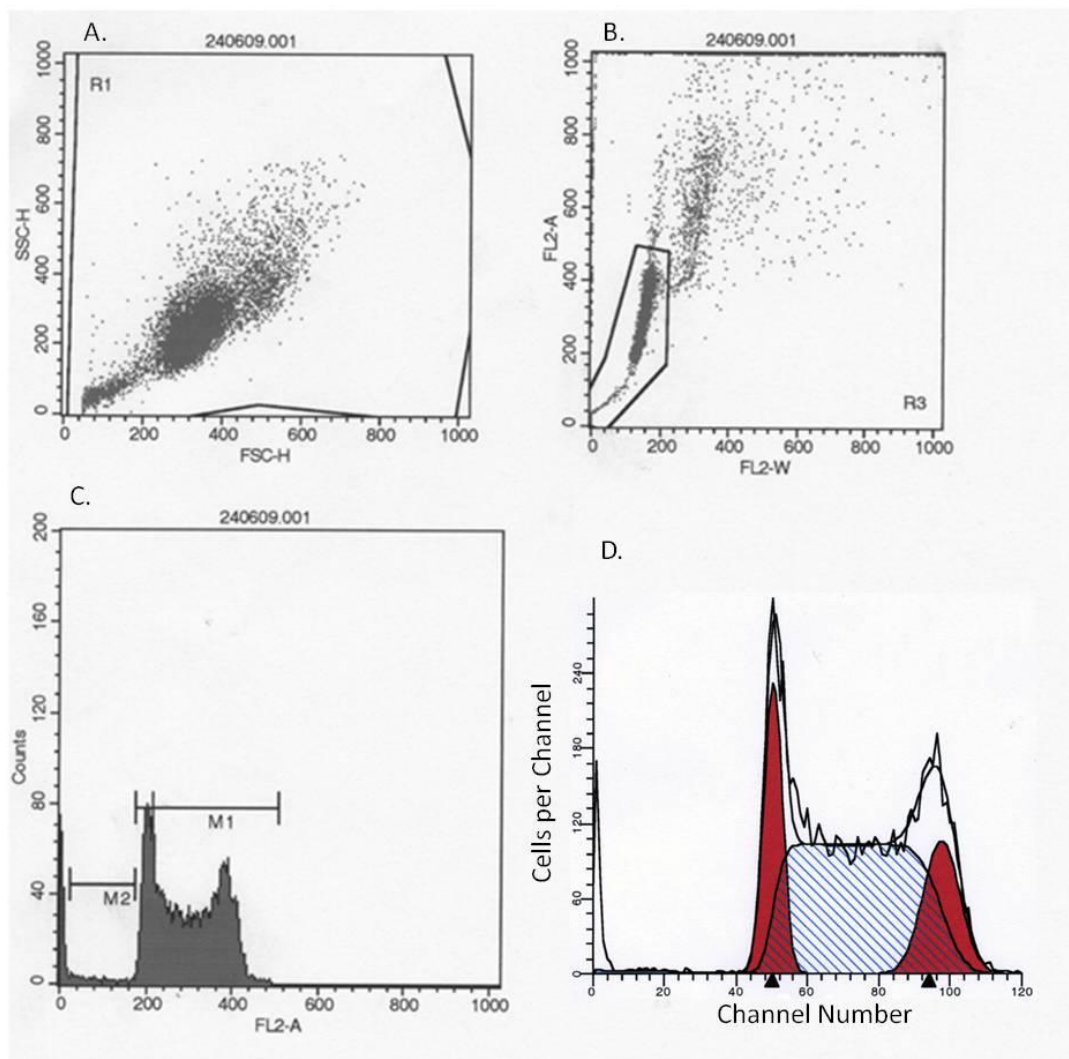
The results of this project highlight the importance of extending this work, to better understand the effects of cancer treatments involving radiotherapy and/or treatment with hypomethylating drugs. Radiotherapy is a valuable and effective cancer treatment due to its ability to cause DNA damage and cell death (Joiner *et al*, 2009). Drugs that induce genome-wide hypomethylation can be used to increase tumour radiosensitivity (Dote *et al*, 2005). However, the long term biological effects of demethylating drugs for normal tissues are currently unknown. This project has demonstrated that catalytic inactivation of the maintenance methyltransferase, which is the main DNMT expressed in somatic cells (Li *et al*, 1992), results in a 10-fold increase of mutation rate at coding genes. Given that 5-azacytidine, 5-azadeoxycytidine and Zebularine all exert their effect by forming a covalent complex with, and effectively trapping, the DNMTs (Champion *et al*, 2010, Zhou *et al*, 2002) the use of such drugs could potentially lead to genomic instability and eventually carcinogenesis.

Finally, DNMT3A and DNMT3B are expressed at very low levels in most mammalian somatic tissues (Lei *et al*, 1996). However, expression of a range of abnormally spliced DNMT3B transcripts is a common occurrence in cancer cells, as is altered gene expression (Beaulieu *et al*, 2002; Ostler *et al*, 2007; Wang *et al*, 2006a and 2006b). The results of this project indicate that whilst absence of a single *de novo* methyltransferase enzyme causes slight but consistent radioresistance, loss of both DNMT3A and DNMT3B causes comparative radiosensitisation. Therefore, it is tempting to speculate that drugs which target both DNMT3A and DNMT3B specifically could

potentially increase tumour cell radiosensitivity whilst minimising the effect of induced genomic instability on normal cells.

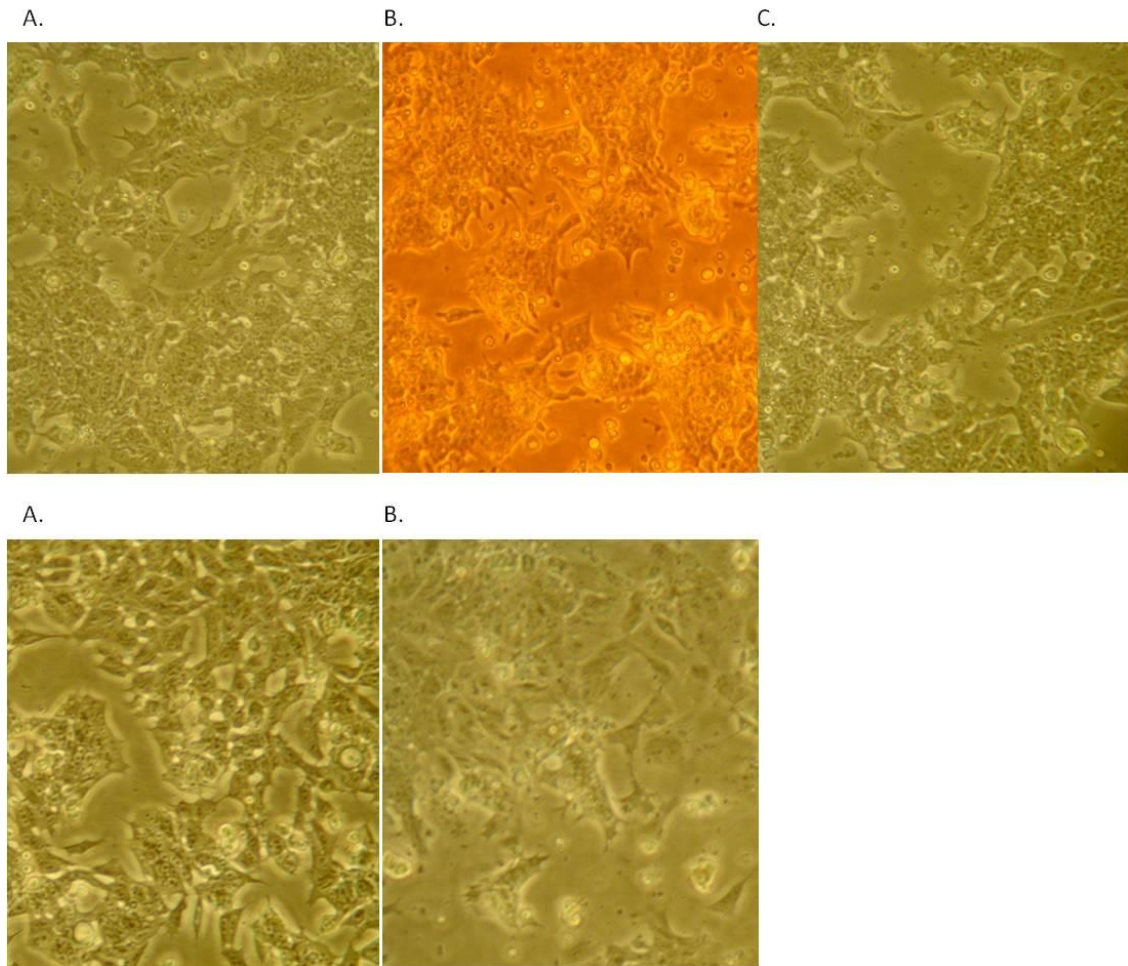
7 Appendices

7.1 Appendix 1



Example of the cell selection/gating processes carried out during cell cycle analysis by flow cytometry. The example shown is of unirradiated J1 (wild type) ESCs. A: Cell debris is excluded using forward-angle light scatter (FSC) and side-angle light scatter (SSC) to select for cells within a certain size and shape limit. B: Aggregates are excluded by selecting for cells within the appropriate area (FL2-A) and width (FL2-W) parameters of their fluorescence peak. C: The gated cells are plotted as a DNA histogram displaying the number of cells per PI fluorescence intensity (FL2-A). D: Analysis of the data by ModFit software determines the proportion of the cells in each phase of the cell cycle.

7.2 Appendix 2



Photographs of the ESC lines growing on gelatinised culture dishes, taken at 10x magnification. None of the ESC lines display any obvious differences in morphology. A: Wild Type ESCs. B: *Dnmt1*^{-/-} ESCs. C: *Dnmt3a3b*^{-/-} ESCs. D: *Dnmt3a*^{-/-} ESCs. E: *Dnmt3b*^{-/-} ESCs.

7.3 Appendix 3

10-14 PDs		Chromosome-type Aberrations						Chromatid-type Aberrations						Other	
		Exchanges				Discontinuity	Exchanges				Discontinuity				
					Reciprocal Translocation			Interchange		Intrachanges					
										Inter-arm		Intra-arm		Complex	
Cell line/condition	Total Metaphases Scored	Dicentric	Centric Ring	Interstitial Deletion	Long Chromosome	Long Satellites	Gaps, Beaks, Fragments	Dicentric	Reciprocal Translocation	Centric Ring	Dicentric	Interstitial Deletion	Isochromatid Deletion	Gaps, Breaks, Fragments	Satellite Associations
Wild Type Sham	119	4	0	0	1	0	5	0	0	0	0	0	0	8	0
Wild Type 1hr Recovery	120	3	0	0	0	0	4	0	0	0	0	0	0	6	0
Wild Type 0hr Recovery	118	0	0	0	0	0	4	0	0	0	0	0	0	6	0
Dnmt1-/- Sham	118	2	0	0	0	0	13	0	0	0	0	0	0	6	1
Dnmt1-/- 1hr Recovery	130	3	0	0	1	0	7	0	0	0	0	0	0	8	0
Dnmt1-/- 0hr Recovery	118	5	0	0	0	0	3	0	0	0	0	0	0	9	0
Dnmt3a3b-/- Sham	120	4	0	0	0	0	2	1	0	1	0	0	1	6	0
Dnmt3a3b-/- 1hr Recovery	112	7	0	0	0	0	2	1	0	0	0	0	0	10	1
Dnmt3a3b-/- 0hr Recovery	120	4	0	0	0	0	4	0	1	0	0	0	0	15	1

Table of raw data 1: the number of each cytogenetic aberration type observed at the 10-14 PD time point post treatment with 0Gy or 3Gy X-rays.

23-25 PDs		Chromosome-type Aberrations						Chromatid-type Aberrations						Other	
		Exchanges				Discontinuity	Exchanges				Discontinuity				
		Dicentric	Centric Ring	Interstitial Deletion	Reciprocal Translocation		Gaps, Beaks, Fragments	Interchange		Intrachanges			Gaps, Breaks, Fragments	Satellite Associations	
					Long Chromosome	Long Satellites		Inter-arm	Intra-arm						
Cell line/condition	Total Metaphases Scored							Dicentric	Reciprocal Translocation	Centric Ring	Dicentric	Interstitial Deletion	Isochromatid Deletion		
Wild Type Sham	119	3	0	0	0	0	8	0	0	0	0	0	0	9	0
Wild Type 1hr Recovery	139	3	0	0	0	1	6	0	0	0	0	0	0	10	0
Dnmt1-/- Sham	119	3	1	0	0	5	7	0	0	0	0	0	0	11	1
Dnmt1-/- 1hr Recovery	120	4	0	0	0	8	3	1	0	0	0	0	0	8	0
Dnmt3a3b-/- Sham	119	7	0	0	0	0	5	0	0	0	0	0	1	8	1
Dnmt3a3b-/- 1hr Recovery	120	4	0	0	0	0	3	0	0	0	0	0	0	7	1

Table of raw data 2: the number of each cytogenetic aberration type observed at the 23-25 PD time point post treatment with 0Gy or 3Gy X-rays.

7.4 Appendix 4

		Chromosome-type Aberrations			
		Exchanges			Discontinuity
Asymmetrical					Break
	Dicentric	Centric Ring	Interstitial Deletion		
Symmetrical					Gap
	Reciprocal Translocation	Pericentric Inversion	Paracentric Inversion		

Figure 1. The appearance of each type of chromosome-type aberration. Adapted from Savage (1999). Only discontinuity and some asymmetrical exchanges (dicentrics and centric rings) are visible using solid staining. Interstitial deletions were difficult to detect reliably, and the symmetrical exchanges were not visible.

		Chromatid-type Aberrations					
		Exchanges					Discontinuity
		Interchange	Inter-arm		Intra-arm		
Asymmetrical							Breaks, Gaps and Fragments
	Dicentric	Centric Ring	Dicentric	Interstitial Deletion	Isochromatid Deletion		
Symmetrical							
	Reciprocal Translocation	Pericentric Inversion	Duplication /Deletion	Paracentric Inversion	Duplication /Deletion		

Figure 2. The appearance of each type of chromatid-type aberration. Adapted from Savage (1999). All forms of discontinuity and interchanges are readily detectable using solid staining, as are inter-arm centric rings and dicentrics. However, inversions, duplications and deletions were very difficult to detect.

7.5 Appendix 5. License Agreement.

OXFORD UNIVERSITY PRESS LICENSE TERMS AND CONDITIONS

Sep 26, 2010

This is a License Agreement between Christine A Armstrong ("You") and Oxford University Press ("Oxford University Press") provided by Copyright Clearance Center ("CCC"). The license consists of your order details, the terms and conditions provided by Oxford University Press, and the payment terms and conditions.

All payments must be made in full to CCC. For payment instructions, please see information listed at the bottom of this form.

License Number	2516450746407
License date	Sep 26, 2010
Licensed content publisher	Oxford University Press
Licensed content publication	Human Molecular Genetics
Licensed content title	The Fanconi anemia pathway is required for the DNA replication stress response and for the regulation of common fragile site stability:
Licensed content author	Niall G. Howlett, Toshiyasu Taniguchi, Sandra G. Durkin, Alan D. D'Andrea, Thomas W. Glover
Licensed content date	1 March 2005
Type of Use	Thesis/Dissertation
Institution name	
Title of your work	DNA Hypomethylation in Radiosensitivity and Genomic Stability
Publisher of your	n/a

work

Expected publication date Sep 2010

Permissions cost 0.00 GBP

Value added tax 0.00 GBP

Total 0.00 GBP

Total 0.00 GBP

Terms and Conditions

STANDARD TERMS AND CONDITIONS FOR REPRODUCTION OF MATERIAL FROM AN OXFORD UNIVERSITY PRESS JOURNAL

1. Use of the material is restricted to the type of use specified in your order details.
2. This permission covers the use of the material in the English language in the following territory: world. If you have requested additional permission to translate this material, the terms and conditions of this reuse will be set out in clause 12.
3. This permission is limited to the particular use authorized in (1) above and does not allow you to sanction its use elsewhere in any other format other than specified above, nor does it apply to quotations, images, artistic works etc that have been reproduced from other sources which may be part of the material to be used.
4. No alteration, omission or addition is made to the material without our written consent. Permission must be re-cleared with Oxford University Press if/when you decide to reprint.
5. The following credit line appears wherever the material is used: author, title, journal, year, volume, issue number, pagination, by permission of Oxford University Press or the sponsoring society if the journal is a society journal. Where a journal is being published on behalf of a learned society, the details of that society must be included in the credit line.
6. For the reproduction of a full article from an Oxford University Press journal for whatever purpose, the corresponding author of the material concerned should be informed of the proposed use. Contact details for the corresponding authors of all Oxford University Press journal contact can be found alongside either the abstract or full text of the article concerned, accessible from www.oxfordjournals.org Should there be a problem clearing these rights, please contact journals.permissions@oxfordjournals.org
7. If the credit line or acknowledgement in our publication indicates that any of the figures, images or photos was reproduced, drawn or modified from an earlier source it will be necessary for you to clear this permission with the original publisher as well. If this

permission has not been obtained, please note that this material cannot be included in your publication/photocopies.

8. While you may exercise the rights licensed immediately upon issuance of the license at the end of the licensing process for the transaction, provided that you have disclosed complete and accurate details of your proposed use, no license is finally effective unless and until full payment is received from you (either by Oxford University Press or by Copyright Clearance Center (CCC)) as provided in CCC's Billing and Payment terms and conditions. If full payment is not received on a timely basis, then any license preliminarily granted shall be deemed automatically revoked and shall be void as if never granted. Further, in the event that you breach any of these terms and conditions or any of CCC's Billing and Payment terms and conditions, the license is automatically revoked and shall be void as if never granted. Use of materials as described in a revoked license, as well as any use of the materials beyond the scope of an unrevoked license, may constitute copyright infringement and Oxford University Press reserves the right to take any and all action to protect its copyright in the materials.

9. This license is personal to you and may not be sublicensed, assigned or transferred by you to any other person without Oxford University Press's written permission.

10. Oxford University Press reserves all rights not specifically granted in the combination of (i) the license details provided by you and accepted in the course of this licensing transaction, (ii) these terms and conditions and (iii) CCC's Billing and Payment terms and conditions.

11. You hereby indemnify and agree to hold harmless Oxford University Press and CCC, and their respective officers, directors, employees and agents, from and against any and all claims arising out of your use of the licensed material other than as specifically authorized pursuant to this license.

12. Other Terms and Conditions:

v1.4

Gratis licenses (referencing \$0 in the Total field) are free. Please retain this printable license for your reference. No payment is required.

If you would like to pay for this license now, please remit this license along with your payment made payable to "COPYRIGHT CLEARANCE CENTER" otherwise you will be invoiced within 48 hours of the license date. Payment should be in the form of a check or money order referencing your account number and this invoice number RLNK10855378.

Once you receive your invoice for this order, you may pay your invoice by credit card. Please follow instructions provided at that time.

**Make Payment To:
Copyright Clearance Center
Dept 001
P.O. Box 843006
Boston, MA 02284-3006**

If you find copyrighted material related to this license will not be used and wish to cancel, please contact us referencing this license number 2516450746407 and noting the reason for cancellation.

Questions? customer@copyright.com or +1-877-622-5543 (toll free in the US) or +1-978-646-2777.



8 References

- Aapola, U., Liiv, I. & Peterson, P. 2002, Imprinting regulator DNMT3L is a transcriptional repressor associated with histone deacetylase activity, *Nucleic acids research*, vol. 30, no. 16, pp. 3602-3608.
- Abrusan, G. & Krambeck, H.J. 2006, The distribution of L1 and Alu retroelements in relation to GC content on human sex chromosomes is consistent with the ectopic recombination model, *Journal of Molecular Evolution*, vol. 63, no. 4, pp. 484-492.
- Adams, B.R., Golding, S.E., Rao, R.R. & Valerie, K. 2010, Dynamic dependence on ATR and ATM for double-strand break repair in human embryonic stem cells and neural descendants, *PLoS one*, vol. 5, no. 4, pp. e10001.
- Aladjem, M.I., Spike, B.T., Rodewald, L.W., Hope, T.J., Klemm, M., Jaenisch, R. & Wahl, G.M. 1998, ESCs do not activate p53-dependent stress responses and undergo p53-independent apoptosis in response to DNA damage, *Current biology : CB*, vol. 8, no. 3, pp. 145-155.
- Amouroux, R., Campalans, A., Epe, B. & Radicella, J.P. 2010, Oxidative stress triggers the preferential assembly of base excision repair complexes on open chromatin regions, *Nucleic acids research*, vol. 38, no. 9, pp. 2878-2890.
- Anderson, R.M., Marsden, S.J., Paice, S.J., Bristow, A.E., Kadhim, M.A., Griffin, C.S. & Goodhead, D.T. 2003, Transmissible and nontransmissible complex chromosome aberrations characterized by three-color and mFISH define a biomarker of exposure to high-LET alpha particles, *Radiation research*, vol. 159, no. 1, pp. 40-48.
- Andrulis, E.D., Neiman, A.M., Zappulla, D.C. & Sternglanz, R. 1998, Perinuclear localization of chromatin facilitates transcriptional silencing, *Nature*, vol. 394, no. 6693, pp. 592-595.
- Armstrong, L., Saretzki, G., Peters, H., Wappler, I., Evans, J., Hole, N., von Zglinicki, T. & Lako, M. 2005, Overexpression of telomerase confers growth advantage, stress resistance, and enhanced differentiation of ESCs toward the hematopoietic lineage, *Stem cells (Dayton, Ohio)*, vol. 23, no. 4, pp. 516-529.
- Artandi, S.E., Chang, S., Lee, S.L., Alson, S., Gottlieb, G.J., Chin, L. & DePinho, R.A. 2000, Telomere dysfunction promotes non-reciprocal translocations and epithelial cancers in mice, *Nature*, vol. 406, no. 6796, pp. 641-645.
- Baird, D.M., Rowson, J., Wynford-Thomas, D. & Kipling, D. 2003, Extensive allelic variation and ultrashort telomeres in senescent human cells, *Nature genetics*, vol. 33, no. 2, pp. 203-207.
- Balestrieri, E., Zanier, R. & Degrossi, F. 2001, Molecular characterisation of camptothecin-induced mutations at the hprt locus in Chinese hamster cells, *Mutation research*, vol. 476, no. 1-2, pp. 63-69.
- Barber, R., Plumb, M.A., Boulton, E., Roux, I. & Dubrova, Y.E. 2002, Elevated mutation rates in the germ line of first- and second-generation offspring of irradiated male mice, *Proceedings of the National Academy of Sciences of the United States of America*, vol. 99, no. 10, pp. 6877-6882.
- Barber, R.C. & Dubrova, Y.E. 2006, The offspring of irradiated parents, are they stable?, *Mutation research*, vol. 598, no. 1-2, pp. 50-60.

- Barber, R.C., Hardwick, R.J., Shanks, M.E., Glen, C.D., Mughal, S.K., Voutounou, M. & Dubrova, Y.E. 2009, The effects of in utero irradiation on mutation induction and transgenerational instability in mice, *Mutation research*, vol. 664, no. 1-2, pp. 6-12.
- Barber, R.C., Hickenbotham, P., Hatch, T., Kelly, D., Topchiy, N., Almeida, G.M., Jones, G.D., Johnson, G.E., Parry, J.M., Rothkamm, K. & Dubrova, Y.E. 2006, Radiation-induced transgenerational alterations in genome stability and DNA damage, *Oncogene*, vol. 25, no. 56, pp. 7336-7342.
- Barreto, G., Schafer, A., Marhold, J., Stach, D., Swaminathan, S.K., Handa, V., Doderlein, G., Maltry, N., Wu, W., Lyko, F. & Niehrs, C. 2007, Gadd45a promotes epigenetic gene activation by repair-mediated DNA demethylation, *Nature*, vol. 445, no. 7128, pp. 671-675.
- Bartek, J. & Lukas, J. 2001, Pathways governing G1/S transition and their response to DNA damage, *FEBS letters*, vol. 490, no. 3, pp. 117-122.
- Baulch, J.E., Raabe, O.G. & Wiley, L.M. 2001, Heritable effects of paternal irradiation in mice on signalling protein kinase activities in F3 offspring, *Mutagenesis*, vol. 16, no. 1, pp. 17-23.
- Beaulieu, N., Morin, S., Chute, I.C., Robert, M.F., Nguyen, H. & MacLeod, A.R. 2002, An essential role for DNA methyltransferase DNMT3B in cancer cell survival, *The Journal of biological chemistry*, vol. 277, no. 31, pp. 28176-28181.
- Bechter, O.E., Shay, J.W. & Wright, W.E. 2004, The frequency of homologous recombination in human ALT cells, *Cell cycle (Georgetown, Tex.)*, vol. 3, no. 5, pp. 547-549.
- Bender, J. 1998, Cytosine methylation of repeated sequences in eukaryotes: the role of DNA pairing, *Trends in biochemical sciences*, vol. 23, no. 7, pp. 252-256.
- Bender, M.A., Awa, A.A., Brooks, A.L., Evans, H.J., Groer, P.G., Littlefield, L.G., Pereira, C., Preston, R.J. & Wachholz, B.W. 1988, Current status of cytogenetic procedures to detect and quantify previous exposures to radiation, *Mutation research*, vol. 196, no. 2, pp. 103-159.
- Benetti, R., Garcia-Cao, M. & Blasco, M.A. 2007, Telomere length regulates the epigenetic status of mammalian telomeres and subtelomeres, *Nature genetics*, vol. 39, no. 2, pp. 243-250.
- Berger, J.M., Gamblin, S.J., Harrison, S.C. & Wang, J.C. 1996, Structure and mechanism of DNA topoisomerase II, *Nature*, vol. 379, no. 6562, pp. 225-232.
- Bhattacharya, S.K., Ramchandani, S., Cervoni, N. & Szyf, M. 1999, A mammalian protein with specific demethylase activity for mCpG DNA, *Nature*, vol. 397, no. 6720, pp. 579-583.
- Blasco, M.A. 2005, Telomeres and human disease: ageing, cancer and beyond, *Nature reviews.Genetics*, vol. 6, no. 8, pp. 611-622.
- Boos, G. & Stopper, H. 2001, DNA methylation influences the decatenation activity of topoisomerase II, *International journal of biological macromolecules*, vol. 28, no. 2, pp. 103-106.
- Borgdorff, V., Pauw, B., van Hees-Stuivenberg, S. & de Wind, N. 2006, DNA mismatch repair mediates protection from mutagenesis induced by short-wave ultraviolet light, *DNA repair*, vol. 5, no. 11, pp. 1364-1372.
- Bourc'his, D., Xu, G.L., Lin, C.S., Bollman, B. & Bestor, T.H. 2001, Dnmt3L and the establishment of maternal genomic imprints, *Science (New York, N.Y.)*, vol. 294, no. 5551, pp. 2536-2539.

- Box, H.C., Budzinski, E.E., Dawidzik, J.B., Wallace, J.C. & Iijima, H. 1998, Tandem lesions and other products in X-irradiated DNA oligomers, *Radiation research*, vol. 149, no. 5, pp. 433-439.
- Branco, M.R. & Pombo, A. 2006, Intermingling of chromosome territories in interphase suggests role in translocations and transcription-dependent associations, *PLoS biology*, vol. 4, no. 5, pp. e138.
- Breen, A.P. & Murphy, J.A. 1995, Reactions of oxyl radicals with DNA, *Free radical biology & medicine*, vol. 18, no. 6, pp. 1033-1077.
- Brena, R.M., Huang, T.H. & Plass, C. 2006, Toward a human epigenome, *Nature genetics*, vol. 38, no. 12, pp. 1359-1360.
- Brock, G.J., Charlton, J. & Bird, A. 1999, Densely methylated sequences that are preferentially localized at telomere-proximal regions of human chromosomes, *Gene*, vol. 240, no. 2, pp. 269-277.
- Brown, T.C. & Jiricny, J. 1987, A specific mismatch repair event protects mammalian cells from loss of 5-methylcytosine, *Cell*, vol. 50, no. 6, pp. 945-950.
- Bryant, P.E. 1984, Enzymatic restriction of mammalian cell DNA using Pvu II and Bam H1: evidence for the double-strand break origin of chromosomal aberrations, *International journal of radiation biology and related studies in physics, chemistry, and medicine*, vol. 46, no. 1, pp. 57-65.
- Buermeyer, A.B., Deschenes, S.M., Baker, S.M. & Liskay, R.M. 1999, Mammalian DNA mismatch repair, *Annual Review of Genetics*, vol. 33, pp. 533-564.
- Burdon, T., Smith, A. & Savatier, P. 2002, Signalling, cell cycle and pluripotency in embryonic stem cells, *Trends in cell biology*, vol. 12, no. 9, pp. 432-438.
- Burks, R.T., Kessis, T.D., Cho, K.R. & Hedrick, L. 1994, Microsatellite instability in endometrial carcinoma, *Oncogene*, vol. 9, no. 4, pp. 1163-1166.
- Calcagnile, O. & Gisselsson, D. 2007, Telomere dysfunction and telomerase activation in cancer--a pathological paradox?, *Cytogenetic and genome research*, vol. 118, no. 2-4, pp. 270-276.
- Caldecott, K.W. 2008, Single-strand break repair and genetic disease, *Nature reviews.Genetics*, vol. 9, no. 8, pp. 619-631.
- Camphausen, K., Burgan, W., Cerra, M., Oswald, K.A., Trepel, J.B., Lee, M.J. & Tofilon, P.J. 2004, Enhanced radiation-induced cell killing and prolongation of gammaH2AX foci expression by the histone deacetylase inhibitor MS-275, *Cancer research*, vol. 64, no. 1, pp. 316-321.
- Camphausen, K., Cerna, D., Scott, T., Sproull, M., Burgan, W.E., Cerra, M.A., Fine, H. & Tofilon, P.J. 2005, Enhancement of *in vitro* and *in vivo* tumour cell radiosensitivity by valproic acid, *International journal of cancer.Journal international du cancer*, vol. 114, no. 3, pp. 380-386.
- Canaani, E., Drezzen, O., Klar, A., Rechavi, G., Ram, D., Cohen, J.B. & Givol, D. 1983, Activation of the c-mos oncogene in a mouse plasmacytoma by insertion of an endogenous intracisternal A-particle genome, *Proceedings of the National Academy of Sciences of the United States of America*, vol. 80, no. 23, pp. 7118-7122.
- Cannon, S.V., Cummings, A. & Teebor, G.W. 1988, 5-Hydroxymethylcytosine DNA glycosylase activity in mammalian tissue, *Biochemical and biophysical research communications*, vol. 151, no. 3, pp. 1173-1179.

- Cao, H. & Wang, Y. 2007, Quantification of oxidative single-base and intrastrand cross-link lesions in unmethylated and CpG-methylated DNA induced by Fenton-type reagents, *Nucleic acids research*, vol. 35, no. 14, pp. 4833-4844.
- Capranico, G., Kohn, K.W. & Pommier, Y. 1990, Local sequence requirements for DNA cleavage by mammalian topoisomerase II in the presence of doxorubicin, *Nucleic acids research*, vol. 18, no. 22, pp. 6611-6619.
- Carnell, A.N. & Goodman, J.I. 2003, The long (LINEs) and the short (SINEs) of it: altered methylation as a precursor to toxicity, *Toxicological sciences : an official journal of the Society of Toxicology*, vol. 75, no. 2, pp. 229-235.
- Caron, R.M., Nagasawa, H., Yu, Y., Pfenning, T., Vetrovs, H. & Little, J.B. 1997, Evidence for a role for genomic instability in radiation-induced mutagenesis, *Radiation oncology investigations*, vol. 5, no. 3, pp. 119-123.
- Carrano, A.V., Minkler, J. & Piluso, D. 1975, On the fate of stable chromosomal aberrations, *Mutation research*, vol. 30, no. 1, pp. 153-156.
- Cervantes, R.B., Stringer, J.R., Shao, C., Tischfield, J.A. & Stambrook, P.J. 2002, Embryonic stem cells and somatic cells differ in mutation frequency and type, *Proceedings of the National Academy of Sciences of the United States of America*, vol. 99, no. 6, pp. 3586-3590.
- Chalitchagorn, K., Shuangshoti, S., Hourpai, N., Kongruttanachok, N., Tangkijvanich, P., Thong-ngam, D., Voravud, N., Sriuranpong, V. & Mutirangura, A. 2004, Distinctive pattern of LINE-1 methylation level in normal tissues and the association with carcinogenesis, *Oncogene*, vol. 23, no. 54, pp. 8841-8846.
- Champion, C., Guianvarc'h, D., Senamaud-Beaufort, C., Jurkowska, R.Z., Jeltsch, A., Ponger, L., Arimondo, P.B. & Guieysse-Peugeot, A.L. 2010, Mechanistic insights on the inhibition of c5 DNA methyltransferases by zebularine, *PLoS one*, vol. 5, no. 8, pp. e12388.
- Chang, J., Watson, W.P., Randerath, E. & Randerath, K. 1993, Bulky DNA-adduct formation induced by Ni(II) *in vitro* and *in vivo* as assayed by 32P-postlabeling, *Mutation research*, vol. 291, no. 2, pp. 147-159.
- Chen, L., MacMillan, A.M., Chang, W., Ezaz-Nikpay, K., Lane, W.S. & Verdine, G.L. 1991, Direct identification of the active-site nucleophile in a DNA (cytosine-5)-methyltransferase, *Biochemistry*, vol. 30, no. 46, pp. 11018-11025.
- Chen, R.Z., Pettersson, U., Beard, C., Jackson-Grusby, L. & Jaenisch, R. 1998, DNA hypomethylation leads to elevated mutation rates, *Nature*, vol. 395, no. 6697, pp. 89-93.
- Chen, T., Hevi, S., Gay, F., Tsujimoto, N., He, T., Zhang, B., Ueda, Y. & Li, E. 2007, Complete inactivation of DNMT1 leads to mitotic catastrophe in human cancer cells, *Nature genetics*, vol. 39, no. 3, pp. 391-396.
- Chen, T., Tsujimoto, N. & Li, E. 2004, The PWWP domain of Dnmt3a and Dnmt3b is required for directing DNA methylation to the major satellite repeats at pericentric heterochromatin, *Molecular and cellular biology*, vol. 24, no. 20, pp. 9048-9058.
- Chen, T., Ueda, Y., Dodge, J.E., Wang, Z. & Li, E. 2003, Establishment and maintenance of genomic methylation patterns in mouse embryonic stem cells by Dnmt3a and Dnmt3b, *Molecular and cellular biology*, vol. 23, no. 16, pp. 5594-5605.

- Cheng, J.C., Yoo, C.B., Weisenberger, D.J., Chuang, J., Wozniak, C., Liang, G., Marquez, V.E., Greer, S., Orntoft, T.F., Thykjaer, T. & Jones, P.A. 2004, Preferential response of cancer cells to zebularine, *Cancer cell*, vol. 6, no. 2, pp. 151-158.
- Choo, K.H.A. 1997, *The Centromere*, Oxford University Press, New York.
- Choy, J.S., Wei, S., Lee, J.Y., Tan, S., Chu, S. & Lee, T.H. 2010, DNA methylation increases nucleosome compaction and rigidity, *Journal of the American Chemical Society*, vol. 132, no. 6, pp. 1782-1783.
- Chubb, J.R., Boyle, S., Perry, P. & Bickmore, W.A. 2002, Chromatin motion is constrained by association with nuclear compartments in human cells, *Current biology : CB*, vol. 12, no. 6, pp. 439-445.
- Chuykin, I.A., Lianguzova, M.S., Pospelova, T.V. & Pospelov, V.A. 2008, Activation of DNA damage response signalling in mouse embryonic stem cells, *Cell cycle (Georgetown, Tex.)*, vol. 7, no. 18, pp. 2922-2928.
- Cimprich, K.A. & Cortez, D. 2008, ATR: an essential regulator of genome integrity, *Nature reviews.Molecular cell biology*, vol. 9, no. 8, pp. 616-627.
- Claij, N. & Te Riele, H. 2002, Methylation tolerance in mismatch repair proficient cells with low MSH2 protein level, *Oncogene*, vol. 21, no. 18, pp. 2873-2879.
- Clutton, S.M., Townsend, K.M., Walker, C., Ansell, J.D. & Wright, E.G. 1996, Radiation-induced genomic instability and persisting oxidative stress in primary bone marrow cultures, *Carcinogenesis*, vol. 17, no. 8, pp. 1633-1639.
- Cooper, T.G., Yeung, C.H., Fetic, S., Sobhani, A. & Nieschlag, E. 2004, Cytoplasmic droplets are normal structures of human sperm but are not well preserved by routine procedures for assessing sperm morphology, *Human reproduction (Oxford, England)*, vol. 19, no. 10, pp. 2283-2288.
- Costello, J.F., Fruhwald, M.C., Smiraglia, D.J., Rush, L.J., Robertson, G.P., Gao, X., Wright, F.A., Feramisco, J.D., Peltomaki, P., Lang, J.C., Schuller, D.E., Yu, L., Bloomfield, C.D., Caligiuri, M.A., Yates, A., Nishikawa, R., Su Huang, H., Petrelli, N.J., Zhang, X., O'Dorisio, M.S., Held, W.A., Cavenee, W.K. & Plass, C. 2000, Aberrant CpG-island methylation has non-random and tumour-type-specific patterns, *Nature genetics*, vol. 24, no. 2, pp. 132-138.
- Cremer, T. & Cremer, C. 2001, Chromosome territories, nuclear architecture and gene regulation in mammalian cells, *Nature reviews.Genetics*, vol. 2, no. 4, pp. 292-301.
- Cruikshanks, H.A. & Tufarelli, C. 2009, Isolation of cancer-specific chimeric transcripts induced by hypomethylation of the LINE-1 antisense promoter, *Genomics*, vol. 94, no. 6, pp. 397-406.
- d'Adda di Fagagna, F., Reaper, P.M., Clay-Farrace, L., Fiegler, H., Carr, P., Von Zglinicki, T., Saretzki, G., Carter, N.P. & Jackson, S.P. 2003, A DNA damage checkpoint response in telomere-initiated senescence, *Nature*, vol. 426, no. 6963, pp. 194-198.
- Daher, A., Varin, M., Lamontagne, Y. & Oth, D. 1998, Effect of pre-conceptional external or internal irradiation of N5 male mice and the risk of leukemia in their offspring, *Carcinogenesis*, vol. 19, no. 9, pp. 1553-1558.
- Dainiak, N. 2002, Hematologic consequences of exposure to ionizing radiation, *Experimental hematology*, vol. 30, no. 6, pp. 513-528.
- Damelin, M. & Bestor, T.H. 2007, Biological functions of DNA methyltransferase 1 require its methyltransferase activity, *Molecular and cellular biology*, vol. 27, no. 11, pp. 3891-3899.

- Damelin, M., Sun, Y.E., Sodja, V.B. & Bestor, T.H. 2005, Decatenation checkpoint deficiency in stem and progenitor cells, *Cancer cell*, vol. 8, no. 6, pp. 479-484.
- Dante, R., Dante-Paire, J., Rigal, D. & Roizes, G. 1992, Methylation patterns of long interspersed repeated DNA and alphoid repetitive DNA from human cell lines and tumours, *Anticancer Research*, vol. 12, no. 2, pp. 559-563.
- Darzynkiewicz, Z., Bruno, S., Del Bino, G., Gorczyca, W., Hotz, M.A., Lassota, P. & Traganos, F. 1992, Features of apoptotic cells measured by flow cytometry, *Cytometry*, vol. 13, no. 8, pp. 795-808.
- Davis, T.L., Yang, G.J., McCarrey, J.R. & Bartolomei, M.S. 2000, The H19 methylation imprint is erased and re-established differentially on the parental alleles during male germ cell development, *Human molecular genetics*, vol. 9, no. 19, pp. 2885-2894.
- de Lange, T. 2005, Shelterin: the protein complex that shapes and safeguards human telomeres, *Genes & development*, vol. 19, no. 18, pp. 2100-2110.
- de Lange, T., Shiue, L., Myers, R.M., Cox, D.R., Naylor, S.L., Killery, A.M. & Varmus, H.E. 1990, Structure and variability of human chromosome ends, *Molecular and cellular biology*, vol. 10, no. 2, pp. 518-527.
- De Silva, I.U., McHugh, P.J., Clingen, P.H. & Hartley, J.A. 2000, Defining the roles of nucleotide excision repair and recombination in the repair of DNA interstrand cross-links in mammalian cells, *Molecular and cellular biology*, vol. 20, no. 21, pp. 7980-7990.
- de Waard, H., de Wit, J., Gorgels, T.G., van den Aardweg, G., Andressoo, J.O., Vermeij, M., van Steeg, H., Hoeijmakers, J.H. & van der Horst, G.T. 2003, Cell type-specific hypersensitivity to oxidative damage in CSB and XPA mice, *DNA repair*, vol. 2, no. 1, pp. 13-25.
- Degrassi, F., De Salvia, R., Tanzarella, C. & Palitti, F. 1989, Induction of chromosomal aberrations and SCE by camptothecin, an inhibitor of mammalian topoisomerase I, *Mutation research*, vol. 211, no. 1, pp. 125-130.
- Deininger, P.L. & Roy-Engel, A.M. 2002, Mobile elements in animal and plant genomes. in *Mobile DNA II*, eds. N.L. Craig, R. Craigie, M. Gellert & A.M. Lambowitz, ASM Press, Washington DC, pp. 1074-1092.
- Denissenko, M.F., Chen, J.X., Tang, M.S. & Pfeifer, G.P. 1997, Cytosine methylation determines hot spots of DNA damage in the human P53 gene, *Proceedings of the National Academy of Sciences of the United States of America*, vol. 94, no. 8, pp. 3893-3898.
- Denissenko, M.F., Pao, A., Tang, M. & Pfeifer, G.P. 1996, Preferential formation of benzo[a]pyrene adducts at lung cancer mutational hotspots in P53, *Science (New York, N.Y.)*, vol. 274, no. 5286, pp. 430-432.
- Dewannieux, M., Dupressoir, A., Harper, F., Pierron, G. & Heidmann, T. 2004, Identification of autonomous IAP LTR retrotransposons mobile in mammalian cells, *Nature genetics*, vol. 36, no. 5, pp. 534-539.
- DeWeese, T.L., Shipman, J.M., Larrier, N.A., Buckley, N.M., Kidd, L.R., Groopman, J.D., Cutler, R.G., te Riele, H. & Nelson, W.G. 1998, Mouse embryonic stem cells carrying one or two defective Msh2 alleles respond abnormally to oxidative stress inflicted by low-level radiation, *Proceedings of the National Academy of Sciences of the United States of America*, vol. 95, no. 20, pp. 11915-11920.
- Dianov, G.L. & Parsons, J.L. 2007, Co-ordination of DNA single strand break repair, *DNA repair*, vol. 6, no. 4, pp. 454-460.

- DiBiase, S.J., Zeng, Z.C., Chen, R., Hyslop, T., Curran, W.J., Jr & Iliakis, G. 2000, DNA-dependent protein kinase stimulates an independently active, nonhomologous, end-joining apparatus, *Cancer research*, vol. 60, no. 5, pp. 1245-1253.
- Dion, V., Lin, Y., Hubert, L., Jr, Waterland, R.A. & Wilson, J.H. 2008, Dnmt1 deficiency promotes CAG repeat expansion in the mouse germline, *Human molecular genetics*, vol. 17, no. 9, pp. 1306-1317.
- Dominguez-Bendala, J. & McWhir, J. 2004, Enhanced gene targeting frequency in ESCs with low genomic methylation levels, *Transgenic research*, vol. 13, no. 1, pp. 69-74.
- Dörr, W. 2009, Pathogenesis of normal-tissue side-effects in *Basic Clinical Radiobiology*, eds. M. Joiner & A. van der Kogel, 4th edn, Hodder Arnold, Great Britain, pp. 169.
- Dote, H., Cerna, D., Burgan, W.E., Carter, D.J., Cerra, M.A., Hollingshead, M.G., Camphausen, K. & Tofilon, P.J. 2005, Enhancement of *in vitro* and *in vivo* tumour cell radiosensitivity by the DNA methylation inhibitor zebularine, *Clinical cancer research : an official journal of the American Association for Cancer Research*, vol. 11, no. 12, pp. 4571-4579.
- Druker, R., Bruxner, T.J., Lehrbach, N.J. & Whitelaw, E. 2004, Complex patterns of transcription at the insertion site of a retrotransposon in the mouse, *Nucleic acids research*, vol. 32, no. 19, pp. 5800-5808.
- Dubrova, Y.E. 2003, Radiation-induced transgenerational instability, *Oncogene*, vol. 22, no. 45, pp. 7087-7093.
- Dubrova, Y.E., Grant, G., Chumak, A.A., Stezhka, V.A. & Karakasian, A.N. 2002, Elevated minisatellite mutation rate in the post-chernobyl families from ukraine, *American Journal of Human Genetics*, vol. 71, no. 4, pp. 801-809.
- Dubrova, Y.E., Plumb, M., Brown, J. & Jeffreys, A.J. 1998, Radiation-induced germline instability at minisatellite loci, *International journal of radiation biology*, vol. 74, no. 6, pp. 689-696.
- Duell, T., Lengfelder, E., Fink, R., Giesen, R. & Bauchinger, M. 1995, Effect of activated oxygen species in human lymphocytes, *Mutation research*, vol. 336, no. 1, pp. 29-38.
- Dunham, M.A., Neumann, A.A., Fasching, C.L. & Reddel, R.R. 2000, Telomere maintenance by recombination in human cells, *Nature genetics*, vol. 26, no. 4, pp. 447-450.
- Edelmann, W., Kroger, B., Goller, M. & Horak, I. 1989, A recombination hotspot in the LTR of a mouse retrotransposon identified in an *in vitro* system, *Cell*, vol. 57, no. 6, pp. 937-946.
- Ehrlich, M. 2002, DNA methylation in cancer: too much, but also too little, *Oncogene*, vol. 21, no. 35, pp. 5400-5413.
- Ehrlich, M., Gama-Sosa, M.A., Huang, L.H., Midgett, R.M., Kuo, K.C., McCune, R.A. & Gehrke, C. 1982, Amount and distribution of 5-methylcytosine in human DNA from different types of tissues of cells, *Nucleic acids research*, vol. 10, no. 8, pp. 2709-2721.
- Ehrlich, M., Jackson, K. & Weemaes, C. 2006, Immunodeficiency, centromeric region instability, facial anomalies syndrome (ICF), *Orphanet journal of rare diseases*, vol. 1, pp. 2.
- Ehrlich, M., Tsien, F., Herrera, D., Blackman, V., Roggenbuck, J. & Tuck-Muller, C.M. 2001, High frequencies of ICF syndrome-like pericentromeric heterochromatin decondensation and breakage in chromosome 1 in a chorionic villus sample, *Journal of medical genetics*, vol. 38, no. 12, pp. 882-884.

- Elliott, B. & Jasin, M. 2002, Double-strand breaks and translocations in cancer, *Cellular and molecular life sciences : CMLS*, vol. 59, no. 2, pp. 373-385.
- Emerit, I. & Cerutti, P.A. 1981, Tumour promoter phorbol-12-myristate-13-acetate induces chromosomal damage via indirect action, *Nature*, vol. 293, no. 5828, pp. 144-146.
- Emerit, I., Levy, A., Cernjavski, L., Arutyunyan, R., Oganessian, N., Pogolian, A., Mejlumian, H., Sarkisian, T., Gulkandarian, M. & Quastel, M. 1994, Transferable clastogenic activity in plasma from persons exposed as salvage personnel of the Chernobyl reactor, *Journal of cancer research and clinical oncology*, vol. 120, no. 9, pp. 558-561.
- Espejel, S., Franco, S., Sgura, A., Gae, D., Bailey, S.M., Taccioli, G.E. & Blasco, M.A. 2002, Functional interaction between DNA-PKcs and telomerase in telomere length maintenance, *The EMBO journal*, vol. 21, no. 22, pp. 6275-6287.
- Esteller, M. 2005, *DNA Methylation: Approaches, Methods and Applications*, 1st edn, CRC Press, USA.
- Esteller, M., Corn, P.G., Baylin, S.B. & Herman, J.G. 2001, A gene hypermethylation profile of human cancer, *Cancer research*, vol. 61, no. 8, pp. 3225-3229.
- Esteve, P.O., Chin, H.G., Smallwood, A., Feehery, G.R., Gangisetty, O., Karpf, A.R., Carey, M.F. & Pradhan, S. 2006, Direct interaction between DNMT1 and G9a coordinates DNA and histone methylation during replication, *Genes & development*, vol. 20, no. 22, pp. 3089-3103.
- Evans, M.J. & Kaufman, M.H. 1981, Establishment in culture of pluripotential cells from mouse embryos, *Nature*, vol. 292, no. 5819, pp. 154-156.
- Feng, Q., Moran, J.V., Kazazian, H.H., Jr & Boeke, J.D. 1996, Human L1 retrotransposon encodes a conserved endonuclease required for retrotransposition, *Cell*, vol. 87, no. 5, pp. 905-916.
- Frankenberg-Schwager, M. 1990, Induction, repair and biological relevance of radiation-induced DNA lesions in eukaryotic cells, *Radiation and environmental biophysics*, vol. 29, no. 4, pp. 273-292.
- Friedberg, E.C. 2001, How nucleotide excision repair protects against cancer, *Nature reviews.Cancer*, vol. 1, no. 1, pp. 22-33.
- Friedman, K.L. & Brewer, B.J. 1995, Analysis of replication intermediates by two-dimensional gel electrophoresis in *Methods in enzymology: DNA replication* Academic Press Inc, USA, pp. 613-627.
- Fuks, F., Burgers, W.A., Brehm, A., Hughes-Davies, L. & Kouzarides, T. 2000, DNA methyltransferase Dnmt1 associates with histone deacetylase activity, *Nature genetics*, vol. 24, no. 1, pp. 88-91.
- Fuks, F., Hurd, P.J., Deplus, R. & Kouzarides, T. 2003, The DNA methyltransferases associate with HP1 and the SUV39H1 histone methyltransferase, *Nucleic acids research*, vol. 31, no. 9, pp. 2305-2312.
- Gagos, S. & Irminger-Finger, I. 2005, Chromosome instability in neoplasia: chaotic roots to continuous growth, *The international journal of biochemistry & cell biology*, vol. 37, no. 5, pp. 1014-1033.
- Gama-Sosa, M.A., Midgett, R.M., Slagel, V.A., Githens, S., Kuo, K.C., Gehrke, C.W. & Ehrlich, M. 1983, Tissue-specific differences in DNA methylation in various mammals, *Biochimica et biophysica acta*, vol. 740, no. 2, pp. 212-219.

- Gama-Sosa, M.A., Slagel, V.A., Trewyn, R.W., Oxenhandler, R., Kuo, K.C., Gehrke, C.W. & Ehrlich, M. 1983, The 5-methylcytosine content of DNA from human tumours, *Nucleic acids research*, vol. 11, no. 19, pp. 6883-6894.
- Gama-Sosa, M.A., Wang, R.Y., Kuo, K.C., Gehrke, C.W. & Ehrlich, M. 1983, The 5-methylcytosine content of highly repeated sequences in human DNA, *Nucleic acids research*, vol. 11, no. 10, pp. 3087-3095.
- Garagna, S., Zuccotti, M., Capanna, E. & Redi, C.A. 2002, High-resolution organization of mouse telomeric and pericentromeric DNA, *Cytogenetic and genome research*, vol. 96, no. 1-4, pp. 125-129.
- Garcia-Cao, M., Gonzalo, S., Dean, D. & Blasco, M.A. 2002, A role for the Rb family of proteins in controlling telomere length, *Nature genetics*, vol. 32, no. 3, pp. 415-419.
- Garcia-Cao, M., O'Sullivan, R., Peters, A.H., Jenuwein, T. & Blasco, M.A. 2004, Epigenetic regulation of telomere length in mammalian cells by the Suv39h1 and Suv39h2 histone methyltransferases, *Nature genetics*, vol. 36, no. 1, pp. 94-99.
- Gaudet, F., Rideout, W.M., 3rd, Meissner, A., Dausman, J., Leonhardt, H. & Jaenisch, R. 2004, Dnmt1 expression in pre- and postimplantation embryogenesis and the maintenance of IAP silencing, *Molecular and cellular biology*, vol. 24, no. 4, pp. 1640-1648.
- Geacintov, N.E., Shahbaz, M., Ibanez, V., Moussaoui, K. & Harvey, R.G. 1988, Base-sequence dependence of noncovalent complex formation and reactivity of benzo[a]pyrene diol epoxide with polynucleotides, *Biochemistry*, vol. 27, no. 22, pp. 8380-8387.
- Geiman, T.M., Sankpal, U.T., Robertson, A.K., Zhao, Y., Zhao, Y. & Robertson, K.D. 2004, DNMT3B interacts with hSNF2H chromatin remodeling enzyme, HDACs 1 and 2, and components of the histone methylation system, *Biochemical and biophysical research communications*, vol. 318, no. 2, pp. 544-555.
- Gilbert, N., Lutz-Prigge, S. & Moran, J.V. 2002, Genomic deletions created upon LINE-1 retrotransposition, *Cell*, vol. 110, no. 3, pp. 315-325.
- Giotopoulos, G., McCormick, C., Cole, C., Zanker, A., Jawad, M., Brown, R. & Plumb, M. 2006, DNA methylation during mouse hemopoietic differentiation and radiation-induced leukemia, *Experimental hematology*, vol. 34, no. 11, pp. 1462-1470.
- Gisselsson, D., Shao, C., Tuck-Muller, C.M., Sogorovic, S., Palsson, E., Smeets, D. & Ehrlich, M. 2005, Interphase chromosomal abnormalities and mitotic missegregation of hypomethylated sequences in ICF syndrome cells, *Chromosoma*, vol. 114, no. 2, pp. 118-126.
- Givan, A.L. 2001, *Flow Cytometry: First Principles*, 2nd edn, Wiley-Liss, USA.
- Goetze, S., Mateos-Langerak, J., Gierman, H.J., de Leeuw, W., Giromus, O., Indemans, M.H., Koster, J., Ondrej, V., Versteeg, R. & van Driel, R. 2007, The three-dimensional structure of human interphase chromosomes is related to the transcriptome map, *Molecular and cellular biology*, vol. 27, no. 12, pp. 4475-4487.
- Gonzalo, S., Garcia-Cao, M., Fraga, M.F., Schotta, G., Peters, A.H., Cotter, S.E., Eguia, R., Dean, D.C., Esteller, M., Jenuwein, T. & Blasco, M.A. 2005, Role of the RB1 family in stabilizing histone methylation at constitutive heterochromatin, *Nature cell biology*, vol. 7, no. 4, pp. 420-428.

- Gonzalo, S., Jaco, I., Fraga, M.F., Chen, T., Li, E., Esteller, M. & Blasco, M.A. 2006, DNA methyltransferases control telomere length and telomere recombination in mammalian cells, *Nature cell biology*, vol. 8, no. 4, pp. 416-424.
- Goodier, J.L., Ostertag, E.M., Du, K. & Kazazian, H.H., Jr 2001, A novel active L1 retrotransposon subfamily in the mouse, *Genome research*, vol. 11, no. 10, pp. 1677-1685.
- Goodier, J.L., Ostertag, E.M. & Kazazian, H.H., Jr 2000, Transduction of 3'-flanking sequences is common in L1 retrotransposition, *Human molecular genetics*, vol. 9, no. 4, pp. 653-657.
- Gopalakrishnan, S., Van Emburgh, B.O., Shan, J., Su, Z., Fields, C.R., Vieweg, J., Hamazaki, T., Schwartz, P.H., Terada, N. & Robertson, K.D. 2009, A novel DNMT3B splice variant expressed in tumour and pluripotent cells modulates genomic DNA methylation patterns and displays altered DNA binding, *Molecular cancer research : MCR*, vol. 7, no. 10, pp. 1622-1634.
- Gorbunova, V., Seluanov, A., Mittelman, D. & Wilson, J.H. 2004, Genome-wide demethylation destabilizes CTG.CAG trinucleotide repeats in mammalian cells, *Human molecular genetics*, vol. 13, no. 23, pp. 2979-2989.
- Goto, T., Mizukami, H., Shirahata, A., Yokomizo, K., Kitamura, Y.H., Sakuraba, K., Saito, M., Ishibashi, K., Kigawa, G., Nemoto, H., Sanada, Y. & Hibi, K. 2010, Methylation of the p16 gene is frequently detected in lymphatic-invasive gastric cancer, *Anticancer Research*, vol. 30, no. 7, pp. 2701-2703.
- Gowher, H., Liebert, K., Hermann, A., Xu, G. & Jeltsch, A. 2005, Mechanism of stimulation of catalytic activity of Dnmt3A and Dnmt3B DNA-(cytosine-C5)-methyltransferases by Dnmt3L, *The Journal of biological chemistry*, vol. 280, no. 14, pp. 13341-13348.
- Greenblatt, M.S., Bennett, W.P., Hollstein, M. & Harris, C.C. 1994, Mutations in the p53 tumour suppressor gene: clues to cancer etiology and molecular pathogenesis, *Cancer research*, vol. 54, no. 18, pp. 4855-4878.
- Griffiths, E.A., Pritchard, S.A., McGrath, S.M., Valentine, H.R., Price, P.M., Welch, I.M. & West, C.M. 2007, Increasing expression of hypoxia-inducible proteins in the Barrett's metaplasia-dysplasia-adenocarcinoma sequence, *British journal of cancer*, vol. 96, no. 9, pp. 1377-1383.
- Grosovsky, A.J., Parks, K.K., Giver, C.R. & Nelson, S.L. 1996, Clonal analysis of delayed karyotypic abnormalities and gene mutations in radiation-induced genetic instability, *Molecular and cellular biology*, vol. 16, no. 11, pp. 6252-6262.
- Guo, G., Wang, W. & Bradley, A. 2004, Mismatch repair genes identified using genetic screens in Blm-deficient embryonic stem cells, *Nature*, vol. 429, no. 6994, pp. 891-895.
- Haik, S., Gauthier, L.R., Granotier, C., Peyrin, J.M., Lages, C.S., Dormont, D. & Boussin, F.D. 2000, Fibroblast growth factor 2 up regulates telomerase activity in neural precursor cells, *Oncogene*, vol. 19, no. 26, pp. 2957-2966.
- Hainaut, P. & Pfeifer, G.P. 2001, Patterns of p53 G-->T transversions in lung cancers reflect the primary mutagenic signature of DNA-damage by tobacco smoke, *Carcinogenesis*, vol. 22, no. 3, pp. 367-374.
- Haines, G.A., Hendry, J.H., Daniel, C.P. & Morris, I.D. 2002, Germ cell and dose-dependent DNA damage measured by the comet assay in murine spermatozoa after testicular X-irradiation, *Biology of reproduction*, vol. 67, no. 3, pp. 854-861.

- Hajkova, P., Jeffries, S.J., Lee, C., Miller, N., Jackson, S.P. & Surani, M.A. 2010, Genome-wide reprogramming in the mouse germ line entails the base excision repair pathway, *Science (New York, N.Y.)*, vol. 329, no. 5987, pp. 78-82.
- Hall, E.J. 2000, *Radiobiology for the Radiologist*, 5th edn, Lippincott Williams and Wilkins, USA.
- Ham, M.F., Takakuwa, T., Luo, W.J., Liu, A., Horii, A. & Aozasa, K. 2006, Impairment of double-strand breaks repair and aberrant splicing of ATM and MRE11 in leukemia-lymphoma cell lines with microsatellite instability, *Cancer science*, vol. 97, no. 3, pp. 226-234.
- Han, J.S. & Boeke, J.D. 2005, LINE-1 retrotransposons: modulators of quantity and quality of mammalian gene expression?, *BioEssays : news and reviews in molecular, cellular and developmental biology*, vol. 27, no. 8, pp. 775-784.
- Hande, M.P., Samper, E., Lansdorp, P. & Blasco, M.A. 1999, Telomere length dynamics and chromosomal instability in cells derived from telomerase null mice, *The Journal of cell biology*, vol. 144, no. 4, pp. 589-601.
- Hannigan, A., Smith, P., Kalna, G., Lo Nigro, C., Orange, C., O'Brien, D.I., Shah, R., Syed, N., Spender, L.C., Herrera, B., Thurlow, J.K., Lattanzio, L., Monteverde, M., Maurer, M.E., Buffa, F.M., Mann, J., Chu, D.C., West, C.M., Patridge, M., Oien, K.A., Cooper, J.A., Frame, M.C., Harris, A.L., Hiller, L., Nicholson, L.J., Gasco, M., Crook, T. & Inman, G.J. 2010, Epigenetic downregulation of human disabled homolog 2 switches TGF-beta from a tumour suppressor to a tumour promoter, *The Journal of clinical investigation*, vol. 120, no. 8, pp. 2842-2857.
- Hansen, R.S., Wijmenga, C., Luo, P., Stanek, A.M., Canfield, T.K., Weemaes, C.M. & Gartler, S.M. 1999, The DNMT3B DNA methyltransferase gene is mutated in the ICF immunodeficiency syndrome, *Proceedings of the National Academy of Sciences of the United States of America*, vol. 96, no. 25, pp. 14412-14417.
- Harley, C.B. 1991, Telomere loss: mitotic clock or genetic time bomb?, *Mutation research*, vol. 256, no. 2-6, pp. 271-282.
- Harley, C.B., Futcher, A.B. & Greider, C.W. 1990, Telomeres shorten during ageing of human fibroblasts, *Nature*, vol. 345, no. 6274, pp. 458-460.
- Harper, K., Lorimore, S.A. & Wright, E.G. 1997, Delayed appearance of radiation-induced mutations at the Hprt locus in murine hemopoietic cells, *Experimental hematology*, vol. 25, no. 3, pp. 263-269.
- Harrison, N.J., Baker, D. & Andrews, P.W. 2007, Culture adaptation of embryonic stem cells echoes germ cell malignancy, *International journal of andrology*, vol. 30, no. 4, pp. 275-81; discussion 281.
- Hartlerode, A.J. & Scully, R. 2009, Mechanisms of double-strand break repair in somatic mammalian cells, *The Biochemical journal*, vol. 423, no. 2, pp. 157-168.
- Hata, K. & Sakaki, Y. 1997, Identification of critical CpG sites for repression of L1 transcription by DNA methylation, *Gene*, vol. 189, no. 2, pp. 227-234.
- Hayata, I., Seki, M., Yoshida, K., Hirashima, K., Sado, T., Yamagiwa, J. & Ishihara, T. 1983, Chromosomal aberrations observed in 52 mouse myeloid leukemias, *Cancer research*, vol. 43, no. 1, pp. 367-373.
- Hayflick, L. 1997, Mortality and immortality at the cellular level. A review, *Biochemistry.Biokhimiia*, vol. 62, no. 11, pp. 1180-1190.

- HAYFLICK, L. 1965, The Limited *in vitro* Lifetime of Human Diploid Cell Strains, *Experimental cell research*, vol. 37, pp. 614-636.
- Hendrich, B., Hardeland, U., Ng, H.H., Jiricny, J. & Bird, A. 1999, The thymine glycosylase MBD4 can bind to the product of deamination at methylated CpG sites, *Nature*, vol. 401, no. 6750, pp. 301-304.
- Henson, J.D., Neumann, A.A., Yeager, T.R. & Reddel, R.R. 2002, Alternative lengthening of telomeres in mammalian cells, *Oncogene*, vol. 21, no. 4, pp. 598-610.
- Hickson, I.D., Davies, S.L., Li, J.L., Levitt, N.C., Mohaghegh, P., North, P.S. & Wu, L. 2001, Role of the Bloom's syndrome helicase in maintenance of genome stability, *Biochemical Society transactions*, vol. 29, no. Pt 2, pp. 201-204.
- Hiyama, E. & Hiyama, K. 2007, Telomere and telomerase in stem cells, *British journal of cancer*, vol. 96, no. 7, pp. 1020-1024.
- Hockel, M. & Vaupel, P. 2001, Tumour hypoxia: definitions and current clinical, biologic, and molecular aspects, *Journal of the National Cancer Institute*, vol. 93, no. 4, pp. 266-276.
- Hockemeyer, D., Sfeir, A.J., Shay, J.W., Wright, W.E. & de Lange, T. 2005, POT1 protects telomeres from a transient DNA damage response and determines how human chromosomes end, *The EMBO journal*, vol. 24, no. 14, pp. 2667-2678.
- Hollstein, M., Shomer, B., Greenblatt, M., Soussi, T., Hovig, E., Montesano, R. & Harris, C.C. 1996, Somatic point mutations in the p53 gene of human tumours and cell lines: updated compilation, *Nucleic acids research*, vol. 24, no. 1, pp. 141-146.
- Holmberg, K., Falt, S., Johansson, A. & Lambert, B. 1993, Clonal chromosome aberrations and genomic instability in X-irradiated human T-lymphocyte cultures, *Mutation research*, vol. 286, no. 2, pp. 321-330.
- Holmes, S.E., Dombroski, B.A., Krebs, C.M., Boehm, C.D. & Kazazian, H.H., Jr 1994, A new retrotransposable human L1 element from the LRE2 locus on chromosome 1q produces a chimaeric insertion, *Nature genetics*, vol. 7, no. 2, pp. 143-148.
- Hong, Y., Cervantes, R.B., Tichy, E., Tischfield, J.A. & Stambrook, P.J. 2007, Protecting genomic integrity in somatic cells and embryonic stem cells, *Mutation research*, vol. 614, no. 1-2, pp. 48-55.
- Hong, Y. & Stambrook, P.J. 2004, Restoration of an absent G1 arrest and protection from apoptosis in embryonic stem cells after ionizing radiation, *Proceedings of the National Academy of Sciences of the United States of America*, vol. 101, no. 40, pp. 14443-14448.
- Honma, M., Sakuraba, M., Koizumi, T., Takashima, Y., Sakamoto, H. & Hayashi, M. 2007, Non-homologous end-joining for repairing I-SceI-induced DNA double strand breaks in human cells, *DNA repair*, vol. 6, no. 6, pp. 781-788.
- Howard, G., Eiges, R., Gaudet, F., Jaenisch, R. & Eden, A. 2008, Activation and transposition of endogenous retroviral elements in hypomethylation induced tumours in mice, *Oncogene*, vol. 27, no. 3, pp. 404-408.
- Howlett, N.G., Taniguchi, T., Durkin, S.G., D'Andrea, A.D. & Glover, T.W. 2005, The Fanconi anemia pathway is required for the DNA replication stress response and for the regulation of common fragile site stability, *Human molecular genetics*, vol. 14, no. 5, pp. 693-701.

- Howlett, S.K. & Reik, W. 1991, Methylation levels of maternal and paternal genomes during preimplantation development, *Development (Cambridge, England)*, vol. 113, no. 1, pp. 119-127.
- Hsiang, Y.H., Hertzberg, R., Hecht, S. & Liu, L.F. 1985, Camptothecin induces protein-linked DNA breaks via mammalian DNA topoisomerase I, *The Journal of biological chemistry*, vol. 260, no. 27, pp. 14873-14878.
- Hsiang, Y.H., Lihou, M.G. & Liu, L.F. 1989, Arrest of replication forks by drug-stabilized topoisomerase I-DNA cleavable complexes as a mechanism of cell killing by camptothecin, *Cancer research*, vol. 49, no. 18, pp. 5077-5082.
- Hsieh, P. & Yamane, K. 2008, DNA mismatch repair: molecular mechanism, cancer, and ageing, *Mechanisms of ageing and development*, vol. 129, no. 7-8, pp. 391-407.
- Hsu, G.W., Huang, X., Luneva, N.P., Geacintov, N.E. & Beese, L.S. 2005, Structure of a high fidelity DNA polymerase bound to a benzo[a]pyrene adduct that blocks replication, *The Journal of biological chemistry*, vol. 280, no. 5, pp. 3764-3770.
- Huang, L., Grim, S., Smith, L.E., Kim, P.M., Nickoloff, J.A., Goloubeva, O.G. & Morgan, W.F. 2004, Ionizing radiation induces delayed hyperrecombination in Mammalian cells, *Molecular and cellular biology*, vol. 24, no. 11, pp. 5060-5068.
- Igarashi, J., Muroi, S., Kawashima, H., Wang, X., Shinjima, Y., Kitamura, E., Oinuma, T., Nemoto, N., Song, F., Ghosh, S., Held, W.A. & Nagase, H. 2008, Quantitative analysis of human tissue-specific differences in methylation, *Biochemical and biophysical research communications*, vol. 376, no. 4, pp. 658-664.
- Ilnytsky, Y., Zemp, F.J., Koturbash, I. & Kovalchuk, O. 2008, Altered microRNA expression patterns in irradiated hematopoietic tissues suggest a sex-specific protective mechanism, *Biochemical and biophysical research communications*, vol. 377, no. 1, pp. 41-45.
- Iskow, R.C., McCabe, M.T., Mills, R.E., Torene, S., Pittard, W.S., Neuwald, A.F., Van Meir, E.G., Vertino, P.M. & Devine, S.E. 2010, Natural mutagenesis of human genomes by endogenous retrotransposons, *Cell*, vol. 141, no. 7, pp. 1253-1261.
- Ito, S., D'Alessio, A.C., Taranova, O.V., Hong, K., Sowers, L.C. & Zhang, Y. 2010, Role of Tet proteins in 5mC to 5hmC conversion, ES-cell self-renewal and inner cell mass specification, *Nature*, vol. 466, no. 7310, pp. 1129-1133.
- Iwabuchi, K., Basu, B.P., Kysela, B., Kurihara, T., Shibata, M., Guan, D., Cao, Y., Hamada, T., Imamura, K., Jeggo, P.A., Date, T. & Doherty, A.J. 2003, Potential role for 53BP1 in DNA end-joining repair through direct interaction with DNA, *The Journal of biological chemistry*, vol. 278, no. 38, pp. 36487-36495.
- Jackson, M., Krassowska, A., Gilbert, N., Chevassut, T., Forrester, L., Ansell, J. & Ramsahoye, B. 2004, Severe global DNA hypomethylation blocks differentiation and induces histone hyperacetylation in embryonic stem cells, *Molecular and cellular biology*, vol. 24, no. 20, pp. 8862-8871.
- Jackson-Grusby, L., Beard, C., Possemato, R., Tudor, M., Fambrough, D., Csankovszki, G., Dausman, J., Lee, P., Wilson, C., Lander, E. & Jaenisch, R. 2001, Loss of genomic methylation causes p53-dependent apoptosis and epigenetic deregulation, *Nature genetics*, vol. 27, no. 1, pp. 31-39.
- Jair, K.W., Bachman, K.E., Suzuki, H., Ting, A.H., Rhee, I., Yen, R.W., Baylin, S.B. & Schuebel, K.E. 2006, De novo CpG island methylation in human cancer cells, *Cancer research*, vol. 66, no. 2, pp. 682-692.

- Jeanpierre, M., Turleau, C., Aurias, A., Prieur, M., Ledest, F., Fischer, A. & Viegas-Pequignot, E. 1993, An embryonic-like methylation pattern of classical satellite DNA is observed in ICF syndrome, *Human molecular genetics*, vol. 2, no. 6, pp. 731-735.
- Jeffreys, A.J., Barber, R., Bois, P., Buard, J., Dubrova, Y.E., Grant, G., Hollies, C.R., May, C.A., Neumann, R., Panayi, M., Ritchie, A.E., Shone, A.C., Signer, E., Stead, J.D. & Tamaki, K. 1999, Human minisatellites, repeat DNA instability and meiotic recombination, *Electrophoresis*, vol. 20, no. 8, pp. 1665-1675.
- Jeltsch, A. 2006, Molecular enzymology of mammalian DNA methyltransferases, *Current topics in microbiology and immunology*, vol. 301, pp. 203-225.
- Jeyapalan, J.N., Mendez-Bermudez, A., Zaffaroni, N., Dubrova, Y.E. & Royle, N.J. 2008, Evidence for alternative lengthening of telomeres in liposarcomas in the absence of ALT-associated PML bodies, *International journal of cancer. Journal international du cancer*, vol. 122, no. 11, pp. 2414-2421.
- Jiang, Y.L., Rigolet, M., Bourc'his, D., Nigon, F., Bokesoy, I., Fryns, J.P., Hulten, M., Jonveaux, P., Maraschio, P., Megarbane, A., Moncla, A. & Viegas-Pequignot, E. 2005, DNMT3B mutations and DNA methylation defect define two types of ICF syndrome, *Human mutation*, vol. 25, no. 1, pp. 56-63.
- Jiricny, J. & Nystrom-Lahti, M. 2000, Mismatch repair defects in cancer, *Current opinion in genetics & development*, vol. 10, no. 2, pp. 157-161.
- Johansson, C., Moller, P., Forchhammer, L., Loft, S., Godschalk, R.W., Langie, S.A., Lumeij, S., Jones, G.D., Kwok, R.W., Azqueta, A., Phillips, D.H., Sozeri, O., Routledge, M.N., Charlton, A.J., Riso, P., Porrini, M., Allione, A., Matullo, G., Palus, J., Stepnik, M., Collins, A.R. & Moller, L. 2010, An ECVAG trial on assessment of oxidative damage to DNA measured by the comet assay, *Mutagenesis*, vol. 25, no. 2, pp. 125-132.
- Joiner, M. & van der Kogel, A. 2009, *Basic Clinical Radiobiology*, 4th edn, Hodder Arnold, Great Britain.
- Joiner, M.C., Van Der Kogel, A.J. & Steel, G.G. 2009, Introduction: the significance of radiobiology and radiotherapy for cancer treatment in *Basic Clinical Radiobiology*, eds. M. Joiner & A. van der Kogel, 4th edn, Edward Arnold, UK, pp. 1.
- Jones, P.A. 1996, DNA methylation errors and cancer, *Cancer research*, vol. 56, no. 11, pp. 2463-2467.
- Jurgens, B., Schmitz-Drager, B.J. & Schulz, W.A. 1996, Hypomethylation of L1 LINE sequences prevailing in human urothelial carcinoma, *Cancer research*, vol. 56, no. 24, pp. 5698-5703.
- Kadhim, M.A., Lorimore, S.A., Hepburn, M.D., Goodhead, D.T., Buckle, V.J. & Wright, E.G. 1994, Alpha-particle-induced chromosomal instability in human bone marrow cells, *Lancet*, vol. 344, no. 8928, pp. 987-988.
- Kadhim, M.A., Lorimore, S.A., Townsend, K.M., Goodhead, D.T., Buckle, V.J. & Wright, E.G. 1995, Radiation-induced genomic instability: delayed cytogenetic aberrations and apoptosis in primary human bone marrow cells, *International journal of radiation biology*, vol. 67, no. 3, pp. 287-293.
- Kadhim, M.A., Macdonald, D.A., Goodhead, D.T., Lorimore, S.A., Marsden, S.J. & Wright, E.G. 1992, Transmission of chromosomal instability after plutonium alpha-particle irradiation, *Nature*, vol. 355, no. 6362, pp. 738-740.

- Kadhim, M.A. & Wright, E.G. 1998, Radiation-induced transmissible chromosomal instability in haemopoietic stem cells, *Advances in space research : the official journal of the Committee on Space Research (COSPAR)*, vol. 22, no. 4, pp. 587-596.
- Kalinich, J.F., Catravas, G.N. & Snyder, S.L. 1989, The effect of gamma radiation on DNA methylation, *Radiation research*, vol. 117, no. 2, pp. 185-197.
- Kalitsis, P., Griffiths, B. & Choo, K.H. 2006, Mouse telocentric sequences reveal a high rate of homogenization and possible role in Robertsonian translocation, *Proceedings of the National Academy of Sciences of the United States of America*, vol. 103, no. 23, pp. 8786-8791.
- Kano, H., Godoy, I., Courtney, C., Vetter, M.R., Gerton, G.L., Ostertag, E.M. & Kazazian, H.H., Jr 2009, L1 retrotransposition occurs mainly in embryogenesis and creates somatic mosaicism, *Genes & development*, vol. 23, no. 11, pp. 1303-1312.
- Kano, Y. & Little, J.B. 1984, Persistence of X-ray-induced chromosomal rearrangements in long-term cultures of human diploid fibroblasts, *Cancer research*, vol. 44, no. 9, pp. 3706-3711.
- Kathe, S.D., Shen, G.P. & Wallace, S.S. 2004, Single-stranded breaks in DNA but not oxidative DNA base damages block transcriptional elongation by RNA polymerase II in HeLa cell nuclear extracts, *The Journal of biological chemistry*, vol. 279, no. 18, pp. 18511-18520.
- Kaufmann, W.K. & Paules, R.S. 1996, DNA damage and cell cycle checkpoints, *The FASEB journal : official publication of the Federation of American Societies for Experimental Biology*, vol. 10, no. 2, pp. 238-247.
- Kaup, S., Grandjean, V., Mukherjee, R., Kapoor, A., Keyes, E., Seymour, C.B., Mothersill, C.E. & Schofield, P.N. 2006, Radiation-induced genomic instability is associated with DNA methylation changes in cultured human keratinocytes, *Mutation research*, vol. 597, no. 1-2, pp. 87-97.
- Kazazian, H.H., Jr & Goodier, J.L. 2002, LINE drive. retrotransposition and genome instability, *Cell*, vol. 110, no. 3, pp. 277-280.
- Kelley, M.R., Kow, Y.W. & Wilson, D.M., 3rd 2003, Disparity between DNA base excision repair in yeast and mammals: translational implications, *Cancer research*, vol. 63, no. 3, pp. 549-554.
- Kendal, W.S. & Frost, P. 1988, Pitfalls and practice of Luria-Delbruck fluctuation analysis: a review, *Cancer research*, vol. 48, no. 5, pp. 1060-1065.
- Khan, S.G., Oh, K.S., Emmert, S., Imoto, K., Tamura, D., Digiovanna, J.J., Shahlavi, T., Armstrong, N., Baker, C.C., Neuburg, M., Zalewski, C., Brewer, C., Wiggs, E., Schiffmann, R. & Kraemer, K.H. 2009, XPC initiation codon mutation in xeroderma pigmentosum patients with and without neurological symptoms, *DNA repair*, vol. 8, no. 1, pp. 114-125.
- Kim, G.D., Ni, J., Kelesoglu, N., Roberts, R.J. & Pradhan, S. 2002, Co-operation and communication between the human maintenance and de novo DNA (cytosine-5) methyltransferases, *The EMBO journal*, vol. 21, no. 15, pp. 4183-4195.
- Kim, J.J. & Tannock, I.F. 2005, Repopulation of cancer cells during therapy: an important cause of treatment failure, *Nature reviews.Cancer*, vol. 5, no. 7, pp. 516-525.
- Kim, M., Trinh, B.N., Long, T.I., Oghamian, S. & Laird, P.W. 2004, Dnmt1 deficiency leads to enhanced microsatellite instability in mouse embryonic stem cells, *Nucleic acids research*, vol. 32, no. 19, pp. 5742-5749.

- Kim, Y.I., Giuliano, A., Hatch, K.D., Schneider, A., Nour, M.A., Dallal, G.E., Selhub, J. & Mason, J.B. 1994, Global DNA hypomethylation increases progressively in cervical dysplasia and carcinoma, *Cancer*, vol. 74, no. 3, pp. 893-899.
- Kinner, A., Wu, W., Staudt, C. & Iliakis, G. 2008, Gamma-H2AX in recognition and signalling of DNA double-strand breaks in the context of chromatin, *Nucleic acids research*, vol. 36, no. 17, pp. 5678-5694.
- Kirkegaard, K. & Wang, J.C. 1985, Bacterial DNA topoisomerase I can relax positively supercoiled DNA containing a single-stranded loop, *Journal of Molecular Biology*, vol. 185, no. 3, pp. 625-637.
- Knipscheer, P., Raschle, M., Smogorzewska, A., Enoiu, M., Ho, T.V., Scharer, O.D., Elledge, S.J. & Walter, J.C. 2009, The Fanconi anemia pathway promotes replication-dependent DNA interstrand cross-link repair, *Science (New York, N.Y.)*, vol. 326, no. 5960, pp. 1698-1701.
- Kochanek, S., Renz, D. & Doerfler, W. 1995, Transcriptional silencing of human Alu sequences and inhibition of protein binding in the box B regulatory elements by 5'-CG-3' methylation, *FEBS letters*, vol. 360, no. 2, pp. 115-120.
- Kochanek, S., Renz, D. & Doerfler, W. 1993, DNA methylation in the Alu sequences of diploid and haploid primary human cells, *The EMBO journal*, vol. 12, no. 3, pp. 1141-1151.
- Kolosha, V.O. & Martin, S.L. 1997, *In vitro* properties of the first ORF protein from mouse LINE-1 support its role in ribonucleoprotein particle formation during retrotransposition, *Proceedings of the National Academy of Sciences of the United States of America*, vol. 94, no. 19, pp. 10155-10160.
- Koniaras, K., Cuddihy, A.R., Christopoulos, H., Hogg, A. & O'Connell, M.J. 2001, Inhibition of Chk1-dependent G2 DNA damage checkpoint radiosensitizes p53 mutant human cells, *Oncogene*, vol. 20, no. 51, pp. 7453-7463.
- Koturbash, I., Baker, M., Loree, J., Kutanzi, K., Hudson, D., Pogribny, I., Sedelnikova, O., Bonner, W. & Kovalchuk, O. 2006, Epigenetic dysregulation underlies radiation-induced transgenerational genome instability *in vivo*, *International journal of radiation oncology, biology, physics*, vol. 66, no. 2, pp. 327-330.
- Koturbash, I., Boyko, A., Rodriguez-Juarez, R., McDonald, R.J., Tryndyak, V.P., Kovalchuk, I., Pogribny, I.P. & Kovalchuk, O. 2007, Role of epigenetic effectors in maintenance of the long-term persistent bystander effect in spleen *in vivo*, *Carcinogenesis*, vol. 28, no. 8, pp. 1831-1838.
- Koturbash, I., Pogribny, I. & Kovalchuk, O. 2005, Stable loss of global DNA methylation in the radiation-target tissue--a possible mechanism contributing to radiation carcinogenesis?, *Biochemical and biophysical research communications*, vol. 337, no. 2, pp. 526-533.
- Kovalchuk, O. & Baulch, J.E. 2008, Epigenetic changes and nontargeted radiation effects--is there a link?, *Environmental and molecular mutagenesis*, vol. 49, no. 1, pp. 16-25.
- Kovalchuk, O., Burke, P., Besplug, J., Slovack, M., Filkowski, J. & Pogribny, I. 2004, Methylation changes in muscle and liver tissues of male and female mice exposed to acute and chronic low-dose X-ray-irradiation, *Mutation research*, vol. 548, no. 1-2, pp. 75-84.
- Kreutzer, D.A. & Essigmann, J.M. 1998, Oxidized, deaminated cytosines are a source of C --> T transitions *in vivo*, *Proceedings of the National Academy of Sciences of the United States of America*, vol. 95, no. 7, pp. 3578-3582.

- Krokan, H.E., Drablos, F. & Slupphaug, G. 2002, Uracil in DNA--occurrence, consequences and repair, *Oncogene*, vol. 21, no. 58, pp. 8935-8948.
- Kuff, E.L. & Lueders, K.K. 1988, The intracisternal A-particle gene family: structure and functional aspects, *Advances in Cancer Research*, vol. 51, pp. 183-276.
- Kuzminov, A. 2001, Single-strand interruptions in replicating chromosomes cause double-strand breaks, *Proceedings of the National Academy of Sciences of the United States of America*, vol. 98, no. 15, pp. 8241-8246.
- Laccone, F. & Christian, W. 2000, A recurrent expansion of a maternal allele with 36 CAG repeats causes Huntington disease in two sisters, *American Journal of Human Genetics*, vol. 66, no. 3, pp. 1145-1148.
- Lan, J., Hua, S., He, X. & Zhang, Y. 2010, DNA methyltransferases and methyl-binding proteins of mammals, *Acta biochimica et biophysica Sinica*, vol. 42, no. 4, pp. 243-252.
- Lander, E.S., Linton, L.M., Birren, B., Nusbaum, C., Zody, M.C., Baldwin, J., Devon, K., Dewar, K., Doyle, M., FitzHugh, W., Funke, R., Gage, D., Harris, K., Heaford, A., Howland, J., Kann, L., Lehoczky, J., LeVine, R., McEwan, P., McKernan, K., Meldrim, J., Mesirov, J.P., Miranda, C., Morris, W., Naylor, J., Raymond, C., Rosetti, M., Santos, R., Sheridan, A., Sougnez, C., Stange-Thomann, N., Stojanovic, N., Subramanian, A., Wyman, D., Rogers, J., Sulston, J., Ainscough, R., Beck, S., Bentley, D., Burton, J., Clee, C., Carter, N., Coulson, A., Deadman, R., Deloukas, P., Dunham, A., Dunham, I., Durbin, R., French, L., Grafham, D., Gregory, S., Hubbard, T., Humphray, S., Hunt, A., Jones, M., Lloyd, C., McMurray, A., Matthews, L., Mercer, S., Milne, S., Mullikin, J.C., Mungall, A., Plumb, R., Ross, M., Shownkeen, R., Sims, S., Waterston, R.H., Wilson, R.K., Hillier, L.W., McPherson, J.D., Marra, M.A., Mardis, E.R., Fulton, L.A., Chinwalla, A.T., Pepin, K.H., Gish, W.R., Chissoe, S.L., Wendl, M.C., Delehaunty, K.D., Miner, T.L., Delehaunty, A., Kramer, J.B., Cook, L.L., Fulton, R.S., Johnson, D.L., Minx, P.J., Clifton, S.W., Hawkins, T., Branscomb, E., Predki, P., Richardson, P., Wenning, S., Slezak, T., Doggett, N., Cheng, J.F., Olsen, A., Lucas, S., Elkin, C., Uberbacher, E., Frazier, M., Gibbs, R.A., Muzny, D.M., Scherer, S.E., Bouck, J.B., Sodergren, E.J., Worley, K.C., Rives, C.M., Gorrell, J.H., Metzker, M.L., Naylor, S.L., Kucherlapati, R.S., Nelson, D.L., Weinstock, G.M., Sakaki, Y., Fujiyama, A., Hattori, M., Yada, T., Toyoda, A., Itoh, T., Kawagoe, C., Watanabe, H., Totoki, Y., Taylor, T., Weissenbach, J., Heilig, R., Saurin, W., Artiguenave, F., Brottier, P., Bruls, T., Pelletier, E., Robert, C., Wincker, P., Smith, D.R., Doucette-Stamm, L., Rubenfield, M., Weinstock, K., Lee, H.M., Dubois, J., Rosenthal, A., Platzer, M., Nyakatura, G., Taudien, S., Rump, A., Yang, H., Yu, J., Wang, J., Huang, G., Gu, J., Hood, L., Rowen, L., Madan, A., Qin, S., Davis, R.W., Federspiel, N.A., Abola, A.P., Proctor, M.J., Myers, R.M., Schmutz, J., Dickson, M., Grimwood, J., Cox, D.R., Olson, M.V., Kaul, R., Raymond, C., Shimizu, N., Kawasaki, K., Minoshima, S., Evans, G.A., Athanasiou, M., Schultz, R., Roe, B.A., Chen, F., Pan, H., Ramser, J., Lehrach, H., Reinhardt, R., McCombie, W.R., de la Bastide, M., Dedhia, N., Blocker, H., Hornischer, K., Nordsiek, G., Agarwala, R., Aravind, L., Bailey, J.A., Bateman, A., Batzoglou, S., Birney, E., Bork, P., Brown, D.G., Burge, C.B., Cerutti, L., Chen, H.C., Church, D., Clamp, M., Copley, R.R., Doerks, T., Eddy, S.R., Eichler, E.E., Furey, T.S., Galagan, J., Gilbert, J.G., Harmon, C., Hayashizaki, Y., Haussler, D., Hermjakob, H., Hokamp, K., Jang, W., Johnson, L.S., Jones, T.A., Kasif, S., Kasprzyk, A., Kennedy, S., Kent, W.J., Kitts, P., Koonin, E.V., Korf, I., Kulp, D., Lancet, D., Lowe, T.M., McLysaght, A., Mikkelsen, T., Moran, J.V., Mulder, N., Pollara, V.J., Ponting, C.P., Schuler, G., Schultz, J., Slater, G., Smit, A.F., Stupka, E., Szustakowski, J., Thierry-Mieg, D., Thierry-Mieg, J., Wagner, L., Wallis, J., Wheeler, R., Williams, A., Wolf, Y.I., Wolfe, K.H., Yang, S.P., Yeh, R.F., Collins, F., Guyer, M.S., Peterson, J., Felsenfeld, A., Wetterstrand, K.A., Patrinos, A., Morgan, M.J., de Jong, P., Catanese, J.J., Osoegawa, K., Shizuya, H., Choi, S., Chen, Y.J. & International Human Genome Sequencing Consortium 2001, Initial sequencing and analysis of the human genome, *Nature*, vol. 409, no. 6822, pp. 860-921.
- Lane, N., Dean, W., Erhardt, S., Hajkova, P., Surani, A., Walter, J. & Reik, W. 2003, Resistance of IAPs to methylation reprogramming may provide a mechanism for epigenetic inheritance in the mouse, *Genesis (New York, N.Y.: 2000)*, vol. 35, no. 2, pp. 88-93.

- Lassmann, M., Hanscheid, H., Gassen, D., Biko, J., Meineke, V., Reiners, C. & Scherthan, H. 2010, *In vivo* formation of gamma-H2AX and 53BP1 DNA repair foci in blood cells after radioiodine therapy of differentiated thyroid cancer, *Journal of nuclear medicine : official publication, Society of Nuclear Medicine*, vol. 51, no. 8, pp. 1318-1325.
- Lee, D.H., O'Connor, T.R. & Pfeifer, G.P. 2002, Oxidative DNA damage induced by copper and hydrogen peroxide promotes CG-->TT tandem mutations at methylated CpG dinucleotides in nucleotide excision repair-deficient cells, *Nucleic acids research*, vol. 30, no. 16, pp. 3566-3573.
- Lee, J.S., Haruna, T., Ishimoto, A., Honjo, T. & Yanagawa, S. 1999, Intracisternal type A particle-mediated activation of the Notch4/int3 gene in a mouse mammary tumour: generation of truncated Notch4/int3 mRNAs by retroviral splicing events, *Journal of virology*, vol. 73, no. 6, pp. 5166-5171.
- Lee, J.T. & Jaenisch, R. 1997, The (epi)genetic control of mammalian X-chromosome inactivation, *Current opinion in genetics & development*, vol. 7, no. 2, pp. 274-280.
- Lei, H., Oh, S.P., Okano, M., Juttermann, R., Goss, K.A., Jaenisch, R. & Li, E. 1996, De novo DNA cytosine methyltransferase activities in mouse embryonic stem cells, *Development (Cambridge, England)*, vol. 122, no. 10, pp. 3195-3205.
- Lei, M., Zaug, A.J., Podell, E.R. & Cech, T.R. 2005, Switching human telomerase on and off with hPOT1 protein *in vitro*, *The Journal of biological chemistry*, vol. 280, no. 21, pp. 20449-20456.
- Lengauer, C., Kinzler, K.W. & Vogelstein, B. 1998, Genetic instabilities in human cancers, *Nature*, vol. 396, no. 6712, pp. 643-649.
- Leteurtre, F., Kohlhagen, G., Fesen, M.R., Tanizawa, A., Kohn, K.W. & Pommier, Y. 1994, Effects of DNA methylation on topoisomerase I and II cleavage activities, *The Journal of biological chemistry*, vol. 269, no. 11, pp. 7893-7900.
- Lethe, B., Lucas, S., Michaux, L., De Smet, C., Godelaine, D., Serrano, A., De Plaen, E. & Boon, T. 1998, LAGE-1, a new gene with tumour specificity, *International journal of cancer. Journal international du cancer*, vol. 76, no. 6, pp. 903-908.
- Li, C.Y., Yandell, D.W. & Little, J.B. 1992, Evidence for coincident mutations in human lymphoblast clones selected for functional loss of a thymidine kinase gene, *Molecular carcinogenesis*, vol. 5, no. 4, pp. 270-277.
- Li, E., Bestor, T.H. & Jaenisch, R. 1992, Targeted mutation of the DNA methyltransferase gene results in embryonic lethality, *Cell*, vol. 69, no. 6, pp. 915-926.
- Li, E. & Bird, A. 2007, DNA methylatin in mammals in *Epigenetics*, eds. C.D. Allis, T. Jenuwein & D. Reinberg, Cold Spring Harbor Press, USA, pp. 341-355.
- Li, J.Y., Pu, M.T., Hirasawa, R., Li, B.Z., Huang, Y.N., Zeng, R., Jing, N.H., Chen, T., Li, E., Sasaki, H. & Xu, G.L. 2007, Synergistic function of DNA methyltransferases Dnmt3a and Dnmt3b in the methylation of Oct4 and Nanog, *Molecular and cellular biology*, vol. 27, no. 24, pp. 8748-8759.
- Limoli, C.L., Giedzinski, E., Morgan, W.F., Swarts, S.G., Jones, G.D. & Hyun, W. 2003, Persistent oxidative stress in chromosomally unstable cells, *Cancer research*, vol. 63, no. 12, pp. 3107-3111.

- Limoli, C.L., Kaplan, M.I., Corcoran, J., Meyers, M., Boothman, D.A. & Morgan, W.F. 1997, Chromosomal instability and its relationship to other end points of genomic instability, *Cancer research*, vol. 57, no. 24, pp. 5557-5563.
- Limoli, C.L., Kaplan, M.I., Giedzinski, E. & Morgan, W.F. 2001, Attenuation of radiation-induced genomic instability by free radical scavengers and cellular proliferation, *Free radical biology & medicine*, vol. 31, no. 1, pp. 10-19.
- Lin, C.H., Hsieh, S.Y., Sheen, I.S., Lee, W.C., Chen, T.C., Shyu, W.C. & Liaw, Y.F. 2001, Genome-wide hypomethylation in hepatocellular carcinogenesis, *Cancer research*, vol. 61, no. 10, pp. 4238-4243.
- Lin, Y., Leng, M., Wan, M. & Wilson, J.H. 2010, Convergent transcription through a long CAG tract destabilizes repeats and induces apoptosis, *Molecular and cellular biology*, vol. 30, no. 18, pp. 4435-4451.
- Lin, Y. & Wilson, J.H. 2009, Diverse effects of individual mismatch repair components on transcription-induced CAG repeat instability in human cells, *DNA repair*, vol. 8, no. 8, pp. 878-885.
- Lin, Y. & Wilson, J.H. 2007, Transcription-induced CAG repeat contraction in human cells is mediated in part by transcription-coupled nucleotide excision repair, *Molecular and cellular biology*, vol. 27, no. 17, pp. 6209-6217.
- Little, J.B., Nagasawa, H., Pfenning, T. & Vetrovs, H. 1997, Radiation-induced genomic instability: delayed mutagenic and cytogenetic effects of X rays and alpha particles, *Radiation research*, vol. 148, no. 4, pp. 299-307.
- Liu, X., Wu, H., Loring, J., Hormuzdi, S., Disteché, C.M., Bornstein, P. & Jaenisch, R. 1997, Trisomy eight in ESCs is a common potential problem in gene targeting and interferes with germ line transmission, *Developmental dynamics : an official publication of the American Association of Anatomists*, vol. 209, no. 1, pp. 85-91.
- Lo, A.W., Sabatier, L., Fouladi, B., Pottier, G., Ricoul, M. & Murnane, J.P. 2002, DNA amplification by breakage/fusion/bridge cycles initiated by spontaneous telomere loss in a human cancer cell line, *Neoplasia (New York, N.Y.)*, vol. 4, no. 6, pp. 531-538.
- Loeb, L.A. 1991, Mutator phenotype may be required for multistage carcinogenesis, *Cancer research*, vol. 51, no. 12, pp. 3075-3079.
- Longo, L., Bygrave, A., Grosveld, F.G. & Pandolfi, P.P. 1997, The chromosome make-up of mouse embryonic stem cells is predictive of somatic and germ cell chimaerism, *Transgenic research*, vol. 6, no. 5, pp. 321-328.
- Loree, J., Koturbash, I., Kutanzi, K., Baker, M., Pogribny, I. & Kovalchuk, O. 2006, Radiation-induced molecular changes in rat mammary tissue: possible implications for radiation-induced carcinogenesis, *International journal of radiation biology*, vol. 82, no. 11, pp. 805-815.
- Lorimore, S.A., Coates, P.J. & Wright, E.G. 2003, Radiation-induced genomic instability and bystander effects: inter-related nontargeted effects of exposure to ionizing radiation, *Oncogene*, vol. 22, no. 45, pp. 7058-7069.
- Lorimore, S.A., Pragnell, I.B., Eckmann, L. & Wright, E.G. 1990, Synergistic interactions allow colony formation *in vitro* by murine haemopoietic stem cells, *Leukemia research*, vol. 14, no. 5, pp. 481-489.

- Lorincz, M.C., Dickerson, D.R., Schmitt, M. & Groudine, M. 2004, Intragenic DNA methylation alters chromatin structure and elongation efficiency in mammalian cells, *Nature structural & molecular biology*, vol. 11, no. 11, pp. 1068-1075.
- Lundblad, V. & Blackburn, E.H. 1993, An alternative pathway for yeast telomere maintenance rescues est1-senescence, *Cell*, vol. 73, no. 2, pp. 347-360.
- Lutsenko, E. & Bhagwat, A.S. 1999, Principal causes of hot spots for cytosine to thymine mutations at sites of cytosine methylation in growing cells. A model, its experimental support and implications, *Mutation research*, vol. 437, no. 1, pp. 11-20.
- MacDonald, D., Boulton, E., Pocock, D., Goodhead, D., Kadhim, M. & Plumb, M. 2001, Evidence of genetic instability in 3 Gy X-ray-induced mouse leukaemias and 3 Gy X-irradiated haemopoietic stem cells, *International journal of radiation biology*, vol. 77, no. 10, pp. 1023-1031.
- Maloisel, L. & Rossignol, J.L. 1998, Suppression of crossing-over by DNA methylation in *Ascombolus*, *Genes & development*, vol. 12, no. 9, pp. 1381-1389.
- Maluf, S.W. & Erdtmann, B. 2001, Genomic instability in Down syndrome and Fanconi anemia assessed by micronucleus analysis and single-cell gel electrophoresis, *Cancer genetics and cytogenetics*, vol. 124, no. 1, pp. 71-75.
- Mantel, C., Guo, Y., Lee, M.R., Kim, M.K., Han, M.K., Shibayama, H., Fukuda, S., Yoder, M.C., Pelus, L.M., Kim, K.S. & Broxmeyer, H.E. 2007, Checkpoint-apoptosis uncoupling in human and mouse embryonic stem cells: a source of karyotypic instability, *Blood*, vol. 109, no. 10, pp. 4518-4527.
- Maraschio, P., Tupler, R., Dainotti, E., Piantanida, M., Cazzola, G. & Tiepolo, L. 1989, Differential expression of the ICF (immunodeficiency, centromeric heterochromatin, facial anomalies) mutation in lymphocytes and fibroblasts, *Journal of medical genetics*, vol. 26, no. 7, pp. 452-456.
- Maraschio, P., Zuffardi, O., Dalla Fior, T. & Tiepolo, L. 1988, Immunodeficiency, centromeric heterochromatin instability of chromosomes 1, 9, and 16, and facial anomalies: the ICF syndrome, *Journal of medical genetics*, vol. 25, no. 3, pp. 173-180.
- Marder, B.A. & Morgan, W.F. 1993, Delayed chromosomal instability induced by DNA damage, *Molecular and cellular biology*, vol. 13, no. 11, pp. 6667-6677.
- Mayer, W., Niveleau, A., Walter, J., Fundele, R. & Haaf, T. 2000, Demethylation of the zygotic paternal genome, *Nature*, vol. 403, no. 6769, pp. 501-502.
- Maynard, S., Swistowska, A.M., Lee, J.W., Liu, Y., Liu, S.T., Da Cruz, A.B., Rao, M., de Souza-Pinto, N.C., Zeng, X. & Bohr, V.A. 2008, Human embryonic stem cells have enhanced repair of multiple forms of DNA damage, *Stem cells (Dayton, Ohio)*, vol. 26, no. 9, pp. 2266-2274.
- McCabe, K.M., Olson, S.B. & Moses, R.E. 2009, DNA interstrand crosslink repair in mammalian cells, *Journal of cellular physiology*, vol. 220, no. 3, pp. 569-573.
- Meehan, T. & Straub, K. 1979, Double-stranded DNA stereoselectively binds benzo(a)pyrene diol epoxides, *Nature*, vol. 277, no. 5695, pp. 410-412.
- Meek, D.W. 2004, The p53 response to DNA damage, *DNA repair*, vol. 3, no. 8-9, pp. 1049-1056.

- Meissner, A., Mikkelsen, T.S., Gu, H., Wernig, M., Hanna, J., Sivachenko, A., Zhang, X., Bernstein, B.E., Nusbaum, C., Jaffe, D.B., Gnirke, A., Jaenisch, R. & Lander, E.S. 2008, Genome-scale DNA methylation maps of pluripotent and differentiated cells, *Nature*, vol. 454, no. 7205, pp. 766-770.
- Menendez, L., Benigno, B.B. & McDonald, J.F. 2004, L1 and HERV-W retrotransposons are hypomethylated in human ovarian carcinomas, *Molecular cancer*, vol. 3, pp. 12.
- Meng, Q., Walker, D.M., Scott, B.R., Seilkop, S.K., Aden, J.K. & Walker, V.E. 2004, Characterization of Hprt mutations in cDNA and genomic DNA of T-cell mutants from control and 1,3-butadiene-exposed male B6C3F1 mice and F344 rats, *Environmental and molecular mutagenesis*, vol. 43, no. 2, pp. 75-92.
- Merlo, A., Mabry, M., Gabrielson, E., Vollmer, R., Baylin, S.B. & Sidransky, D. 1994, Frequent microsatellite instability in primary small cell lung cancer, *Cancer research*, vol. 54, no. 8, pp. 2098-2101.
- Metcalf, D. 1990, The induction and inhibition of differentiation in normal and leukaemic cells, *Philosophical transactions of the Royal Society of London. Series B, Biological sciences*, vol. 327, no. 1239, pp. 99-109.
- Miki, Y., Nishisho, I., Horii, A., Miyoshi, Y., Utsunomiya, J., Kinzler, K.W., Vogelstein, B. & Nakamura, Y. 1992, Disruption of the APC gene by a retrotransposal insertion of L1 sequence in a colon cancer, *Cancer research*, vol. 52, no. 3, pp. 643-645.
- Milligan, J.R., Tran, N.Q., Ly, A. & Ward, J.F. 2004, Peptide repair of oxidative DNA damage, *Biochemistry*, vol. 43, no. 17, pp. 5102-5108.
- Miniou, P., Bourc'his, D., Molina Gomes, D., Jeanpierre, M. & Viegas-Pequignot, E. 1997, Undermethylation of Alu sequences in ICF syndrome: molecular and in situ analysis, *Cytogenetics and cell genetics*, vol. 77, no. 3-4, pp. 308-313.
- Miniou, P., Jeanpierre, M., Blanquet, V., Sibella, V., Bonneau, D., Herbelin, C., Fischer, A., Niveleau, A. & Viegas-Pequignot, E. 1994, Abnormal methylation pattern in constitutive and facultative (X inactive chromosome) heterochromatin of ICF patients, *Human molecular genetics*, vol. 3, no. 12, pp. 2093-2102.
- Miniou, P., Jeanpierre, M., Bourc'his, D., Coutinho Barbosa, A.C., Blanquet, V. & Viegas-Pequignot, E. 1997, alpha-satellite DNA methylation in normal individuals and in ICF patients: heterogeneous methylation of constitutive heterochromatin in adult and fetal tissues, *Human genetics*, vol. 99, no. 6, pp. 738-745.
- Mitalipova, M.M., Rao, R.R., Hoyer, D.M., Johnson, J.A., Meisner, L.F., Jones, K.L., Dalton, S. & Stice, S.L. 2005, Preserving the genetic integrity of human embryonic stem cells, *Nature biotechnology*, vol. 23, no. 1, pp. 19-20.
- Mizuno, S., Chijiwa, T., Okamura, T., Akashi, K., Fukumaki, Y., Niho, Y. & Sasaki, H. 2001, Expression of DNA methyltransferases DNMT1, 3A, and 3B in normal hematopoiesis and in acute and chronic myelogenous leukemia, *Blood*, vol. 97, no. 5, pp. 1172-1179.
- Mognato, M., Ferraro, P., Canova, S., Sordi, G., Russo, A., Cherubini, R. & Celotti, L. 2001, Analysis of mutational effects at the HPRT locus in human G(0) phase lymphocytes irradiated *in vitro* with gamma rays, *Mutation research*, vol. 474, no. 1-2, pp. 147-158.
- Monk, M., Boubelik, M. & Lehnert, S. 1987, Temporal and regional changes in DNA methylation in the embryonic, extraembryonic and germ cell lineages during mouse embryo development, *Development (Cambridge, England)*, vol. 99, no. 3, pp. 371-382.

- Morgan, H.D., Dean, W., Coker, H.A., Reik, W. & Petersen-Mahrt, S.K. 2004, Activation-induced cytidine deaminase deaminates 5-methylcytosine in DNA and is expressed in pluripotent tissues: implications for epigenetic reprogramming, *The Journal of biological chemistry*, vol. 279, no. 50, pp. 52353-52360.
- Morgan, W.F. 2003, Is there a common mechanism underlying genomic instability, bystander effects and other nontargeted effects of exposure to ionizing radiation?, *Oncogene*, vol. 22, no. 45, pp. 7094-7099.
- Morris, T. & Thacker, J. 1993, Formation of large deletions by illegitimate recombination in the HPRT gene of primary human fibroblasts, *Proceedings of the National Academy of Sciences of the United States of America*, vol. 90, no. 4, pp. 1392-1396.
- Morse, B., Rotherg, P.G., South, V.J., Spandorfer, J.M. & Astrin, S.M. 1988, Insertional mutagenesis of the myc locus by a LINE-1 sequence in a human breast carcinoma, *Nature*, vol. 333, no. 6168, pp. 87-90.
- Mortusewicz, O., Schermelleh, L., Walter, J., Cardoso, M.C. & Leonhardt, H. 2005, Recruitment of DNA methyltransferase I to DNA repair sites, *Proceedings of the National Academy of Sciences of the United States of America*, vol. 102, no. 25, pp. 8905-8909.
- Mothersill, C., Crean, M., Lyons, M., McSweeney, J., Mooney, R., O'Reilly, J. & Seymour, C.B. 1998, Expression of delayed toxicity and lethal mutations in the progeny of human cells surviving exposure to radiation and other environmental mutagens, *International journal of radiation biology*, vol. 74, no. 6, pp. 673-680.
- Mouse Genome Sequencing Consortium, Waterston, R.H., Lindblad-Toh, K., Birney, E., Rogers, J., Abril, J.F., Agarwal, P., Agarwala, R., Ainscough, R., Alexandersson, M., An, P., Antonarakis, S.E., Attwood, J., Baertsch, R., Bailey, J., Barlow, K., Beck, S., Berry, E., Birren, B., Bloom, T., Bork, P., Botcherby, M., Bray, N., Brent, M.R., Brown, D.G., Brown, S.D., Bult, C., Burton, J., Butler, J., Campbell, R.D., Carninci, P., Cawley, S., Chiaromonte, F., Chinwalla, A.T., Church, D.M., Clamp, M., Clee, C., Collins, F.S., Cook, L.L., Copley, R.R., Coulson, A., Couronne, O., Cuff, J., Curwen, V., Cutts, T., Daly, M., David, R., Davies, J., Delehaanty, K.D., Deri, J., Dermitzakis, E.T., Dewey, C., Dickens, N.J., Diekhans, M., Dodge, S., Dubchak, I., Dunn, D.M., Eddy, S.R., Elnitski, L., Emes, R.D., Eswara, P., Eyas, E., Felsenfeld, A., Fewell, G.A., Flicek, P., Foley, K., Frankel, W.N., Fulton, L.A., Fulton, R.S., Furey, T.S., Gage, D., Gibbs, R.A., Glusman, G., Gnerre, S., Goldman, N., Goodstadt, L., Grafham, D., Graves, T.A., Green, E.D., Gregory, S., Guigo, R., Guyer, M., Hardison, R.C., Haussler, D., Hayashizaki, Y., Hillier, L.W., Hinrichs, A., Hlavina, W., Holzer, T., Hsu, F., Hua, A., Hubbard, T., Hunt, A., Jackson, I., Jaffe, D.B., Johnson, L.S., Jones, M., Jones, T.A., Joy, A., Kamal, M., Karlsson, E.K., Karolchik, D., Kasprzyk, A., Kawai, J., Keibler, E., Kells, C., Kent, W.J., Kirby, A., Kolbe, D.L., Korf, I., Kucherlapati, R.S., Kulbokas, E.J., Kulp, D., Landers, T., Leger, J.P., Leonard, S., Letunic, I., Levine, R., Li, J., Li, M., Lloyd, C., Lucas, S., Ma, B., Maglott, D.R., Mardis, E.R., Matthews, L., Mauceli, E., Mayer, J.H., McCarthy, M., McCombie, W.R., McLaren, S., McLay, K., McPherson, J.D., Meldrim, J., Meredith, B., Mesirov, J.P., Miller, W., Miner, T.L., Mongin, E., Montgomery, K.T., Morgan, M., Mott, R., Mullikin, J.C., Muzny, D.M., Nash, W.E., Nelson, J.O., Nhan, M.N., Nicol, R., Ning, Z., Nusbaum, C., O'Connor, M.J., Okazaki, Y., Oliver, K., Overton-Larty, E., Pachter, L., Parra, G., Pepin, K.H., Peterson, J., Pevzner, P., Plumb, R., Pohl, C.S., Poliakov, A., Ponce, T.C., Ponting, C.P., Potter, S., Quail, M., Reymond, A., Roe, B.A., Roskin, K.M., Rubin, E.M., Rust, A.G., Santos, R., Sapojnikov, V., Schultz, B., Schultz, J., Schwartz, M.S., Schwartz, S., Scott, C., Seaman, S., Searle, S., Sharpe, T., Sheridan, A., Shownkeen, R., Sims, S., Singer, J.B., Slater, G., Smit, A., Smith, D.R., Spencer, B., Stabenau, A., Stange-Thomann, N., Sugnet, C., Suyama, M., Tesler, G., Thompson, J., Torrents, D., Trevaskis, E., Tromp, J., Ucla, C., Ureta-Vidal, A., Vinson, J.P., Von Niederhausern, A.C., Wade, C.M., Wall, M., Weber, R.J., Weiss, R.B., Wendl, M.C., West, A.P., Wetterstrand, K., Wheeler, R., Whelan, S., Wierzbowski, J., Willey, D., Williams, S., Wilson, R.K., Winter, E., Worley, K.C., Wyman, D., Yang, S., Yang, S.P., Zdobnov, E.M., Zody, M.C. & Lander, E.S. 2002, Initial sequencing and comparative analysis of the mouse genome, *Nature*, vol. 420, no. 6915, pp. 520-562.

- Munshi, A., Kurland, J.F., Nishikawa, T., Tanaka, T., Hobbs, M.L., Tucker, S.L., Ismail, S., Stevens, C. & Meyn, R.E. 2005, Histone deacetylase inhibitors radiosensitize human melanoma cells by suppressing DNA repair activity, *Clinical cancer research : an official journal of the American Association for Cancer Research*, vol. 11, no. 13, pp. 4912-4922.
- Murnane, J.P., Sabatier, L., Marder, B.A. & Morgan, W.F. 1994, Telomere dynamics in an immortal human cell line, *The EMBO journal*, vol. 13, no. 20, pp. 4953-4962.
- Nabetani, A. & Ishikawa, F. 2009, Unusual telomeric DNAs in human telomerase-negative immortalized cells, *Molecular and cellular biology*, vol. 29, no. 3, pp. 703-713.
- Nagase, H. & Ghosh, S. 2008, Epigenetics: differential DNA methylation in mammalian somatic tissues, *The FEBS journal*, vol. 275, no. 8, pp. 1617-1623.
- Nan, X., Ng, H.H., Johnson, C.A., Laherty, C.D., Turner, B.M., Eisenman, R.N. & Bird, A. 1998, Transcriptional repression by the methyl-CpG-binding protein MeCP2 involves a histone deacetylase complex, *Nature*, vol. 393, no. 6683, pp. 386-389.
- Narayan, A., Tuck-Muller, C., Weissbecker, K., Smeets, D. & Ehrlich, M. 2000, Hypersensitivity to radiation-induced non-apoptotic and apoptotic death in cell lines from patients with the ICF chromosome instability syndrome, *Mutation research*, vol. 456, no. 1-2, pp. 1-15.
- Ng, H.H. & Bird, A. 1999, DNA methylation and chromatin modification, *Current opinion in genetics & development*, vol. 9, no. 2, pp. 158-163.
- Niedernhofer, L.J., Lalai, A.S. & Hoeijmakers, J.H. 2005, Fanconi anemia (cross)linked to DNA repair, *Cell*, vol. 123, no. 7, pp. 1191-1198.
- Nilausen, K. & Green, H. 1965, Reversible arrest of growth in G1 of an established fibroblast line (3T3), *Experimental cell research*, vol. 40, no. 1, pp. 166-168.
- Norris, D.P., Patel, D., Kay, G.F., Penny, G.D., Brockdorff, N., Sheardown, S.A. & Rastan, S. 1994, Evidence that random and imprinted Xist expression is controlled by preemptive methylation, *Cell*, vol. 77, no. 1, pp. 41-51.
- Nowell, P.C. 1976, The clonal evolution of tumour cell populations, *Science (New York, N.Y.)*, vol. 194, no. 4260, pp. 23-28.
- Ohki, I., Shimotake, N., Fujita, N., Jee, J., Ikegami, T., Nakao, M. & Shirakawa, M. 2001, Solution structure of the methyl-CpG binding domain of human MBD1 in complex with methylated DNA, *Cell*, vol. 105, no. 4, pp. 487-497.
- Oka, M., Rodic, N., Graddy, J., Chang, L.J. & Terada, N. 2006, CpG sites preferentially methylated by Dnmt3a *in vivo*, *The Journal of biological chemistry*, vol. 281, no. 15, pp. 9901-9908.
- Okada, Y., Yamagata, K., Hong, K., Wakayama, T. & Zhang, Y. 2010, A role for the elongator complex in zygotic paternal genome demethylation, *Nature*, vol. 463, no. 7280, pp. 554-558.
- Okano, M., Bell, D.W., Haber, D.A. & Li, E. 1999, DNA methyltransferases Dnmt3a and Dnmt3b are essential for de novo methylation and mammalian development, *Cell*, vol. 99, no. 3, pp. 247-257.
- Okano, M. & Li, E. 2002, Genetic analyses of DNA methyltransferase genes in mouse model system, *The Journal of nutrition*, vol. 132, no. 8 Suppl, pp. 2462S-2465S.

- Okano, M., Xie, S. & Li, E. 1998, Cloning and characterization of a family of novel mammalian DNA (cytosine-5) methyltransferases, *Nature genetics*, vol. 19, no. 3, pp. 219-220.
- Olive, P.L. & Banath, J.P. 2006, The comet assay: a method to measure DNA damage in individual cells, *Nature protocols*, vol. 1, no. 1, pp. 23-29.
- Ooi, S.K., Qiu, C., Bernstein, E., Li, K., Jia, D., Yang, Z., Erdjument-Bromage, H., Tempst, P., Lin, S.P., Allis, C.D., Cheng, X. & Bestor, T.H. 2007, DNMT3L connects unmethylated lysine 4 of histone H3 to de novo methylation of DNA, *Nature*, vol. 448, no. 7154, pp. 714-717.
- Osheroff, N. 1986, Eukaryotic topoisomerase II. Characterization of enzyme turnover, *The Journal of biological chemistry*, vol. 261, no. 21, pp. 9944-9950.
- Oshida, K., Iwanaga, E., Miyamoto-Kuramitsu, K. & Miyamoto, Y. 2008, An *in vivo* comet assay of multiple organs (liver, kidney and bone marrow) in mice treated with methyl methanesulfonate and acetaminophen accompanied by hematology and/or blood chemistry, *The Journal of toxicological sciences*, vol. 33, no. 5, pp. 515-524.
- Ostler, K.R., Davis, E.M., Payne, S.L., Gosalia, B.B., Exposito-Cespedes, J., Le Beau, M.M. & Godley, L.A. 2007, Cancer cells express aberrant DNMT3B transcripts encoding truncated proteins, *Oncogene*, vol. 26, no. 38, pp. 5553-5563.
- Oswald, J., Engemann, S., Lane, N., Mayer, W., Olek, A., Fundele, R., Dean, W., Reik, W. & Walter, J. 2000, Active demethylation of the paternal genome in the mouse zygote, *Current biology : CB*, vol. 10, no. 8, pp. 475-478.
- Packer, A.I., Manova, K. & Bachvarova, R.F. 1993, A discrete LINE-1 transcript in mouse blastocysts, *Developmental biology*, vol. 157, no. 1, pp. 281-283.
- Pardee, A.B. 2002, Regulation of the cell cycle in *The cancer handbook*, ed. M. Alison, John Wiley and Sons, USA, pp. 13-24.
- Paull, T.T., Rogakou, E.P., Yamazaki, V., Kirchgessner, C.U., Gellert, M. & Bonner, W.M. 2000, A critical role for histone H2AX in recruitment of repair factors to nuclear foci after DNA damage, *Current biology : CB*, vol. 10, no. 15, pp. 886-895.
- Pavlicek, A., Jabbari, K., Paces, J., Paces, V., Hejnar, J.V. & Bernardi, G. 2001, Similar integration but different stability of Alus and LINEs in the human genome, *Gene*, vol. 276, no. 1-2, pp. 39-45.
- Pawlik, T.M. & Keyomarsi, K. 2004, Role of cell cycle in mediating sensitivity to radiotherapy, *International journal of radiation oncology, biology, physics*, vol. 59, no. 4, pp. 928-942.
- Peterson, C.L. & Cote, J. 2004, Cellular machineries for chromosomal DNA repair, *Genes & development*, vol. 18, no. 6, pp. 602-616.
- Piskareva, O., Denmukhametova, S. & Schmatchenko, V. 2003, Functional reverse transcriptase encoded by the human LINE-1 from baculovirus-infected insect cells, *Protein expression and purification*, vol. 28, no. 1, pp. 125-130.
- Pogribny, I., Raiche, J., Slovack, M. & Kovalchuk, O. 2004, Dose-dependence, sex- and tissue-specificity, and persistence of radiation-induced genomic DNA methylation changes, *Biochemical and biophysical research communications*, vol. 320, no. 4, pp. 1253-1261.

- Pommier, Y., Capranico, G., Orr, A. & Kohn, K.W. 1991, Local base sequence preferences for DNA cleavage by mammalian topoisomerase II in the presence of amsacrine or teniposide, *Nucleic acids research*, vol. 19, no. 21, pp. 5973-5980.
- Pommier, Y., Orr, A., Kohn, K.W. & Riou, J.F. 1992, Differential effects of amsacrine and epipodophyllotoxins on topoisomerase II cleavage in the human c-myc protooncogene, *Cancer research*, vol. 52, no. 11, pp. 3125-3130.
- Ponnaiya, B., Cornforth, M.N. & Ullrich, R.L. 1997, Radiation-induced chromosomal instability in BALB/c and C57BL/6 mice: the difference is as clear as black and white, *Radiation research*, vol. 147, no. 2, pp. 121-125.
- Pradhan, S. & Esteve, P.O. 2003, Mammalian DNA (cytosine-5) methyltransferases and their expression, *Clinical immunology (Orlando, Fla.)*, vol. 109, no. 1, pp. 6-16.
- Prasad, R., Beard, W.A., Strauss, P.R. & Wilson, S.H. 1998, Human DNA polymerase beta deoxyribose phosphate lyase. Substrate specificity and catalytic mechanism, *The Journal of biological chemistry*, vol. 273, no. 24, pp. 15263-15270.
- Protic-Sabljić, M. & Kraemer, K.H. 1985, One pyrimidine dimer inactivates expression of a transfected gene in xeroderma pigmentosum cells, *Proceedings of the National Academy of Sciences of the United States of America*, vol. 82, no. 19, pp. 6622-6626.
- Pulukuri, S.M. & Rao, J.S. 2006, CpG island promoter methylation and silencing of 14-3-3sigma gene expression in LNCaP and Tramp-C1 prostate cancer cell lines is associated with methyl-CpG-binding protein MBD2, *Oncogene*, vol. 25, no. 33, pp. 4559-4572.
- Quentin, Y. 1994, A master sequence related to a free left Alu monomer (FLAM) at the origin of the B1 family in rodent genomes, *Nucleic acids research*, vol. 22, no. 12, pp. 2222-2227.
- Radicella, J.P., Dherin, C., Desmaze, C., Fox, M.S. & Boiteux, S. 1997, Cloning and characterization of hOGG1, a human homolog of the OGG1 gene of *Saccharomyces cerevisiae*, *Proceedings of the National Academy of Sciences of the United States of America*, vol. 94, no. 15, pp. 8010-8015.
- Rai, K., Huggins, I.J., James, S.R., Karpf, A.R., Jones, D.A. & Cairns, B.R. 2008, DNA demethylation in zebrafish involves the coupling of a deaminase, a glycosylase, and gadd45, *Cell*, vol. 135, no. 7, pp. 1201-1212.
- Raiche, J., Rodriguez-Juarez, R., Pogribny, I. & Kovalchuk, O. 2004, Sex- and tissue-specific expression of maintenance and de novo DNA methyltransferases upon low dose X-irradiation in mice, *Biochemical and biophysical research communications*, vol. 325, no. 1, pp. 39-47.
- Ramsahoye, B.H. 2002, Nearest-neighbor analysis, *Methods in molecular biology (Clifton, N.J.)*, vol. 200, pp. 9-15.
- Ramsahoye, B.H., Biniszkiewicz, D., Lyko, F., Clark, V., Bird, A.P. & Jaenisch, R. 2000, Non-CpG methylation is prevalent in embryonic stem cells and may be mediated by DNA methyltransferase 3a, *Proceedings of the National Academy of Sciences of the United States of America*, vol. 97, no. 10, pp. 5237-5242.
- Razin, A. & Szyf, M. 1984, DNA methylation patterns. Formation and function, *Biochimica et biophysica acta*, vol. 782, no. 4, pp. 331-342.
- Reid, R.J., Benedetti, P. & Bjornsti, M.A. 1998, Yeast as a model organism for studying the actions of DNA topoisomerase-targeted drugs, *Biochimica et biophysica acta*, vol. 1400, no. 1-3, pp. 289-300.

- Reik, W. & Walter, J. 2001, Genomic imprinting: parental influence on the genome, *Nature reviews.Genetics*, vol. 2, no. 1, pp. 21-32.
- Riballo, E., Kuhne, M., Rief, N., Doherty, A., Smith, G.C., Recio, M.J., Reis, C., Dahm, K., Fricke, A., Krempler, A., Parker, A.R., Jackson, S.P., Gennery, A., Jeggo, P.A. & Lobrich, M. 2004, A pathway of double-strand break rejoining dependent upon ATM, Artemis, and proteins locating to gamma-H2AX foci, *Molecular cell*, vol. 16, no. 5, pp. 715-724.
- Robertson, K.D., Uzvolgyi, E., Liang, G., Talmadge, C., Sumegi, J., Gonzales, F.A. & Jones, P.A. 1999, The human DNA methyltransferases (DNMTs) 1, 3a and 3b: coordinate mRNA expression in normal tissues and overexpression in tumours, *Nucleic acids research*, vol. 27, no. 11, pp. 2291-2298.
- Rofstad, E.K., Sundfor, K., Lyng, H. & Trope, C.G. 2000, Hypoxia-induced treatment failure in advanced squamous cell carcinoma of the uterine cervix is primarily due to hypoxia-induced radiation resistance rather than hypoxia-induced metastasis, *British journal of cancer*, vol. 83, no. 3, pp. 354-359.
- Rogakou, E.P., Boon, C., Redon, C. & Bonner, W.M. 1999, Megabase chromatin domains involved in DNA double-strand breaks *in vivo*, *The Journal of cell biology*, vol. 146, no. 5, pp. 905-916.
- Rogakou, E.P., Pilch, D.R., Orr, A.H., Ivanova, V.S. & Bonner, W.M. 1998, DNA double-stranded breaks induce histone H2AX phosphorylation on serine 139, *The Journal of biological chemistry*, vol. 273, no. 10, pp. 5858-5868.
- Rollins, R.A., Haghghi, F., Edwards, J.R., Das, R., Zhang, M.Q., Ju, J. & Bestor, T.H. 2006, Large-scale structure of genomic methylation patterns, *Genome research*, vol. 16, no. 2, pp. 157-163.
- Roman-Gomez, J., Jimenez-Velasco, A., Agirre, X., Cervantes, F., Sanchez, J., Garate, L., Barrios, M., Castillejo, J.A., Navarro, G., Colomer, D., Prosper, F., Heiniger, A. & Torres, A. 2005, Promoter hypomethylation of the LINE-1 retrotransposable elements activates sense/antisense transcription and marks the progression of chronic myeloid leukemia, *Oncogene*, vol. 24, no. 48, pp. 7213-7223.
- Romney, C.A., Paulauskis, J.D., Nagasawa, H. & Little, J.B. 2001, Multiple manifestations of X-ray-induced genomic instability in Chinese hamster ovary (CHO) cells, *Molecular carcinogenesis*, vol. 32, no. 3, pp. 118-127.
- Roos, W.P., Christmann, M., Fraser, S.T. & Kaina, B. 2007, Mouse embryonic stem cells are hypersensitive to apoptosis triggered by the DNA damage O(6)-methylguanine due to high E2F1 regulated mismatch repair, *Cell death and differentiation*, vol. 14, no. 8, pp. 1422-1432.
- Rothkamm, K., Kruger, I., Thompson, L.H. & Lobrich, M. 2003, Pathways of DNA double-strand break repair during the mammalian cell cycle, *Molecular and cellular biology*, vol. 23, no. 16, pp. 5706-5715.
- Rougier, N., Bourc'his, D., Gomes, D.M., Niveleau, A., Plachot, M., Paldi, A. & Viegas-Pequignot, E. 1998, Chromosome methylation patterns during mammalian preimplantation development, *Genes & development*, vol. 12, no. 14, pp. 2108-2113.
- Royle, N.J., Mendez-Bermudez, A., Gravani, A., Novo, C., Foxon, J., Williams, J., Cotton, V. & Hidalgo, A. 2009, The role of recombination in telomere length maintenance, *Biochemical Society transactions*, vol. 37, no. Pt 3, pp. 589-595.
- Ryan, A.J., Squires, S., Strutt, H.L. & Johnson, R.T. 1991, Camptothecin cytotoxicity in mammalian cells is associated with the induction of persistent double strand breaks in replicating DNA, *Nucleic acids research*, vol. 19, no. 12, pp. 3295-3300.

- Sandhu, J., Kaur, B., Armstrong, C., Talbot, C.J., Steward, W.P., Farmer, P.B. & Singh, R. 2009, Determination of 5-methyl-2'-deoxycytidine in genomic DNA using high performance liquid chromatography-ultraviolet detection, *Journal of chromatography.B, Analytical technologies in the biomedical and life sciences*, vol. 877, no. 20-21, pp. 1957-1961.
- Sanford, J.P., Clark, H.J., Chapman, V.M. & Rossant, J. 1987, Differences in DNA methylation during oogenesis and spermatogenesis and their persistence during early embryogenesis in the mouse, *Genes & development*, vol. 1, no. 10, pp. 1039-1046.
- Santos, F. & Dean, W. 2004, Epigenetic reprogramming during early development in mammals, *Reproduction (Cambridge, England)*, vol. 127, no. 6, pp. 643-651.
- Santos, F., Hendrich, B., Reik, W. & Dean, W. 2002, Dynamic reprogramming of DNA methylation in the early mouse embryo, *Developmental biology*, vol. 241, no. 1, pp. 172-182.
- Saretzki, G., Armstrong, L., Leake, A., Lako, M. & von Zglinicki, T. 2004, Stress defense in murine embryonic stem cells is superior to that of various differentiated murine cells, *Stem cells (Dayton, Ohio)*, vol. 22, no. 6, pp. 962-971.
- Saretzki, G., Walter, T., Atkinson, S., Passos, J.F., Bareth, B., Keith, W.N., Stewart, R., Hoare, S., Stojkovic, M., Armstrong, L., von Zglinicki, T. & Lako, M. 2008, Downregulation of multiple stress defense mechanisms during differentiation of human embryonic stem cells, *Stem cells (Dayton, Ohio)*, vol. 26, no. 2, pp. 455-464.
- Savage, J.R. 2002, Reflections and meditations upon complex chromosomal exchanges, *Mutation research*, vol. 512, no. 2-3, pp. 93-109.
- Savage, J.R. 1980, Chromosomal aberrations as indicators of mutagenicity, *Clinical and experimental dermatology*, vol. 5, no. 2, pp. 139-145.
- Savage, J.R. 1976, Classification and relationships of induced chromosomal structural changes, *Journal of medical genetics*, vol. 13, no. 2, pp. 103-122.
- Savage, J.R.K. 1999, An Introduction to Chromosomal Aberrations, *Atlas of Genetics and Cytogenetics in Oncology and Haematology*, .
- Savatier, P., Lapillonne, H., van Grunsven, L.A., Rudkin, B.B. & Samarut, J. 1996, Withdrawal of differentiation inhibitory activity/leukemia inhibitory factor up-regulates D-type cyclins and cyclin-dependent kinase inhibitors in mouse embryonic stem cells, *Oncogene*, vol. 12, no. 2, pp. 309-322.
- Sawyer, J.R., Swanson, C.M., Wheeler, G. & Cunniff, C. 1995, Chromosome instability in ICF syndrome: formation of micronuclei from multibranching chromosomes 1 demonstrated by fluorescence in situ hybridization, *American Journal of Medical Genetics*, vol. 56, no. 2, pp. 203-209.
- Saxonov, S., Berg, P. & Brutlag, D.L. 2006, A genome-wide analysis of CpG dinucleotides in the human genome distinguishes two distinct classes of promoters, *Proceedings of the National Academy of Sciences of the United States of America*, vol. 103, no. 5, pp. 1412-1417.
- Schermelleh, L., Haemmer, A., Spada, F., Rosing, N., Meilinger, D., Rothbauer, U., Cardoso, M.C. & Leonhardt, H. 2007, Dynamics of Dnmt1 interaction with the replication machinery and its role in postreplicative maintenance of DNA methylation, *Nucleic acids research*, vol. 35, no. 13, pp. 4301-4312.

- Schmidt, P. & Kiefer, J. 1998, Deletion-pattern analysis of alpha-particle and X-ray induced mutations at the HPRT locus of V79 Chinese hamster cells, *Mutation research*, vol. 421, no. 2, pp. 149-161.
- Schmitz, K.M., Schmitt, N., Hoffmann-Rohrer, U., Schafer, A., Grummt, I. & Mayer, C. 2009, TAF12 recruits Gadd45a and the nucleotide excision repair complex to the promoter of rRNA genes leading to active DNA demethylation, *Molecular cell*, vol. 33, no. 3, pp. 344-353.
- Setlow, R.B. 1974, The wavelengths in sunlight effective in producing skin cancer: a theoretical analysis, *Proceedings of the National Academy of Sciences of the United States of America*, vol. 71, no. 9, pp. 3363-3366.
- Sharif, J., Muto, M., Takebayashi, S., Suetake, I., Iwamatsu, A., Endo, T.A., Shinga, J., Mizutani-Koseki, Y., Toyoda, T., Okamura, K., Tajima, S., Mitsuya, K., Okano, M. & Koseki, H. 2007, The SRA protein Np95 mediates epigenetic inheritance by recruiting Dnmt1 to methylated DNA, *Nature*, vol. 450, no. 7171, pp. 908-912.
- Shay, J.W. & Wright, W.E. 2005, Senescence and immortalization: role of telomeres and telomerase, *Carcinogenesis*, vol. 26, no. 5, pp. 867-874.
- Shen, J.C., Rideout, W.M., 3rd & Jones, P.A. 1994, The rate of hydrolytic deamination of 5-methylcytosine in double-stranded DNA, *Nucleic acids research*, vol. 22, no. 6, pp. 972-976.
- Shen, L., Kondo, Y., Guo, Y., Zhang, J., Zhang, L., Ahmed, S., Shu, J., Chen, X., Waterland, R.A. & Issa, J.P. 2007, Genome-wide profiling of DNA methylation reveals a class of normally methylated CpG island promoters, *PLoS genetics*, vol. 3, no. 10, pp. 2023-2036.
- Shen-Ong, G.L. & Cole, M.D. 1982, Differing populations of intracisternal A-particle genes in myeloma tumours and mouse subspecies, *Journal of virology*, vol. 42, no. 2, pp. 411-421.
- Shiota, K., Kogo, Y., Ohgane, J., Imamura, T., Urano, A., Nishino, K., Tanaka, S. & Hattori, N. 2002, Epigenetic marks by DNA methylation specific to stem, germ and somatic cells in mice, *Genes to cells : devoted to molecular & cellular mechanisms*, vol. 7, no. 9, pp. 961-969.
- Shukla, R., Liu, T., Geacintov, N.E. & Loechler, E.L. 1997, The major, N2-dG adduct of (+)-anti-B[a]PDE shows a dramatically different mutagenic specificity (predominantly, G --> A) in a 5'-CGT-3' sequence context, *Biochemistry*, vol. 36, no. 33, pp. 10256-10261.
- Shulman, M.J., Collins, C., Connor, A., Read, L.R. & Baker, M.D. 1995, Interchromosomal recombination is suppressed in mammalian somatic cells, *The EMBO journal*, vol. 14, no. 16, pp. 4102-4107.
- Sinha, R.P. & Hader, D.P. 2002, UV-induced DNA damage and repair: a review, *Photochemical & photobiological sciences : Official journal of the European Photochemistry Association and the European Society for Photobiology*, vol. 1, no. 4, pp. 225-236.
- Smallwood, A., Esteve, P.O., Pradhan, S. & Carey, M. 2007, Functional cooperation between HP1 and DNMT1 mediates gene silencing, *Genes & development*, vol. 21, no. 10, pp. 1169-1178.
- Song, F., Smith, J.F., Kimura, M.T., Morrow, A.D., Matsuyama, T., Nagase, H. & Held, W.A. 2005, Association of tissue-specific differentially methylated regions (TDMs) with differential gene expression, *Proceedings of the National Academy of Sciences of the United States of America*, vol. 102, no. 9, pp. 3336-3341.

- Sonoda, E., Sasaki, M.S., Morrison, C., Yamaguchi-Iwai, Y., Takata, M. & Takeda, S. 1999, Sister chromatid exchanges are mediated by homologous recombination in vertebrate cells, *Molecular and cellular biology*, vol. 19, no. 7, pp. 5166-5169.
- Sowers, L.C., Shaw, B.R. & Sedwick, W.D. 1987, Base stacking and molecular polarizability: effect of a methyl group in the 5-position of pyrimidines, *Biochemical and biophysical research communications*, vol. 148, no. 2, pp. 790-794.
- Speit, G., Schutz, P., Bonzheim, I., Trenz, K. & Hoffmann, H. 2004, Sensitivity of the FPG protein towards alkylation damage in the comet assay, *Toxicology letters*, vol. 146, no. 2, pp. 151-158.
- Steinert, S., Shay, J.W. & Wright, W.E. 2004, Modification of subtelomeric DNA, *Molecular and cellular biology*, vol. 24, no. 10, pp. 4571-4580.
- Stoilov, L., Darroudi, F., Meschini, R., van der Schans, G., Mullenders, L.H. & Natarajan, A.T. 2000, Inhibition of repair of X-ray-induced DNA double-strand breaks in human lymphocytes exposed to sodium butyrate, *International journal of radiation biology*, vol. 76, no. 11, pp. 1485-1491.
- Strick, T.R., Croquette, V. & Bensimon, D. 2000, Single-molecule analysis of DNA uncoiling by a type II topoisomerase, *Nature*, vol. 404, no. 6780, pp. 901-904.
- Sulewska, A., Niklinska, W., Kozłowski, M., Minarowski, L., Naumnik, W., Niklinski, J., Dabrowska, K. & Chyczewski, L. 2007, Detection of DNA methylation in eucaryotic cells, *Folia histochemica et cytobiologica / Polish Academy of Sciences, Polish Histochemical and Cytochemical Society*, vol. 45, no. 4, pp. 315-324.
- Suzuki, K., Ojima, M., Kodama, S. & Watanabe, M. 2003, Radiation-induced DNA damage and delayed induced genomic instability, *Oncogene*, vol. 22, no. 45, pp. 6988-6993.
- Symer, D.E., Connelly, C., Szak, S.T., Caputo, E.M., Cost, G.J., Parmigiani, G. & Boeke, J.D. 2002, Human I1 retrotransposition is associated with genetic instability *in vivo*, *Cell*, vol. 110, no. 3, pp. 327-338.
- Tachibana, M., Matsumura, Y., Fukuda, M., Kimura, H. & Shinkai, Y. 2008, G9a/GLP complexes independently mediate H3K9 and DNA methylation to silence transcription, *The EMBO journal*, vol. 27, no. 20, pp. 2681-2690.
- Taddei, A., Maison, C., Roche, D. & Almouzni, G. 2001, Reversible disruption of pericentric heterochromatin and centromere function by inhibiting deacetylases, *Nature cell biology*, vol. 3, no. 2, pp. 114-120.
- Tadokoro, Y., Ema, H., Okano, M., Li, E. & Nakauchi, H. 2007, De novo DNA methyltransferase is essential for self-renewal, but not for differentiation, in hematopoietic stem cells, *The Journal of experimental medicine*, vol. 204, no. 4, pp. 715-722.
- Takai, D., Yagi, Y., Habib, N., Sugimura, T. & Ushijima, T. 2000, Hypomethylation of LINE1 retrotransposon in human hepatocellular carcinomas, but not in surrounding liver cirrhosis, *Japanese journal of clinical oncology*, vol. 30, no. 7, pp. 306-309.
- Takebayashi, S., Tamura, T., Matsuoka, C. & Okano, M. 2007, Major and essential role for the DNA methylation mark in mouse embryogenesis and stable association of DNMT1 with newly replicated regions, *Molecular and cellular biology*, vol. 27, no. 23, pp. 8243-8258.
- Tanaka, I. & Ishihara, H. 1995, Unusual long target duplication by insertion of intracisternal A-particle element in radiation-induced acute myeloid leukemia cells in mouse, *FEBS letters*, vol. 376, no. 3, pp. 146-150.

- Tanaka, K., Kohda, A., Toyokawa, T., Ichinohe, K. & Oghiso, Y. 2008, Chromosome aberration frequencies and chromosome instability in mice after long-term exposure to low-dose-rate gamma-irradiation, *Mutation research*, vol. 657, no. 1, pp. 19-25.
- Tawa, R., Kimura, Y., Komura, J., Miyamura, Y., Kurishita, A., Sasaki, M.S., Sakurai, H. & Ono, T. 1998, Effects of X-ray irradiation on genomic DNA methylation levels in mouse tissues, *Journal of radiation research*, vol. 39, no. 4, pp. 271-278.
- Tchou, J., Kasai, H., Shibutani, S., Chung, M.H., Laval, J., Grollman, A.P. & Nishimura, S. 1991, 8-oxoguanine (8-hydroxyguanine) DNA glycosylase and its substrate specificity, *Proceedings of the National Academy of Sciences of the United States of America*, vol. 88, no. 11, pp. 4690-4694.
- Tice, R.R., Agurell, E., Anderson, D., Burlinson, B., Hartmann, A., Kobayashi, H., Miyamae, Y., Rojas, E., Ryu, J.C. & Sasaki, Y.F. 2000, Single cell gel/comet assay: guidelines for *in vitro* and *in vivo* genetic toxicology testing, *Environmental and molecular mutagenesis*, vol. 35, no. 3, pp. 206-221.
- Tichy, E.D. & Stambrook, P.J. 2008, DNA repair in murine embryonic stem cells and differentiated cells, *Experimental cell research*, vol. 314, no. 9, pp. 1929-1936.
- Tiepolo, L., Maraschio, P., Gimelli, C., Cuoco, C., Gargani, G.F. & Romano, C. 1978, Concurrent Instability at Specific Sites of Chromosomes 1, 9 and 16 Resulting in Multi-Branched Structures, *Clinical Genetics*, vol. 14, pp. 313-314.
- Tommasi, S., Denissenko, M.F. & Pfeifer, G.P. 1997, Sunlight induces pyrimidine dimers preferentially at 5-methylcytosine bases, *Cancer research*, vol. 57, no. 21, pp. 4727-4730.
- Tornaletti, S. & Pfeifer, G.P. 1995, Complete and tissue-independent methylation of CpG sites in the p53 gene: implications for mutations in human cancers, *Oncogene*, vol. 10, no. 8, pp. 1493-1499.
- Tsubouchi, S. & Matsuzawa, T. 1974, Rapid radiation cell death and cell proliferation in intestinal epithelium after 1000-rad irradiation, *Radiation research*, vol. 57, no. 3, pp. 451-458.
- Tsuda, H., Maynard-Currie, C.E., Reid, L.H., Yoshida, T., Edamura, K., Maeda, N., Smithies, O. & Jakobovits, A. 1997, Inactivation of the mouse HPRT locus by a 203-bp retroposon insertion and a 55-kb gene-targeted deletion: establishment of new HPRT-deficient mouse embryonic stem cell lines, *Genomics*, vol. 42, no. 3, pp. 413-421.
- Tsumura, A., Hayakawa, T., Kumaki, Y., Takebayashi, S., Sakaue, M., Matsuoka, C., Shimotohno, K., Ishikawa, F., Li, E., Ueda, H.R., Nakayama, J. & Okano, M. 2006, Maintenance of self-renewal ability of mouse embryonic stem cells in the absence of DNA methyltransferases Dnmt1, Dnmt3a and Dnmt3b, *Genes to cells : devoted to molecular & cellular mechanisms*, vol. 11, no. 7, pp. 805-814.
- Tuck-Muller, C.M., Narayan, A., Tsien, F., Smeets, D.F., Sawyer, J., Fiala, E.S., Sohn, O.S. & Ehrlich, M. 2000, DNA hypomethylation and unusual chromosome instability in cell lines from ICF syndrome patients, *Cytogenetics and cell genetics*, vol. 89, no. 1-2, pp. 121-128.
- Uchida, T., Wada, C., Wang, C., Egawa, S., Ohtani, H. & Koshiba, K. 1994, Genomic instability of microsatellite repeats and mutations of H-, K-, and N-ras, and p53 genes in renal cell carcinoma, *Cancer research*, vol. 54, no. 14, pp. 3682-3685.
- Umar, A., Buermeier, A.B., Simon, J.A., Thomas, D.C., Clark, A.B., Liskay, R.M. & Kunkel, T.A. 1996, Requirement for PCNA in DNA mismatch repair at a step preceding DNA resynthesis, *Cell*, vol. 87, no. 1, pp. 65-73.

- Valeri, N., Gasparini, P., Fabbri, M., Braconi, C., Veronese, A., Lovat, F., Adair, B., Vannini, I., Fanini, F., Bottoni, A., Costinean, S., Sandhu, S.K., Nuovo, G.J., Alder, H., Gafa, R., Calore, F., Ferracin, M., Lanza, G., Volinia, S., Negrini, M., McIlhatton, M.A., Amadori, D., Fishel, R. & Croce, C.M. 2010, Modulation of mismatch repair and genomic stability by miR-155, *Proceedings of the National Academy of Sciences of the United States of America*, vol. 107, no. 15, pp. 6982-6987.
- Valerie, K. & Povirk, L.F. 2003, Regulation and mechanisms of mammalian double-strand break repair, *Oncogene*, vol. 22, no. 37, pp. 5792-5812.
- van Attikum, H. & Gasser, S.M. 2005, ATP-dependent chromatin remodeling and DNA double-strand break repair, *Cell cycle (Georgetown, Tex.)*, vol. 4, no. 8, pp. 1011-1014.
- van Loon, A.A., Timmerman, A.J., van der Schans, G.P., Lohman, P.H. & Baan, R.A. 1992, Different repair kinetics of radiation-induced DNA lesions in human and murine white blood cells, *Carcinogenesis*, vol. 13, no. 3, pp. 457-462.
- van Luenen, H.G., Colloms, S.D. & Plasterk, R.H. 1993, Mobilization of quiet, endogenous Tc3 transposons of *Caenorhabditis elegans* by forced expression of Tc3 transposase, *The EMBO journal*, vol. 12, no. 6, pp. 2513-2520.
- Van Sloun, P.P., Jansen, J.G., Weeda, G., Mullenders, L.H., van Zeeland, A.A., Lohman, P.H. & Vrieling, H. 1999, The role of nucleotide excision repair in protecting embryonic stem cells from genotoxic effects of UV-induced DNA damage, *Nucleic acids research*, vol. 27, no. 16, pp. 3276-3282.
- van Steensel, B., Smogorzewska, A. & de Lange, T. 1998, TRF2 protects human telomeres from end-to-end fusions, *Cell*, vol. 92, no. 3, pp. 401-413.
- vanAnkeren, S.C., Murray, D. & Meyn, R.E. 1988, Induction and rejoining of gamma-ray-induced DNA single- and double-strand breaks in Chinese hamster AA8 cells and in two radiosensitive clones, *Radiation research*, vol. 116, no. 3, pp. 511-525.
- Vance, M.M., Baulch, J.E., Raabe, O.G., Wiley, L.M. & Overstreet, J.W. 2002, Cellular reprogramming in the F3 mouse with paternal F0 radiation history, *International journal of radiation biology*, vol. 78, no. 6, pp. 513-526.
- Vermeulen, K., Van Bockstaele, D.R. & Berneman, Z.N. 2003, The cell cycle: a review of regulation, deregulation and therapeutic targets in cancer, *Cell proliferation*, vol. 36, no. 3, pp. 131-149.
- Vire, E., Brenner, C., Deplus, R., Blanchon, L., Fraga, M., Didelot, C., Morey, L., Van Eynde, A., Bernard, D., Vanderwinden, J.M., Bollen, M., Esteller, M., Di Croce, L., de Launoit, Y. & Fuks, F. 2006, The Polycomb group protein EZH2 directly controls DNA methylation, *Nature*, vol. 439, no. 7078, pp. 871-874.
- Wahlfors, J., Hiltunen, H., Heinonen, K., Hamalainen, E., Alhonen, L. & Janne, J. 1992, Genomic hypomethylation in human chronic lymphocytic leukemia, *Blood*, vol. 80, no. 8, pp. 2074-2080.
- Wakeford, R. 2004, The cancer epidemiology of radiation, *Oncogene*, vol. 23, no. 38, pp. 6404-6428.
- Wang, H., Zeng, Z.C., Bui, T.A., Sonoda, E., Takata, M., Takeda, S. & Iliakis, G. 2001, Efficient rejoining of radiation-induced DNA double-strand breaks in vertebrate cells deficient in genes of the RAD52 epistasis group, *Oncogene*, vol. 20, no. 18, pp. 2212-2224.

- Wang, J., Walsh, G., Liu, D.D., Lee, J.J. & Mao, L. 2006, Expression of Delta DNMT3B variants and its association with promoter methylation of p16 and RASSF1A in primary non-small cell lung cancer, *Cancer research*, vol. 66, no. 17, pp. 8361-8366.
- Wang, J.C. 2002, Cellular roles of DNA topoisomerases: a molecular perspective, *Nature reviews.Molecular cell biology*, vol. 3, no. 6, pp. 430-440.
- Wang, K.Y. & James Shen, C.K. 2004, DNA methyltransferase Dnmt1 and mismatch repair, *Oncogene*, vol. 23, no. 47, pp. 7898-7902.
- Wang, L., Wang, J., Sun, S., Rodriguez, M., Yue, P., Jang, S.J. & Mao, L. 2006, A novel DNMT3B subfamily, DeltaDNMT3B, is the predominant form of DNMT3B in non-small cell lung cancer, *International journal of oncology*, vol. 29, no. 1, pp. 201-207.
- Wang, R.C., Smogorzewska, A. & de Lange, T. 2004, Homologous recombination generates T-loop-sized deletions at human telomeres, *Cell*, vol. 119, no. 3, pp. 355-368.
- Ward, J.F. 1988, DNA damage produced by ionizing radiation in mammalian cells: identities, mechanisms of formation, and reparability, *Progress in nucleic acid research and molecular biology*, vol. 35, pp. 95-125.
- Watanabe, D., Suetake, I., Tada, T. & Tajima, S. 2002, Stage- and cell-specific expression of Dnmt3a and Dnmt3b during embryogenesis, *Mechanisms of development*, vol. 118, no. 1-2, pp. 187-190.
- Watson, G.E., Lorimore, S.A., Clutton, S.M., Kadhim, M.A. & Wright, E.G. 1997, Genetic factors influencing alpha-particle-induced chromosomal instability, *International journal of radiation biology*, vol. 71, no. 5, pp. 497-503.
- Watson, G.E., Pocock, D.A., Papworth, D., Lorimore, S.A. & Wright, E.G. 2001, *In vivo* chromosomal instability and transmissible aberrations in the progeny of haemopoietic stem cells induced by high- and low-LET radiations, *International journal of radiation biology*, vol. 77, no. 4, pp. 409-417.
- Watson, J.D. 1972, Origin of concatemeric T7 DNA, *Nature: New biology*, vol. 239, no. 94, pp. 197-201.
- Watt, F. & Molloy, P.L. 1988, Cytosine methylation prevents binding to DNA of a HeLa cell transcription factor required for optimal expression of the adenovirus major late promoter, *Genes & development*, vol. 2, no. 9, pp. 1136-1143.
- Weber, M., Hellmann, I., Stadler, M.B., Ramos, L., Paabo, S., Rebhan, M. & Schubeler, D. 2007, Distribution, silencing potential and evolutionary impact of promoter DNA methylation in the human genome, *Nature genetics*, vol. 39, no. 4, pp. 457-466.
- White, J. & Dalton, S. 2005, Cell cycle control of embryonic stem cells, *Stem cell reviews*, vol. 1, no. 2, pp. 131-138.
- Widschwendter, M., Jiang, G., Woods, C., Muller, H.M., Fiegl, H., Goebel, G., Marth, C., Muller-Holzner, E., Zeimet, A.G., Laird, P.W. & Ehrlich, M. 2004, DNA hypomethylation and ovarian cancer biology, *Cancer research*, vol. 64, no. 13, pp. 4472-4480.
- Winter, R.B., Berg, O.G. & von Hippel, P.H. 1981, Diffusion-driven mechanisms of protein translocation on nucleic acids. 3. The Escherichia coli lac repressor--operator interaction: kinetic measurements and conclusions, *Biochemistry*, vol. 20, no. 24, pp. 6961-6977.

- Wohrle, D., Salat, U., Glaser, D., Mucke, J., Meisel-Stosiek, M., Schindler, D., Vogel, W. & Steinbach, P. 1998, Unusual mutations in high functioning fragile X males: apparent instability of expanded unmethylated CGG repeats, *Journal of medical genetics*, vol. 35, no. 2, pp. 103-111.
- Wong, K.K., Maser, R.S., Bachoo, R.M., Menon, J., Carrasco, D.R., Gu, Y., Alt, F.W. & DePinho, R.A. 2003, Telomere dysfunction and Atm deficiency compromises organ homeostasis and accelerates ageing, *Nature*, vol. 421, no. 6923, pp. 643-648.
- Wouters, B.G. & Begg, A.C. 2009, in *Basic Clinical Radiobiology*, eds. M. Joiner & A. van der Kogel, 4th edn, Edward Arnold, UK, pp. 11.
- Wright, E.G. 2010, Manifestations and mechanisms of non-targeted effects of ionizing radiation, *Mutation research*, vol. 687, no. 1-2, pp. 28-33.
- Wright, W.E. & Shay, J.W. 2005, Telomere biology in aging and cancer, *Journal of the American Geriatrics Society*, vol. 53, no. 9 Suppl, pp. S292-4.
- Wu, S.C. & Zhang, Y. 2010, Active DNA demethylation: many roads lead to Rome, *Nature reviews.Molecular cell biology*, vol. 11, no. 9, pp. 607-620.
- Xin, Z. & Broccoli, D. 2004, Manipulating mouse telomeres: models of tumourigenesis and aging, *Cytogenetic and genome research*, vol. 105, no. 2-4, pp. 471-478.
- Xu, G.L., Bestor, T.H., Bourc'his, D., Hsieh, C.L., Tommerup, N., Bugge, M., Hulten, M., Qu, X., Russo, J.J. & Viegas-Pequignot, E. 1999, Chromosome instability and immunodeficiency syndrome caused by mutations in a DNA methyltransferase gene, *Nature*, vol. 402, no. 6758, pp. 187-191.
- Yamamoto, H., Min, Y., Itoh, F., Imsumran, A., Horiuchi, S., Yoshida, M., Iku, S., Fukushima, H. & Imai, K. 2002, Differential involvement of the hypermethylator phenotype in hereditary and sporadic colorectal cancers with high-frequency microsatellite instability, *Genes, chromosomes & cancer*, vol. 33, no. 3, pp. 322-325.
- Yang, Q., Zheng, Y.L. & Harris, C.C. 2005, POT1 and TRF2 cooperate to maintain telomeric integrity, *Molecular and cellular biology*, vol. 25, no. 3, pp. 1070-1080.
- Yang, S., Smit, A.F., Schwartz, S., Chiaromonte, F., Roskin, K.M., Haussler, D., Miller, W. & Hardison, R.C. 2004, Patterns of insertions and their covariation with substitutions in the rat, mouse, and human genomes, *Genome research*, vol. 14, no. 4, pp. 517-527.
- Yee, C.J., Roodi, N., Verrier, C.S. & Parl, F.F. 1994, Microsatellite instability and loss of heterozygosity in breast cancer, *Cancer research*, vol. 54, no. 7, pp. 1641-1644.
- Yoder, J.A., Walsh, C.P. & Bestor, T.H. 1997, Cytosine methylation and the ecology of intragenomic parasites, *Trends in genetics : TIG*, vol. 13, no. 8, pp. 335-340.
- Yoon, J.H., Smith, L.E., Feng, Z., Tang, M., Lee, C.S. & Pfeifer, G.P. 2001, Methylated CpG dinucleotides are the preferential targets for G-to-T transversion mutations induced by benzo[a]pyrene diol epoxide in mammalian cells: similarities with the p53 mutation spectrum in smoking-associated lung cancers, *Cancer research*, vol. 61, no. 19, pp. 7110-7117.
- You, Y.H., Li, C. & Pfeifer, G.P. 1999, Involvement of 5-methylcytosine in sunlight-induced mutagenesis, *Journal of Molecular Biology*, vol. 293, no. 3, pp. 493-503.

- Zheng, H., Wang, X., Warren, A.J., Legerski, R.J., Nairn, R.S., Hamilton, J.W. & Li, L. 2003, Nucleotide excision repair- and polymerase eta-mediated error-prone removal of mitomycin C interstrand cross-links, *Molecular and cellular biology*, vol. 23, no. 2, pp. 754-761.
- Zhou, L., Cheng, X., Connolly, B.A., Dickman, M.J., Hurd, P.J. & Hornby, D.P. 2002, Zebularine: a novel DNA methylation inhibitor that forms a covalent complex with DNA methyltransferases, *Journal of Molecular Biology*, vol. 321, no. 4, pp. 591-599.
- Zhu, B., Zheng, Y., Angliker, H., Schwarz, S., Thiry, S., Siegmann, M. & Jost, J.P. 2000, 5-Methylcytosine DNA glycosylase activity is also present in the human MBD4 (G/T mismatch glycosylase) and in a related avian sequence, *Nucleic acids research*, vol. 28, no. 21, pp. 4157-4165.
- Zilberman, D. 2007, The human promoter methylome, *Nature genetics*, vol. 39, no. 4, pp. 442-443.
- Zou, Y., Misri, S., Shay, J.W., Pandita, T.K. & Wright, W.E. 2009, Altered states of telomere deprotection and the two-stage mechanism of replicative aging, *Molecular and cellular biology*, vol. 29, no. 9, pp. 2390-2397.
- Zou, Y., Sfeir, A., Gryaznov, S.M., Shay, J.W. & Wright, W.E. 2004, Does a sentinel or a subset of short telomeres determine replicative senescence?, *Molecular biology of the cell*, vol. 15, no. 8, pp. 3709-3718.